

# Design and synthesis of reactive building blocks for multicomponent polymer systems : new options for poly(2,6-dimethyl-1,4-phenylene ether)

**Citation for published version (APA):**

Aert, van, H. A. M. (1997). *Design and synthesis of reactive building blocks for multicomponent polymer systems : new options for poly(2,6-dimethyl-1,4-phenylene ether)*. [Phd Thesis 1 (Research TU/e / Graduation TU/e), Chemical Engineering and Chemistry]. Technische Universiteit Eindhoven. <https://doi.org/10.6100/IR491737>

**DOI:**

[10.6100/IR491737](https://doi.org/10.6100/IR491737)

**Document status and date:**

Published: 01/01/1997

**Document Version:**

Publisher's PDF, also known as Version of Record (includes final page, issue and volume numbers)

**Please check the document version of this publication:**

- A submitted manuscript is the version of the article upon submission and before peer-review. There can be important differences between the submitted version and the official published version of record. People interested in the research are advised to contact the author for the final version of the publication, or visit the DOI to the publisher's website.
- The final author version and the galley proof are versions of the publication after peer review.
- The final published version features the final layout of the paper including the volume, issue and page numbers.

[Link to publication](#)

**General rights**

Copyright and moral rights for the publications made accessible in the public portal are retained by the authors and/or other copyright owners and it is a condition of accessing publications that users recognise and abide by the legal requirements associated with these rights.

- Users may download and print one copy of any publication from the public portal for the purpose of private study or research.
- You may not further distribute the material or use it for any profit-making activity or commercial gain
- You may freely distribute the URL identifying the publication in the public portal.

If the publication is distributed under the terms of Article 25fa of the Dutch Copyright Act, indicated by the "Taverne" license above, please follow below link for the End User Agreement:

[www.tue.nl/taverne](http://www.tue.nl/taverne)

**Take down policy**

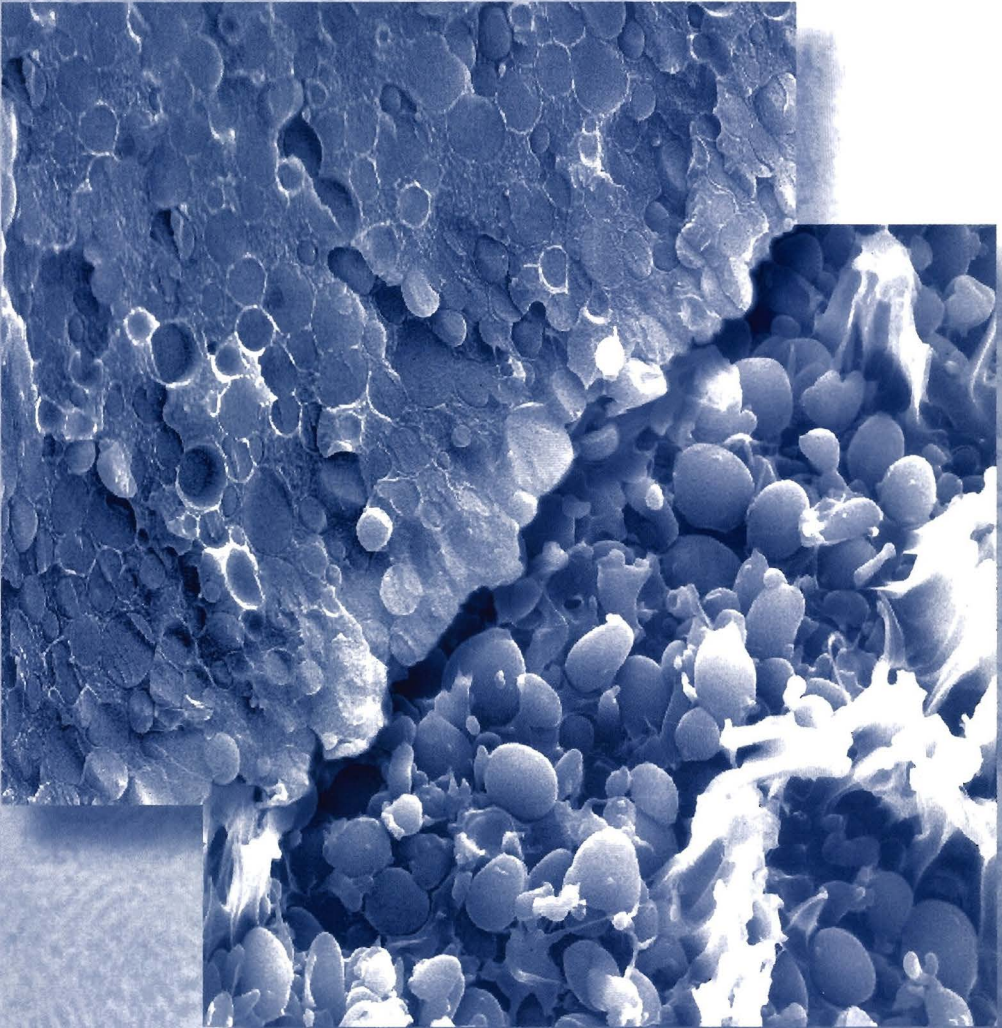
If you believe that this document breaches copyright please contact us at:

[openaccess@tue.nl](mailto:openaccess@tue.nl)

providing details and we will investigate your claim.

# Design and Synthesis of Reactive Building Blocks for Multicomponent Polymer Systems

*New options for poly(2,6-dimethyl-1,4-phenylene ether)*



**Huib van Aert**



**Design and Synthesis of Reactive Building Blocks  
for Multicomponent Polymer Systems**

New options for poly(2,6-dimethyl-1,4-phenylene ether)

CIP-DATA LIBRARY TECHNISCHE UNIVERSITEIT EINDHOVEN

Aert, Huub A.M. van

Design and synthesis of reactive building blocks for multicomponent polymer systems : new options for poly(2,6-dimethyl-1,4-phenylene ether) / by Huub A.M. van Aert. - Eindhoven : Technische Universiteit Eindhoven, 1997.

Proefschrift. -

ISBN 90-386-0968-X

NUGI 813

Trefw.: multicomponent polymeren / polymeren ; synthese / blokpolymeren

Subject headings: multicomponent polymers / block copolymers / polymer blends / redistribution

Copyright © 1997 H.A.M. van Aert

Omslagontwerp: Ben Mobach, TUE

Druk: Universiteitsdrukkerij TUE

**Cover:** Electron micrographs of multicomponent polymer systems, on front cover: two scanning electron microscopy pictures of fracture surfaces of blends containing poly(butylene terephthalate) (PBT) and poly(2,6-dimethyl-1,4-phenylene ether) (PPE), either using reactive PPE or unmodified PPE; on the full cover: a transmission electron micrograph from a cryosection of a poly(bisphenol A carbonate)-poly(dimethylsiloxane) multiblock copolymer film.



**Design and Synthesis of Reactive Building Blocks  
for Multicomponent Polymer Systems**

New options for poly(2,6-dimethyl-1,4-phenylene ether)

PROEFSCHRIFT

ter verkrijging van de graad van doctor aan de  
Technische Universiteit Eindhoven, op gezag van  
de Rector Magnificus, prof.dr. M. Rem, voor een  
commissie aangewezen door het College van  
Dekanen in het openbaar te verdedigen op  
dinsdag 27 mei 1997 om 16.00 uur

door

HUBERTUS ADRIANUS MARIA VAN AERT

geboren te Huijbergen

Dit proefschrift is goedgekeurd door de promotoren:

prof.dr. E.W. Meijer

en

prof.dr. P.J. Lemstra

Copromotor:

dr.ir. M.H.P. van Genderen



## Contents

### Chapter 1

General introduction	1
1.1 Poly(2,6-dimethyl-1,4-phenylene ether), a versatile polymer	1
1.2 Reactive oligomers and telechelic polymers	2
1.3 Polymer blends	3
1.4 Block copolymers	6
1.5 Aim and scope of this thesis	9
1.6 References	10

### Chapter 2

The precipitation polymerization of 2,6-dimethylphenol; control over molecular weight of PPE	15
2.1 Introduction	15
2.2 Results and discussion	17
2.3 Conclusions	21
2.4 Experimental	21
2.5 References	23

### Chapter 3

Modified poly(2,6-dimethyl-1,4-phenylene ether)s prepared by redistribution	25
3.1 Introduction	25
3.2 Results and discussion	28
3.2.1 Redistribution using CuCl/DMAP catalysts	31
3.2.2 Redistribution using Cu(NO <sub>3</sub> ) <sub>2</sub> ·3H <sub>2</sub> O/N-methylimidazole (NMI) catalysts	36
3.2.3 Use of TMDPQ as oxidant	37
3.2.4 The role of base	42
3.3 Conclusions	46
3.4 Experimental	47
3.5 References and notes	52

### Chapter 4

Star-shaped poly(2,6-dimethyl-1,4-phenylene ether)	55
4.1 Introduction	55
4.2 Results and discussion	57
4.2.1 Materials	57
4.2.2 Star-shaped PPEs in solution	59

4.2.3	Blends of star-shaped PPE and linear PS	62
4.3	Conclusions	65
4.4	Experimental	65
4.5	References	66

### Chapter 5

Endgroup modification of poly(2,6-dimethyl-1,4-phenylene ether) using phase-transfer-catalysis	69
--	----

5.1	Introduction	69
5.2	Results and discussion	72
5.2.1	Trioctyl methyl ammonium chloride as phase-transfer catalyst	72
5.2.2	Tetrabutylammonium hydroxide as phase-transfer catalyst	74
5.3	Conclusions	76
5.4	Experimental	77
5.5	References	79

### Chapter 6

Reactive compatibilization of blends of poly(2,6-dimethyl-1,4-phenylene ether) and poly(butylene terephthalate)	83
---	----

6.1	Introduction	84
6.2	Results and discussion	87
6.2.1	Poly(butylene terephthalate) and blend studies	87
6.2.2	Blends of PBT and carboxylic-acid-modified PPE	87
6.2.3	Blends of PBT and methyl ester-modified PPE	93
6.2.4	Blends of PBT and hydroxyalkyl-modified PPE	94
6.2.5	Blends of PBT and amino-terminated PPE	95
6.2.6	Blends of PBT and <i>t</i> -BOC-protected amino-functionalized PBT	97
6.2.7	Type of reaction, esterification versus amidation	99
6.3	Conclusions	100
6.4	Experimental	100
6.5	References	101

### Chapter 7

Poly(2,6-dimethyl-1,4-phenylene ether)-poly(dimethylsiloxane) triblock copolymers	105
---	-----

7.1	Introduction	105
7.2	Results and discussion	107
7.2.1	Synthesis	107
7.2.2	Electronmicroscopy	108
7.2.3	Small Angle X-ray Scattering	110
7.2.4	Solid state NMR	113
7.3	Conclusions	118
7.4	Experimental	118



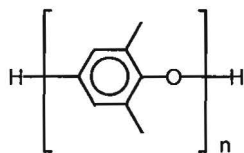
7.5	References	120
<i>Chapter 8</i>		
Poly(bisphenol A carbonate)-poly(dimethylsiloxane) multiblock copolymers		123
8.1	Introduction	123
8.2	Results and discussion	124
8.3	Conclusions	132
8.4	Experimental	133
8.5	References	134
<i>Chapter 9</i>		
Microphase-separated multiblock copolymers of poly(dimethyl siloxane) and photo-crosslinkable polyesters		137
9.1	Introduction	137
9.2	Results and discussion	139
9.2.1	Synthesis of cinnamate derivatives and siloxane copolymers	139
9.2.2	Thermal properties of the copolymers	143
9.2.3	X-ray scattering experiments	145
9.2.4	Photo-crosslinking experiments	148
9.3	Conclusions	151
9.4	Experimental	151
9.5	References	155
<i>Summary</i>		157
<i>Samenvatting</i>		159
<i>Curriculum Vitae</i>		161
<i>Dankwoord</i>		163

# Chapter 1

## General introduction

### 1.1 Poly(2,6-dimethyl-1,4-phenylene ether), a versatile polymer

Poly(2,6-dimethyl-1,4-phenylene ether) (PPE) (1.1) is an amorphous thermoplast, possessing a high glass transition temperature,  $T_g$ , of approximately 210 °C and exhibits excellent properties, such as a high toughness, a high dimensional stability, a good flame retardancy and a low moisture uptake. The facile synthesis of PPE by the oxidative coupling polymerization of 2,6-dimethylphenol, as discovered by A.S. Hay in 1956, attracted considerable commercial interest.<sup>1</sup> However, the high glass transition temperature,  $T_g$ , of ca. 210 °C of PPE, requires high melt processing temperatures in the range of 300–350 °C and under these conditions, considerable degradation occurs. PPE is therefore regarded as an intractable polymer. This problem was overcome by the discovery that PPE forms homogeneous blends with polystyrene having a lower  $T_g$ , which could be extruded and molded at 225–275 °C, far below the temperature where decomposition of PPE takes place. This has led to the development of PPE-polystyrene blends under the Noryl<sup>®</sup> resin trademark of General Electric Plastics, which became a major family of engineering plastics. An alternative route to reduce the viscosity of PPE is the use of reactive solvents. The use epoxy resins as reactive solvents for PPE has been explored recently by Venderbosch.<sup>2</sup> For many years the homogeneous blends with polystyrene were essentially the sole PPE products manufactured. However, more recently *heterogeneous* blends with polyamides and polyesters have been produced, which often requires modification of PPE in order to provide the required compatibilization.



1.1

Nowadays, polymeric materials are known for the great versatility of their macroscopic performances, promoted by the precise control of their primary structure. Polymers of a fairly low molecular weight, bearing specific reactive endgroups at one or both sides, often play an important role in the production of advanced polymeric materials.<sup>3,4</sup> These reactive polymers particularly



contribute to the development of a diversity of block- and graft- and, more recently, star-shaped copolymers with their specific chain architecture.

Well-defined modified PPEs, which are required for the application in block copolymers, are only reported in literature to a limited extent. The aim of our study is the preparation of modified PPEs with facile control over the molecular weight and the nature of the endgroups, in order to obtain well-defined chain microstructures and polymer architectures. Our main interest is to use these modified PPEs in block copolymers and blends in order to investigate the morphology in these multicomponent polymer systems. PPE is therefore combined with polymers having divergent properties, such as crystalline polyesters and low- $T_g$  polysiloxanes. The controlled synthesis of modified PPEs and their study in block copolymers and blends can enlarge the knowledge on this widely employed polymer and can open pathways for new polymeric materials.

Each subject discussed in this thesis is introduced in its own Chapter and their introductory topics are not given here. The next paragraphs, however, will review the most important general aspects of reactive oligomers and telechelics, blends and block copolymers. Special attention will be given to the phase segregation in blends and block copolymers.

## 1.2 Reactive oligomers and telechelic polymers

The term “reactive oligomers” is used for oligomers with deliberately introduced reactive groups, which are utilized for further reactions. This category of reactive oligomers comprises linear chains bearing one reactive endgroup, designated as end-reactive oligomers, and telechelics, i.e. polymers that possess as many functional groups as they have extremities. The term “telechelic” was first introduced in order to describe polybutadienes<sup>5</sup> having carboxyl and hydroxyl endgroups, based on the Greek words “telos” = end and “chele” = claw. The term telechelics is not limited to linear oligomers possessing one or two reactive groups, but (preferably regularly) branched structures having multiple functional endgroups are also included within the category of telechelics. Important examples of these multiple systems are known as star polymers<sup>6,7</sup> and dendritic polymers.<sup>8-10</sup> Star polymers are obtained either by coupling of a monofunctional polymer with a multifunctional reagent to obtain a core with branches (arm first method), or by the polymerization using a multifunctional initiator (core first method). Well-defined dendritic polymers (dendrimers) are, on the other hand, produced through a controlled sequence of reactions using multifunctional reagents in a divergent or convergent approach. Poly(propylene imine) dendrimers, as commercially produced by DSM, are synthesized via a divergent procedure.<sup>11</sup> A repetitive addition of a primary amine to two equivalents of acrylonitrile, followed by hydrogenation of the resulting nitrile moieties with Raney cobalt in a hydrogen atmosphere, afford the desired amine-terminated poly(propylene

imine) dendrimers. The convergent approach is initially reported by Fréchet<sup>12</sup> and co-workers for the synthesis of aromatic polyether dendrimers. The convergent approach is, however, less optimal to prepare highly functional telechelics than the divergent approach.

The main interest in reactive oligomers and telechelics is their use as building blocks for the production of segmented copolymers and polymer networks. The industrial interest in telechelics was stimulated by the development of thermoplastic elastomers (TPEs) consisting of ABA triblock and multiblock copolymers. Well-known examples of TPEs are styrene-butadiene-styrene (SBS) and styrene-isoprene-styrene triblock copolymers.<sup>13,14</sup> A large number of synthetic methods for the preparation of well-defined reactive oligomers and telechelics polymers have been developed.<sup>15-20</sup> Tailor-made reactive polymers are often prepared via living polymerizations through one of the following processes: anionic,<sup>21-23</sup> cationic,<sup>24,25</sup> free-radical,<sup>26-28</sup> metathesis<sup>29,30</sup> and group-transfer<sup>31</sup> polymerization. Besides living polymerizations more classical methods, such as stepwise polymerizations, are still used to produce reactive polymers as well.<sup>20,32</sup> In this thesis the preparation of polymers with a well-defined chain architecture and nature of endgroups are described, such as star-shaped PPEs and polymers with reactive chain ends, like telechelics of PPE, poly(bisphenol A carbonate) (PC), poly(dimethylsiloxane) (PDMS), and unsaturated polyesters. These modified polymers are used in multicomponent polymer systems like blends and block copolymers.

### 1.3 Polymer blends

Polymer blends are mixtures of at least two macromolecular species, polymers and/or copolymers. From an industrial point of view, polymer blends fill the deficiency in price/performance of existing homopolymers with relatively minor capital investment, compared to the development of a new macromolecule. Polymer blends represent one of the fastest growing sectors of polymer industry.<sup>33,34</sup>

Polymer blends are either miscible or immiscible. It is convenient to define miscibility as the ability to be mixed at a molecular level to produce one homogeneous phase. The miscibility behaviour of a polymer blend is determined by the thermodynamics of this multicomponent polymer system,<sup>35-42</sup> and is obtained when the Gibbs free energy of mixing is negative and  $\partial^2 \Delta G_m / \partial \phi_B^2 > 0$ . The free energy of mixing ( $\Delta G_m$ ) is composed of an enthalpic term and entropic term:  $\Delta G_m = \Delta H_m - T \Delta S_m$ , where  $\Delta H_m$  is the enthalpy of mixing,  $\Delta S_m$  is the entropy of mixing and  $T$  the absolute temperature. A more detailed discussion of the thermodynamics of polymer blends is described in reviews by Utracki,<sup>42</sup> van de Grampel,<sup>34</sup> Walsh<sup>36</sup> and Macknight.<sup>37</sup>

In order to predict the phase behavior of a system, one needs to describe the free energy of a polymer mixture by a model. The Flory-Huggins mean-field theory was one of the first models to be applied to describe the thermodynamics of polymer mixtures. Already more than 50 years ago Flory<sup>39</sup> and Huggins<sup>40,41</sup> independently estimated this change in free energy  $\Delta G_m$  employing a lattice model:  $\Delta G_m/nk_B T = \phi_A/N_A \ln\phi_B + \phi_B/N_B \ln(\phi_B) + \phi_A\phi_B\chi$ , in which  $n (= n_A N_A + n_B N_B)$  denotes the total number of segments,  $k_B$  is the Boltzman constant,  $T$  the temperature,  $n_A$  and  $n_B$  the number of polymer molecules A and B consisting of  $N_A$  respectively  $N_B$  segments,  $\chi$  the Flory-Huggins segment-segment interaction parameter, and  $\phi_A$  and  $\phi_B$  the volume fractions of polymers A and B, respectively ( $\phi_A + \phi_B = 1$ ). The first two terms account for the entropy  $\Delta S_m = -nk_B(\phi_A/N_A \ln\phi_A + \phi_B/N_B \ln\phi_B)$ . Because mixing increases the systems randomness, it naturally increases  $\Delta S_m$  and thereby decreases the free energy of mixing. The third term represents the enthalpy of mixing  $\Delta H_m = nk_B T \phi_A \phi_B \chi$ . Since the entropy of mixing in polymer blends is very small (large  $N_A$  and  $N_B$ ), polymer miscibility is determined by the enthalpy. Usually, the enthalpy is unfavorable and the polymers are not expected to be miscible. Mixing can, however, be predicted to occur under three circumstances.<sup>36</sup> (1) If the polymers have low molecular weight then the entropy will not be negligible and may outweigh an unfavorable enthalpy of mixing. (2) If the enthalpy is positive but very small, then a small entropy of mixing may be sufficient. This might occur when the polymers are very similar chemically and physically. For example, copolymers with similar composition are expected to be miscible. (3) If the enthalpy is negative then two polymers are expected to be miscible. This might occur when there is a favorable interaction ( $\chi < 0$ ) like hydrogen bonding.

Using the Flory-Huggins mean-field theory a phase-diagram of a binary polymer blend can be predicted. When the stability criterion,  $\partial^2 \Delta G_m / \partial \phi_B^2 > 0$ , is not satisfied, the system is unstable and phase separation proceeds via spinodal decomposition. The spinodal ( $\partial^2 \Delta G_m / \partial \phi_B^2 = 0$ ), shown in Figure 1.1., defines the limit of metastability in a phase diagram. All points inside the spinodal represent unstable systems. The coexistence curve or binodal is the curve in the phase diagram defining the coexisting phases of the system. Equilibrium is obtained when  $\Delta \mu_i(\phi') = \Delta \mu_i(\phi'')$ , where the superscripts ' and '' refer to separate phases and  $\Delta \mu_i$  denotes the difference between the chemical potential in the mixture and the pure state for component  $i$ . In the region between the spinodal and binodal, the system is metasable and the phase separation occurs via a nucleation and growth mechanism. At the critical point the equilibrium (binodal) and stability (spinodal) curves coincide and  $\partial^2 \Delta G_m / \partial \phi_B^2 = 0$  and  $\partial^3 \Delta G_m / \partial \phi_B^3 = 0$ . Using the Flory-Huggins theory, simple explicit conditions for the critical state can be derived:  $\phi_C = N_A^{1/2} / (N_A^{1/2} + N_B^{1/2})$  and  $\chi_C = (N_A^{1/2} + N_B^{1/2})^2 / 2N_A N_B$ . In a theoretical phase diagram<sup>35</sup> for a symmetric ( $N_A = N_B \equiv N$ ) binary mixture of linear homopolymers, as shown in Figure 1.1,  $\phi_C = 0.5$  and  $\chi_C = 2/N$ . At  $\phi_C = 0.5$  phase separation occurs for  $\chi N > 2$ .

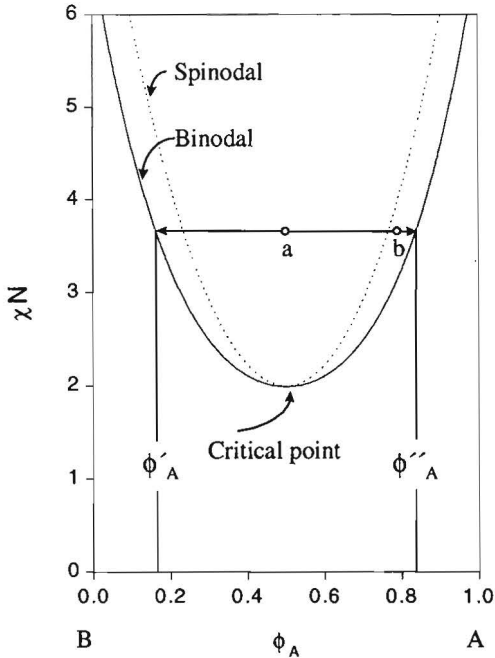


**Figure 1.1:** Theoretical phase diagram for a symmetric mixture of linear homopolymers A and B; inside the equilibrium (solid) curve, two phases exist with compositions  $\phi'_A$  and  $\phi''_A$ ; in the metastable region (such as point b), phase separation occurs by a nucleation and growth mechanism, while an unstable mixture (such as point a) spontaneously demixes.

Only a limited number of miscible blends are known in literature, e.g. the blend of PPE and atactic PS, and the blend of poly(etherimide) (PEI) and poly(etherether ketone) (PEEK).<sup>33,34</sup> Polymer-polymer miscibility is often restricted to situations where specific interactions, i.e. hydrogen bonding,<sup>43-46</sup> are present. Another example of specific interactions which can cause miscibility in polymer blends is electron-donor-acceptor complexation.<sup>47-50</sup> Experimentally, however, many polymer blends are miscible without the presence of specific interactions. These polymer blends have in common that at least one component is a random copolymer and miscibility is attributed to the so called intramolecular repulsion effect.<sup>51-55</sup> Intramolecular interactions may outweigh intermolecular repulsion and cause two polymers to have a net interaction and become miscible. An typical example is a blend of PPE with a random copolymer of *ortho*-chlorostyrene and *para*-chlorostyrene.<sup>56</sup> PPE is not miscible with the homopolymers poly(*ortho*-chlorostyrene) or poly(*para*-chlorostyrene) and poly(*ortho*-chlorostyrene) is not miscible with poly(*para*-chlorostyrene). However, PPE is miscible with poly((*ortho*-chlorostyrene)<sub>x</sub>-co-(*para*-chlorostyrene)<sub>1-x</sub>) at 200 °C for 0.3 < x < 0.8.

Most applied blends are used as structural materials consisting of two or more phases. The properties of an immiscible blend are determined, to a large extent, by the morphology i.e. the

particle size, shape and distribution of the components. The main problem of such a morphology is its intrinsic instability in the molten state. The morphology changes continuously and adapts to changes in shear- and elongational stress, deformation rate, total strain, processing time and temperature.<sup>57-60</sup> In order to transfer the desired properties to the final product, it is important to gain control of the morphology during the various processing steps involved. Development of new multiphase polymer blends is related to two key variables: control of the interfacial properties and the obtained microstructure. The term compatibilization is used to denote any of a variety of techniques that will improve the interfacial adhesion in a multiphase polymer system. A compatible blend stands for an immiscible polymer blend that has been modified to possess commercially attractive properties.<sup>42</sup> Compatible blends are mechanically processable blends, which generally do not give a large phase segregation. Numerous commercial compatible blends have been developed, such as blends of poly(bisphenol A carbonate) (PC) and poly(butylene terephthalate) (PBT) and blends of polyamide with PPE. Nowadays, a lot of research on immiscible blends focuses on control of the multiphase morphology. Control of the interfacial interactions and reactive compatibilization plays an important role.<sup>61-69</sup> Reactive compatibilization is often referred to as reactive processing or reactive blending. Using this method the interfacial agent is formed *in-situ*. Reactive blending is used in Chapter 6 to compatibilize the immiscible blend of PPE and PBT. From the view of cost, this technique is more useful than the addition of a specially tailored, usually expensive copolymer.

## 1.4 Block copolymers

Block copolymers are often employed for control of the interfacial properties in multiphase polymer systems. To improve the mechanical properties of immiscible polymer blends, block copolymers having blocks of the same chemical structure as the phases in the heterogeneous blend, may be added to the mixture. When these block copolymers localize at the interface between the immiscible polymers, the interfacial tension will be lowered and the interface consequently broadened. Localization of the block copolymers at the interface is thermodynamically the most favorable because this will reduce to number of unfavorable interactions between the A and B segments of the homopolymers A and B. The reduced interfacial tension will give rise to smaller domains and will stabilize the blend morphology. Furthermore, an improved interfacial adhesion will yield better mechanical properties. Copolymers capable of improving the interfacial properties can be premade or can be prepared *in-situ* during processing.<sup>33,61,70</sup> The use of simple diblock copolymers,<sup>71,72</sup> but also other architectures like triblock,<sup>73</sup> star-shaped block<sup>74</sup> and multiblock<sup>75</sup> copolymers, as interfacial agents is reported. Besides block copolymers also graft<sup>76,77</sup> and random copolymers<sup>78</sup> are reported as interfacial agent.

Besides for their use as compatibilizing agents, block copolymers<sup>79</sup> have gained considerable importance both in scientific studies and in industrial applications.<sup>13,80-90</sup> The interest in these products arises from their specific microstructure, which gives rise to unique physical and mechanical properties and specific morphologies. A wide variety of block copolymers with well-defined structures have been prepared from styrene and diene monomers, and are being studied extensively.<sup>13</sup> Block copolymers with poly(vinylpyridine) (PVP) segments are widely investigated as well, e.g. in polystyrene-PVP diblock copolymers.<sup>91</sup> Useful properties of block copolymers are often derived from the thermodynamically driven phase segregation of unlike blocks, leading to microphase separation in the solid state<sup>35</sup> or micellization in solution.<sup>80,92-94</sup> In block copolymers the different types of components present in blocks are covalently bonded together, and thereby preventing the phase separation on a macroscopic scale and therefore leading to quantitative differences in phase behavior as a comparison to polymer blends. While in symmetric binary mixtures of linear homopolymers demixing occurs for  $\phi = 0.5$  when  $\chi N > 2$  ( $N$  defined as number of segments  $N \equiv N_A = N_B$ ) (see Figure 1.1), in a symmetric A-B diblock copolymer phase separation occurs for  $\chi N > 10$  at  $f_A = 0.5$  ( $N$  defined as total degree of polymerization  $N = N_A + N_B$ , and  $f_A$  the volume fraction of component A in the block copolymer) as reported by Vavasour.<sup>95</sup> A theoretical phase diagram<sup>95</sup> for A-B diblock copolymers is shown in Figure 1.2. The critical point is given by  $f_A = 0.5$  and  $\chi N = 10$ .

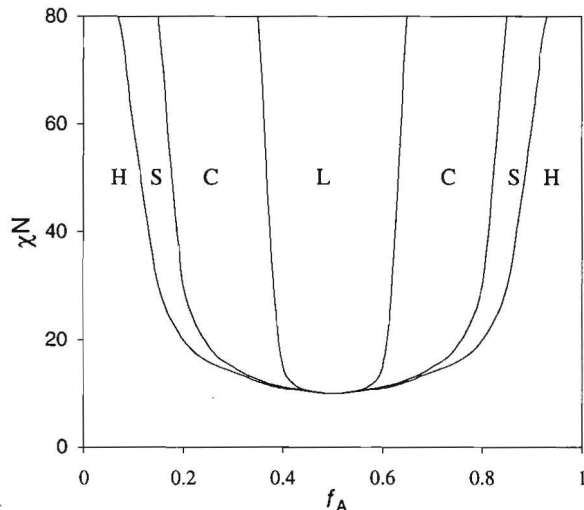


**Figure 1.2:** Theoretical phase diagram for A-B diblock copolymers; H, S, C, and L represent homogeneous, spherical, cylindrical and lamellar phases, respectively.

Like in polymer blends, the phase behavior of block copolymers is dependent on the product  $\chi N$  (where  $N$  is the polymerization index and  $\chi$  is the Flory parameter characterizing the interaction of monomers A-B). Increasing  $\chi N$  leads to an increase in the segregation power and sharper



microdomain boundaries.<sup>35</sup> When  $\chi > 0$ , a decrease in segment-segment contacts reduces the enthalpy ( $\Delta H$ ) of the system. This process can occur locally, segregating A and B blocks. Segregation is opposed by the associated loss in the entropy ( $\Delta S$ ) of the system caused by localization of block-block junction points at interfaces and by stretching of the chains in order to maintain a uniform density. The entropy of the block copolymer scales with  $\Delta S \sim N^{-1}$ . For  $\chi N \gg 10$ , the “strong segregation limit” (SSL) is obtained. The “weak segregation limit” (WSL) is obtained for  $\chi N \approx 10$ . For  $\chi N \ll 10$ , entropic effects dominate and block copolymers exist in a spatially homogeneous state.

In the strong segregation limit, several characteristic morphologies have been identified. Examples of ordered structures at thermodynamic equilibrium are spheres in a body centered cubic (bcc) lattice, cylinders in a hexagonal (hex) lattice and alternating lamellae. The existence of stable morphologies consisting of spheres, cylinders and lamellae is known already as a classical picture reported by Molau.<sup>96</sup> Figure 1.3 shows the changes in morphology as a function of the A-content in an A-B block copolymer as known from this classical picture.<sup>96</sup> Other equilibrium microdomain morphologies located between the cylinder and lamellar phases are described by Bates<sup>81,97</sup> and Thomas.<sup>87,98,99</sup>

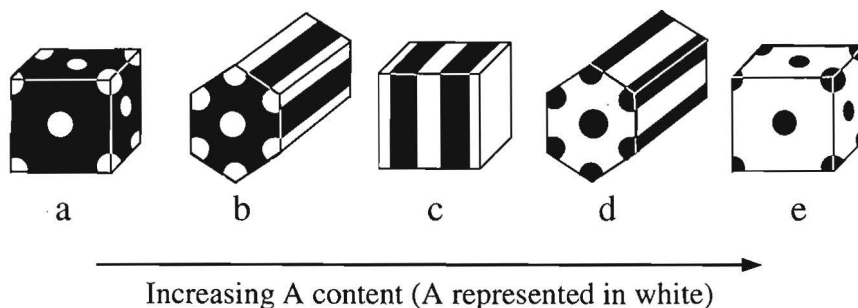


**Figure 1.3:** Changes in morphology of the ordered structure with A-content in an A-B block copolymer: a) spheres of A in matrix of B, b) cylinders of A in matrix of B, c) alternating A and B lamellae, d) cylinders of B in matrix of A, e) spheres of B in matrix of A.

The phase-separated domains in microphase-separated block copolymers can not grow macroscopically because of the chemical connection between the independent polymer blocks. Instead, the phase-separated domains are restricted in size to a scale comparable to the unperturbed chain dimensions of a single chain with the same length. For unperturbed chain dimensions the domain spacing scales with  $\overline{M}_n^\alpha$  with  $\alpha = 1/2$ . The exact scaling of the domain spacings (d) with molecular weight of the blocks present in the block copolymer is more complex.<sup>100</sup> In weakly segregating block polymers the chains are not appreciably distorted ( $d \sim \overline{M}_n^{1/2}$ ).<sup>106</sup> For strongly segregating block copolymers, however, both experimentally<sup>101-104</sup> and theoretically,<sup>105-107</sup> it was

found that the domain spacing scales with  $\overline{M}_n^\alpha$  with  $\alpha = 2/3$ . This higher power  $\alpha = 2/3$ , is caused by the fact that the blocks are more stretched in strongly segregating block copolymers. Some exceptions are known for this scaling ( $d \sim \overline{M}_n^{2/3}$ ) in strongly segregating block copolymers,<sup>108,109</sup> probably due to kinetic limitations to equilibrium morphology.

Scattering techniques<sup>110</sup> and electron microscopy<sup>80</sup> are in particular suitable for evaluation of the structural parameters of block copolymers. Transmission Electron Microscopy (TEM) provides a direct image of the microstructure, provided that the electron density difference between the different blocks is sufficient. In many cases selective staining is required. However, deducing the three-dimensional structure from TEM analyses is difficult. In addition, due to the small sections of samples examined and the possible effects of staining and sample deformation during microtoming and analysis, the ability to obtain quantitative information on the relevant length scales is limited. Additional information can be obtained using Small Angle X-Ray Scattering (SAXS). SAXS performed on bulk samples provides information on a global scale, allowing more quantitative determination of the microstructure (length scales 10–500 nm). The majority of detailed experimental data discussed in the literature concerns the microphase segregation in styrene-diene block copolymers.<sup>111-113</sup> Advances in theory and parallel development in experimental techniques gave a deeper insight into the physical properties of block copolymers. The expansion to experimental studies using other block copolymers is now in progress, e.g. for siloxane based block copolymers as described in Chapters 7–9 of this thesis.

## 1.5 Aim and scope of this thesis

The aim of our study is the preparation of novel well-defined polymeric architectures in general, and of systems based on poly(2,6-dimethyl-1,4-phenylene ether) in particular. In order to arrive at the stage that PPEs can be used in a variety of new combinations with other polymers, it is a prerequisite to develop versatile synthetic routes to oligo- and poly(2,6-dimethyl-1,4-phenylene ether)s with different reactive groups. The current industrial status of PPEs requires new synthetic strategies which in principle can be used at a larger scale. However, the use of defect-free well-defined samples of reactive PPEs are required to obtain a comprehensive insight into the formation of the new architectures prepared. The controlled synthesis of functional PPEs and their study in block copolymers and blends will enlarge the knowledge on this widely employed polymer and can open pathways for new polymeric materials. Combination of PPE with other polymers in block copolymers and blends allows investigation of the morphology in these multicomponent polymer systems, while the knowledge obtained can be used to study block copolymers and blends without PPE as well.

In Chapter 2, the control of chain length in the oxidative coupling polymerization of 2,6-dimethylphenol,<sup>114</sup> yielding well-defined PPE is described. The polymers so obtained are used throughout our investigations and serve as models for commercial PPE. Chapter 3 describes the use of PPE redistribution as a novel technique to prepare reactive PPEs with the easy adjustment of the chain length.<sup>115,116</sup> Depending on the reacting phenolic compound, desired reaction time and product purity, different catalyst systems are employed. Redistribution is also used in Chapter 4 to prepare multifunctional star shaped PPE.<sup>115,117,118</sup> The physical properties of these star-shaped PPEs and the influence of their specific chain conformation on miscibility behavior with linear polystyrene (PS) is investigated. Endgroup modification of the phenolic head units is described in Chapter 5. Using phase-transfer catalysis several endgroups are introduced. The morphology of compatibilized PPE/poly(butylene terephthalate) (PBT) blends obtained by reactive extrusion is investigated, as described in Chapter 6. In Chapters 7, 8 and 9 the microphase separation of siloxane block copolymers is studied. Chapter 7 describes the synthesis and characterization of PPE-PDMS-PPE triblock copolymers, prepared via PPE-redistribution. The knowledge obtained from the previous Chapters, especially on microphase separation in block copolymers, brought us in Chapters 8 and 9 to study block copolymers for developing systems without PPE. Chapter 8 describes the synthesis and characterization of PC-PDMS multiblock copolymers. The influence of crystallization of the polycarbonate blocks on mechanical properties and microstructure is investigated. Chapter 9 describes the synthesis of multiblock copolymers of PDMS and unsaturated polyesters.<sup>119</sup> The selective crosslinking of these block copolymers with polarized light leading to anisotropy has been investigated.

## 1.6 References

1. Hay, A.S. *J. Polym. Sci., Polym. Chem. Ed.*, **34**, 1369 (1996).
2. Venderbosch, R.W., "Processing of intractable polymers using reactive solvents", PhD thesis, Eindhoven University of Technology, The Netherlands, (1995).
3. Jerome, R. and Vanhoorne, P. *Trends Polym. Sci.*, **2**, 382 (1994).
4. Gnanou, Y. *J. Macromol. Sci., Rev. Macromol. Chem. Phys.*, **C36**, 77 (1996).
5. Uraneck, C.A., Hsiesh, H.L. and Buck, O.G. *J. Polym. Sci.*, **46**, 535 (1960).
6. Rein, D., Rempp, P. and Lutz, P.J. *Makromol. Chem., Macromol. Symp.*, **67**, 237 (1993).
7. Roovers, J. *Trends Polym. Sci.*, **2**, 294 (1994).
8. Voit, B.I. *Acta Polym.* **46**, 87 (1995).
9. Tomalia, D.A., Naylor, A., Goddard III, W. *Angew. Chem. Int. Ed. Engl.*, **29**, 138 (1990).
10. Newkome, G.R., Moorefield, C.N. and Vögtle, F. "Dendritic Molecules", VCH Verlagsgesellschaft mbH, Weinheim, (1996).
11. De Brabander-van den Berg, E.M.M., Nijenhuis, A, Mure, M., Keulen, J., Reintjes, R., Vandenbooren, F., Bosman, B., De Raat, R., Frijns, T. Van der Wal, S. Castelijns, M., Put, J. and Meijer, E.W. *Macromol. Symp.*, **77**, 138 (1994).

12. Hawker, C. and Fréchet, J.M.J. *J. Chem. Soc., Chem. Commun.*, 110 (1990).
13. Quirk, R.P., Kinning, D.J. and Fetters, L.J. *Compr. Polym. Sci.*, **7**, 1 (1989).
14. Fredrickson, G.H. and Bates, F.S. *Ann. Rev. Mater. Sci.*, **26**, 501 (1996).
15. Tezuka, Y. *Prog. Polym. Sci.*, **17**, 471 (1992).
16. Percec, V., Pugh, C., Nuyken, O. and Pask, S. *Compr. Polym. Sci.*, **6**, 281 (1989).
17. Jerome, R., Henriouille-Granville, M., Boutevin, B. and Robin, J.J. *Prog. Polym. Sci.*, **16**, 837 (1991).
18. Rempp, R. *Macromol. Symp.*, **60**, 209 (1992).
19. Boutevin B. *Adv. Polym. Sci.*, **94**, 69 (1990).
20. Van Caeter, P. and Goethals, E.J. *Trends Polym. Sci.*, **3**, 227 (1995).
21. Szwarc, M. *Adv. Polym. Sci.*, **49**, 1 (1983).
22. Quirk, R.P. *Compr. Polym. Sci.*, *1th suppl.*, 83 (1992).
23. Hirao, A. and Nakahama, S. *Trends Polym. Sci.*, **2**, 267 (1994).
24. Nuyken, O., Kroner, H., Riess, G., Oh, S. and Ingrisich, S. *Macromol. Symp.*, **101**, 29 (1996).
25. Kennedy, J.P. *Macromol. Chem., Macromol. Symp.*, **51**, 169 (1991).
26. Otsu, T. and Tazaki, T. *Polym. Bull.*, **16**, 277 (1986).
27. Turner, S. and Blevins, R. *Macromolecules*, **23**, 1856 (1990).
28. Hammouch, S.O. and Catala, J.M., *Macromol. Rapid Commun.*, **17**, 149 (1996).
29. Breslow, D.S. *Progress Polym. Sci.*, **18**, 1141 (1993).
30. Gibson, V.C. *Adv. Mater.*, **6**, 37 (1994).
31. Webster, O. and Anderson, B. "New Methods for Polymer Synthesis", Ed. Mijs, W., Plenum Press, New York, (1992).
32. Klee, J.E. *Acta Polym.*, **45**, 73 (1994).
33. Utracki, L.A. *Polym. Eng. Sci.*, **35**, 2 (1995).
34. Van de Grampel, H.T. *Rapra. Rev.*, **5**, 1 (1991).
35. Bates, F.S. *Science*, **251**, 898 (1991).
36. Walsh, D.J. *Compr. Polym. Sci.*, **2**, 135 (1989).
37. MacKnight, W.J. and Karasz, F.E. *Compr. Polym. Sci.*, **7**, 111 (1989).
38. Rostami, S. "Multicomponent Polymer Systems", Chapter 3, eds. Miles, I.S. and Rostami, S., Longman Scientific & Technical, Essex, (1992).
39. Flory, P.J. *J. Chem. Phys.*, **10**, 51 (1942).
40. Huggins, M. *J. Phys. Chem.*, **46**, 151 (1942).
41. Huggins, M. *J. Am. Chem. Soc.*, **64**, 1721 (1942).
42. Utracki, L.A. "Polymer alloys and blends, thermodynamics and rheology", Hanser Publishers, New York, (1989).
43. Coleman, M.M. and Painter, P.C. *Prog. Polym. Sci.*, **20**, 1 (1995).
44. Lange, R.F.M. and Meijer, E.W. *Macromolecules*, **28**, 782 (1995).
45. Cowie, J.M.G. and Reilly, A.A.N. *J. Appl. Polym. Sci.*, **47**, 1155 (1993).
46. Hobbie, E.K. and Han C.C. *J. Chem. Phys.*, **105**, 738 (1996).
47. Pugh, C. and Percec, V. *Macromolecules*, **19**, 65 (1986).
48. Schneider, H.A., Cantow, H.J., Lutz, P. and Nothfleet-Neto, H. *Macromol. Chem. Suppl.*, **8**, 89 (1984).

49. Simmons, A. and Natansohn, A. *Macromolecules*, **25**, 1272 (1992).
50. Karcha, R.J. and Porter, R.S. *J. Polym. Sci., Polym. Phys. Ed.*, **31**, 821 (1993).
51. Angerman, H., Hadziioannou, G. and ten Brinke, G. *Phys. Rev. E*, **50**, 3808 (1994).
52. Jiang, M. Huang, Y. and Xie, J. *Macromol. Chem. Phys.*, **196**, 803 (1995).
53. Paul, D.R. and Barlow, J.W. *Polymer*, **25**, 753 (1984).
54. Ten Brinke, G., Karasz, F.E. and Macknight, W.J. *Macromolecules*, **16**, 1827 (1983).
55. Jacobson, S.H., Gordon, D.J. Nelson, G.V. and Ballazs, A. *Adv. Mater.*, **4**, 198 (1992).
56. Ten Brinke, G., "Thermodynamica van polymeersystemen", reader, State University of Groningen, The Netherlands, (1989).
57. Van Gisbergen, J.G.M. "Electron beam irradiation of polymer blends", PhD thesis, Eindhoven University of Technology, The Netherlands, (1991).
58. Elmendorp, J.J. and van der Vegt, A.K. "Two-phase polymer systems, progress in polymer processing", Ed. Utracki, L.A., Hanser Publishers, New York, (1991).
59. Elemans, P.H.M. "Modelling of the processing of incompatible polymer blends", PhD thesis, Eindhoven University of Technology, The Netherlands, (1989).
60. Jansen, J.M.H. "Dynamics of liquid-liquid mixing", PhD thesis, Eindhoven University of Technology, The Netherlands, (1993).
61. Markham, R.L. *Adv. Polym. Techn.*, **10**, 231 (1990),
62. Aiji, A. and Utracki, L.A. *Polym. Eng. Sci.*, **36**, 1574 (1996).
63. Favis, B.D. *Can. J. Chem. Eng.*, **69**, 619 (1991).
64. Xanthos, M. and Dadli, S.S. *Polym. Eng. Sci.*, **31**, 929 (1991).
65. Gaylord, N.G. *J. Macromol. Sci., Chem.*, **A26**, 1211 (1989).
66. Bonner, J.G. and Hope, P.S. "Polymer Blends and Alloys", Chapter 3, Eds. Folkes, M.J. and Hope, P.S., Blackie Academic & Professional, Glasgow, (1993).
67. Brown, S.B. "Reactive Extrusion", Chapter 4, ed. Xanthos, X., Oxford University Press, Oxford, (1992).
68. Kumpf, R.J., Wiggins, J.S. and Pielartzik, H., *Trends Polym. Sci.*, **3**, 132 (1995).
69. Rösch, J., Warth, H., Müller, P., Schäfer, R., Wörner, C., Friedrich, C., Kressler, J. and Müllhaupt, R. *Makromol. Chem., Macromol. Symp.*, **102**, 241 (1996).
70. Sundararaj, U and Macosko. C.W. *Macromolecules*, **28**, 2647 (1995).
71. Macosko, C.W., Guégan, P., Khandpur, A.K., Nakayama, A., Marechal, P. and Inoue T. *Macromolecules*, **29**, 5590 (1996).
72. Coumans, W.J., Heikens, D. and Sjoerdsma, S.D. *Polymer*, **21**, 103 (1980).
73. Brown, H.R., Krappe, U. and Stadler, R. *Macromolecules*, **29**, 6582 (1996).
74. Mityata, K., Watanabe, Y., Itaya, T., Tanigaki, T. and Inoue, K. *Macromolecules*, **29**, 3694 (1996).
75. Trostyanskaya, E.B., Zemskov, M.B. and Mikhasenok, O.Y. *Plast Massy*, **11**, 28 (1983).
76. Jannasch, P., Gunnarson, O. and Wesslen, B. *J. Appl. Polym. Sci.*, **59**, 619 (1996).
77. Eklind, H. Schantz, S., Maurer, F.H.J., Jannash, P. and Wesslen, B. *Macromolecules*, **29**, 984 (1996).
78. Dai, C.A., Dair, B.J., Ober, C.K., Kramer, E.J., Hui, C.Y., and Jelinski, J.W. *Phys. Rev. L*, **73**, 2472 (1994).

79. IUPAC Commission on Macromolecular Nomenclature, *Pure Appl. Chem.*, **57**, 1427 (1985).
80. Brown, R.A., Masters, A.J., Price, C. and Yuan, X.F. *Compr. Polym. Sci.*, **2**, 155 (1989).
81. Bates, F.S., Schulz, M.F., Khandpur, A.K., Förster, S., Rosedale, J.H., Almdal, K. and Mortensen, K. *Faraday Discuss.*, **98**, 7 (1994).
82. Richards, R.W. "Multicomponent Polymer Systems", Chapter 4, Eds. Miles, I.S. and Rostami, S., Longman Scientific & Technical, Essex, (1992).
83. Aggarwal, S.L. *Polymer*, **17**, 938 (1976).
84. Meier, D.J. *J. Polym. Sci., Part C*, 81 (1969), *J. Polym. Sci., Phys. Ed.*, **34**, 1819 (1996).
85. Sakurai, S. *Trends Polym. Sci.*, **3**, 90 (1995).
86. Goodman, I. *Compr. Polym. Sci.*, **6**, 369 (1989).
87. Thomas, E.L. and Lescanec, R.L. *Phil. Trans. R. Soc. Lond.*, **348**, 149 (1994).
88. Leibler, L. *Macromolecules*, **13**, 1602 (1980).
89. Matsen, M.W. and Bates, F.S. *Macromolecules*, **29**, 1091 (1996).
90. Semenov, A.N. *Macromolecules*, **26**, 6617 (1993).
91. Schulz, M.F., Khandpur, A.K., Bates, F.S., Almdal, K., Mortensen, K., Hajduk, D.A. and Gruner, S.M. *Macromolecules*, **29**, 2857 (1996).
92. Gao, Z. and Eisenberg, A. *Macromolecules*, **26**, 7353 (1993).
93. Zhang, L. Barlow, R.J. and Eisenberg, A. *Macromolecules*, **28**, 6055 (1995).
94. Moffitt, M. Khougaz, K. and Eisenberg, A. *Acc. Chem. Res.*, **29**, 95 (1996).
95. Vavasour, J.D. and Whitmore M.D. *Macromolecules*, **25**, 5477 (1992).
96. Molau, G.E. "Colloidal and Morphological Behavior of Block Copolymers", ed. Molau, G.E., Plenum Press. New York, (1971).
97. Matsen, M.W. and Bates, F.S. *Macromolecules*, **29**, 7641 (1996).
98. Thomas, E.L., Anderson, D.M., Henkee, C.S. and Hofmann, D. *Nature*, **344**, 598 (1988).
99. Thomas, E.L., Alward, D.B., Kinning, D.J., Martin, D.C., Handlin, D.L. and Fetters, L.J. *Macromolecules*, **19**, 2197 (1986).
100. Halperin, A., Tirrell, M. and Lodge, T.P. *Adv. Polym. Sci.*, **100**, 33 (1992).
101. Hashimoto, T., Shibayama, M. and Kawai, H. *Macromolecules*, **13**, 1237 (1980).
102. Hashimoto, T., Fujimura, M. and Kawai, H. *Macromolecules*, **13**, 1660 (1980).
103. Hashimoto, T. Tanaka, H. and Hasegawa H. *Macromolecules*, **18**, 1864 (1985).
104. Hashimoto, T. *Macromolecules*, **15**, 1549 (1982).
105. Ohta, T. and Kawasaki, K. *Macromolecules*, **19**, 2621 (1986).
106. Melenkevitz, J. and Muthukumar, M. *Macromolecules*, **24**, 4199 (1991).
107. Semenov, A.N. *Soc. Phys. JETP*, **61**, 733 (1985).
108. Bates, F.S., Berney, C.V. and Cohen, R.E. *Macromolecules*, **16**, 1101 (1983).
109. Hadziioannou, G. and Skoulios, A. *Macromolecules*, **15**, 258 (1982).
110. Lodge, T. *Microchim. Acta*, **116**, 1 (1994).
111. Sakurai, S., Kawada, H., Hashimoto, T. and Fetters, L.J. *Macromolecules*, **26**, 5796 (1993).
112. Khandpur, A.K., Förster, S., Bates, F.S., Hamley, I.W., Ryan, A.J., Bras, W., Almdal, K. and Mortensen, K. *Macromolecules*, **28**, 8796 (1995).

- 113 . Inoue, T., Soen, T., Hashimoto, T. and Kawai, H. *J. Polym. Sci., Part A-2*, **7**, 1283 (1969).
- 114 . Van Aert, H.A.M., Venderbosch, R.W., van Genderen, M.H.P., Meijer, E.W. and Lemstra, P.J. *J. Macromol. Sci., Pure Appl. Chem.*, **A32**, 515 (1995).
- 115 . Van Aert, H.A.M., Burkard, M.E.M., Jansen, J.F.G.A., van Genderen, M.H.P. and Meijer, E.W., Oevering, H. and Werumeus Buning, G.H. *Macromolecules*, **28**, 7967 (1995).
- 116 . Van Aert, H.A.M., van Genderen, M.H.P., van Steenpaal, G.J.M.L., Nelissen, L.N.I.H., Meijer, E.W. and Liska, J. *Macromolecules*, submitted.
- 117 . Van Aert, H.A.M., van Genderen, M.H.P. and Meijer, E.W., *Polym. Bull.*, **37**, 273 (1996).
- 118 . Oevering, H., Werumeus Buning, G.H., Meijer, E.W., van Aert, H.A.M. and Out, G.J.J. PTC Int. Pat. Appl. WO 96/01865, (1996).
- 119 . Van Aert, H.A.M., Fischer, H., Sijbesma, R.P., de Waal, B.F.M., Broer, D. and Meijer, E.W. *Acta Polym.*, manuscript in preparation.

## Chapter 2

### The precipitation polymerization of 2,6-dimethylphenol; control over molecular weight of PPE

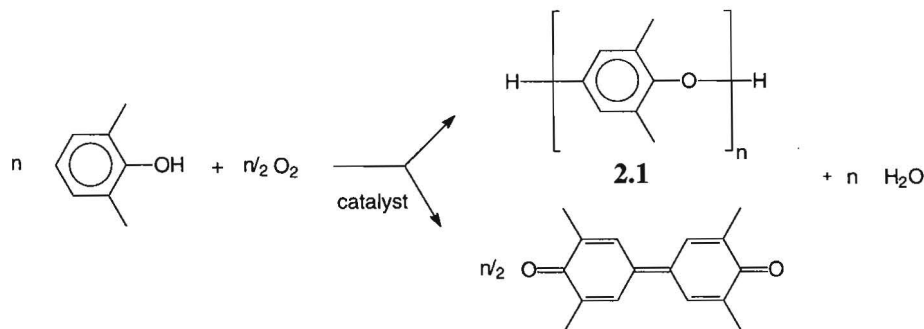
#### Summary

*Precipitation polymerization of 2,6-dimethylphenol gives well-defined monofunctional polymers in high yields using oxygen and copper/amine catalysts. The molecular weights are easily adjusted by using a particular solvent/non-solvent volume ratio; in this case a toluene/2-propanol mixture is employed. The addition of more toluene results in a precipitated polymer with a higher molecular weight. The molecular weights are independent of the ligand system of the catalyst used. Products are characterized with a combination of NMR and GPC techniques. Molecular weight characterization by FD-MS is applicable for very low molecular weight PPE. In contrast to the industrial polymerization, no or hardly any side reactions, like incorporation of secondary amines (e.g. di-n-butylamine) and tetramethyldiphenoquinone, are observed in the presented precipitation polymerization of 2,6-dimethylphenol.*

#### 2.1 Introduction

The oxidative polymerization of 2,6-dimethylphenol (DMP) (Scheme 2.1), as discovered by Hay<sup>1,2</sup> results in high molecular weight poly(2,6-dimethyl-1,4-phenylene ether) (PPE) (**2.1**). However, using this method several side reactions can occur as well. One side reaction is due to the copper-amine complexes, which are well-known catalysts in the oxidative coupling polymerization of DMP; secondary amines, which are used as a ligand for copper, are often incorporated into the polymer by means of a Mannich base type endgroup.<sup>3</sup> Another side reaction yields the coloured TMDPQ (3,5,3',5'-tetramethyl-4,4'-diphenoquinone) (Scheme 2.1), which can also be incorporated into the polymer by the quinone-coupling reaction between PPE and TMDPQ. This reaction leads to a bifunctional polymer with two OH-functionalities.<sup>4</sup> Both Mannich base- and TMDPQ-incorporation are regarded as side reactions in the PPE synthesis that lead to materials with undesired properties. The impurities that are often present in commercial PPE grades are shown in Chart 2.1.





**Scheme 2.1:** Oxidative coupling of 2,6-dimethylphenol.

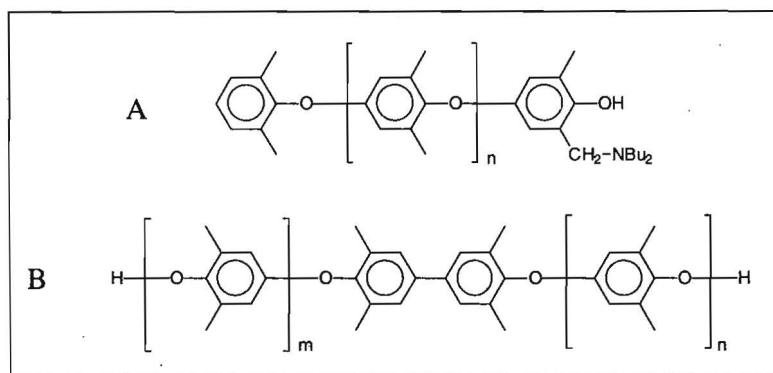


**Chart 2.1:** Impurities in PPE: A. Mannich base endgroups, B. TMDPQ incorporation.

Recently, low molecular weight PPE for use in block copolymers of well-defined architectures has attracted considerable interest.<sup>5-10</sup> Several methods are available for the preparation of low molecular weight PPE. The polymerization of 4-bromo-2,6-dimethylphenolate in the presence of an oxidizing agent is described by Price.<sup>11</sup> A more elegant approach is based on the phase-transfer catalysed polymerization of 4-bromo-2,6-dimethylphenol in the presence of either 2,4,6-trimethylphenol or 4-*tert*-butyl-2,6-dimethylphenol.<sup>12</sup> However, a number of side reactions are detected; 2,4,6-trimethylphenol can undergo an oxidative dealkylation, which leads to 4,4'-dihydroxy-3,3',5,5'-tetramethyldiphenylmethane units. In the phase-transfer catalysed depolymerization of PPE in the presence of either 2,4,6-trimethyl or 4-*tert*-butyl-2,6-dimethylphenol no side reactions occur,<sup>13</sup> but the polydispersity is large ( $D = 3-7$ ). Finally, low molecular weight polymers are prepared if the polymerization is stopped at low conversion.<sup>14</sup>

In this Chapter, precipitation polymerization is used in order to prepare low molecular weight polymers without impurities. These well-defined oligomers are employed in Chapter 5 for the

preparation of more reactive oligomers. An additional advantage of this technique is that the molecular weight distribution will be narrow due to the precipitation method. In the past a number of papers, mainly patents, concerning the polymerization of 2,6-dimethylphenol in a poor solvent or in a solvent/non-solvent mixture were published, however, no details on the polymers prepared are given.<sup>15-18</sup>

## 2.2 Results and discussion

The traditional Cu(I)Cl-amine catalytic system was employed in the precipitation polymerization of 2,6-dimethylphenol (DMP). The polarity of the reaction mixture was adjusted with a solvent mixture of toluene (solvent for PPE) and 2-propanol (non-solvent for PPE). The systems studied consisted of solvent compositions between 100% 2-propanol and 80% 2-propanol/20% toluene. Two different Cu(I)Cl-amine catalysts were used; Cu(I)Cl with a combination of *N,N'*-di-*t*-butylethylenediamine (DBEDA) and di-*n*-butylamine (DBA), being secondary amines, or Cu(I)Cl with *N,N,N',N'*-tetraethylethylenediamine (TEED), an example of a tertiary amine (Chart 2.2). A high amine/Cu(I)Cl ratio was used and DMP was added slowly, in order to prevent the formation of TMDPQ. The polymers that are precipitated from the reaction mixture were purified by reprecipitation from chloroform in methanol. Characterization of the polymers was performed with <sup>1</sup>H- and <sup>13</sup>C-NMR spectroscopy, GPC and field desorption mass spectrometry.

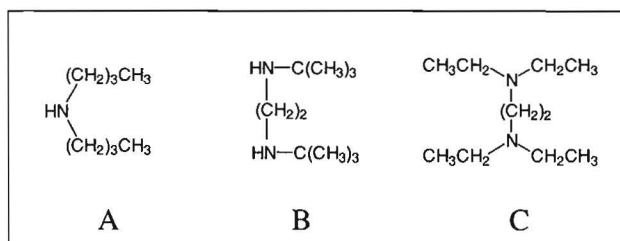


Chart 2.2: Employed amines; A. DBA, B. DBEDA, C. TEED.

The results of two series of polymerizations using the two different catalyst systems are presented in Table 2.1. For both ligand systems a similar molecular weight is obtained for a particular solvent/nonsolvent mixture as indicated in Figure 2.1. The polydispersity index D determined from the GPC measurements is smaller when a solvent is used with a higher polarity, which is caused by an earlier precipitation in more polar solvents. From Figure 2.1 it is concluded that the molecular weight can be regulated easily by adjustment of the solvent composition. The results obtained from <sup>1</sup>H-NMR spectroscopy and GPC are similar, so the Mark-Houwink equation remains useful even with the low molecular weight polymers. The results from NMR are probably slightly more accurate because here the determination of molecular weight is direct and no calibration is required. Molecular weights are determined directly from <sup>1</sup>H-NMR by comparing of the peaks of the

endgroups with those of the repeating unit.<sup>19</sup> The accuracy of the determination of the molecular weights and polydispersity index with GPC depends predominantly on the analysis of the chromatograms, determination of the base line and detection of the beginning and end of the peak, and the calibration curve determined with standard polystyrene specimens.

**Table 2.1:** Molecular weight as function of solvent composition

toluene / 2-propanol volume ratio	amine ligand system	$\bar{M}_n$ (kg/mol) <sup>1</sup> H-NMR	$\bar{M}_n$ (kg/mol) GPC	D GPC
0/100	DBA/DBEDA	2.75	2.80	1.66
	TEED	2.70	3.30	1.95
5/95	DBA/DBEDA	3.30	3.00	1.75
	TEED	3.40	3.40	2.05
10/90	DBA/DBEDA	4.50	4.50	1.71
	TEED	4.55	4.50	1.96
15/85	DBA/DBEDA	5.50	6.00	2.04
	TEED	5.75	5.10	2.09
20/80	DBA/DBEDA	7.50	6.90	2.22
	TEED	7.40	6.50	2.22

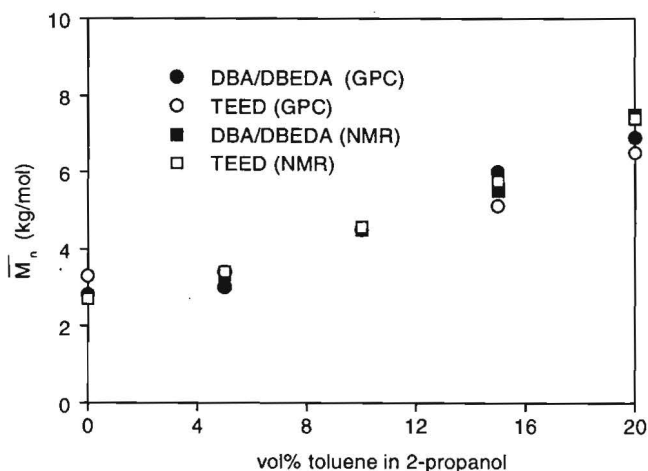


**Figure 2.1:** Molecular weight of precipitated PPE, as determined with <sup>1</sup>H-NMR (■ & □) and GPC (● & ○), for various catalysts.

Field desorption mass spectrometry (FD-MS), as developed in 1969 by Beckey,<sup>20</sup> has undergone a rapid development since then, and has proved to be a powerful tool in polymer

characterization.<sup>21-23</sup> We used FD-MS for detection of impurities, like Mannich base type endgroups and TMDPQ incorporation. The use of FD-MS is illustrated for a PPE with low molecular weight, because this technique is more powerful for low molecular weight oligomers. In Figure 2.2 the FD-MS spectrum is shown for a polymer with  $\overline{M}_n = 1.5$  kg/mol (according to <sup>1</sup>H-NMR). This polymer is prepared by precipitation polymerization in methanol. A lower molecular weight polymer with a more narrow molecular weight distribution ( $D = 1.46$  as determined from GPC) is obtained when methanol is used as solvent as compared with the polymerization in 2-propanol ( $D = 1.66$  as determined from GPC). All oligomeric species are separately detectable in the FD-MS spectrum and differ the mass of one repeating unit (120 amu). In the low molecular weight region smaller peaks due to doubly-charged ions are present as well. No peaks that can be assigned to side products are detected. From the FD-MS spectrum it can be calculated that  $\overline{M}_n = 1.62$  kg/mol,  $\overline{M}_w = 2.05$  kg/mol and  $D = 1.26$ . The polydispersity index estimated from FD-MS is lower than the one obtained with GPC possibly because high molecular weight PPE is more difficult to ionise. For polymers with  $\overline{M}_n > 1.50$  kg/mol the polydispersity index is even smaller than 1.26. Therefore, accurate molecular weight determination using FD-MS seems only applicable for very low molecular weight samples of PPE. Therefore, we used FD-MS in particular for detection of side products, like PPEs with incorporated secondary amines or TMDPQ. Also higher molecular weight PPE samples, prepared from precipitation polymerization in toluene/2-propanol mixtures, didn't show the presence of side products.

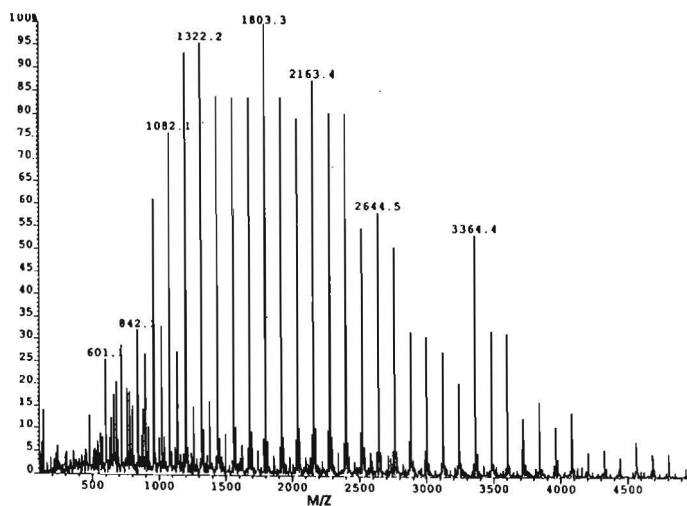
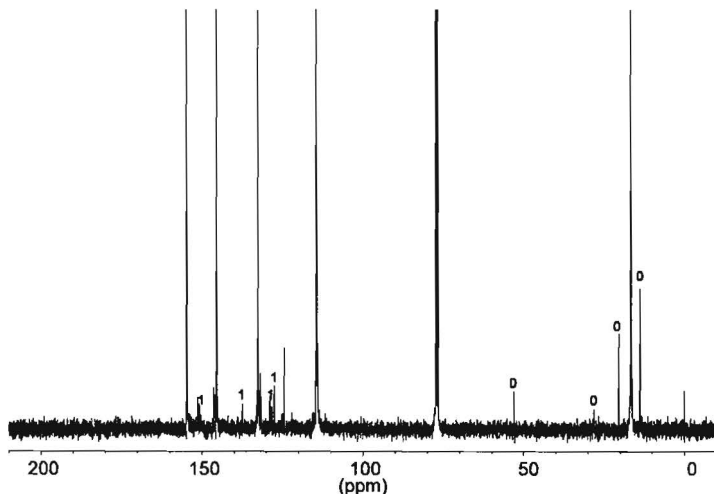


Figure 2.2: FD-MS spectrum of PPE;  $\overline{M}_n = 1.50$  kg/mol.

The mixture of DBEDA and DBA, frequently used by General Electric Plastics, is a well-known ligand system<sup>24</sup> and can lead to Mannich base type endgroups.<sup>3</sup> TEED is a tertiary amine and can therefore not lead to a Mannich base type endgroup. For example, when DBA is used, the phenolic

endgroup can contain a dibutylamine group attached to the *ortho*-methyl group. According to White, amine incorporation can be detected by  $^{13}\text{C}$ -NMR spectroscopy.<sup>3</sup> In order to investigate the occurrence of these side reactions in our precipitation polymerization, we have compared the  $^{13}\text{C}$ -NMR spectrum of a commercial polymer, PPE-1, with  $\overline{M}_n = 11.0$  kg/mol (Figure 2.3), with that of a polymer with  $\overline{M}_n = 2.75$  kg/mol prepared by precipitation polymerization (Figure 2.4). The commercial polymer is prepared with the DBA/DBEDA-ligand system. In the  $^{13}\text{C}$ -NMR spectrum some peaks of Mannich base type endgroups are detected ( $\delta = 53.1, 28.3, 20.5,$  and  $13.9$  ppm). The  $^{13}\text{C}$ -NMR spectrum shows also some DPQ incorporation ( $\delta = 154.3, 137.4, 127.7,$  and  $127.3$  ppm). The peaks from amine and DPQ incorporation are higher or equal in size in comparison with the peaks of the unmodified endgroups ( $\delta = 154.7, 151.4, 146.4, 131.4, 128.9, 124.9, 124.5,$  and  $114.1$  ppm) as assigned in the structural formula. Figure 2.4 shows the  $^{13}\text{C}$ -NMR spectrum of a polymer with  $\overline{M}_n = 2.75$  kg/mol, made with the DBA/DBEDA ligand system by precipitation polymerization. The  $^{13}\text{C}$ -NMR spectra of the polymers made with the DBEDA/DBA ligand system show no or hardly any peaks of amine or TMDPQ incorporation within the limit of detection. The signal-to-noise ratio is higher in comparison with the spectrum of the commercial polymer, PPE-1, because endgroup peaks are much higher due to the low molecular weight. In the polymer prepared with TEED also no additional peaks have been determined.



**Figure 2.3:**  $^{13}\text{C}$ -NMR spectrum of PPE-1 made with the DBA/DBEDA-ligand system;  $\overline{M}_n = 11.0$  kg/mol; the resonances marked with 0 and 1 are assigned to Mannich base type endgroups and TMDPQ incorporation, respectively.

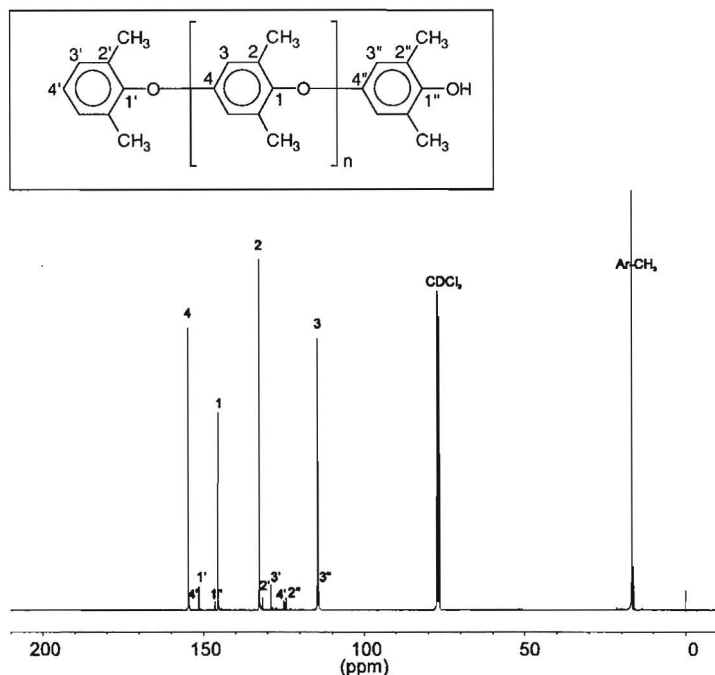


**Figure 2.4:**  $^{13}\text{C}$ -NMR spectrum of PPE made with the DBA/DBEDA-ligand system;  $\overline{M}_n = 2.75$  kg/mol.

## 2.3 Conclusions

Precipitation polymerization in the oxidative coupling polymerization of 2,6-dimethylphenol gives well-defined monofunctional polymers in high yields. Products can be well characterized with a combination of NMR and GPC techniques. The molecular weights which are obtained using these techniques are consistent. Molecular weight characterization by FD-MS is applicable for very low molecular weight PPE. No or hardly any side reactions, like incorporation of secondary amines and TMDPQ, are observed. The molecular weights can easily be adjusted by using a particular solvent composition, and are independent of the used ligand system.

## 2.4 Experimental

### Materials:

2,6-Dimethylphenol (DMP) was supplied by General Electric Plastics and recrystallized from *n*-hexane. *N,N'*-di-*t*-butylethylene diamine (DBEDA), di-*n*-butylamine (DBA) and the commercial PPE grade PPE-1 (IV = 0.4 dL/g) were used as obtained from General Electric Plastics. *N,N,N',N'*-tetraethylethylene diamine (TEED)

99+% pure was obtained from Janssen Chimica. Cu(I)Cl, chloroform, toluene, and 2-propanol were obtained p.a. from Merck. Methanol was used extra pure from Lamers & Pleuger.

### Techniques

The molecular weights were determined using 400 MHz  $^1\text{H-NMR}$  by comparing the aromatic C–H peaks of the endgroups (tail unit:  $\delta$  7.09, m, 3H, aromatic C–H and head unit:  $\delta$  6.47, s, 2H, aromatic C–H) with those of the repeating unit. A reproducible number average molecular weight could be calculated within an accuracy of 5%. The peak assignments were taken from Percec et al.<sup>19</sup>  $^1\text{H-NMR}$  and  $^{13}\text{C-NMR}$  spectra were recorded in  $\text{CDCl}_3$  on a Bruker AM-400 spectrometer at 400.13 and 100.62 MHz respectively. All  $^1\text{H-NMR}$  and  $^{13}\text{C-NMR}$  spectra were referenced to TMS ( $\delta = 0$  ppm) and  $\text{CDCl}_3$  (77 ppm), respectively. The molecular weights were determined also with Size Exclusion Chromatography (SEC) in chloroform at 25 °C using the universal calibration method with a set of standard polystyrene specimens. From SEC, using the Mark-Houwink equation with  $K_{\text{PPE}} = 48.3 \times 10^{-3}$  ml/g and  $a_{\text{PPE}} = 0.64$ ,<sup>25</sup> the  $\overline{M}_n$ ,  $\overline{M}_w$  and  $D = \overline{M}_w / \overline{M}_n$  were calculated. Field desorption mass spectrometry was performed at the Max-Planck-Institut für Polymerforschung in Mainz, Germany.

### Precipitation polymerization of DMP:

A 1 L jacketed flask was thermostated at 40 °C. A gas mixture of 80%  $\text{N}_2$  and 20%  $\text{O}_2$  was let through with a gas flow of 2 mL/s. 2 g (0.016 mol) DMP, 1.39 g (0.008 mol) DBEDA and 10.44 g (0.08 mol) DBA were dissolved in 416 mL solvent/nonsolvent mixture (vide infra). When the reaction mixture was heated to 35 °C, the reaction was started by the addition of 0.4 g (0.004 mol) CuCl to the reaction mixture. Then 48 g (0.39 mol) DMP in 250 mL solvent/non-solvent mixture was added slowly in 1 hour. After a reaction time of 5 hours the precipitated polymer was filtered, washed with methanol, and dried in vacuum at 60 °C. The polymer was reprecipitated twice from 250 ml chloroform in 3 L methanol.

Other polymers were prepared in a similar way. Solvent/non-solvent mixtures of 2-propanol with 0–20% v/v toluene were used in order to prepare different molecular weights. The addition of more toluene results in a higher molecular weight. Also, the tertiary amine TEED is used as ligand in polymerizations with the same solvent compositions. Here 8.7 g (0.051 mol) TEED is used instead of the DBEDA/DBA-ligand system as described above. All polymer yields are between 85 and 95%. Molecular weights were determined by SEC and  $^1\text{H-NMR}$ . Solvent = 2-propanol / ligand system = DBA/DBEDA:  $\overline{M}_n = 2.75$  kg/mol (NMR),  $\overline{M}_n = 2.80$  kg/mol (SEC),  $D = 1.66$ . Solvent: 2-propanol / ligand TEED:  $\overline{M}_n = 2.70$  kg/mol (NMR),  $\overline{M}_n = 3.30$  kg/mol (SEC),  $D = 1.95$ . Solvent = 95 % (v/v) 2-propanol, 5 % (v/v) toluene / ligand system = DBA/DBEDA:  $\overline{M}_n = 3.30$  kg/mol (NMR),  $\overline{M}_n = 3.00$  kg/mol (SEC),  $D = 1.75$ . Solvent = 95 % (v/v) 2-propanol, 5 % (v/v) toluene / ligand TEED:  $\overline{M}_n = 3.40$  kg/mol (NMR),  $\overline{M}_n = 3.40$  kg/mol (SEC),  $D = 2.05$ . Solvent = 90 % (v/v) 2-propanol, 10 % (v/v) toluene / ligand system = DBA/DBEDA:  $\overline{M}_n = 4.50$  kg/mol (NMR),  $\overline{M}_n = 4.50$  kg/mol (SEC),  $D = 1.71$ . Solvent = 90 % (v/v) 2-propanol, 10 % (v/v) toluene / ligand TEED:  $\overline{M}_n = 4.55$  kg/mol (NMR),  $\overline{M}_n = 4.50$  kg/mol (SEC),  $D = 1.96$ . Solvent = 85 % (v/v) 2-propanol, 15 % (v/v) toluene / ligand system = DBA/DBEDA:  $\overline{M}_n = 5.50$  kg/mol (NMR),  $\overline{M}_n = 6.00$  kg/mol (SEC),  $D = 2.04$ . Solvent = 85 % (v/v) 2-propanol, 15 % (v/v) toluene / ligand TEED:  $\overline{M}_n = 5.75$  kg/mol (NMR),  $\overline{M}_n = 5.10$  kg/mol (SEC),  $D = 2.09$ . Solvent = 80 % (v/v) 2-propanol, 20 % (v/v) toluene / ligand system = DBA/DBEDA:  $\overline{M}_n = 7.50$  kg/mol (NMR),  $\overline{M}_n = 6.90$  kg/mol (SEC),  $D = 2.22$ . Solvent = 80 % (v/v) 2-

propanol, 20 % (v/v) toluene / ligand TEED:  $\overline{M}_n = 7.40$  kg/mol (NMR),  $\overline{M}_n = 6.50$  kg/mol (SEC), D = 2.22.

## 2.5 References

1. Hay, A.S., Blanchard, H.S., Endres, G.F. and Eutace J.W. *J. Am. Chem. Soc.*, **81**, 6335 (1959).
2. Hay, A.S. *J. Polym. Sci.*, **58**, 581 (1962).
3. White, D.M. and Nye, S.A. *Macromolecules*, **23**, 1318 (1990).
4. White, D.M. *J. Polym. Sci., Polym. Chem. Ed.*, **19**, 1367 (1981).
5. Percec, V. and Wang, J.H. *Makromol. Chem., Macromol. Symp.*, **54/55**, 561 (1992).
6. Viersen, F.J., Colantuoni P. and Marmalis, I. *Angew. Makromol. Chem.*, **206**, 111 (1993).
7. Percec, V. and Nava, H. *Makromol. Chem., Rapid Commun.*, **5**, 319 (1984).
8. Chao, H.S.I., Hovatter, T.W., Johnson, B.C. and Rice, S.T. *J. Polym. Sci., Polym. Chem. Ed.*, **27**, 3371 (1989).
9. Heyde, G. and Heitz, W. *Makromol. Chem.*, **194**, 2741 (1993).
10. Stehlicek, J. and Puffr, R. *Collect. Czech. Chem. Commun.*, **58**, 2574 (1993).
11. Staffin, G.D. and Price C.C. *J. Am. Chem. Soc.*, **82**, 3632 (1960).
12. Percec, V. and Wang, J.M. *J. Polym. Sci., Polym. Chem. Ed.*, **29**, 63 (1991).
13. Percec, V. and Wang, J.M. *Polym. Bull.*, **24**, 71 (1990).
14. Reuben, J. and Biswas, A. *Macromolecules*, **24**, 648 (1991).
15. Tacke, P. and Freitag, D. Ger. Offen. DE 3529093 A1, (1987).
16. Bataskova, P., Spousta, E., Rehakova, M., Fil, J., and Elefantova, D. Czech. Pat. Appl. CS 227586 B, (1986).
17. Kawaki, T., Nishizawa, C., Nizutani, M. and Sakakib, Y. Eur. Pat. Appl. EP 153074 A2, (1985).
18. Cao, W. *Huaxue Shijie*, **25**, 326 (1984).
19. Nava, H. and Percec, V. *J. Polym. Sci., Polym. Chem. Ed.*, **24**, 965 (1986).
20. Becky, H.D. *Angew. Chem.*, **81**, 662 (1969).
21. Saito, J., Waki, H., Teramae N. and Tanaka, S. *Progress in Organic Coatings*, **15**, 311 (1988).
22. Tottszer, A.I., Neumann, G.M., Derrick, P.J. and Willett, G.D. *J. Phys. D: Appl. Phys.*, **21**, 1713 (1988).
23. Blease, T.G., Paterson, G.A. and Scrivens, J.M. *Brit. Pol. J.*, **21**, 37 (1989).
24. Mobly, D.P. *J. Polym. Sci., Polym. Chem. Ed.*, **22**, 3202 (1984).
25. Kurata, M. Tsunashima, Y. "Polymer Handbook", Eds. Brandrup, J. Immergut, E.H., Wiley-Interscience, New York, VII/21 (1989).





## Chapter 3

### Modified poly(2,6-dimethyl-1,4-phenylene ether)s prepared by redistribution

#### Summary

*Redistribution of poly(2,6-dimethyl-1,4-phenylene ether) (PPE) with a phenolic compound yields a depolymerized polymer having the phenolic compound incorporated as tail end. The molecular weight of the product is adjusted with the ratio phenol over PPE repeating units. PPE oligomers and telechelics with a large variety of endgroups, including reactive endgroups, can be prepared in this way. Furthermore, block copolymers can be prepared by reacting a phenol terminated polymer in a redistribution with PPE. This is illustrated by the reaction of phenol terminated polystyrene with PPE, leading to polystyrene-PPE diblock copolymers. TMDPQ or copper/amine catalysts can be used as catalyst depending on the reacting phenolic compound, desired reaction time and product purity. For a fast PPE redistribution with ortho-unsubstituted phenols, without any oxidation of methyl substituents of PPE chain, the use of TMDPQ is preferred. For the preparation of pure oligomers and block copolymers, a slow redistribution using copper catalysts in the absence of oxygen is preferred.*

#### 3.1 Introduction

The conventional synthesis of poly(2,6-dimethyl-1,4-phenylene ether) (PPE) is based on the oxidative coupling mechanism of 2,6-dimethylphenol (DMP) as discovered by Hay.<sup>1-5</sup> It is well known that during the oxidative coupling polymerization of DMP, redistribution reactions simultaneously occur. The most widely accepted mechanism<sup>6-11</sup> for these reactions is based on phenoxy radicals, as outlined in Figures 3.1 and 3.2. Chain elongation is the result of coupling of these radicals via the formation of a quinol ether on the free *para*-position of a tail-end or monomer phenol ring, whereas redistribution involves a coupling to a quinone ketal on the *para*-position of a headgroup phenol ring. This ketal unit can either dissociate or undergo an intramolecular rearrangement,<sup>9,12-14</sup> in which the cyclohexadienone acetal group moves to an adjacent unit on the polymer chain. The oligomers with 2,6-dimethylphenol tail ends can be linked with the oligomers with substituted tail ends via this intramolecular rearrangement, in which quinol ether intermediates are present like in the oxidative coupling mechanism. Usually, the oxidative coupling is catalyzed with a CuCl/amine complex in the presence of oxygen. The

amines, such as pyridine, *N,N'*-di-*t*-butylethylenediamine (DBEDA), 4-*N,N'*-(dimethylamino)pyridine (DMAP) and *N,N,N',N'*-tetramethylethylenediamine (TMEDA), serve both as ligand for the copper ions and as bases to form phenolate anions, which are more easily oxidized. Besides the desired C–O coupling, C–C coupling of dimethylphenol can occur to form 3,3',5,5'-tetramethylbicyclohexylidene-2,2',5,5'-tetraene-4,4'-dion (3,3',5,5'-tetramethyl-4,4'-diphenoquinone, TMDPQ) which itself can serve as oxidant, leading to 3,3',5,5'-tetramethyl-biphenyl-4,4'-diol (3,3',5,5'-tetramethyl-4,4'-bisphenol). This bisphenol is subsequently incorporated into the polymer, yielding telechelics.<sup>15</sup>

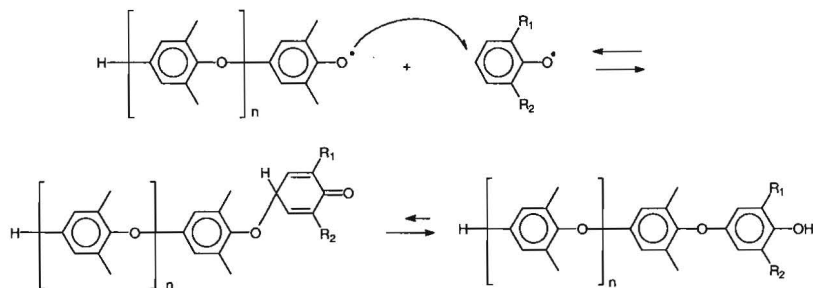


**Figure 3.1:** Oxidative coupling via quinol ether intermediates.

Tail-end functionalized PPE can in principle be obtained by copolymerization.<sup>16–27</sup> When using (besides the DMP) a *para*-functionalized phenol, which can only partake in the redistribution reactions, this phenol will always end up as tail-end of PPE.<sup>28,29</sup> However, rapid oxidative coupling will usually lead to large amounts of non-functionalized PPE as well. Furthermore, if one wants to use the commercially easily available *ortho*-unsubstituted phenols, extensive crosslinking<sup>9,30</sup> and methyl group oxidation<sup>31,32</sup> will occur.

In this Chapter, we report a method to perform redistribution reactions without oxidative coupling.<sup>33</sup> This involves the use of copper catalysts either in the absence of oxygen, viz. CuCl/DMAP (ratio 1:1,6) under an inert argon atmosphere, or with ligands of low basicity, viz. Cu(NO<sub>3</sub>)<sub>2</sub>·3H<sub>2</sub>O/*N*-methylimidazole (NMI) (ratio 1:20) in air. These mild catalysts allow the tail-end introduction of various phenols, both *ortho*-substituted and *ortho*-unsubstituted, without oxidative side reactions. Since the added phenol was usually in excess with respect to the polymer, the redistribution results in a depolymerization. In contrast to the copolymerization technique, redistribution leads to PPE that is over 95% functionalized.

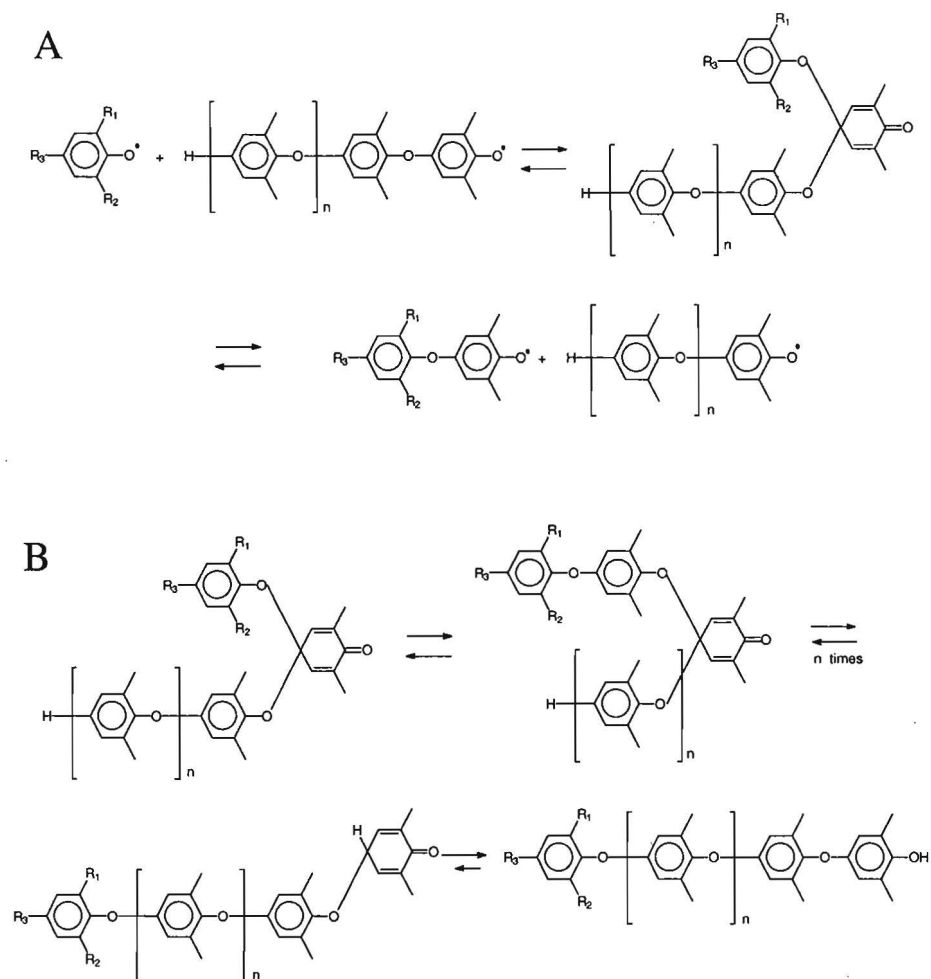


**Figure 3.2:** Redistribution (A) and intramolecular rearrangement (B) via ketal intermediates.

Furthermore, in this Chapter we explore the scope and limitations of the clean redistribution reactions for the tail-end functionalization of PPE. A large range of mono- and difunctional phenols will be incorporated, and the formation of block copolymers between polystyrene and PPE will be demonstrated. Also, we will introduce TMDPQ as a much faster catalyst for the redistribution reactions. Although TMDPQ gives some side products, for practical applications its speed far outweighs these problems.

## 3.2 Results and discussion

When PPE and a phenol are mixed together, the PPE is decreased in molecular weight in proportion to the degree of reaction with the phenol. Upon addition of 2,6-dimethylphenol (DMP) or the PPE-dimer 4-(2,6-dimethylphenoxy)-2,6-dimethylphenol to a high molecular weight PPE, the latter is depolymerized yielding low molecular weight oligomers. The progress of the polymer molecular weight decrease during the redistribution reaction using the PPE-dimer is illustrated in the SEC analyses, presented in Figure 3.3. We used for this reaction a  $\text{Cu}(\text{NO}_3)_2 \cdot 3\text{H}_2\text{O}/\text{NMI}$  catalyst, which hardly gives any polymerization due to the weakly basic ligands and the absence of additional base. A typical reaction time using this catalyst is 1–3 weeks using chloroform as solvent. In the PPE redistribution with DMP or PPE-dimer the reaction product has the same structure as the starting polymer. Due to the addition of the phenol the polymer has a bimodal molecular weight distribution but this becomes more monomodal during the equilibration reaction.

If the redistribution reaction is performed with a functional phenol, the reaction product has a different structure than the starting PPE. Whereas the starting polymer has a 2,6-dimethylphenoxy tail end, in the reaction product the functional phenol is incorporated as tail end, for example 4-*tert*-butyl-2,6-dimethylphenol (TBDMP). Due to the low oxidation potential of TBDMP, redistribution could be performed without the addition of any catalyst under air. When the reactions are performed under argon similar reaction rates are obtained. The ease of formation of phenoxy radicals in PPE is shown by a preliminary Electron Spin Resonance (ESR) experiment. PPE dissolved in  $\text{CDCl}_3$  already shows the existence of 2,6-dimethylphenoxy endgroup radicals without the addition of an oxidant. In the ESR spectrum a septet signal with a hyperfine coupling of 5.6 Gauss is observed, similar to 2,6-dimethylphenoxy radicals described in literature.<sup>34,35</sup> Even though residual copper from the oxidative coupling might still be present in the PPE, no signals from copper are detected in the ESR spectrum. It is known that  $\text{CHCl}_3$  and  $\text{CDCl}_3$  can initiate radical chain reactions. This is an additional reason, beside its low oxidation potential, why for TBDMP redistribution no catalyst is needed.

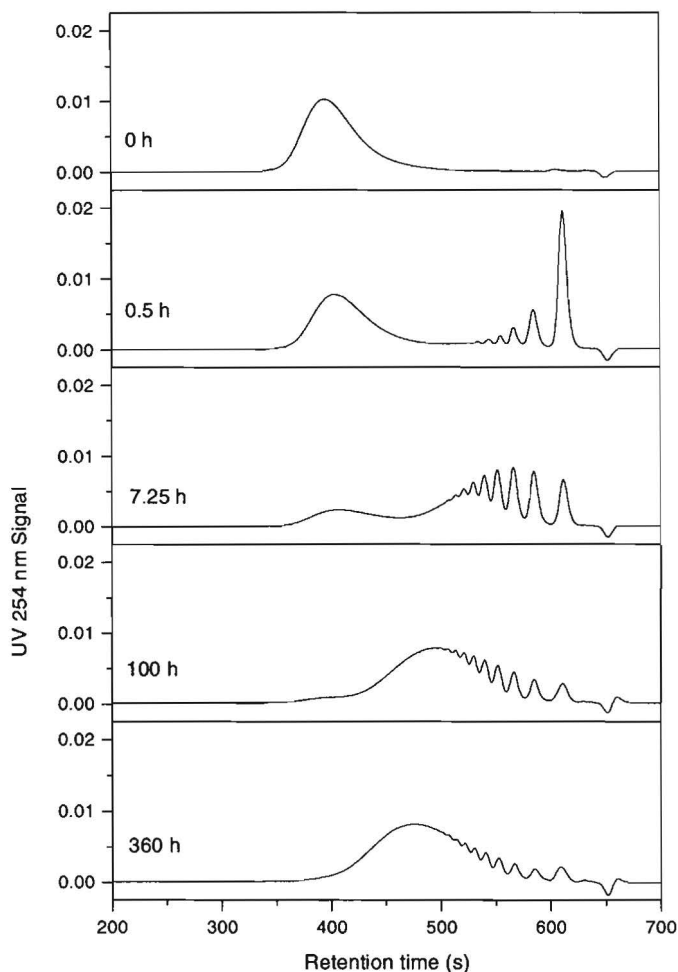


**Figure 3.3:** SEC analyses of redistribution PPE with PPE-dimer, monitored in time.

During the redistribution with TBDMP, monofunctional PPE with a 2,6-dimethylphenoxy tail end is converted to a PPE with a *tert*-butyl substituent at its tail end. When the redistribution reaction is complete, all polymer chains contain a *tert*-butyl group at their tail end and almost no polymer chains are present with a 2,6-dimethylphenoxy tail end. This can be clearly seen from an HPLC analysis of the redistribution product, in which unfunctionalized PPE oligomers (total < 5%) are detected as small peaks in between the large peaks from the oligomers with a *tert*-butyl tail end (Figure 3.4). The small peaks were identified as oligomers with a 2,6-dimethylphenoxy tail end or as telechelic PPE containing a tetramethylbiphenol unit by the

comparison with some model compounds, such as low molecular weight PPE oligomers. UV detection at 200 nm and 270 nm was used to differentiate between oligomers with a 2,6-dimethylphenoxy tail end (visible at 200 nm) and oligomers with incorporated tetramethylbiphenol (visible at 200 and 270 nm). Peaks A, B, and C, indicated in Figure 3.4, are typical peaks for oligomers with *tert*-butyl endgroups, incorporated biphenyl units and 2,6-dimethylphenyl endgroups, respectively. Additional evidence for a complete redistribution was obtained from the  $^1\text{H-NMR}$  spectrum (Figure 3.5) of the precipitated product, in which only the endgroups of the modified PPE are present and no multiplet signal of the aromatic protons of the 2,6-dimethylphenoxy tail units of the starting PPE could be detected at a chemical shift of 7.09 ppm.

The observed complete redistribution, which leads to product consisting of predominantly tail-end modified PPEs and hardly any unmodified PPEs with a 2,6-dimethylphenoxy tail end, can be explained by the intermolecular rearrangement, that occurs next to the redistribution reaction (Figure 3.2). In the intermolecular rearrangement mechanism quinol ether intermediates are present, like in the oxidative coupling mechanism.

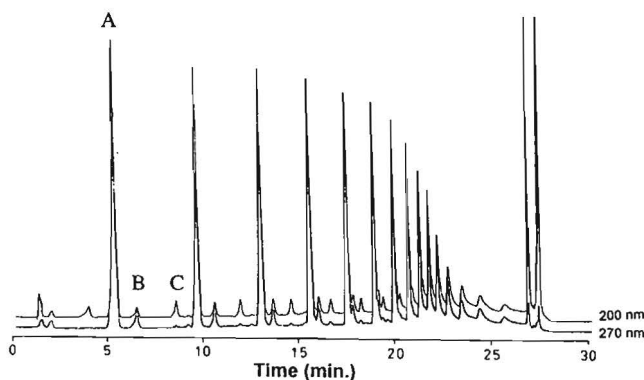


**Figure 3.4:** HPLC analysis of PPE redistribution with 4-*tert*-butyl-2,6-dimethylphenol, obtained by evaporation of the solvent after 336 hours reaction time, UV detection at 200 and 270 nm; Peaks A, B, and C are typical peaks for oligomers with *tert*-butyl endgroups, incorporated biphenyl units and 2,6-dimethylphenyl endgroups, respectively.

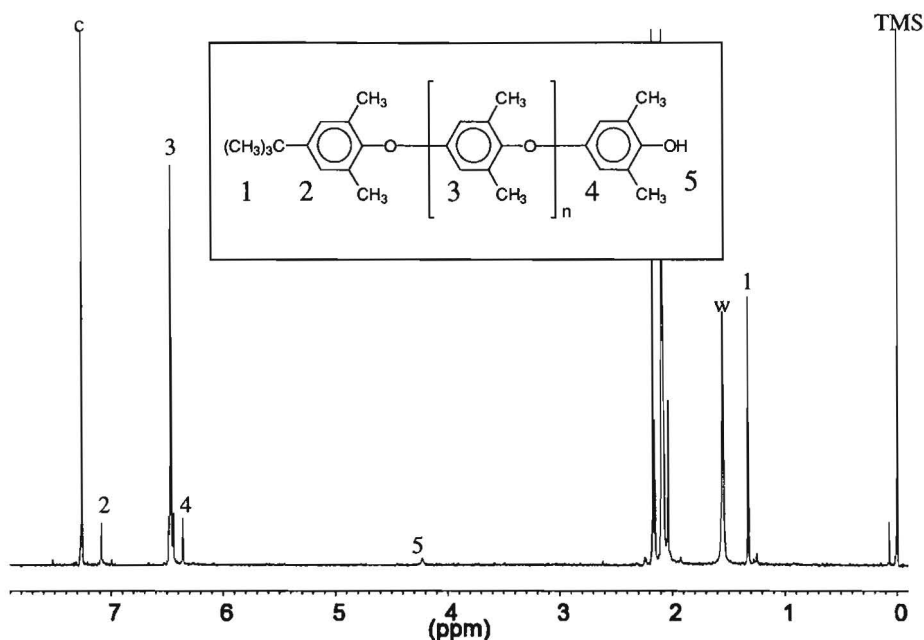


**Figure 3.5:**  $^1\text{H-NMR}$  spectrum ( $\text{CDCl}_3$ , 400 MHz) of the precipitated product from a PPE redistribution with 4-*tert*-butyl-2,6-dimethylphenol after 336 hours reaction time; the signals marked with *w* and *c* are assigned to residual  $\text{H}_2\text{O}$  and  $\text{CHCl}_3$ , respectively.

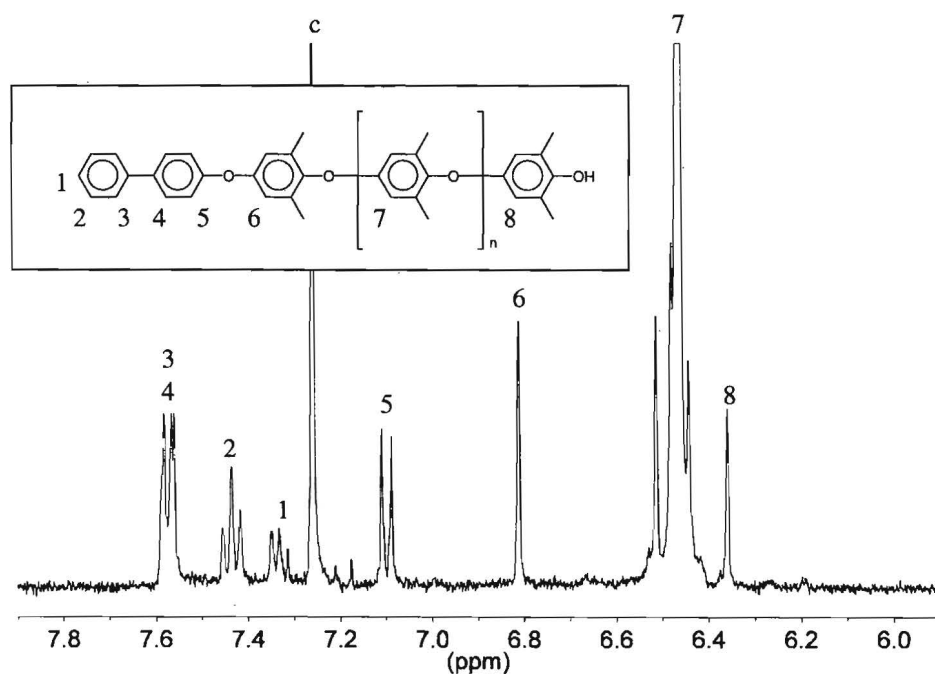
Attempted reactions of 4-*tert*-butyl-2,6-dimethylphenol with methoxy-terminated PPE didn't result in a redistribution, which is consistent with the necessity of a phenolic endgroup in the quinone-ketal redistribution mechanism. Other experiments reported in literature also show the requirement of phenolic endgroups on both of the reacting species.<sup>36-38</sup> Recently Baesjou<sup>39</sup> and coworkers found that 4-(2',6'-dimethylphenoxy)-2,6-dimethyl anisole didn't react in a redistribution in contrast to the PPE-dimer with a free phenolic endgroup.

### 3.2.1 Redistribution using $\text{CuCl}/\text{DMAP}$ catalysts

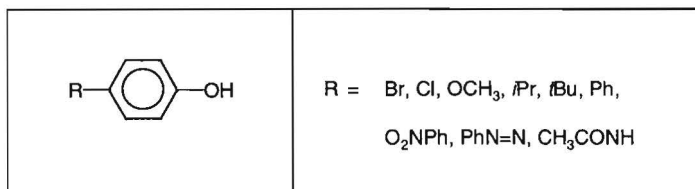
When a  $\text{CuCl}/\text{DMAP}$  catalyst is employed in the PPE redistribution, oxidation of the methyl substituents can occur in the presence of oxygen. This oxidation, leading to ill-defined structures, can be suppressed by performing the reaction in the absence of oxygen, although redistribution rates are low. Under these mild conditions, also *ortho*-unsubstituted phenols can be incorporated as a tail end in PPE, without any crosslinking via the *ortho*-positions. This is in contrast to the oxidative coupling of phenol with only one *ortho*-substituent and an open *para* position, which usually yield highly branched and coloured polymers.



A variety of endgroups can be introduced by reacting different types of phenols in a PPE redistribution. Examples of *ortho*-unsubstituted phenols with a functional group at the *para*-position, which can be incorporated successfully as tail end using the CuCl/DMAP catalysts, are listed in Chart 3.1. The functional groups at the *para*-position are stable under the reaction conditions employed. As an example a  $^1\text{H-NMR}$  spectrum of a reaction product from a PPE redistribution with 4-phenylphenol, using a CuCl/DMAP catalyst is shown in Figure 3.6. This spectrum shows no evidence for crosslinking via the *ortho*-positions. The proton at the *ortho*-position (indicated as proton 5) is shown by a doublet signal in the expected integral ratio in comparison with other protons from the endgroup (protons – [integral ratio]: 5/(3+4) – [1/2]; 5/2 – [1/1]; 5/1 – [2/1]; 5/6 – [1/1])

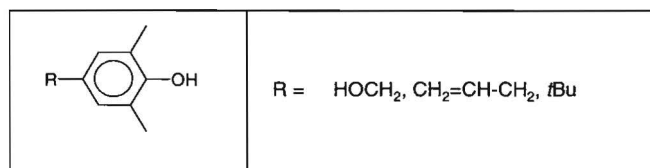


**Figure 3.6.**  $^1\text{H-NMR}$  spectrum (aromatic region) of the reprecipitated reaction product from PPE redistribution with 4-phenylphenol; the signal marked with *c* is assigned to residual  $\text{CHCl}_3$ .

**Chart 3.1**

Usually, phenols with electron-donating substituents react more rapidly in a redistribution due to their lower oxidation potential. A phenol with an electron-withdrawing substituent, like 4-nitrophenol, barely shows any reactivity. If we introduce a phenyl group as spacer, like in 4-nitrophenylphenol, or if a phenol like 3-nitrophenol with the nitro-substituent in the *meta*-position is used, then a higher reactivity is found.

*Ortho*-methyl substituted phenols are intrinsically more reactive due to the electron-donating methyl groups. The ones we employed in a PPE redistribution using the CuCl/DMAP catalyst are listed in Chart 3.2. Typical reaction times employed for the *ortho*-methyl substituted phenols are 1–2 weeks, whereas *ortho*-unsubstituted phenols are reacted usually for 3–4 weeks. TBDMP redistribution without the use of catalyst was already discussed before. Slightly improved reaction rates were found in a reaction under argon in the presence of a CuCl/DMAP catalyst. The TBDMP conversion is also higher when a catalyst is employed. At a reaction time of 300 h the TBDMP-conversion without catalyst is 70%, while with the CuCl/DMAP catalyst the TBDMP-conversion is 90%. The allyl-terminated PPE, prepared by redistribution with 4-allyl-2,6-dimethylphenol, is a precursor for various other functionalities. We converted the allyl-terminated PPE to a hydroxypropyl-terminated PPE by a hydroboration/oxidation reaction using bicyclo[3.3.1]nonan-9-one (9-BBN) using a procedure described for allyl-terminated poly(methylmethacrylate).<sup>40</sup>

**Chart 3.2**

We tried to introduce a hydroxyalkyl substituent by redistribution with 4-hydroxymethyl-2,6-dimethylphenol, but reaction of this phenol predominantly yields a telechelic polymer with two PPE arms on a tetramethylbisphenol formaldehyde core. Most probably this is due to the condensation reaction of two hydroxymethyl endgroups. This is consistent with copolymerization experiments of 4-hydroxymethyl-2,6-dimethylphenol with 4-bromo-2,6-

dimethylphenol as described by Percec.<sup>41</sup> A more rational design for telechelic PPE would be the use of bisphenols during redistribution. E.g. the telechelic product obtained above can also be obtained from a redistribution with bis(3,5-dimethyl-4-hydroxyphenyl)-methane (tetramethylbisphenol formaldehyde, BPF) (Chart 3.3,  $R_1 = \text{CH}_3$ ,  $R_2 = \text{H}$ ). This was tested with the CuCl/DMAP catalyst for other bisphenols as listed in Chart 3.3. The *ortho*-methyl substituted bisphenols give higher reaction rates, analogous to the *ortho*-methyl substituted phenols, and yielded the desired telechelics.

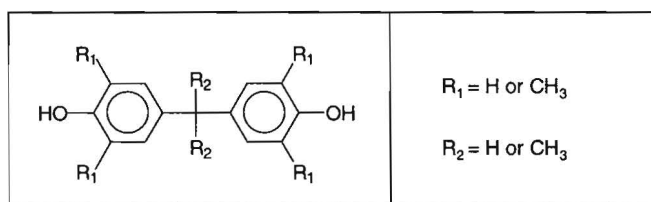


**Chart 3.3**

When using *ortho*-unsubstituted bisphenols in the PPE-redistribution, reaction occurs surprisingly only at one side of the bisphenol yielding a different type of telechelic, presumably due to a higher oxidation potential. This phenomenon will be illustrated in more detail later.

Redistribution experiments can also be used for the preparation of block copolymers. To obtain pure block copolymers, redistribution reactions should be performed using copper catalysts with low basic ligands or in the absence of oxygen. Therefore, we used CuCl/DMAP catalysts in the absence of oxygen for the block copolymer synthesis. In this investigation, we employed 4-hydroxyphenyl-terminated polystyrene, prepared by anionic polymerization, as reacting model compound in the PPE redistribution (Figure 3.7).<sup>42</sup> The PS-PPE diblock copolymers, which are prepared in this way, are characterized by Size Exclusion Chromatography (SEC) with THF as eluent. The chromatograms are shown in Figure 3.8. SEC analyses of the starting polystyrene material implementing either a UV (254 nm) or RI detector overlap completely. Determined molecular weights are uncorrected and relative to a set of polystyrene standards. In case of the SEC analyses of the PS-PPE copolymers, the UV detector detects a higher apparent molecular weight than the RI detector. This is caused by the higher UV absorbance of PPE in comparison with PS. Block copolymers with a higher molecular weight contain a higher fraction of PPE, and are more easily detected by UV than by RI detection. Furthermore, the determined SEC peaks are monomodal and symmetrical, which suggests that block copolymer formation has occurred. The determined molecular weights are summarized in Table 3.1. The employed phenol-terminated polystyrene is used as a model compound in the block copolymer synthesis via redistribution. The used polystyrene can be

replaced by any phenol-terminated polymer, yielding numerous types of block copolymers, which will be e.g. in Chapter 7 of this thesis.

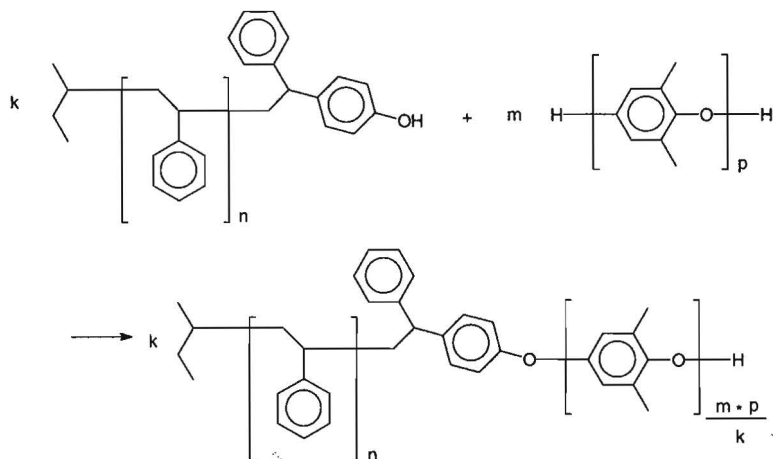


Figure 3.7: PPE redistribution with phenol-terminated PS

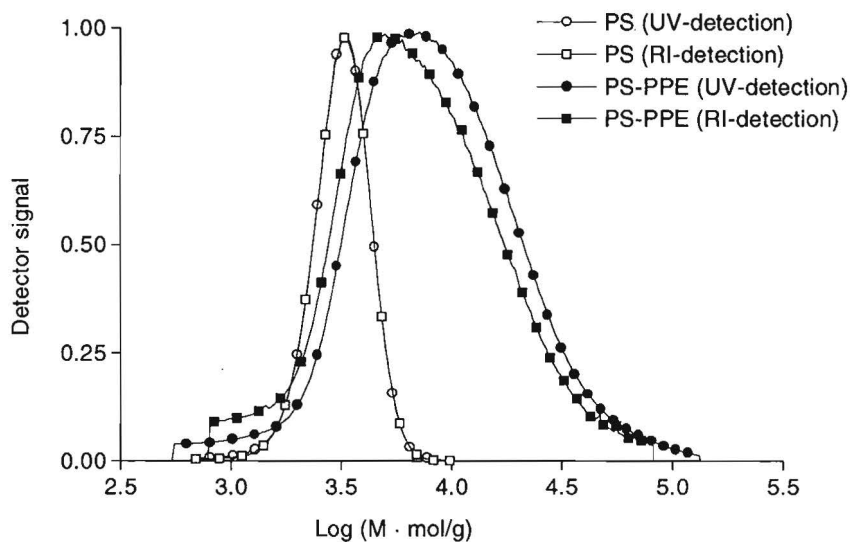


Figure 3.8: SEC chromatograms of phenol-terminated PS and prepared PS-PPE diblock copolymers, detector signal as a function of the logarithm of the apparent molecular weight.

**Table 3.1:** Uncorrected molecular weights as determined by SEC.

Polymer type/ detector	$\bar{M}_n$ (kg/mol)	$\bar{M}_w$ (kg/mol)	D
PS			
UV detector	2.97	3.28	1.11
RI detector	3.00	3.29	1.10
PS-PPE			
UV-detector	5.99	12.40	2.07
RI-detector	4.66	10.80	2.32

### 3.2.2 Redistribution using $\text{Cu}(\text{NO}_3)_2 \cdot 3\text{H}_2\text{O}$ /N-methylimidazole (NMI) catalysts

Where as reactions catalyzed by a  $\text{CuCl}/\text{DMAP}$  catalyst preferentially are performed in the absence of air, reactions using the  $\text{Cu}(\text{NO}_3)_2 \cdot 3\text{H}_2\text{O}/\text{NMI}$  catalyst can be performed under air, which allows for a more convenient experimental setup. This catalyst is tested for redistributions with DMP and the PPE dimer as already presented before. Slightly higher redistribution rates are obtained when TBDMP is reacted in the presence of the  $\text{Cu}(\text{NO}_3)_2 \cdot 3\text{H}_2\text{O}/\text{NMI}$  catalyst in comparison with an experiment in the absence of a catalyst. No large difference in reaction rates using the  $\text{Cu}(\text{NO}_3)_2 \cdot 3\text{H}_2\text{O}/\text{NMI}$  catalyst or the  $\text{CuCl}/\text{DMAP}$  catalyst under argon is observed for redistribution with TBDMP. The bisphenol 4,4'-bis(4-hydroxy-3,5-dimethylphenyl)pentanoic acid (Chart 3.5;  $\text{R}_1 = \text{CH}_3$  and  $\text{R}_2 = \text{H}$ ) could also be incorporated successfully when reacted in chloroform and shows that redistribution is feasible in the presence of carboxylic acid functional groups without any side reactions. An advantage of the  $\text{Cu}(\text{NO}_3)_2 \cdot 3\text{H}_2\text{O}/\text{NMI}$  catalyst in comparison to the  $\text{CuCl}/\text{DMAP}$  catalyst is that hardly any oxidation of the methyl substituents of the PPE occurs. Even when reactions are put under argon atmosphere still some minor oxidation can occur when the  $\text{CuCl}/\text{DMAP}$  catalyst is using during long reaction times.

To prevent the formation of TMDPQ via C–C coupling of formed 2,6-dimethylphenol during redistribution, we used a high ligand-copper ratio ( $L/\text{Cu} = 20$ ). Lower  $L/\text{Cu}$  ratios can cause the formation of TMDPQ, which can be incorporated into PPE as well. This is in good agreement with the results previously reported in polymerization reactions.<sup>43–46</sup> If the  $\text{CuCl}/\text{DMAP}$  catalyst is used a lower  $L/\text{Cu}$  ratio of 1.6 could be used, however still some minor TMDPQ formation can occur.

### 3.2.3 Use of TMDPQ as oxidant

Redistributions using copper catalysts did show clean redistributions, however, reaction rates are rather slow. To overcome this drawback TMDPQ is used as an oxidant. Reaction of TMDPQ with the phenolic endgroup of PPE will initially generate a phenoxy radical endgroup and the dipheno-semiquinone. The semiquinone can couple with a polymer radical to form a quinone ketal (Figure 3.9) or abstract a hydrogen from a phenol to form 3,3',5,5'-tetramethylbiphenyl-4,4'-diol. Under the action of TMDPQ hydrogen abstraction can presumably also occur from added functional phenols and resulting phenoxy radicals can react in the redistribution reactions. TMDPQ can also lead to oxidative coupling, but only when a base is present, this will be illustrated later by an example.

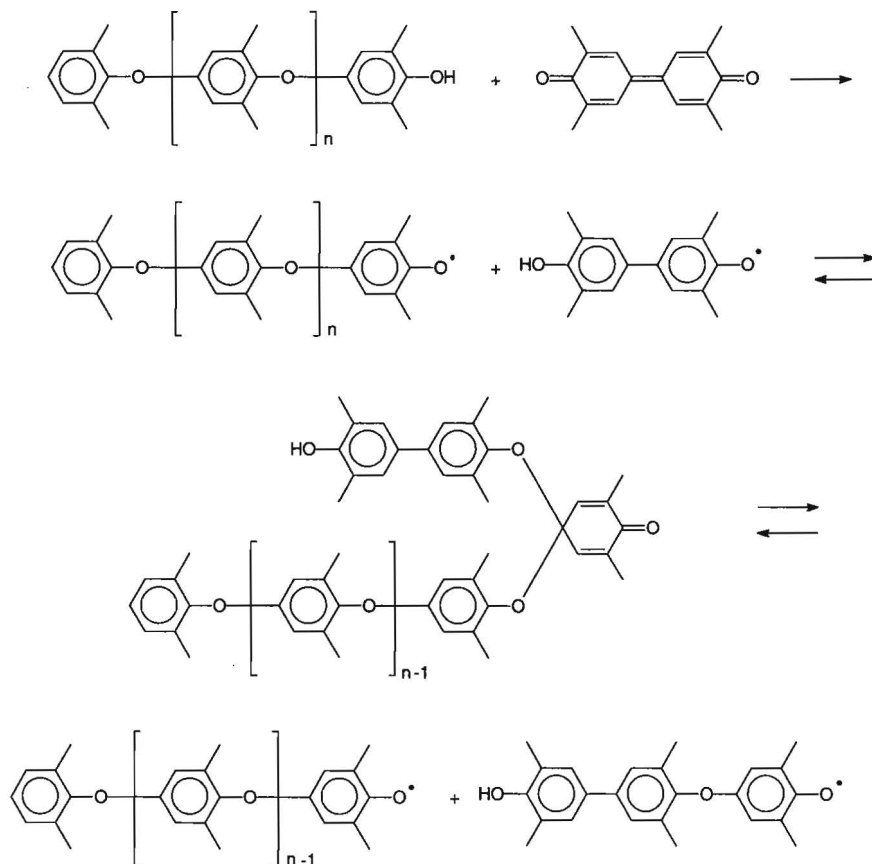


Figure 3.9: Reaction of TMDPQ with PPE.

Redistributions using TMDPQ are much faster, even in the absence of oxygen (reaction time 3–5 hours), but yield less pure products because TMDPQ is also incorporated in the polymer. However, the speed far outweighs this disadvantage, especially for large scale applications.<sup>47</sup> Also the PPE that is used for the redistribution is of different quality in these applications. While in the redistribution experiments with copper catalysts, as described before, well-defined PPEs prepared by precipitation polymerization are used, redistributions using TMDPQ as oxidant are performed using commercially available PPE grades. Already 80–100 % of the polymer chains in these commercially available PPE grades contain a tetramethylbiphenyl unit derived from TMDPQ. The aromatic C–H protons of the tetramethylbiphenyl unit coming from TMDPQ are visible at 7.36 ppm in the <sup>1</sup>H-NMR spectrum. Besides this tetramethylbiphenyl unit, commercially available PPE also contains Mannich base type end groups. In particular, signals belonging to Mannich base end groups derived from di-*n*-butylamine are visible in the <sup>1</sup>H-NMR spectrum. Assignments of the proton signals from these di-*n*-butylamine Mannich base type end groups are described by Mitui.<sup>48,49</sup>

The incorporation of TMDPQ also means that the catalyst is consumed and that the redistribution will not reach completion. Therefore, increased phenol incorporation is observed, when the TMDPQ is added gradually instead of a addition of all TMDPQ at the beginning of the reaction. Due to incomplete redistribution, the reaction product contains, besides the modified PPEs with the reacted phenol incorporated as a tail end, also unfunctionalized polymers, either with a 2,6-dimethylphenoxy tail or telechelic PPE with incorporated tetramethylbiphenyl. The aromatic C–H protons of the 2,6-dimethylphenoxy tail units are visible as a multiplet signal at 7.09 ppm in the <sup>1</sup>H-NMR spectrum.

*Ortho*-methyl substituted phenols typically can yield PPE chains of which 80 mol% contains functionalized endgroups, 15 mol% contains a tetramethylbiphenyl unit and 5 mol% has a 2,6-dimethylphenoxy tail end as determined by <sup>1</sup>H-NMR spectroscopy. An optimized reaction of PPE with *ortho*-unsubstituted phenols using TMDPQ as oxidant typically yields 35 mol% unfunctionalized PPE containing a tetramethyl biphenyl unit, 5 mol% unfunctionalized PPE with 2,6-dimethylphenoxy tail ends and 60 mol% modified PPE. The lower percentage is due to the fact that the formed 3,3',5,5'-tetramethyl-4,4'-biphenol derived from TMDPQ is more easily incorporated than the phenols without a methyl group at the *ortho*-positions. Despite the fact that not all PPE molecules are functionalized, these PPEs are still very useful in applications like reactive extrusion.

PPE redistribution with phenols, including some functional ones, was described in detail by White.<sup>50</sup> The use of TMDPQ in redistribution reactions has extensively been studied by General Electric Plastics,<sup>51-54</sup> for phenols also containing functional groups like carboxylic acid

functionalities.<sup>55</sup> The use of commercially available *ortho*-unsubstituted phenols (Chart 3.4) is investigated in a PPE redistribution using TMDPQ as oxidant.

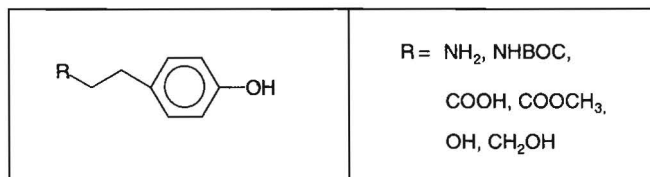


**Chart 3.4**

Some of these functional phenols barely dissolve in toluene, which is the best commercially applicable solvent for PPE. Therefore, we predissolve these functional phenols in methanol and perform the reactions in a mixture of toluene and methanol (5–10 vol%). The solubility in toluene or toluene/methanol mixtures can be improved further by attaching a facilely removable protective group onto the functional groups. The solubility of tyramine (4-aminoethylphenol) can be enhanced by a *tert*-butoxy carbonyl (*t*-BOC) protective group. The *t*-BOC-group is readily removable using trifluoroacetic acid or by heat, for instance during polymer extrusion. The solubility of carboxylic acids is increased by transforming them to their methyl esters. Elevated reaction temperatures (ca. 60 °C) are used to improve solubility of phenols and PPE. Since electron transfer reactions play an important role in the redistribution, only a small influence of temperature on reaction rate is observed.

Besides by improvement of the solubility of the reacting phenol, the intrinsic reactivity of the phenol is influenced by the type of substituent. Usually, phenols with electron-donating substituents react more rapidly in a redistribution due to their lower oxidation potential.<sup>33</sup> *Ortho*-methyl substituted functional phenols are not commercially available, so we investigated functional tetramethylbisphenols, which easily can be synthesized via an acid catalyzed condensation of 2,6-dimethylphenol and functional ketones, e.g. 4-oxo-pentanoic acid. Functional bisphenols tested in a PPE redistribution employing TMDPQ as oxidant are listed in Chart 3.5.



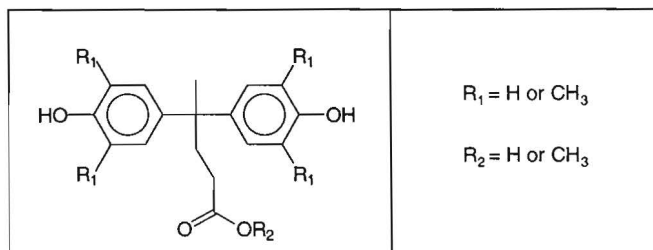
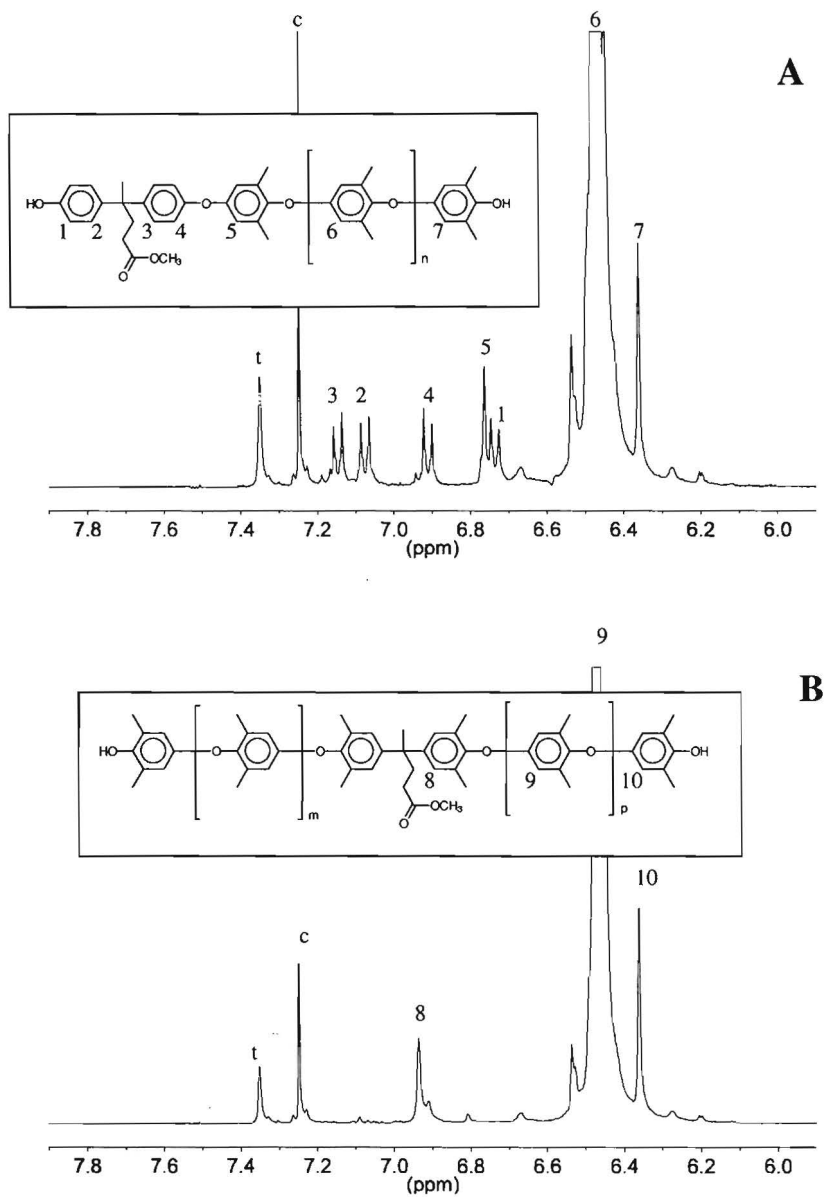


Chart 3.5

As reported above for redistributions with bisphenol acetone (BPA) or bisphenol formaldehyde (BPF) and their *ortho*-methyl substituted derivatives, *ortho*-unsubstituted bisphenols react only at one side of the bisphenol while *ortho*-methyl substituted bisphenols react at both sides of the bisphenol. Also for the bisphenol derived from 4-oxo-pentanoic acid the same phenomenon occurs, as is illustrated in a  $^1\text{H-NMR}$  spectrum of a product from redistribution with an *ortho*-unsubstituted bisphenol, 4,4'-bis(4-hydroxyphenyl)pentanoic acid methyl ester (Figure 3.10A). The  $^1\text{H-NMR}$  spectrum of this bisphenol, which is incorporated at the tail end, typically shows 4 doublet signals of the aromatic protons. Furthermore, the  $^1\text{H-NMR}$  spectrum shows a singlet belonging to the aromatic C-H protons of the 2,6-dimethylphenoxy unit adjacent to the bisphenol tail unit at 6.77 ppm. A similar singlet was observed for the aromatic protons in the penultimate benzene ring in PPEs modified with *ortho*-unsubstituted phenols (Chart 3.1 and 3.4) at their tail end. Redistribution with *ortho*-methyl substituted bisphenols yields telechelics with two PPE arms. This is illustrated by the  $^1\text{H-NMR}$  spectrum (Figure 3.10B) of a redistribution product from 4,4'-bis(4-hydroxy-3,5-dimethylphenyl)pentanoic acid methyl ester.



**Figure 3.10:** A:  $^1\text{H-NMR}$  spectrum of a reprecipitated product from PPE redistribution with 4,4'-bis(4-hydroxyphenyl)pentanoic acid methyl ester, B:  $^1\text{H-NMR}$  spectrum of reprecipitated product from a PPE redistribution with 4,4'-bis(4-hydroxy-3,5-dimethyl phenyl)pentanoic acid methyl ester; the signals marked with t and c are assigned to incorporated TMDPQ and  $\text{CHCl}_3$ , respectively.

### 3.2.4 The role of base

The necessity of a base for the oxidative polymerization<sup>18,56-60</sup> is confirmed by reactions of TMDPQ with 2,6-dimethylphenol (DMP) in the presence or absence of a base. If TMDPQ is brought into reaction with DMP in equimolar amounts, almost no oligomers are formed as determined by size exclusion chromatography (SEC) (Figure 3.11). Only the biphenol and TMDPQ are present in the reaction product and no oxidative coupling occurs. The <sup>1</sup>H-NMR spectrum (Figure 3.12) of the reaction mixture of DMP and TMDPQ shows that no C–O coupling but only C–C coupling occurs because signals of 2,6-dimethylphenoxy repeating units at 6.5 ppm are absent. The C–C coupling leads to formation of 3,3',5,5'-tetramethyl-biphenyl-4,4'-diol. This is consistent with the necessity of a high amine/copper ratio to prevent C–C coupling during the copper-catalyzed oxidative polymerization of DMP.<sup>43-46</sup>

However, when base is present, e.g. a combination of DMAP and pyridine, higher molecular weight oligomers are formed. All these oligomers contain the biphenyl unit coming from TMDPQ (Chart 3.6). When a base is present, the rate of oxidative coupling can be increased since DMP generates more easily the phenolate anion, from which the phenoxy radical is formed. This is consistent with the necessity of a base to produce a phenolate as an intermediate in the copper-catalyzed oxidative polymerization. The slower reaction of DMP with TMDPQ in comparison with the reaction of TMDPQ with a polymeric phenol endgroup can be explained by the higher redox potential of the monomeric species.<sup>29</sup>

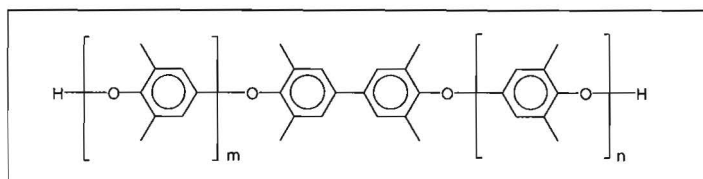
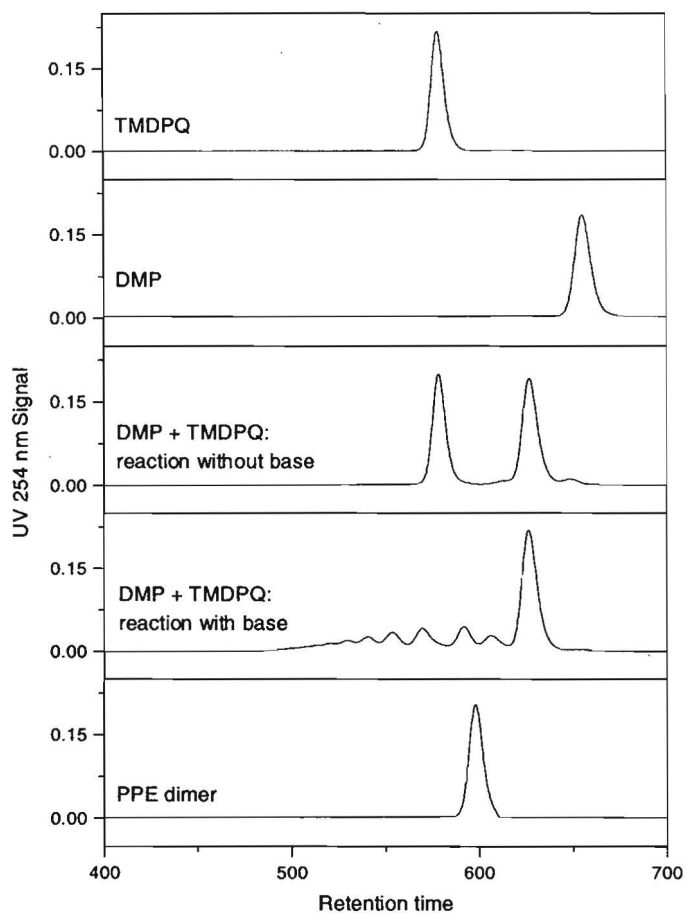
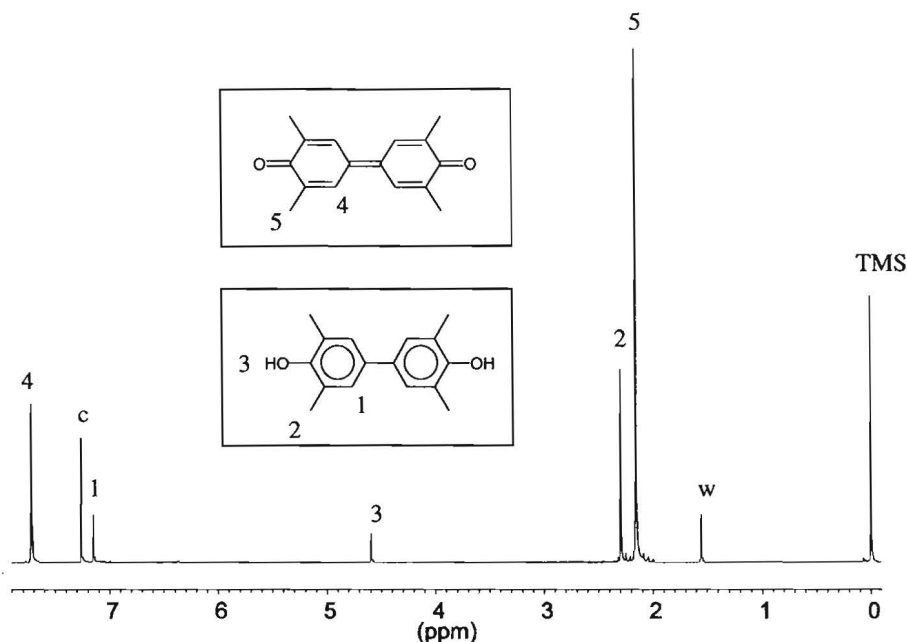


Chart 3.6



**Figure 3.11:** SEC of reaction products of DMP and TMDPQ, in the presence or absence of pyridine/DMAP, including SEC of references like DMP, TMDPQ and 4-(2,6-dimethylphenoxy)-2,6-dimethylphenol (PPE-dimer), the reactions of DMP with TMDPQ yield product mixtures containing 3,3',5,5'-tetramethylbiphenyl-4,4'-diol.



**Figure 3.12:**  $^1\text{H-NMR}$  spectrum in  $\text{CDCl}_3$  of the reaction product from reaction of DMP and TMDPQ in the absence of a base; the signals marked with w and c are assigned to residual  $\text{H}_2\text{O}$  and  $\text{CHCl}_3$ , respectively.

The importance of an additional base for the occurrence of oxidative coupling besides the redistribution with TMDPQ as oxidant is illustrated by experiments with *para*-unsubstituted phenols, as presented in Chart 3.7.

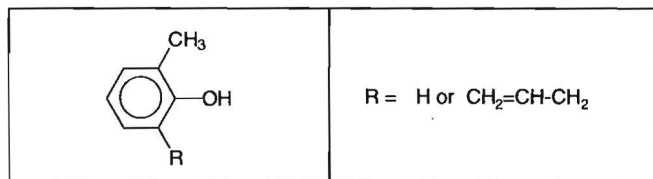


**Chart 3.7**

When redistributions are performed with *para*-unsubstituted phenols, like *o*-cresol, in the absence of a base the reacting phenol is only incorporated at the polymer tail end. This can be seen clearly from the  $^1\text{H-NMR}$  spectrum of a redistribution product with *o*-cresol, as shown in Figure 3.13A. The cresol unit at the tail end of the polymer shows as expected one triplet of the *para*-C-H proton, one doublet of the *ortho*-C-H proton and two overlapping signals of the *meta*-C-H protons in the aromatic region. Furthermore a singlet is shown for the penultimate

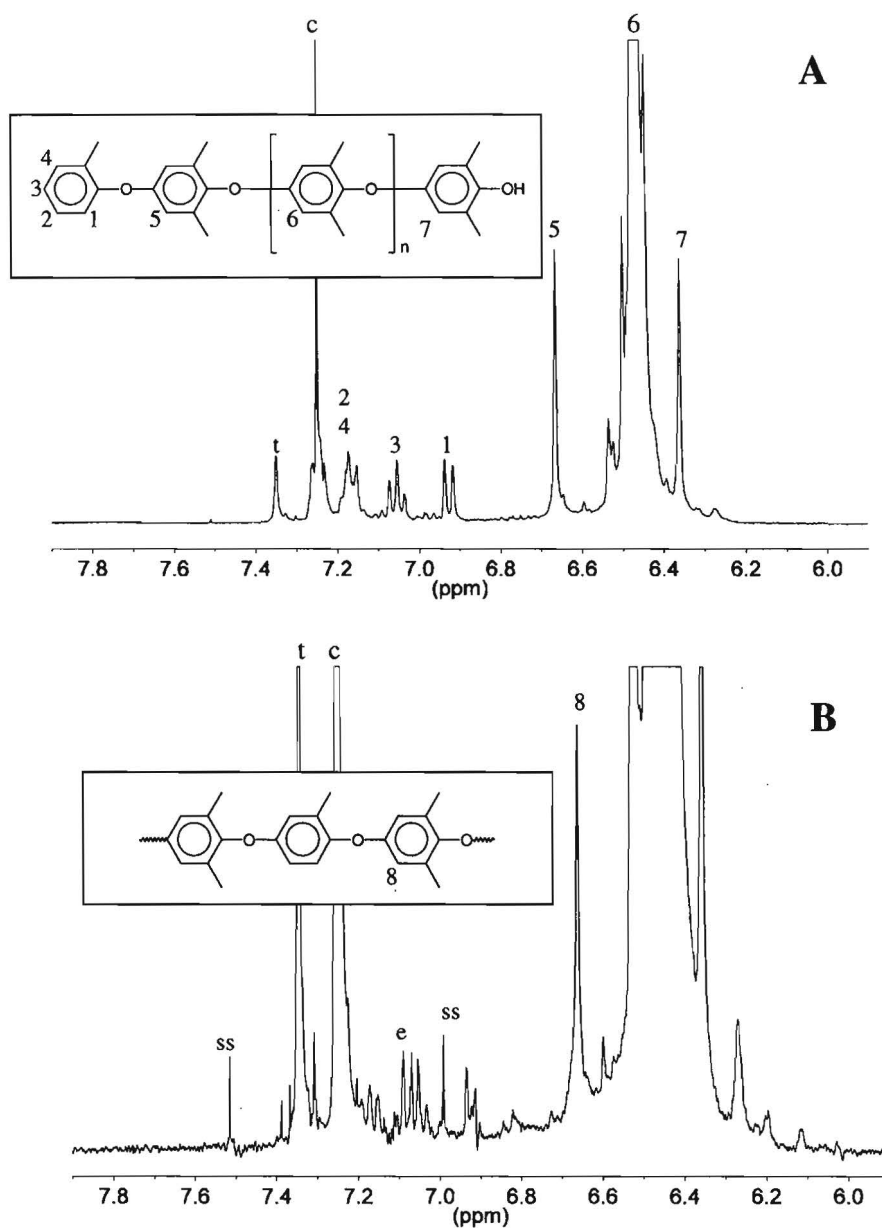


**Figure 3.13:**  $^1\text{H-NMR}$  spectrum of precipitated reaction product of redistribution with *o*-cresol; A without addition of pyridine/DMAP, B with addition of pyridine/DMAP; the signals marked with *t*, *c*, *ss* and *e* are assigned to incorporated TMDPQ, residual  $\text{CHCl}_3$ , spinning side bands and 2,6-dimethylphenoxy tail units, respectively.

2,6-dimethylphenoxy unit. All peaks have the expected integral ratios. The singlet for the aromatic C–H of the penultimate unit is shifted slightly upfield in comparison to one in a redistribution with a *ortho*-unsubstituted phenol. Presumably, when a base is absent a dimethyl-substituted ketal (Figure 3.1,  $R_1 = \text{H}$  and  $R_2 = \text{CH}_3$ ) is formed more easily than a monomethyl substituted quinol ether (Figure 3.2,  $R_1 = R_3 = \text{H}$  and  $R_2 = \text{CH}_3$ ).

When additional base, like a pyridine/DMAP combination, is added, incorporation also occurs in the middle of the chain and considerable higher molecular weights are obtained. The aromatic C–H protons of a 2,6-dimethylphenoxy units, adjacent to a cresol unit show a singlet at 6.67 ppm in the  $^1\text{H-NMR}$  spectrum as depicted in Figure 3.13B. This signal has a larger integral in comparison with a signal from two aromatic C–H protons of a cresol tail unit. Consequently, more aromatic C–H protons of a 2,6-dimethylphenoxy units adjacent to a cresol unit are present. Besides *ortho*-cresol tail units, additional signals are present at 7.09 ppm in the  $^1\text{H-NMR}$  spectrum (Figure 3.13B), presumably coming from 2,6-dimethylphenoxy tail units. Most probably the reaction product consists of a mixture with different polymer structures, i.e. either with 2,6-dimethylphenoxy or cresol tail units and either with or without one or more cresol units in the middle of the polymer chain.

### 3.3 Conclusions

A facile method is described for the preparation of functional PPE oligomers or telechelics. Redistribution of PPE with a phenolic compound yields a product with that phenolic compound incorporated as tail end. A large variety of endgroups, including reactive endgroups, can be introduced in this way. Phenolic compounds which dissolve in a good solvent for PPE and are not too deactivated caused by steric hindrance or electron-withdrawing substituents are suitable for the described redistribution reaction. Furthermore, block copolymers can be prepared by reacting a phenol terminated polymer in a redistribution with PPE.

Depending on the reacting phenolic compound, desired reaction time and product purity, TMDPQ or copper/amine systems can be used as a catalyst. For a fast PPE redistribution with *ortho*-unsubstituted phenols, without any oxidation of methyl substituents of the PPE chain, we prefer the use of TMDPQ. For the preparation of pure oligomers and block copolymers, we prefer a slow redistribution using copper catalysts in the absence of oxygen, especially when *ortho*-methyl substituted phenols are employed.

### 3.4 Experimental

#### Materials:

DMP, TMDPQ and internal grades of PPE, PPE-1 (IV = 0.40 dL/g, toluene, 30°C) and PPE-2 (IV = 0.46 dL/g, toluene, 30°C), were supplied by General Electric Plastics, Bergen op Zoom. The DMP was recrystallized from *n*-hexane before use. Low molecular weight PPEs were obtained using a precipitation polymerization method.<sup>61</sup> CuCl 99% pure, 4-dimethylaminopyridine (DMAP) 99% pure, 4-oxo-pentanoic acid 98+% pure, *N*-methylimidazole 99%, *p*-toluenesulfonic acid monohydrate 99% pure and a 1 M solution of tetrabutylammonium fluoride (TBAF) in THF were obtained from Acros. 4,4'-Bis(4-hydroxyphenyl)pentanoic acid >98% pure and 4-phenylphenol >95% pure were obtained from Fluka. Tetramethylbisphenol acetone<sup>62</sup> and 4-*tert*-butyl-2,6-dimethylphenol<sup>63</sup> were prepared according to literature procedures. The solvents chloroform, hexane, pyridine, THF, methanol and toluene and copper(II) nitrate trihydrate were used p.a. from Merck. Ethylenediaminetetraacetic acid trisodiumsalt hydrate (EDTA) 95% pure, *ortho*-cresol 99+% pure, benzoyl peroxide 97% and  $\alpha,\alpha'$ -2,3,5,6-*para*-xylene were obtained from Aldrich. The PPE-dimer, 4-(2,6-dimethylphenoxy)-2,6-dimethylphenol was obtained from P.J. Baesjou from the Leiden Institute of Chemistry, Leiden University, Leiden, The Netherlands. The TBDMS-protected 4-hydroxyphenyl terminated polystyrene was prepared by M. Hempenius, Twente University of Technology, the Netherlands, using a literature procedure.<sup>42</sup>

#### Techniques:

<sup>1</sup>H-NMR spectra were obtained using a 400 MHz Bruker AM-400 spectrometer using CDCl<sub>3</sub> or CD<sub>3</sub>OD as solvent. All  $\delta$  values were given in ppm downfield from tetramethylsilane at 0 ppm. Functionality contents are calculated using 2,3,5,6-hexachloro-*p*-xylene as an internal standard (400 MHz CDCl<sub>3</sub>; 2H,  $\delta$  = 4.93 ppm). HPLC analysis is performed using a HP 1090 HPLC with a reversed phase column, type 10007C18 and a diode array detector. A gradient from a 30% acetonitrile/water mixture to 100% acetonitrile at 40 °C was employed during 20 minutes. The presented Size Exclusion Chromatography (SEC) analysis in Figure 3.3 was performed at room temperature using chloroform as eluent, a LC-10AT Shimadzu liquid chromatograph with a PL gel column (particle size: 5  $\mu$ m, pore size: 500 Å, length: 300 mm, internal diameter: 7.5 mm) and UV detection at 254 nm using a Linear UVIS-205 absorbance detector. Molecular weight determination of all other PPEs was performed using SEC at General Electric Plastics using a chloroform/ethanol mixture (98/2 v/v) as eluent at 40 °C. Dibutyl amine (50 ppm) is added to prevent tailing. Equipment used for this analysis are: a Waters 150-CV ALC/GPC apparatus, PL gel columns 10<sup>3</sup> and 10<sup>5</sup> Å and a Waters 490E programmable multiwavelength detector (PPE detected at 280 nm, polystyrene standards detected at 254 nm). SEC analyses of low molecular weight oligomers as presented in Figure 3.3 were performed at room temperature using chloroform as eluent and a PL gel column (particle size: 5  $\mu$ m, pore size 500 Å, length 300 mm, internal diameter 7.5 mm) The PS-PPE block copolymers are analysed by SEC with THF as eluent at 40 °C using a Waters model 510 SEC apparatus, 2 Shodex KF 80-M linear columns, a Waters 410 differential refractometer and a Waters 486 tunable absorbance detector (UV detection at 254 nm). Element analysis has been performed using a Perkin Elmer CHN analyser type 2400. Melting points were measured with a heating rate of 2 °C/min using a Stuart Scientific SMP2 Melting point apparatus.



*Synthesis of bis(3,5-dimethyl-4-hydroxyphenyl)pentanoic acid:*

DMP (597.0 g, 4.89 mol) and 4-oxo-pentanoic acid (levulinic acid) (283.7 g, 2.44 mol) are dissolved at 60 °C, solution of 715 mL of 37% HCl is slowly added. Subsequently 7 gram (36.8 mmol) of p-toluenesulfonic acid monohydrate is added. The reaction mixture is reacted for 5 days at 60 °C, then 3 L water is added. The product is filtrated and washed with 0.5 L water. The filtrated product is recrystallized twice from toluene and dried in a vacuum oven. Reaction yield: 80% <sup>1</sup>H-NMR (400 MHz, CD<sub>3</sub>OD): δ 1.46 (3H, s, CH<sub>3</sub>), 2.14 (12H, s, CH<sub>3</sub>), 2.31 (2H, t, J = 8.1 Hz, CH<sub>2</sub>-COOH), 2.05 (2H, t, J = 8.1 Hz, CH<sub>2</sub>-CH<sub>2</sub>-COOH), 6.72 (4H, s, Ar-H), 4.69 (2H, s, Ar-OH). <sup>13</sup>C-NMR (400 MHz, CD<sub>3</sub>OD): δ 176.6 (CH<sub>3</sub>C(Ar)<sub>2</sub>CH<sub>2</sub>CH<sub>2</sub>COOH), 152.0 (arom. C1), 141.6 (arom. C4), 128.3 (arom. C3), 124.9 (arom. C2), 45.1 (CH<sub>3</sub>C(Ar)<sub>2</sub>CH<sub>2</sub>CH<sub>2</sub>COOH), 37.8 (CH<sub>3</sub>C(Ar)<sub>2</sub>CH<sub>2</sub>CH<sub>2</sub>COOH), 31.1 (CH<sub>3</sub>C(Ar)<sub>2</sub>CH<sub>2</sub>CH<sub>2</sub>COOH), 28.2 (CH<sub>3</sub>C(Ar)<sub>2</sub>CH<sub>2</sub>CH<sub>2</sub>COOH), 16.9 (Ar-CH<sub>3</sub>). mp 202 °C Anal. Calcd for C<sub>21</sub>H<sub>22</sub>O<sub>4</sub>: C, 73.66; H, 7.65; Found: C, 73.46; H, 7.62.

The experimental procedures described in this experimental section for redistribution experiments are typical examples and are also valid for other phenols

*Redistribution of 4-tert-butyl-2,6-dimethylphenol with PPE:*

PPE (10 gram,  $\overline{M}_n = 3.5$  kg/mol, 83.17 mmol of dimethylphenoxy repeating units, prepared by precipitation polymerization<sup>61</sup> was dissolved in toluene (100 mL). Upon the addition of TBDMP (4.55 g, 25.5 mmol) the PPE is depolymerized to low molecular weight oligomers. After a reaction time of 13 days the reaction mixture was precipitated into methanol. <sup>1</sup>H-NMR (CDCl<sub>3</sub>): δ 1.33 (9H, s, C(CH<sub>3</sub>)<sub>3</sub> tail endgroup), 7.09 (2H, s, arom. C-H tail endgroup), 6.36 (2H, s, arom. C-H head endgroup),  $\overline{M}_n = 1.19$  kg/mol.

*PPE redistribution with DMP using a Cu(NO<sub>3</sub>)<sub>2</sub>·3H<sub>2</sub>O / NMI catalyst:*

A mixture of Cu(NO<sub>3</sub>)<sub>2</sub>·3H<sub>2</sub>O (0.053 g, 0.22 mmol) and *N*-methylimidazole (0.355 g, 4.3 mmol) was added to a solution of PPE-OH (1.07 g,  $\overline{M}_n = 7.3$  kg/mol) and DMP (0.617 g, 5.0 mmol) in chloroform (10 mL). The reaction was performed in the presence of air at room temperature. Reaction samples were taken, extracted subsequently with an aqueous 10 wt% EDTA solution and an aqueous 37% HCl and then the product was obtained by evaporation of the chloroform.

*PPE redistribution with 4-(2,6-dimethylphenoxy)-2,6-dimethylphenol (PPE-dimer) using a Cu(NO<sub>3</sub>)<sub>2</sub>·3H<sub>2</sub>O / NMI catalyst:*

A mixture of Cu(NO<sub>3</sub>)<sub>2</sub>·3H<sub>2</sub>O (0.025 g, 0.10 mmol) and *N*-methylimidazole (0.175 g, 2.1 mmol) was added to a solution of PPE-OH (0.233 g,  $\overline{M}_n = 7.3$  kg/mol) and the PPE-dimer (0.200 g, 0.83 mmol) in chloroform (10 mL). The reaction was performed in the presence of air at room temperature. Reaction samples were taken, extracted subsequently with an aqueous 10 wt% EDTA solution and aqueous 37% HCl and then the product was obtained by evaporation of the chloroform.

*PPE redistribution with 4,4'-bis(4-hydroxy-3,5-dimethylphenyl)pentanoic acid using a  $\text{Cu}(\text{NO}_3)_2 \cdot 3\text{H}_2\text{O}$  / NMI catalyst:*

PPE-OH (1.57 g,  $\overline{M}_n = 7.3$  kg/mol) and 4,4'-bis(4-hydroxy-3,5-dimethylphenyl)pentanoic acid (0.595 g, 1.74 mmol) were dissolved in chloroform (10 mL) at 60 °C. When all PPE and most of the added bisphenol were dissolved, the reaction mixture was allowed to cool to room temperature. Then a mixture of  $\text{Cu}(\text{NO}_3)_2 \cdot 3\text{H}_2\text{O}$  (0.098 g, 0.40 mmol) and *N*-methylimidazole (0.663 g, 8.1 mmol) in chloroform (10 mL) was added. The reaction was performed in the presence of air at room temperature. Reaction samples were taken, extracted subsequently with an aqueous 10 wt% EDTA solution and a aqueous 37% HCl and then the product was obtained by evaporation of the chloroform.

*PPE redistribution with 4-phenylphenol using a  $\text{CuCl}/\text{DMAP}$  catalyst*

PPE-1 (2.54 g), 4-phenylphenol (0.82 g, 4.31 mmol), CuCl (0.010 g, 0.10 mmol) and DMAP (0.020 g, 0.16 mmol) were set under argon by repeated evacuation of the flask and filling with argon. The reaction was started by the addition of 30 mL chloroform. After 17 days the reaction mixture extracted with a 10 wt% EDTA solution and a 10 wt% HCl solution and precipitated into methanol (300 mL). The precipitated polymer was collected by filtration and dried in a vacuum oven at 90 °C. The number average molecular weight of the precipitated polymer is determined using  $^1\text{H-NMR}$  spectroscopy:  $\overline{M}_n = 2.33$  kg/mol.  $^1\text{H-NMR}$  (400 MHz,  $\text{CDCl}_3$ ):  $\delta$  7.57 (4H, m, arom. *ortho* C3-H and arom. *meta* C4-H biphenyl tail end group), 7.43 (2H, t,  $J=7.6$  Hz, arom. *meta* C2-H biphenyl tail end group), 7.34 (1H, m, arom. C1-H biphenyl tail endgroup), 7.10 (2H, d,  $J=8.6$  Hz, arom. *ortho* C5-H biphenyl tail endgroup), 6.81 (2H, s, C6-H arom. penultimate 2,6-dimethylphenoxy unit at tail end), 6.36 (2H, s, arom. C8-H 2,6-dimethyl phenolic head unit).

*PPE redistribution with 4-(2-hydroxyethyl)phenol using TMDPQ:*

PPE-1 (30.14 g) was dissolved in toluene (300 mL) at 60 °C. Subsequently, 4-(2-hydroxyethyl) phenol (1.811 g, 13.1 mmol) dissolved in methanol (15 mL) was added. The reaction was started by the addition of TMDPQ (0.3024 g, 1.26 mol). After 4 hours reaction time, the reaction mixture was precipitated in methanol (3.5 L). The precipitated polymer was collected by filtration and dried in a vacuum oven at 90 °C. The obtained polymer was reprecipitated from a 10 wt% chloroform solution in a 10-fold excess of methanol. Yield precipitated product: 28.0 gram.  $^1\text{H-NMR}$  (400 MHz,  $\text{CDCl}_3$ ):  $\delta$  3.88 (2H, t,  $J=6.4$  Hz,  $\text{HOCH}_2$ ), 2.87 (2H, t,  $J=6.5$  Hz,  $\text{CH}_2\text{-Ar}$ ), 7.21 (2H, d,  $J=8.4$  Hz, *ortho* C3-H arom. tail end group), 7.00 (2H, d,  $J=8.6$  Hz, *meta* C4-H arom. tail end group), 6.77 (2H, s, C-H arom. penultimate unit at tail end), 6.37 (2H, s, arom. C3-H head unit). Functionality (phenol) content in precipitated polymer: 1.85 wt%. Uncorrected molecular weights determined by SEC, eluent  $\text{CHCl}_3$ , using polystyrene standard specimen:  $\overline{M}_n = 6.59$  kg/mol and  $\overline{M}_w = 15.55$  kg/mol.

*PPE redistribution with 4,4'-bis(4-hydroxyphenyl)pentanoic acid methyl ester using TMDPQ:*

PPE-1 (30.01 g) was dissolved in toluene (300 mL) at 60 °C. Subsequently, the 4,4'-bis(4-hydroxyphenyl)pentanoic acid methyl ester (3.94 g, 13.1 mmol) dissolved in methanol (30 mL) was added. The reaction was started by the addition of TMDPQ (0.300 g, 1.25 mol). After 3 hours reaction time, the reaction mixture was precipitated in methanol (4 L). The precipitated polymer was collected by filtration and dried in a vacuum oven at 90 °C. The obtained polymer was reprecipitated from a 10 wt% chloroform solution in a 10-fold excess of methanol. Yield of precipitated product: 29.4 gram.  $^1\text{H-NMR}$

NMR (400 MHz,  $\text{CDCl}_3$ ):  $\delta$  3.62 (3H, s,  $\text{OCH}_3$ ), 7.15 (2H, d,  $J=8.8$  Hz, arom. C2-H tail end group), 7.08 (2H, d,  $J=8.7$  Hz, arom. C3-H tail end group), 6.91 (2H, d,  $J=8.7$  Hz, C4-H arom. tail end group), 6.74 (2H, d,  $J=8.6$  Hz, arom. C1-H tail end group), 6.76 (2H, s, C5-H arom. penultimate unit at tail end),  $\delta$  6.37 (2H, s, arom. C3-H head unit). Functionality (phenol) content in precipitated polymer: 3.56 wt%. Uncorrected molecular weights determined by SEC, eluent  $\text{CHCl}_3$ , using polystyrene standard specimen:  $\overline{M}_n = 7.00$  g/mol and  $\overline{M}_w = 17.65$  g/mol.

*PPE redistribution with 4,4'-bis(4-hydroxy-3,5-dimethylphenyl)pentanoic acid methyl ester using TMDPQ:*

PPE-1 (10.00 g) was dissolved in toluene (100 mL) at 60 °C. Subsequently, 4,4'-bis(4-hydroxy-3,5-dimethylphenyl)pentanoic acid methyl ester (0.7722 g, 2.17 mmol) was dissolved in methanol (10 mL) was added. The reaction was started by the addition of TMDPQ (0.033 g, 0.14 mol). After 1 and 2 hours reaction time again TMDPQ is added ( $2 \times 0.033$  gram, 0.14 mol). After 5 hours total reaction time, the reaction mixture was precipitated in methanol (1.5 l). The precipitated polymer was collected by filtration and dried in a vacuum oven at 90 °C. The obtained polymer was reprecipitated from a 10 wt% chloroform solution in a 10-fold excess of methanol. Yield precipitated product: 9.60 gram.  $^1\text{H-NMR}$  (400 MHz,  $\text{CDCl}_3$ ):  $\delta$  3.65 (3H, s,  $\text{OCH}_3$ ), 6.93 (4H, s, arom. C-H bisphenol core unit), 6.36 (2H, s, C3-H arom. head unit). Functionality (phenol) content in precipitated polymer: 5.79 wt%. Uncorrected molecular weights determined by SEC, eluent =  $\text{CHCl}_3$ , using polystyrene standard specimen:  $\overline{M}_n = 5.80$  kg/mol and  $\overline{M}_w = 16.00$  kg/mol.

*PPE redistribution with 4,4'-bis(4-hydroxy-3,5-dimethylphenyl)pentanoic acid using benzoyl peroxide:*

PPE-1 (10.01 g) was set under argon by repeated evacuation of the flask and filling with argon. Toluene (100 mL), distilled from sodium, was added to the PPE powder and PPE was dissolved at 90 °C. Subsequently, the 4,4'-bis(4-hydroxy-3,5-dimethyl-phenyl)pentanoic acid (0.250 g, 0.73 mmol) dissolved in methanol (5 mL) was added. The reaction was started by the addition of benzoyl peroxide (0.100 g, 0.41 mol). After 3 hours reaction time, the reaction mixture was precipitated in methanol (1.2 L). The precipitated polymer was collected by filtration and dried in a vacuum oven at 90 °C. The obtained polymer was reprecipitated from a 10 wt% chloroform solution in a 10-fold excess of methanol. Yield of precipitated product: 9.62 gram.  $^1\text{H-NMR}$  (400 MHz,  $\text{CDCl}_3$ ):  $\delta$  6.94 (4H, s, arom. C-H bisphenol core unit), 6.36 (2H, s, C3-H arom. head unit). Functionality (phenol) content in precipitated polymer: 1.76 wt%. Uncorrected molecular weights determined by SEC, eluent =  $\text{CHCl}_3$ , using polystyrene standard specimen:  $\overline{M}_n = 9.50$  kg/mol and  $\overline{M}_w = 24.50$  kg/mol.

*Preparation of PS-PPE diblock copolymers via redistribution*

The anionically prepared polystyrene (PS), initiated by *sec*-butyl lithium, was terminated by a 1,1-divinylethene derivative containing a *tert*-butyl-dimethylsilyl (TBDMS) protected phenol, 1-(4-*tert*-butyldimethylsiloxyphenyl)-1-phenylethylene, according to a literature procedure.<sup>42</sup> Deprotection of the TBDMS group was performed using tetrabutyl ammonium fluoride (TBAF) in THF according to the following procedure: 0.594 g of PS terminated with a TBDMS protected phenolic endgroup ( $\overline{M}_n = 3.0$  kg/mol) was dissolved in 15 mL THF, 1 mL of a 1 M solution of TBAF in THF was added. After 4 days reaction at room temperature the reaction mixture was extracted twice with an aqueous 15 wt%

HCl solution and precipitated into methanol. The obtained product was collected by filtration and dried in a vacuum oven at 60 °C. SEC (THF) :  $\overline{M}_n = 3.0$  kg/mol,  $\overline{M}_w = 3.3$  kg/mol,  $D = 1.1$ .

Redistribution of the phenol-terminated PS and PPE was performed according to the following experimental procedure: 0.222 g of phenol-terminated PS ( $\overline{M}_n = 3.0$  kg/mol), 0.230 g of PPE-1, 0.031 g of DMAP and 0.016 g of CuCl were set under argon by repeated evacuation of the flask and filling with argon. The reaction was started by the addition of chloroform (15 mL). After reaction during 1 week at room temperature, the reaction mixture was precipitated into methanol. The obtained product was collected by filtration and dried in a vacuum oven at 60 °C.

#### *Redistribution of ortho-cresol with PPE under the action of TMDPQ*

PPE-2 (4.98 g, 41.4 mol of 2,6-dimethylphenoxy repeating units) was dissolved in toluene (50 mL) at 60 °C. Then *o*-cresol (1.15 g, 10.6 mmol), dissolved in methanol (5 mL) was added and the reaction was started upon the addition of TMDPQ (0.0502 g, 0.21 mmol). After a reaction time of 4 hours, the reaction mixture was precipitated into methanol. The product was reprecipitated twice from chloroform into methanol. <sup>1</sup>H-NMR (CDCl<sub>3</sub>):  $\delta$  6.66 (2H, s, arom. C-H penultimate tail endgroup), 7.15 (1H, t,  $J = 2.7$  Hz, arom. *para*-C-H tail endgroup), 6.93 (1H, d,  $J = 8.1$  Hz, arom. *ortho*-C-H tail endgroup), 7.17 (2H, m, arom. *meta*-C-H's tail endgroup). Uncorrected molecular weights determined by SEC, eluent=CHCl<sub>3</sub>, using polystyrene standard specimen:  $\overline{M}_n = 20.20$  kg/mol and  $\overline{M}_w = 5.07$  kg/mol.

#### *Redistribution of ortho-cresol with PPE under the action of TMDPQ and base*

PPE-2 (5.00 g, 41.6 mmol dimethylphenoxy repeating units) and DMAP (0.531 g, 4.35 mmol) are dissolved in a toluene (25 mL) and pyridine (25 mL) at 60 °C. Then *o*-cresol (1.19 g, 11.0 mmol), dissolved in methanol (5 mL) was added and the reaction was started by the addition of TMDPQ (0.0504 g, 0.21 mmol). After a reaction time of 4 hours, the reaction mixture was precipitated into methanol. The product was reprecipitated twice from chloroform into methanol. Uncorrected molecular weights determined by SEC, eluent = CHCl<sub>3</sub>, using polystyrene standard specimen:  $\overline{M}_n = 42.00$  kg/mol and  $\overline{M}_w = 14.50$  kg/mol.

#### *Reaction of DMP with TMDPQ:*

*In the absence of base:* TMDPQ (0.8307 g, 3.46 mol) and DMP (0.4765 g, 3.90 mol) are dissolved in toluene (5 mL) and reacted for 5 hours at 60 °C. The reaction is stopped by evaporation of the solvent. The reaction product consist of a mixture of TMDPQ and 4,4'-bis(3,5-dimethyl)biphenyl in a molar ratio of 4/1, as determined by <sup>1</sup>H-NMR spectroscopy. <sup>1</sup>H-NMR (CDCl<sub>3</sub>) TMDPQ: 7.72 (4H, s, arom. C-H), 2.16 (12H, s, CH<sub>3</sub>). <sup>1</sup>H-NMR (CDCl<sub>3</sub>) 4,4'-bis(3,5-dimethyl)biphenyl: 7.15 (4H, s, arom. C-H), 4.59 (1H, s, OH), 2.30 (12H, s, CH<sub>3</sub>).

*In the presence of base:* TMDPQ (0.8290 g, 3.45 mol), DMP (0.4745 g, 3.88 mol) and DMAP (0.0570 g, 0.467 mmol) are dissolved in pyridine (5 mL) and reacted for 5 hours at 60 °C. The reaction is stopped by evaporation of the solvent. Then the reaction mixture is dissolved into chloroform and extracted with 10 wt% HCl solution, to remove pyridine and DMAP. Subsequently, the chloroform is evaporated.

### 3.5 References and notes

1. Hay, A.S., *J. Polym. Sci., Polym. Chem. Ed.*, **34**, 1369 (1996).
2. Hay, A.S., Blanchard, H.S., Endres; G.F. and Eutance J.W. *J. Am. Chem. Soc.*, **81**, 6335 (1959).
3. Hay, A.S. *J. Polym. Sci.*, **58**, 581 (1962).
4. Hay A.S. and Endres, G.F. *Polym. Lett.*, **3**, 887 (1965).
5. Hay A.S. *Adv. Polym. Sci.*, **4**, 496 (1967).
6. Cooper, G.D. *Ann. New York Acad. Sci.*, **159**, 278 (1969).
7. Percec, V., Wang, J.H. and Clough, R.S. *Macromol. Chem., Macromol. Symp.*, **54/55**, 275 (1992).
8. Viersen, F.J., Renkema, J., Challa G. and Reedijk J. *J. Polym. Sci., Polym. Chem. Ed.*, **30**, 901 (1992).
9. White, D.M. *Compr. Polym. Sci.*, **5**, 473 (1989).
10. Cooper, G.D. and Karchmann, A. *Adv. Chem. Ser.*, **91**, 660 (1969).
11. Finkbeiner, H.L., Hay, A.S. and White, D.M., "Polymerization Processes", Vol. 29, Eds. Schildknecht C.E., Skeist, I., Wiley, New York, 537 (1977).
12. Finkbeiner, H.L., Endres, G.F., Blanchard, H.S. and Eustance, J.W. *SPE Trans.*, **2**, 110, (1962).
13. Finkbeiner, H.L., Endres, G.F., Blanchard, H.S. and Eustance, J.W. *Polym. Prep., Am. Chem. Soc., Div. Polym. Chem.*, **2**, 340 (1961).
14. White D.M. *Polym. Prep., Am. Chem. Soc., Div. Polym. Chem.*, **9**, 663 (1968).
15. White, D. M. *J. Polym. Sci. Polym. Chem. Ed.*, **19**, 1367 (1981).
16. Koch, W., Risse, W. and Freitag, D. *Macromol. Chem.*, **12**, 105 (1985).
17. Risse, W., Heitz, W., Freitag, D. and Bottenbruch, L. *Macromol. Chem.*, **186**, 1835 (1985).
18. Chen, W., Challa, G. and Reedijk, J. *Polym. Commun.*, **32**, 518 (1991).
19. Nava, H. and Percec, V. *J. Polym. Sci., Polym. Chem. Ed.*, **24**, 986 (1986).
20. Wang, J.H. and Percec, V. *Polym. Bull.*, **25**, 25 (1991).
21. Cooper G.D., Bennett J.G. and Factor A. *Polym. Prep., Am. Chem. Soc., Div. Polym. Chem.*, **13**, 551 (1972).
22. Kowalczyk, U., Bartmann, M., Mügge, J. and Neugebauer, W. Eur. Pat. Appl. EP 0,468,162 A1, (1991).
23. Kowalczyk, U., Bartmann M. and Poll H.G., U.S. US 5,128,422, (1992).
24. Kowalczyk, U., Bartmann, M., Mügge, J. and Neugebauer, W. Eur. Pat. Appl. EP 0,468,162 A1, (1991).
25. Kowalczyk, U., Bartmann M. and Poll G. Eur. Pat. Appl. EP 0,391,031 A2, (1990).
26. Neugebauer W., Bartmann, M. and Kowalczyk, U. U.S. US 5,039,781, (1991).
27. Tsukahara T., Nishimura H., Aritomi M., Arashiro Y. and Yamauchi S. Eur. Pat. Appl. EP 0,530,442 A1 (1992).
28. Heitz, W. *Angew. Makromol. Chem.*, **223**, 135 (1994).

29. Koch, W., Risse, W. and Heitz, W. *Macromol. Chem., Suppl.*, **12**, 105 (1985).
30. Less branching can be achieved by using a bulky amine as part of the catalyst to block the open *ortho*-position as described by: Hay, A.S. and Endres, G.F. *J. Polym. Sci., Polym. Lett. Ed.*, **3**, 887 (1965).
31. Usami, T., Kogawa, Y., Takayama, S. and Toyama, T. *Eur. Polym. J.*, **26**, 699 (1990).
32. Picket, J.E., *Polym. Degrad. Stab.*, **44**, 119 (1994).
33. Van Aert, H.A.M., Burkard, M.E.M., Jansen, J.F.G.A., van Genderen, M.H.P., Meijer, E.W., Oevering, H. and Werumeus Buning, G.H. *Macromolecules*, **28**, 7967 (1995).
34. Tsuruya, S., Kinumi, K., Hagi, K. and Masai, M. *J. Mol. Catal.*, **22**, 47 (1983).
35. Huysmans, W.G.B. and Waters, W.A. *J. Chem. Soc. (B)*, 1163 (1967).
36. Heitz, W. *Pure & Appl. Chem.*, **67**, 1951 (1995).
37. Bartmann, M. and Kowalczyk, U., *Makromol. Chem.*, **189**, 2285 (1988).
38. Finkbeiner, H.L., Endres, G.F., Blanchard, H.S. and Eustance, J.W. *SPE Trans.*, **2**, 112 (1962).
39. Baesjou, P.J. "The copper-catalyzed oxidative coupling of 2,6-dimethylphenol", PhD thesis, State University of Leiden, The Netherlands, (1997).
40. Kaitayama, T., Nakagawa, O., Kishiro, S., Nisjiura, K. and Hatada, K. *Eur. Polym. J.*, **25**, 707 (1993).
41. Wang, J.H. and Percec, V. *Polym. Bull.*, **25**, 25 (1991).
42. Quirk, R.P. and Zhu, L.F. *Makromol. Chem.*, **190**, 487 (1989).
43. Viersen, F.J., Wilson, J.C., Challa, G. and Reedijk, J. *Polym. Adv. Technol.*, **6**, 144 (1995).
44. Endres, G.F., Hay, A.S., Eustance, J.W. and Kwiatek, J. *SPE trans.*, **2**, 109 (1962).
45. Endres, G.F., Hay, A.S. and Eustance, J.W. *J. Org. Chem.*, **28**, 1300 (1963).
46. Viersen, F.J., Challa, G. and Reedijk, J. *Recl. Trav. Chim. Pays-Bas*, **109**, 97 (1990).
47. For large scale utilization of the preparation of functional PPEs via redistribution, besides TMDPQ also benzoyl peroxide can be a suitable oxidant. Peroxides are known to initiate fast redistribution of PPE with phenols lacking a functional group. Preliminary research has shown that benzoylperoxide also can be used in redistribution of PPE with phenols containing functional groups, see: Chao, H.S.I. and Whalen, J.M. *React. Polym.*, **15**, 9 (1991). To optimize the reaction conditions further research is required.
48. Mitui, A., Kanayama, A., Takayama, S. and Takeda, K. *Kobunshi Ronbunshi*, **51**, 157 (1994).
49. Takayama, S., Mitsui, A. and Takeda, K. *Kobunshi Ronbunshi*, **51**, 479 (1994).
50. White, D.M. *J. Org. Chem.*, **34**, 297 (1969).
51. Cooper, G.D., Gilbert, A.R. and White, D.M. Brit. Pat. Appl. BP 1,119,914 (1968).
52. White, D.M. U.S. US 3,367,978 (1968).
53. Cooper, G.D. and Gilbert, A.R. U.S. US 3,496,236 (1970).
54. Aycock, D.F. and Dert, V. Eur. Pat. Appl. EP 0,550,209 A2, (1993).
55. Yates III, J.B. and White, D.M. Eur. Pat. Appl. EP 0,315,822 A1, (1989).
56. Viersen, F.J., Challa, G. and Reedijk, J. *Recl. Trav. Chim. Pays-Bas*, **108**, 247 (1989).
57. Viersen, F.J., Challa, G. and Reedijk, J. *Polymer*, **31**, 1361 (1990).
58. Viersen, F.J., Challa, G. and Reedijk, J. *Polymer*, **31**, 1368 (1990).

- 59 . Tullemans, A.H.J., Bouwman, E., de Graaff, R.A.G., Driessen, W.L. and Reedijk, J. *Recl. Trav. Chim. Pays-Bas*, **109**, 70 (1990).
- 60 . Challa, G. and Chen, W. *Macromol. Chem., Macromol. Symp.*, **59**, 59 (1992).
- 61 . Van Aert, H.A.M., Venderbosch, R.W., van Genderen, M.H.P., Lemstra, P.J. and Meijer, E.W. *J. Macromol. Sci., Pure & Appl. Chem.*, **A32**, 515 (1995).
- 62 . Curtis, R.F. *J. Chem. Soc.*, 415 (1962).
- 63 . Percec, V. and Wang, J.H. *J. Polym. Sci., Polym. Chem. Ed.*, **29**, 63 (1991).

## Chapter 4

### Star-shaped poly(2,6-dimethyl-1,4-phenylene ether)

#### Summary

*The properties of star-shaped poly(2,6-dimethyl-1,4-phenylene ether) (PPE), as prepared by the redistribution of PPE and tyrosine-modified poly(propylene imine) dendrimers, are studied in solution and in blends with linear polystyrene (1 : 1 weight ratio). Star polymers with constant armlength but increasing number of arms show the same hydrodynamic volume as measured by Size Exclusion Chromatography (SEC), but decreasing hydrodynamic radius as measured by Dynamic Light Scattering (DLS). This is caused by the restricted free-draining in the starpolymers at high numbers of arms, also leading to a decrease in intrinsic viscosities. Star-shaped polymers with a high number of PPE arms (16, 32 or 64) give inhomogeneous blends with linear polystyrene, in contrast to the miscible combination of linear polystyrene with linear PPE or star-shaped polymers with a low number (4 or 8) of PPE arms.*

#### 4.1 Introduction

Star-shaped polymers are gaining interest because of their characteristic rheological properties and their dilute-solution properties.<sup>1-5</sup> The interest for branched polymers, in general, arises from their compactness and enhanced segmental density as compared to their linear counterparts of the same molecular weight. Therefore, the star-shaped polymers resemble the hard-sphere model more closely than linear polymers, especially when the number of arms in the star polymer increases.<sup>6,7</sup> There are two basic influences of the topological constraints in star-branched polymers:<sup>8</sup> (1) The local average polymer density increases relative to that of a linear chain. (2) Cooperative motion of the chain is restricted by the constrained segmental motion with the branches. The first effect is particularly important in the investigation of dilute solution properties, while the second effect dominates at high concentrations as proposed by Douglas.<sup>8</sup> Generally, it was found experimentally that starpolymers have lower intrinsic viscosities as compared to linear polymers of the same molecular weight.<sup>6,9,10</sup> These observations can be explained by the Flory-Fox equation,<sup>11</sup>  $[\eta] = \Phi R^3/M$ , in which  $[\eta]$  denotes the intrinsic viscosity,  $R$  the root-mean-square-radius,  $M$  the molecular weight and  $\Phi$  a



universal constant. The ratio of intrinsic viscosities of star-branched and linear polymers, respectively, having the same molecular weight can be predicted theoretically,<sup>4,12</sup> and decreases for larger number of arms.

Phase-separation in blends of linear polymers has been investigated widely.<sup>13</sup> A theoretical investigation on the influence of short chain branching on the miscibility of binary polymer blends and its application to polyolefin mixtures is described by Freed.<sup>14</sup> Several experimental studies about mixtures of branched polymers with their linear counterpart are reported. The liquid-liquid phase separation in binary blends of branched polyethylenes with linear polyethylenes is described in detail.<sup>15-17</sup> In contrast to studies about phase separation in branched/linear polymer systems, the phase behavior of star/linear polymer systems has not been investigated to a large extent. The dynamics of polymer blends made out of linear and star-shaped polymers is studied theoretically.<sup>18-20</sup> Roovers<sup>21</sup> and Struglinski<sup>22</sup> studied the viscoelastic properties and relaxation behaviour of binary mixtures of linear and star polybutadienes. Phase-separation kinetics of mixtures of linear and star-shaped polymers of different nature have been studied experimentally for star-shaped polystyrene and linear poly(vinyl methyl ether).<sup>23-25</sup> In this case, however, the corresponding mixtures of their linear polymers already show phase separation. The minimum of the cloud-point curve of the star/linear system is several degrees lower in comparison to the linear/linear system. Hardly any investigations are reported on phase separation in linear/star polymer blends, using polymers that give homogeneous blends of their linear analogues. By mixing both linear and star-shaped poly( $\epsilon$ -caprolactam) (PCL) with styrene-acrylonitrile copolymers (SAN) partially miscible blends can be produced, which show one glass transition temperature. It appears that only a fraction of the PCL chains is miscible with the SAN resulting in moderately elevated glass-transition temperatures.<sup>26</sup> The SAN chains are unable to penetrate in an efficient manner into the core region. This is consistent with a model of an impermeable core from which the arms of the star diffuse outward.<sup>27</sup> In this miscibility study a 6-arm star PCL is used. Increasing the number of arms will probably give a more pronounced phase-separation.

The blends of linear PS and linear PPE were recognized as being homogeneous at all compositions,<sup>28-31</sup> but some microheterogeneities can be detected by solid-state NMR<sup>32</sup> and pressure can cause phase separation of this blend.<sup>33</sup> Using the PPE redistribution, star-shaped PPE can be prepared with facile control of the number of PPE arms,<sup>34,35</sup> as schematically shown in Figure 4.1. As core, well-defined poly(propylene imine) dendrimers,<sup>36</sup> with an exact number of end groups varying from 4, 8, 16, 32 to 64 are used. After a modification with protected amino acids, like *tert*-butyloxycarbonyl (*t*-BOC) protected phenylalanine or tyrosine, a rigid shell is obtained.<sup>37,38</sup> These dendrimers have been used as dendritic box for encapsulation of guest molecules. Because of their well-defined structure and rigid shell, these

dendrimers are very useful in star polymers as a conformationally frozen core with a well-defined number of end groups. The tyrosine-modified dendrimers, which have phenolic end groups, are reactive in a redistribution reaction with PPE to give star-shaped PPE (Figure 4.2). The arm length of the star-branched PPE is easily regulated by the employed phenol/PPE ratio. These star polymers with a well-defined number of arms will be nice model compounds to study miscibility of linear/star blends. The aim of this research is the investigation of the miscibility behaviour of these star polymers with linear polystyrene (PS) with variation of the number of arms of the PPE star polymer.

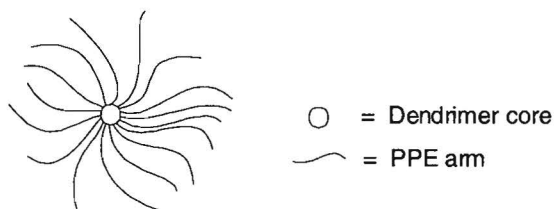


**Figure 4.1:** Schematic representation of a star polymer.

## 4.2 Results and discussion

### 4.2.1 Materials

The star-shaped PPEs are prepared by a redistribution reaction of PPE with a multifunctional phenol.<sup>34,35</sup> Redistribution experiments using *para-tert*-butyl-calix-[*n*]arenes<sup>39</sup> ( $n = 4$  or  $8$ ) yields star-shaped PPEs.<sup>40</sup> However, the reactivity of these calixarenes is rather low due to the specific orientation of the hydrogen-bonded phenolic endgroups. Poly(propylene imine) dendrimers modified with phenolic endgroups are studied in more detail in the PPE redistribution because they contain a well-defined number of endgroups. This approach yields star polymers with a poly(propylene imine) dendrimer core and 4, 8, 16, 32, or 64 polymer arms, depending on the dendrimer generation. For example, using DAB-*dendr*-(NH<sub>2</sub>)<sub>64</sub>, a modified dendrimer with 64 tyrosine endgroups (DAB-*dendr*-(NH-*t*-BOC-L-Tyr)<sub>64</sub>) can be prepared. Redistribution of this *N-t*-BOC-protected tyrosine modified dendrimer with 61.8 moles of PPE ( $\bar{M}_n = 11.2$  kg/mol) yields a 64-arm star-shaped PPE (Figure 4.2) with an estimated average arm length of 90 PPE repeating units.

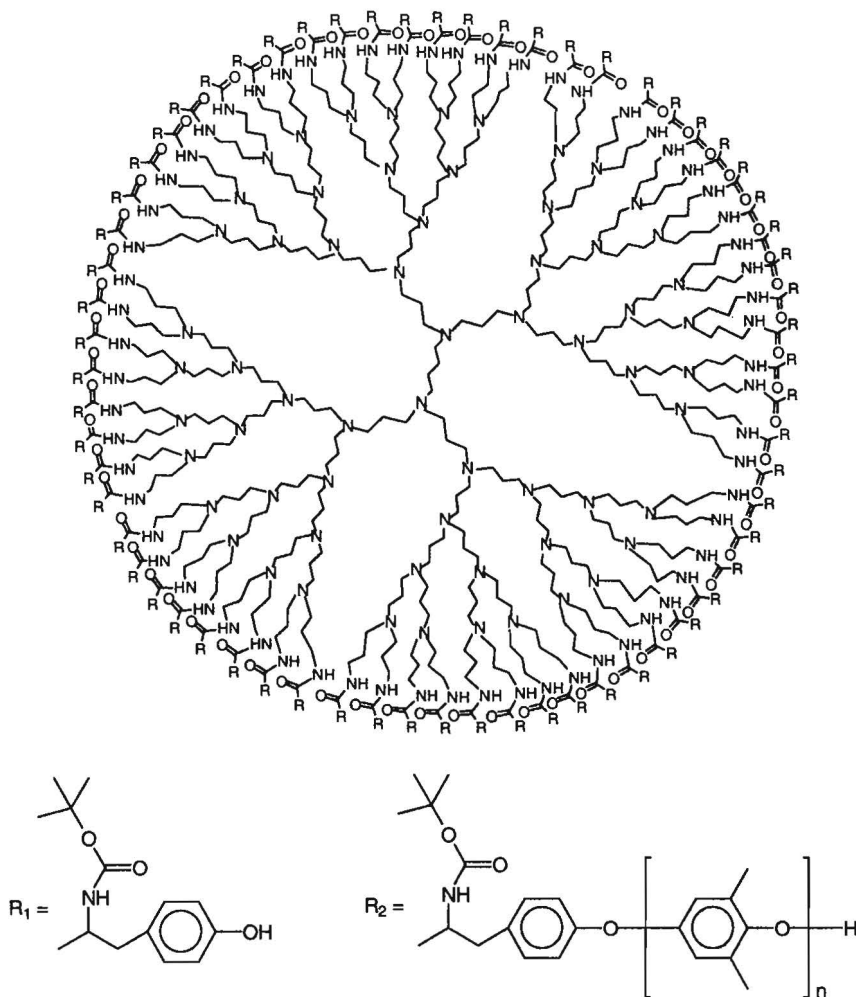


**Figure 4.2:** Dendritic structure using  $R = R_1$ :  $(DAB-dendr-(NH-t-BOC-L-Tyr))_{64}$  and using  $R = R_2$ : 64-arm PPE star-shaped polymer prepared from  $(DAB-dendr-(NH-t-BOC-L-Tyr))_{64}$

The number of phenolic endgroups can be varied by reacting the fifth-generation (64 end groups) amino-terminated poly(propylene imine) dendrimers with a mixture of *t*-Boc-protected hydroxysuccinimide-activated esters of L-tyrosine and D-phenylalanine. Employing these modified dendrimers in the PPE redistribution only the number of arms is varied but not the size of the dendritic core which is constant for each generation. Now that we can easily control the number of arms of the PPE star polymers, it is interesting to study its influence on physical behaviour in solution and in blends with PS.

Due to the long reaction times some methyl-group oxidation can not be avoided. This causes broadening of the signals in the  $^1\text{H-NMR}$  spectra. From NMR, it can not be concluded how many PPE arms are attached to the dendrimer core. We only used  $^1\text{H-NMR}$  spectroscopy to verify whether the dendrimer signals (e.g. *tert*-butyl) are in the expected integral ratio with signals from PPE. *Ortho*-methyl substituted phenols are supposed to give a more easy characterization, due to the shorter reaction time required, which leads to less methyl-group oxidation. For example, tetraphenols prepared from condensation of 2,6-dimethylphenol and a dialdehyde,<sup>41</sup> like 1,1,5,5-tetrakis(4-hydroxy-3,5-dimethylphenyl)pentane, are proposed to give a more efficient redistribution yielding more well-defined 4-armed star-shaped PPEs. The fact that we have indeed star-shaped PPE arises from their characteristic properties in solution and in blends with PS.

The star polymers are characterized by a number of techniques, including SEC and their properties in blends with polystyrene are investigated. The results of these studies are discussed below and confirm the structures assigned.

#### 4.2.2 Star-shaped PPEs in solution

Size Exclusion Chromatography (SEC) can be a powerful tool for characterization of star-branched polymers,<sup>42-45</sup> especially when a Low-Angle Laser Light Scattering detector (LALLS) is implemented. However, in our case the star polymers gave too low scattering intensities to obtain reliable data from LALLS. When chloroform was used as an eluent, the star polymers showed strong interaction with the SEC-column, in contrast to linear analogues. However when tetrahydrofuran (THF) was employed as eluent, the polymer-column interaction was strongly reduced, possibly due to solvation of the phenolic endgroups of the polymer arms by THF. Moreover, chloroform is a better solvent for PPE than THF, therefore polymer arms could be more collapsed when dissolved in THF and shield the polar core. When chloroform was applied as solvent in the DLS experiments star polymers showed large aggregates, while in THF the star polymers showed single particle behaviour.<sup>46</sup> Therefore, THF is preferred as solvent for the study of star polymers in solution.

Star-shaped PPEs with an estimated armlength of 22.5 units from different dendritic core generations and therefore with a different number of arms, show the same hydrodynamic volume in SEC, as shown in Figure 4.3. The difference in core-size is not expressed in a hydrodynamic volume change but only in an increase in segmental density. Furthermore, we characterized star polymers with the same core-size but a different number of arms caused by

partial modification with tyrosine endgroups. These star polymers are prepared from a 5th generation poly(propylene imine) dendrimer, modified with a mixture of tBOC-protected hydroxysuccinimide activated esters of L-tyrosine and D-phenylalanine. Only the tyrosine endgroups will react with PPE in a redistribution. In this case polymers prepared from 20% and 40% tyrosine-modified dendrimers showed lower hydrodynamic volume, probably due to less extended polymer arms (Figure 4.4).

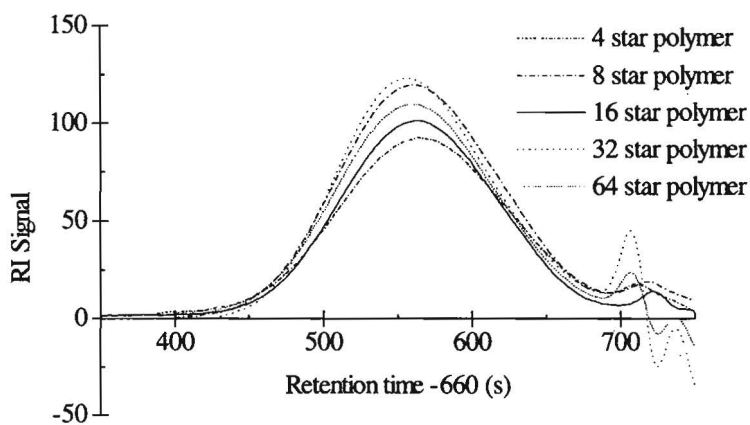


**Figure 4.3:** SEC plots of PPE star polymers with an estimated armlength of 22.5 units, prepared from different dendrimer core generations; eluent = THF.

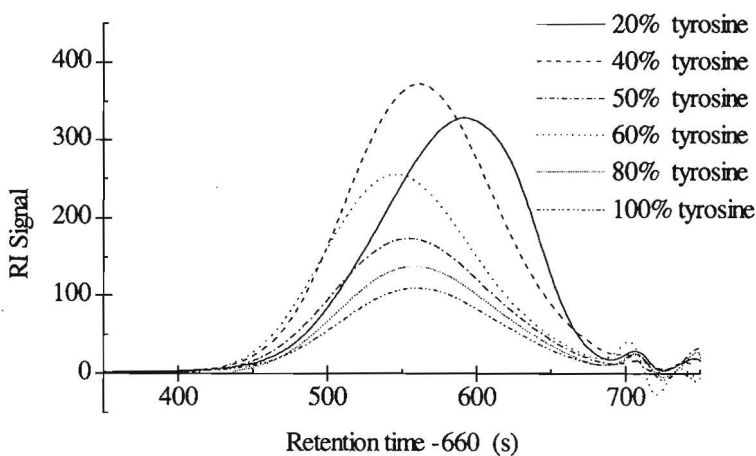


**Figure 4.4:** SEC plots of PPE star polymers with an estimated armlength of 22.5 units prepared from a 5th generation dendrimer core with variation of the tyrosine/ phenylalanine ratio; eluent = THF.

Star polymers with the same hydrodynamic volume as detected by SEC, however, show a large deviation in measured hydrodynamic radius ( $R_H$ ) by DLS (Table 4.1). The  $R_H$  increases with the number of arms. This increase is proposed to be caused by a decreased free-draining in the starpolymers containing more densely packed PPE arms at high number of arms.

**Table 4.1:** Hydrodynamic radii measured by DLS in THF

dendrimer generation (endgroups)	tyrosine/phenylalanine ratio	estimated number of PPE arms	average degree of polymerization (PPE units)	$R_H$ (nm)
5 (64)	0/100	0	0	2.1
5 (64)	20/80	12.8	22.5	2.4
5 (64)	50/50	32	22.5	3.4
5 (64)	80/20	51.2	22.5	4.0
5 (64)	100/0	64	22.5	5.7
4 (32)	100/0	32	22.5	4.2
2 (8)	100/0	8	22.5	3.7

Star polymers with the same dendritic core but an increasing number of PPE arms of the same estimated length show a lower refractive index increment ( $dn/dc$ ), while star polymers with same arm length prepared from different dendrimer generations show a constant  $dn/dc$ . The  $dn/dc$  is higher for the dendritic core than for the PPE arms. Therefore only qualitative data could be obtained using SEC implementing a visco-detector and refractive index (RI) detector. The measured intrinsic viscosities (IV) from this visco-detector decrease when the number of arms is increased, either by increasing the dendrimer generation or tyrosine/phenylalanine ratio (Table 4.2). These lower IVs of starpolymers with a high number and more densely packed PPE arms are in agreement with the theoretical predictions using a phantom-chain model for star-shaped polymers by Ganazzoli.<sup>4</sup>

**Table 4.2:** Intrinsic viscosities in THF measured by SEC/viscometer.

polymer type	dendrimer generation	tyrosine/phenylalanine ratio	estimated number of arms	average arm length (PPE-units)	batch IV (dL/g)
linear	-	0/0	1	39	0.157
star	2	100/0	8	22.5	0.052
star	5	100/0	64	22.5	0.041
star	5	40/60	25.6	22.5	0.081

### 4.2.3 Blends of star-shaped PPE and linear PS

The miscibility behaviour of blends is usually investigated by determination of glass transition ( $T_g$ ) temperatures. As a reference, we determined the  $T_g$ s by differential scanning calorimetry (DSC) of the star polymers, which are used in blends with linear polystyrene (PS). We observed an independence of  $T_g$  on the core generation of the star polymers by DSC and no large differences are observed in  $T_g$  of the star-shaped PPEs in comparison with a linear PPE (Table 4.3). This is in agreement with the theoretical treatment of the  $T_g$  of dendritic polymers as described by Stutz.<sup>47</sup> In star or dendritic polymers the glass temperature only depends on the molecular weight of a dendron, but not on the molecular weight of the whole molecule. Therefore  $T_g$  is governed primarily by the backbone glass temperature and depends little on grafting functionality. Only minor differences in  $T_g$  between linear macromolecule and dendritic structure are obtained, since the influences of endgroups and branching compensate each other to a large extent, as reported by Stutz.<sup>47</sup>

**Table 4.3:** Glass transition temperatures as measured by DSC, heating rate 20 °C /min, second heating run.

polymer type	estimated number of arms	average arm length (repeating units)	$T_g$ (°C)
linear PS	1	909	107.0
linear PPE	1	93	209.1
star PPE	4	90	210.4
star PPE	8	90	211.1
star PPE	16	90	209.8
star PPE	32	90	209.9
star PPE	64	90	211.2

Both star-branched PPEs and linear PPE are employed in blends with linear polystyrene at a 1:1 (w/w) ratio. Glass transition temperatures were determined by dynamic mechanical thermal analysis (DMTA). The homogeneous linear PPE-linear PS blend shows a single  $\tan\delta$  peak after extrusion as expected (Figure 4.5). When a 4-arm star polymer is extruded with linear polystyrene, a slightly broadened  $\tan\delta$  peak is observed (Figure 4.6). A further broadening is observed for the 8-arm star polymer. Beyond 8 arms two  $\tan\delta$  peaks are observed, indicating that phase separation occurs (Figure 4.7). The extruded samples clearly show that the liquid-liquid demixing is enhanced for higher number of arms of the star polymer. Extruded blends of polystyrene either with 4- or 8-arm star-shaped PPE are transparent and show high toughness. Phase separation becomes more pronounced when the number of arms of the star-branched PPE is increased. Extruded blends with 32- or 64-arm star-shaped PPE are opaque and extremely brittle. Moreover, blends with highly branched PPE show severe delamination. The DMTA results are summarized in Table 4.4. The phase-separation of polystyrene and PPE star polymers becomes more pronounced at high number of arms.

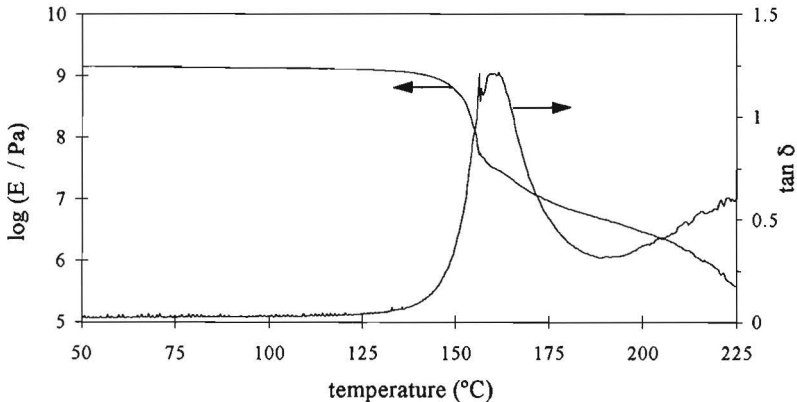


**Figure 4.5:** DMTA scan of a blend with 50 wt% linear PS and 50 wt% linear PPE.



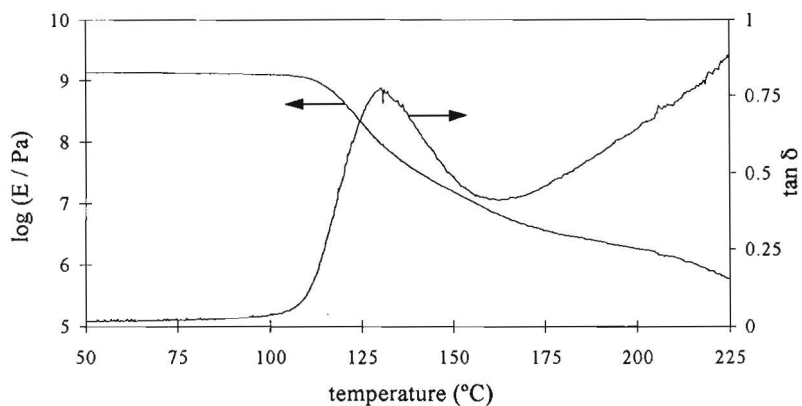


Figure 4.6: DMTA scan of a blend with 50 wt% 4-arm PPE star and 50 wt% linear PS.

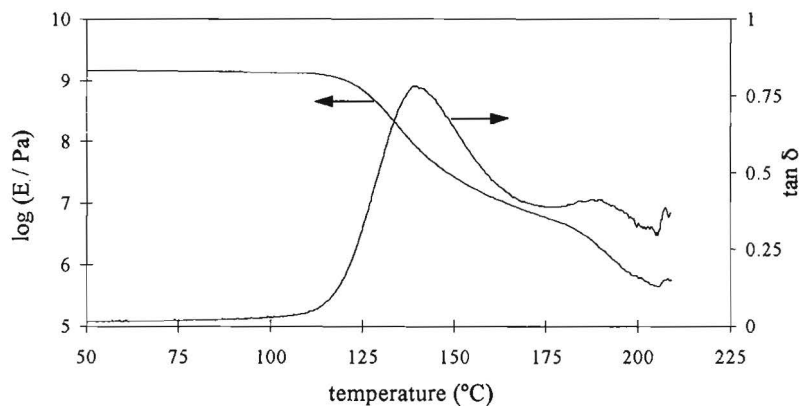


Figure 4.7: DMTA scan of a blend with 50 wt% 64-arm star PPE and 50 wt% linear PS.

Table 4.4:  $\text{Tan}\delta$  peaks as measured by DMTA.

blend type PS/PPE	first $\text{tan}\delta$ peak ( $^{\circ}\text{C}$ )	second $\text{tan}\delta$ peak ( $^{\circ}\text{C}$ )
linear/ linear	160	-
linear/ 4-star	132	-
linear/ 8-star	154	-
linear/ 16-star	139	174 <sup>a</sup>
linear/ 32-star	129	167
linear/ 64-star	140	189

<sup>a</sup> no clear  $\text{tan}\delta$  peak, sample specimen breaks at 184  $^{\circ}\text{C}$

### 4.3 Conclusions

Star-shaped PPEs can be obtained by redistribution of PPE with phenol-modified poly(propylene imine) dendrimers. Star-shaped polymers with a high number of PPE arms give rise to inhomogeneous blends with linear polystyrene. The widening of the damping peak<sup>48</sup> indicates a decreased miscibility upon increasing the number of arms. The specific chain conformation of the starpolymers is reflected in the solution properties. Star polymers with constant armlength but increasing number of arms show the same hydrodynamic volume as measured by SEC, but decreasing hydrodynamic radius as measured by DLS. This confirms the dense packing of the polymer arms of the star-shaped PPE. Intrinsic viscosities decrease at higher number of arms, as was predicted theoretically for star-shaped polymers.<sup>4,11</sup>

### 4.4 Experimental

#### *Materials*

Linear PS (N5000) is obtained from 'Bredase Polystyreen Maatschappij' ( $\overline{M}_n = 80.0$  kg/mol,  $M_w=260000$  g/mol). Linear PPE (PPE-1) is obtained from General Electric Plastics ( $\overline{M}_n = 14.5$  kg/mol,  $\overline{M}_w = 30.2$  kg/mol). Low molecular weight PPEs were obtained using a precipitation polymerization method (Chapter 2). CuCl 99% pure and 4-dimethylaminopyridine (DMAP) 99% pure were obtained from Acros. The solvents chloroform, DMSO and methanol were used p.a. from Merck. Ethylenediaminetetraacetic acid trisodiumsalt hydrate (EDTA) 95% pure was obtained from Aldrich.

#### *Techniques*

SEC as presented in figures 4 and 5 is performed using THF (40 °C) as eluent, 2 Shodex KF 80-M linear columns (8 \* 300 mm), a differential refractive index detector (RI) detector and a flow rate of 1 ml/min. DLS measurements are performed using a ALV/SP-86 goniometer with a Spectra Physics series 2000 Ar<sup>+</sup> laser (514.5 nm, 300 mW). Intrinsic viscosities are measured using SEC implementing a viscodetector (Viscotec Model 40), using THF (40 °C) as eluent, 3 APS linear columns and a flow rate of 1 ml/min. Glass transition temperatures ( $T_g$ ) of these polymers are measured using a Differential Scanning Calorimeter (Perkin Elmer DSC-7) during the second heating run with a heating rate of 20 °C/min. Testing specimens of polymer blends that were approximately 20 mm long, 2 mm thick and 4 mm wide are prepared by compression moulding at 220 °C during 5 minutes. These specimens are investigated by dynamical thermal analysis (DMTA) (Polymer Laboratories, MKIII) in the tensile mode with a heating rate of 2 °C/min and a frequency of 1 Hz.

#### *Preparation of the star-shaped PPEs:*

PPE redistribution experiments of mixed phenylalanine/tyrosine-modified poly(propylene imine) dendrimers are performed in chloroform, while 100% tyrosine-modified dendrimers are reacted in chloroform/DMSO mixtures due to low solubility of tyrosine-modified dendrimers in chloroform. All

redistributions take place under inert argon atmosphere, at room temperature during 18 days using Pyrex glass vessels. As an example the preparation of 16-arm PPE star polymer with an armlength of 22.5 PPE units is described. To a solution of 1.11 g PPE ( $\overline{M}_n = 5.52$  kg/mol) in 30 mL chloroform, 0.150 g of the DAB-*dendr*-(NH-*t*-BOC-L-Tyr)<sub>16</sub> dissolved in 2 mL DMSO is added slowly. Subsequently 0.0114 g CuCl and 0.0242 g 4-dimethylaminopyridine (DMAP) is added. After 18 days reaction time the reaction mixture is extracted subsequently with an aqueous 10 wt% EDTA solution, water, and an aqueous 10 wt% HCl solution. Phase separation during extraction was improved by centrifugation. The chloroform solution was then partially evaporated at a rotary evaporator until a volume of 15 mL and then precipitated in 200 mL chloroform. The precipitated polymer was collected by filtration and dried in a vacuum oven at 60 °C.

#### *Preparation of PPE/PS blends*

The 50/50 (w/w) PPE/PS blends were prepared using a laboratory-scale mini-extruder, which operates continuously or batchwise. The device consists of two co-rotating, closely intermeshing, self-wiping, conical screws and is equipped with a recurrent loop and valve system. The device allows processing small quantities of material (volume = 6 cm<sup>3</sup>) at temperatures up to ~ 400 °C in a way equivalent to large-scale industrial co-rotating twin screw extruders. All star/linear and linear/linear blends in a 1 : 1 (w/w) ratio were extruded at 230 °C, during 3 minutes.

## 4.5 References

1. Roovers, J. *Trends Polym. Sci.*, **2**, 294 (1994).
2. Grest, G.S., Fetters, L.J., Huang, J.S. and Richter, "Advances in Chemical Physics", volume 94, eds. Prigogine, I. and Rice, S.A., John Wiley & Sons Inc., New York, 67 (1996).
3. Fetters, L.J., Kiss, A.D., Pearson, D.S., Quack, G.F. and Vitus, F.J. *Macromolecules*, **26**, 647 (1993).
4. Ganazzolli, F., Allegra, G., Colombo, E. and De Vitis, M. *Macromolecules*, **28**, 1076 (1995).
5. Richter, D., Jucknischke, O., Willner, L., Fetters, L.J., Lin, M., Huang, J.S., Roovers, J., Toporovski, C. and Zhou, L.L. *J. Phys. IV*, **3**, 3 (1993).
6. Roovers, J. and Martin, J.E. *J. Polym. Sci., Polym. Phys. Ed.*, **27**, 2513 (1989).
7. Bauer, B.J., Fetters, L.J., Graessley, W.W., Hadjichristidis, N. and Quack, G.F. *Macromolecules*, **22**, 2337 (1989).
8. Douglas, J.F., Roovers, J. and Freed, K.F. *Macromolecules*, **23**, 4168 (1990).
9. Frater, D.J., Mays, J.W. and Jackson C. *J. Polym. Sci., Polym. Phys. Ed.*, **35**, 141 (1997).
10. Kuwano, K., Nagata, K., Nagasawa, M. and Hibino, H. *Kobunshi Ronbunshu*, **53**, 165 (1996).
11. Zimm, B.H. and Kilb, R.W. *J. Polym. Sci.*, **37**, 19 (1959); *J. Polym. Sci., Polym. Phys. Ed.*, **34**, 1367 (1996).
12. Freire, J.J., Rey, A., Bishop, M. and Clarke, J.H.R. *Macromolecules*, **24**, 6494 (1991).
13. Utracki, L.A. *Polym. Eng. Sci.*, **35**, 2 (1995).

- 14 . Freed, K.F. and Dudowicz, J. *Macromolecules*, **29**, 625 (1996).
- 15 . Hill, M.J. *Polymer*, **35**, 1991(1994).
- 16 . Mumby, S.J., Sher, P. and van Ruiten, J. *Polymer*, **36**, 2921(1995).
- 17 . Puig, C.C, Odell, J.A., Hill, M.J., Barham, P.J. and Folkes, M.J. *Polymer*, **35**, 2453 (1994).
- 18 . Clarke, N. and McLeish, T.C.B. *J. Chem. Phys.*, **99**, 10034(1993).
- 19 . Feng, H., Feng, Z. and Shen, L. *Macromolecules*, **27**, 7840 (1994).
- 20 . Sikorski, A., Kolinski, A. and Skolnick, J. *Macromol. Theory Simul.*, **3**, 715 (1994).
- 21 . Roovers, J. *Macromolecules*, **20**, 148 (1987).
- 22 . Struglinski, M.J., Graessley, W.W. and Fetters, L.J. *Macromolecules*, **21**, 783 (1988).
- 23 . Russell, T.P., Fetters, L.J., Clark, J.C., Bauer, B.J. and Han, C.C. *Macromolecules*, **23**, 654 (1990).
- 24 . Factor, B.J., Russell, T.P., Smith, B.A., Fetters, L.J., Bauer, B.J. and Han, C.C. *Macromolecules*, **23**, 4452 (1990).
- 25 . Faust, A.B., Sremcich, P.S. and Gilmer, J.W. *Macromolecules*, **22**, 1250 (1989).
- 26 . Gorda, K.R. and Peiffer, D.G. *J. Appl. Polym. Sci.*, **50**, 1977 (1993).
- 27 . Birshstein, T.M., Zhulina E.B. and Borisov, O.V. *Polymer*, **27**, 1078 (1986).
- 28 . Bair, H.E. *Polym. Eng. Sci.*, **10**, 247 (1970).
- 29 . Yee, A.F. *Polym. Eng. Sci.*, **17**, 213 (1977).
- 30 . Shultz, A.R. and Beach, B.M. *Macromolecules*, **7**, 902 (1974).
- 31 . Maconnachie, A., Kambour, R.P., White, D.M., Rostami, S. and Walsh, D.J. *Macromolecules*, **17**, 2645 (1984).
- 32 . Li, S., Dickinson, C. and Chien, J.C.W. *J. Appl. Polym. Sci.*, **43**, 1111 (1991).
- 33 . Nelissen, L., Nies, E. and Lemstra, P.J. *Polymer Commun.*, **31**, 122 (1990).
- 34 . Van Aert, H.A.M., Burkard, M.E.M., Jansen, J.F.G.A., van Genderen, M.H.P., Meijer, E.W., Oevering, H. and Werumeus Buning, G.H. *Macromolecules*, **28**, 7967(1995)
- 35 . Oevering, H., Werumeus Buning, G.H., Meijer, E.W., van Aert, H.A.M. and Out, G.J.J. Int. Patent WO 96/01865 (1996).
- 36 . De Brabander-van den Berg, E.M.M. and Meijer, E.W. *Angew. Chem., Int. Ed. Engl.*, **32**, 1308 (1993).
- 37 . Jansen, J.F.G.A., de Brabander-van de Berg, E.M.M. and Meijer E.W. *Science*, **266**, 1226 (1994).
- 38 . Jansen, J.F.G.A., Peerlings, H.W.I., de Brabander-van den Berg, E.M.M. and Meijer, E.W. *Angew. Chem., Int. Ed. Engl.*, **34**, 1206 (1995).
- 39 . Gutsche, C.D. "Calixarenes", J. F. Stoddard ed., The Royal Society of Chemistry, Cambridge, (1989).
- 40 . Burkard, M.E.M. "Synthese en karakterisering van poly(fenyleen ether) sterpolymeren", Undergraduate report, Eindhoven University of Technology, (1994).
- 41 . Lee, M-C., Ho, T-H. and Wang, C-S. *J. Appl. Polym. Sci.*, **62**, 217 (1996).
- 42 . Taromi, F.A., Grunbiscic-Gallot, Z. and Rempp, P. *Eur. Polym. J.*, **25**, 1183(1989).
- 43 . Lesec, J. and Millequant, M. *Int. J. Polym. Anal. Characterization*, **2**, 305 (1996).
- 44 . Lesec, J. and Millequant, M. *Polym. Mat. Sci. Eng.*, **69**, 265 (1993).

- 45 . Lesec, J., Millequant, M., Patin, M., Teyssie, P. *Adv. Chem. Ser.*, 247, 167 (1995).
- 46 . Moussaïd, A. private communication.
- 47 . Stutz, H. *J. Polym. Sci., Polym. Phys. Ed.*, **33**, 333 (1995).
- 48 . Ward, I.M., "Mechanical properties of solid polymers", second edition, John Wiley & Sons, Chichester, 175 (1990).

## Chapter 5

### Endgroup modification of poly(2,6-dimethyl-1,4-phenylene ether) using phase-transfer catalysis

#### Summary

*Endgroup modification of poly(2,6-dimethyl-1,4-phenylene ether) (PPE) has been performed with phase-transfer catalysis and endgroups like cyano, amino, allyl, methoxy, nitro and carboxylic acid are introduced. Trioctylmethylammonium chloride (TOMA) and tetrabutylammonium hydroxide (TBAH) are used as phase-transfer catalyts. The functionalized PPEs can be used as precursor for larger polymeric structures or the endgroups can be converted into other endgroups. This is illustrated by the conversion of allylic endgroups into hydroxypropyl endgroups by a hydroboration/oxidation reaction. All described endgroup modifications of monofunctional PPEs are also applicable to bifunctional telechelic PPEs.*

#### 5.1 Introduction

Poly(2,6-dimethyl-1,4-phenylene ether) (PPE) belongs to a class important engineering plastics.<sup>1</sup> Main-chain and endgroup functionalization of this widely employed polymer is an important topic of research because these modified polymers can be used as precursors for block<sup>2-16</sup> and graft copolymers<sup>17-26</sup> and in polymer blends to influence miscibility.<sup>27-29</sup>

PPE with amino endgroups can for example be used in blends of PPE and epoxy resin,<sup>30</sup> or in thermoplastic elastomers based on PPE and 1,4-polyisoprene.<sup>2</sup> Cyano endgroups are prepared because these endgroups can be converted to amino and carboxylic acid functionalities, which are reactive towards for example epoxy resins, polyesters and polyamides. The hydrogenation of polymeric nitrile groups into amino groups is studied in detail in our laboratory in the synthesis of poly(propylene imine) dendrimers.<sup>31,32</sup> Allylic endgroups can be converted to various useful functionalities, like epoxy, carboxylic acid, and hydroxyl. These allyl functionalities can be epoxidized by a number of peracids,<sup>33</sup> of which *m*-chloroperbenzoic acid has been the most often used. Hydroboration<sup>34-37</sup> of the allyl functionality and subsequent oxidation can give a hydroxy endgroup. These hydroxyalkyl-substituted PPEs are suitable as compatibilizing agent for PPE/polyester blends, which is described in Chapter 6. Besides reactive endgroups, non-reactive endgroups in PPE, like methoxy, are also of interest.<sup>30</sup>

Main chain functionalization<sup>38-49</sup> can be accomplished by electrophilic substitution reactions on the aromatic ring of PPE, radical substitution reactions on the methyl groups of PPE and metallation of PPE with organometallic compounds. For example, carboxylated PPE has been prepared by metallation of PPE with *n*-butyllithium followed by a treatment with an excess of carbon dioxide.<sup>19</sup> This carboxylated PPE was modified with a caprolactam endgroup and then used as macro-initiator in the anionic graft copolymerization of  $\epsilon$ -caprolactam. Main chain functionalization often yields ill-defined products due to multiple reaction sites.

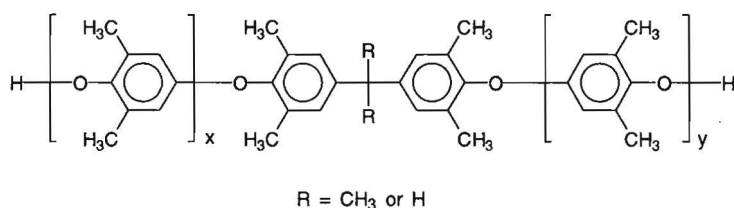
In contrast to the main-chain functionalization, a well-defined location of functional groups is obtained using endgroup functionalization. Besides endgroup modification at the 2,6-dimethylphenoxy tail end of PPE (Chapter 3), endgroup modification at the phenolic head endgroups is feasible. The phenolic head group can react as a nucleophile with several electrophiles. However, the reactivity of the phenolic endgroup is rather low. The terminal hydroxyl groups of PPE are less acidic than the hydroxyl group of phenol, due to electron-donating effects of the methyl groups at the *ortho*-positions and the etheric oxygen in the *para*-position. Although the acidity of the phenol decreases when *ortho*-methyl groups are present, the nucleophilicity of the formed phenolate will be higher. Furthermore, the steric influence of the two methyl groups is significant in reactions with bulky electrophiles. Also, the conformational behaviour of PPE in solution influences conversion. In non-polar solvents the terminal hydroxyl groups are less accessible than in more polar solvents. On the other hand PPE is insoluble in strongly polar solvents.

Nevertheless, numerous functional endgroups can be introduced in PPE, as is mainly described in patent literature.<sup>50-66</sup> For example, Campbell<sup>9,10</sup> used PPEs functionalized with fumaric acid, maleic anhydride or trimellitic anhydride acid chloride for the preparation of polycarbonate-PPE copolymers. Grutke<sup>21</sup> used norbornene-functionalized PPEs as a macromonomer in a ring-opening olefin metathesis polymerization (ROMP). Sato<sup>22</sup> used bis-carboxylic-acid-functionalized PPE for the synthesis of thermotropic liquid-crystalline aromatic polyester-*graft*-PPE copolymers. In most of these described modification reactions, functionalization is obtained by an ester linkage of PPE with reactants like acid chlorides or anhydrides. Modification by ether linkage is preferred, because the phenolic esters are less stable. This is caused by the good leaving group character of phenolates, which are formed during decomposition or hydrolysis of the phenolic esters. In particular, electron-deficient phenolates have a good leaving group character. Especially modification routes involving an ether linkage using phase-transfer catalysis (PTC) can give effective functionalizations.

Phase-transfer catalysis (PTC), a term which has been coined by Starks,<sup>67</sup> has become an active subject of research with deep implications, especially in preparative organic, organometallic and polymer chemistry. The use of phase-transfer catalysis for the synthesis of low molecular weight

phenol ethers is described by McKillop.<sup>68</sup> His method involves alkylation of the phenoxide ion with an alkyl halide or sulphate ester in a methylene chloride-water system at room temperature. A quaternary ammonium salt is used as the effective reagent for the transport of the phenoxide ion between the two phases. A review on developments in polymer synthesis by PTC is given by Percec.<sup>69</sup> Coupling and capping reactions on PPE using PTC, resulting in different endgroups, have been introduced by White.<sup>70,71</sup> For example, PPE was endcapped with acetic anhydride and coupling reactions were performed using isophthaloyl chloride, which results in chain-extended PPEs with higher molecular weight. In particular, PTC was often employed in the preparation of PPE-macromonomers<sup>23-26</sup> by Percec, reacting *p*-chloromethyl styrene.<sup>72-74</sup>

Since the phenolic endgroups of poly(2,6-dimethyl-1,4-phenylene ether) have a low reactivity, introducing more reactive endgroups, like amino-endgroups, is an important topic in our laboratory. The scope of etherification of the phenolic endgroup is investigated using phase-transfer catalysis, leading to endgroups such as cyano, amino, allyl, methoxy, nitro and carboxylic acid. These modification reactions are investigated for monofunctional PPEs, but also for  $\alpha,\omega$ -bishydroxy functional PPE telechelics as presented in Scheme 5.1. These bifunctional telechelic PPEs were prepared by PPE redistribution with bisphenols.<sup>75-77</sup> We are mainly interested in modification of low molecular weight polymers, which can be used as building block in larger macromolecular structures, like block copolymers. These low molecular weight polymers are easier to characterize.



**Scheme 5.1:**  $\alpha,\omega$ -bishydroxy functional PPE telechelics.

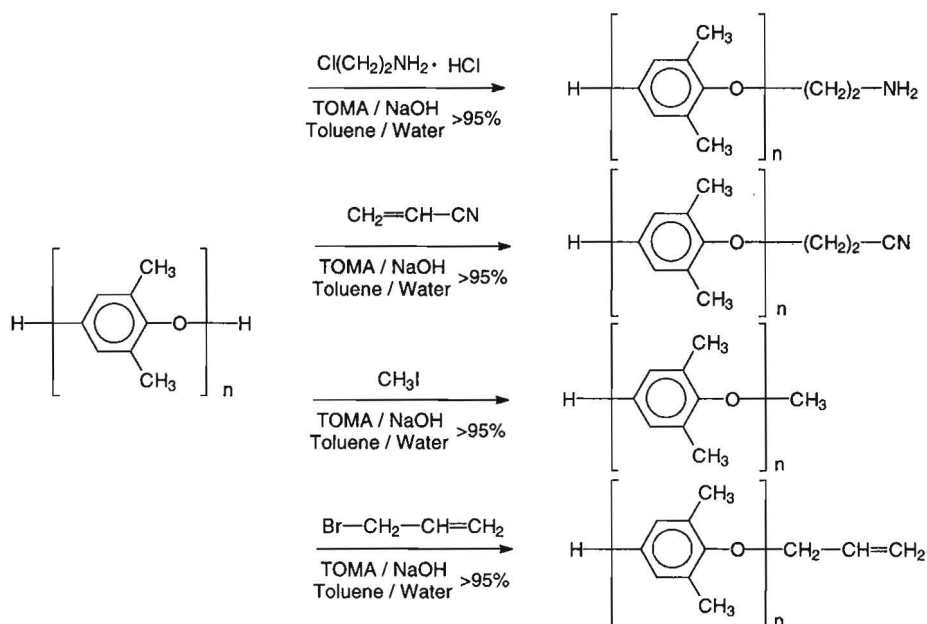
The scope of etherification of the phenolic endgroup using of phase transfer catalysis leading to a variety of endgroups is described in this Chapter. These ether-modified PPEs are generally more stable than ester-modified PPEs, which are most often described in literature. Phase transfer catalysis is used to enhance the reactivity of the phenolic endgroup.



## 5.2 Results and discussion

### 5.2.1 Trioctyl methyl ammonium chloride as phase-transfer catalyst

The phenolic endgroup was modified using different reagents as illustrated in Scheme 5.2. The following reagents were used: acrylonitrile, 2-chloroethylamine hydrochloride, allyl bromide and iodomethane, in a reaction with PPE under the action of base and trioctyl methylammonium chloride (TOMA). With these reagents the following endgroups respectively are introduced: cyano, amino, allylic and methoxy-endgroups. In our investigation, we usually employ TOMA as a phase-transfer catalyst in the two-phase system of toluene and water. NaOH is used as base to produce the phenolate anion. With the trioctylmethylammonium cation as counterion, the PPE remains dissolved in toluene. If no phase-transfer agent is used, some of the PPE can precipitate as the sodium salt.



**Scheme 5.2:** Endgroup modifications of PPE using TOMA.

For the modification with amino endgroups using chloroethylamine hydrochloride, we used a procedure as described in patent literature,<sup>78-81</sup> but we investigated oligomeric PPEs, both mono- and bifunctional, with lower molecular weight for clear determination of endgroups using <sup>1</sup>H-NMR spectroscopy. All reactions occur in high yields (> 95%) within the detection limit of the <sup>1</sup>H-NMR spectroscopy, not only for monofunctional PPEs but also for bifunctional PPE telechelics.

The polymers are characterized with  $^1\text{H-NMR}$  spectroscopy. The modified polymers show additional peaks of the introduced endgroup, illustrated by the  $^1\text{H-NMR}$  spectrum (Figure 5.1) of the amino-endcapped polymer. The spectrum of this amino-endcapped polymer, precipitated in methanol, shows next to the PPE signals two additional signals at 3.06 and 3.76 ppm. When the polymer is precipitated in acidified methanol the polymeric amino-HCl salt will precipitate (3.40 and 4.02 ppm). The reaction with chloroethylamine hydrochloride occurs probably via aziridine<sup>82</sup> in a nucleophilic substitution. The spectrum of the cyano-endcapped polymer prepared with acrylonitrile also shows signals from the acrylonitrile-water adduct (2.65 and 3.75 ppm). After reprecipitation these peaks disappear. The modified polymer has two additional triplet signals (2.79 and 3.94 ppm). The reaction with acrylonitrile is a Michael addition and has to be performed at low reaction temperature (room temperature) to prevent the retro-Michael reaction. Also, no large excess of NaOH should be employed or acrylonitrile polymerization will occur. The methoxy-endcapped polymer has one extra peak at 3.67 ppm. The allyl-terminated polymer shows additional peaks at 6.10 (m), 5.41 (d), 5.24 (d) and 4.26 ppm (d). The Williamson syntheses with iodomethane and allyl bromide can also be performed at elevated temperatures.

Synthesis of hydroxypropyl-terminated PPEs is feasible starting from the allyl-terminated PPEs. Hydroboration is performed using bicyclo[3.3.1]nonan-9-one (9-BBN), but the use of  $\text{BH}_3\text{-THF}$  is also practicable. In the oxidation with an aqueous  $\text{H}_2\text{O}_2/\text{NaOH}$  solution,  $\text{H}_2\text{O}$  addition occurs in an anti-Markovnikov manner yielding the alcohol. Via extraction and precipitation, the side-product 1,5-dihydroxycyclooctane is easily removed. A disadvantage for preparation of the hydroxypropyl endgroups is that more than one reaction is required, i.e. the reaction with allyl bromide and the hydroboration/oxidation reaction. However, these reactions are very efficient and products are obtained in high yields (> 95%). Also bisallyl-terminated PPE telechelics easily can be converted into the hydroxypropyl derivatives. However, we prefer the use of 9-BBN in the hydroboration of bisallyl compounds. When  $\text{BH}_3\text{-THF}$  is used, network formation occurs and low polymer concentrations are necessary to obtain complete reaction. The hydroxyalkyl-functionalized PPEs are very useful in the reactive compatibilization of PPE/polyester blends, as discussed in Chapter 6. Alternative methods to produce hydroxyalkyl functionalities at PPE phenolic endgroups are less efficient, like reactions of the phenolic endgroup or its phenolate anion with ethylene oxide, ethylene carbonate,  $\gamma$ -butyrolactone,  $\epsilon$ -caprolactone, 3-bromopropanol or 2-bromoethanol. No quantitative modification of the phenolic endgroup could be obtained using these reagents.

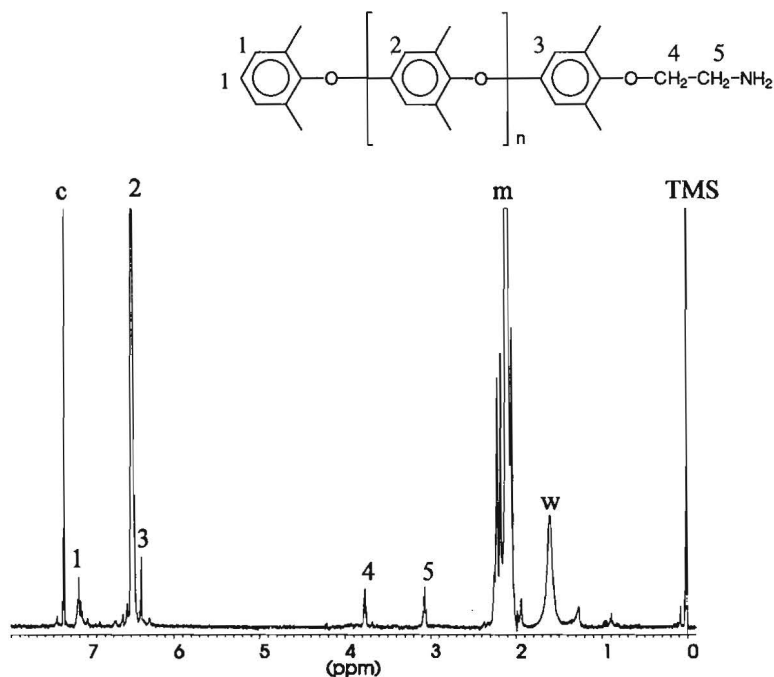
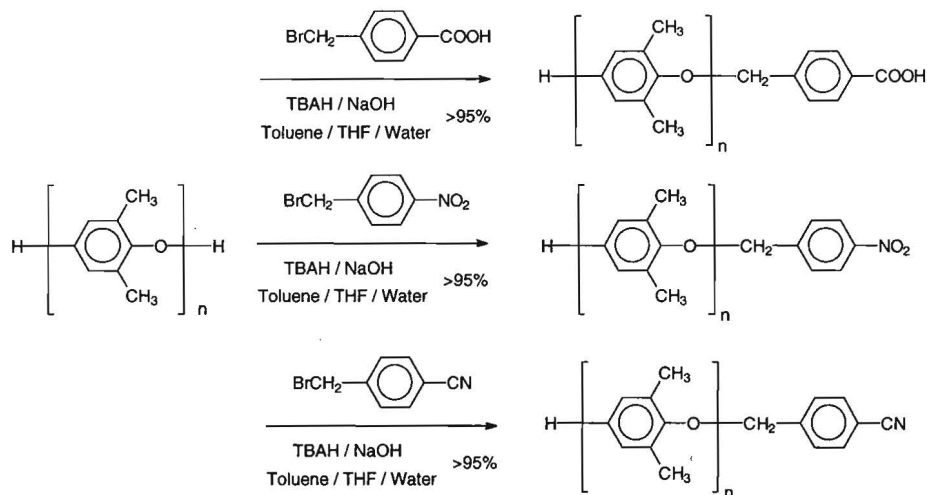


**Figure 5.1:**  $^1\text{H-NMR}$  spectrum in  $\text{CDCl}_3$  of amino-encapped PPE (neutral form); the signals marked with *c*, *m* and *w* are assigned to  $\text{CHCl}_3$ , PPE methyl groups and  $\text{H}_2\text{O}$ , respectively.

## 5.2.2 Tetrabutylammonium hydroxide as phase-transfer catalyst

Analogous to a synthetic procedure for the preparation of PPE macromonomers reacting PPE with *para*-chloromethylstyrene, described by Percec,<sup>72-74</sup> we also reacted several benzylic halides with PPE. Carboxylic acid, nitro and cyano endgroups are introduced at the PPE phenolic endgroup via reaction of respectively  $\alpha$ -bromo-*p*-toluic acid,  $\alpha$ -bromo-*p*-tolunitrile and 4-nitrobenzyl bromide as presented in Scheme 5.3. For this purpose, we used tetrabutylammonium hydroxide (TBAH) as phase transfer catalyst, because it was used successfully in the reaction of a similar benzyl halide by Percec.<sup>72-74</sup> In these modifications the polymer is dissolved in a mixture of toluene and THF. THF is added not only to improve the accessibility of the phenolic endgroup, but also to improve the solubility of the polar reagents, especially for  $\alpha$ -bromo-*p*-toluic acid. Solubility of the carboxylic acid can also be improved by reacting its methyl ester. Sato<sup>22</sup> introduces bis-carboxylic acids at the phenolic endgroup by reaction of a benzyl bromide with two methyl esters followed by a basic hydrolysis yielding the bis-carboxylic acid. The carboxylic-acid-modified PPEs are used in the reactive compatibilization of PPE/polyester blends. The benzyl-bromide-modified PPEs show in the  $^1\text{H-NMR}$  spectrum two additional doublets in the aromatic region and one singlet for the methylene

unit. The aromatic region of a  $^1\text{H-NMR}$  spectrum of a biscyano-endcapped PPE-telechelic with a tetramethylbisphenol acetone core is shown in Figure 5.2.



**Scheme 5.3:** Endgroup modifications of PPE using TBAH

All modifications performed occur in high yields (>95%) within the detection limit of the  $^1\text{H-NMR}$  spectroscopy and reaction yields are mainly influenced by fractionation during precipitation. No difference is observed in effectiveness of the performed modifications using benzyl bromides either for mono-functional PPEs or bifunctional PPE telechelics.

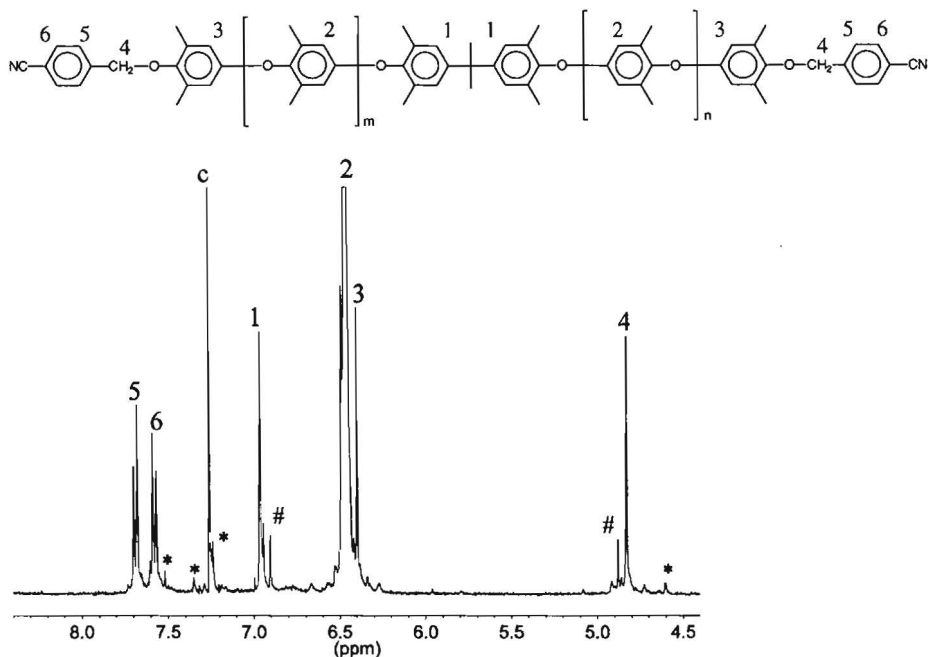


**Figure 5.2:** Aromatic region of the  $^1\text{H-NMR}$  spectrum of biscyano-encapped PPE telechelics, the signals marked with c, \*, # are assigned to chloroform, impurities and most probably structures in which 4-cyanobenzyl unit is attached directly to the BPA unit, respectively.

### 5.3 Conclusions

Phase-transfer catalysis is a useful technique for endgroup modification of poly(2,6-dimethyl-1,4-phenylene ether). Different groups at the phenolic end can be introduced like: cyano, amino, allyl, methoxy, nitro and carboxylic acid endgroups. These functionalized PPEs can readily be employed as reactive PPEs, or the endgroups can be converted to other endgroups. For example, the allyl groups are easily converted into hydroxypropyls by a hydroboration/oxidation reaction. The carboxylic-acid- and hydroxypropyl-functionalized PPEs are used in reactive compatibilization of PPE / polybutylene terephthalate (PBT) blends as described in Chapter 6. All described endgroup modifications of monofunctional PPEs are also applicable on bifunctional telechelic PPEs.

## 5.4 Experimental

### Materials

2-Chloroethylamine hydrochloride was used in a 70% aqueous solution from Acros. Acrylonitrile, 99+%, inhibited with 35–45 ppm hydroquinone monomethyl ether, iodomethane 99% pure, allyl bromide 99% pure and  $\alpha$ -bromo-*p*-toluic acid 97% pure were obtained from Acros. The phase transfer catalyst trioctylmethylammonium chloride was obtained as Aliquat 336 from Aldrich.  $\alpha$ -Bromo-*p*-tolunitrile 99% pure and a 0.5 molar solution of 9-BBN in THF was obtained from Aldrich. 4-Nitrobenzyl bromide with a purity of  $\geq 97\%$  was obtained from Fluka. Tetrabutylammonium hydroxide (TBAH) was used in a 40% aqueous solution from Merck. Sodium hydroxide pellets and toluene were obtained analytically pure from Merck. The employed monofunctional PPE was prepared using precipitation polymerization of 2,6-dimethylphenol<sup>83,84</sup> and bifunctional telechelic PPE was prepared by PPE redistribution with bisphenols.<sup>75-75</sup>

### Techniques

<sup>1</sup>H-NMR spectra were recorded in CDCl<sub>3</sub> on a Bruker AM-400 spectrometer at 400.13 MHz. All  $\delta$  values were given in ppm downfield from tetramethylsilane. Number average molecular weights were determined by comparison of the <sup>1</sup>H-NMR signals of the endgroups with those of the repeating unit.<sup>73</sup> IR spectra recorded on a Perkin Elmer 1600 series FT-IR spectrometer.

All products were obtained as off white powders after precipitation in methanol. All described reactions occur quantitatively, within the detection limit of the <sup>1</sup>H-NMR spectroscopy and reaction yields in general > 95% are only influenced by fractionation of the polymer occurring during precipitation.

### Michael addition with acrylonitrile

0.75 g of PPE-OH,  $\overline{M}_n = 2.69$  kg/mol, was dissolved in 7.5 mL toluene. Subsequently were added: 0.5 g TOMA and 0.02 g NaOH in 0.5 mL water. Then 15 mL acrylonitrile was slowly added at room temperature. After 2 days stirring at room temperature, the polymer solution was precipitated in a 10-fold excess of methanol. <sup>1</sup>H-NMR (CDCl<sub>3</sub>):  $\delta$  2.79 (2H, t, J = 5.0 Hz, CH<sub>2</sub>CN), 3.94 (2H, t, J = 5.0 Hz, OCH<sub>2</sub>), 7.09 (3H, m, arom. C-H tail-unit), 6.47 (~75H, broad s, arom. C-H repeating unit), 6.37 (2H, s, arom. C-H head unit), 2.09 (~225H, broad s, CH<sub>3</sub> repeating unit).  $\overline{M}_n = 4.8$  kg/mol as determined using <sup>1</sup>H-NMR spectroscopy. IR: 2250.8 cm<sup>-1</sup> CN-stretch

### Williamson synthesis with iodomethane

0.54 g PPE-OH,  $\overline{M}_n = 2.75$  kg/mol, was dissolved in 4 mL toluene, 0.08 g TOMA and 0.02 g NaOH in 0.25 mL water were added subsequently. Then 2.5 mL of iodomethane was slowly added. After a reaction time of 12 hours at room temperature the polymer solution was precipitated in a 10-fold excess methanol. <sup>1</sup>H-NMR (CDCl<sub>3</sub>):  $\delta$  3.67 (3H, s, OCH<sub>3</sub>), 7.09 (3H, m, arom. C-H tail-unit), 6.47 (~54H, broad s, arom. C-H repeating unit), 6.37 (2H, s, arom. C-H head unit), 2.09 (~162H, broad s, CH<sub>3</sub> repeating unit).  $\overline{M}_n = 3.5$  kg/mol as determined using <sup>1</sup>H-NMR spectroscopy. IR: 2857.3 cm<sup>-1</sup> (OCH<sub>3</sub> absorption)

*Nucleophilic substitution with chloroethylamine hydrochloride*

13.4 g PPE-OH,  $\overline{M}_n = 2.62$  g/mol, was dissolved in 100 mL toluene. 5.2 g TOMA and 6.14 g NaOH in 7 mL water were added subsequently. The reaction mixture was heated to 90 °C. After 15 minutes 12.7 g of a 70 wt% aqueous solution of chloroethylamine-HCl was slowly added. After 48 hours reaction at a temperature of 90 °C the polymer solution is precipitated in methanol.  $^1\text{H-NMR}$  ( $\text{CDCl}_3$ ):  $\delta$  3.06 (2H, t,  $J = 4.8$  Hz,  $\text{CH}_2\text{NH}_2$ ), 3.76 (2H, t,  $J = 4.8$  Hz,  $\text{OCH}_2$ ), 7.09 (3H, m, arom. C-H tail-unit), 6.47 (~60H, broad s, arom. C-H repeating unit), 6.37 (2H, s, arom. C-H head unit), 2.09 (~180H, broad s,  $\text{CH}_3$  repeating unit).  $\overline{M}_n = 3.9$  kg/mol as determined using  $^1\text{H-NMR}$  spectroscopy.

If the precipitation is performed in acidified methanol then the  $\text{PPE-NH}_3^+\text{Cl}^-$  salt will precipitate. ( $^1\text{H-NMR}$  ( $\text{CDCl}_3$ ):  $\delta$  3.40 (2H, broad s,  $\text{CH}_2\text{NH}_3^+\text{Cl}^-$ ) 4.02 (2H, broad s,  $\text{OCH}_2$ ), 7.09 (3H, m, arom. C-H tail-unit), 6.47 (~59H, broad s, arom. C-H repeating unit), 6.34 (2H, s, arom. C-H head unit), 2.09 (~177H, broad s,  $\text{CH}_3$  repeating unit).  $\overline{M}_n = 3.8$  kg/mol as determined using  $^1\text{H-NMR}$  spectroscopy.

*Williamson synthesis with allyl bromide*

PPE-OH (12.4 g,  $\overline{M}_n = 1.97$  kg/mol) was dissolved in 130 mL toluene. Subsequently were added: 5.1 g TOMA and 1.0 g NaOH in 1 mL water. Allyl bromide (25 mL) was slowly added at room temperature and after 12 hours the polymer solution was precipitated in methanol.  $^1\text{H-NMR}$  ( $\text{CDCl}_3$ ):  $\delta$  6.10 (1H, m,  $\text{CH}_2\text{-CH}=\text{CH}_2$ ), 5.41 (1H, d,  $J = 17.2$  Hz,  $\text{CH}_2\text{-CH}=\text{CH}_2$  *cis* towards  $\text{OCH}_2$ ), 5.24 (1H, d,  $J = 10.4$  Hz,  $\text{CH}_2\text{-CH}=\text{CH}_2$  *trans* towards  $\text{OCH}_2$ ), 4.26 (2H, d,  $J = 5.4$  Hz,  $\text{OCH}_2$ ), 7.09 (3H, m, arom. C-H tail-unit), 6.47 (~38H, broad s, arom. C-H repeating unit), 6.36 (2H, s, arom. C-H head unit), 2.09 (~114H, broad s,  $\text{CH}_3$  repeating unit).  $\overline{M}_n = 2.6$  kg/mol as determined using  $^1\text{H-NMR}$  spectroscopy.

*Hydroboration/oxidation of allylic terminated PPEs*

Allylic terminated telechelic PPE (7.1 g,  $\overline{M}_n = 3.48$  kg/mol, tetramethyl bisphenol acetone core) is dissolved in THF (200 mL), distilled from Na/benzophenone. The polymer solution is cooled in an ice-bath to approxim. 0 °C. A 0.5 M solution of 9-BBN in THF (41 mL) is slowly added and the reaction mixture was stirred for at least 6 hours at 0 °C. Then a mixture of an aqueous NaOH solution (1.8 g in 12 mL  $\text{H}_2\text{O}$ ) and a 30% aqueous  $\text{H}_2\text{O}_2$  solution (2.4 mL) was slowly added. Especially the first drops should be added cautiously, since the reaction occurs vigorously. The reaction mixture was stirred overnight and was allowed to warm up to room temperature. The solvent was partially evaporated and after an extraction with chloroform/water, the organic layer was precipitated into methanol.  $^1\text{H-NMR}$  ( $\text{CDCl}_3$ ):  $\delta$  6.97 (4H, s, arom. C-H TMBPA core unit) 3.92 (4H, m,  $\text{CH}_2\text{OH}$  and  $\text{ArCH}_2$ ), 6.37 (4H, s, arom. C-H 2,6-dimethylphenoxy head-units), 6.47 (~72H, broad s, arom. C-H repeating unit), 2.09 (~216H, broad s,  $\text{CH}_3$  repeating unit).  $\overline{M}_n = 4.9$  kg/mol as determined using  $^1\text{H-NMR}$  spectroscopy. IR:  $\nu_{\text{OH}} 3564.1$   $\text{cm}^{-1}$

*Reaction of PPE with 4-nitrobenzyl bromide*

1.42 g PPE-OH,  $\overline{M}_n = 3.65$  kg/mol, was dissolved in a mixture of toluene (20 mL) and THF (20 mL). Subsequently were added: 0.19 g NaOH in 0.5 mL  $\text{H}_2\text{O}$  and 0.84 g of 4-nitrobenzyl bromide. After one hour 0.25 g of an aqueous 40 wt% TBAH solution was added. After 1 day, the solvent was partially evaporated, some chloroform was added and the reaction mixture was extracted with a 10 wt% aqueous HCl solution. The chloroform layer was subsequently precipitated into methanol.  $^1\text{H-NMR}$  ( $\text{CDCl}_3$ ):  $\delta$  8.26 (2H, d,  $J = 8.7$  Hz, arom. C(3)-H of 4-nitrophenyl endgroup), 7.64 (2H, d,  $J = 8.6$  Hz, arom. C(2)-H of 4-nitrophenyl endgroup), 4.88 (2H, s,  $\text{OCH}_2$ ), 7.09 (3H, m, arom. C-H tail-unit), 6.47 (~68H, broad s, arom. C-H repeating

unit), 2.09 (~205H, broad s, CH<sub>3</sub> repeating unit).  $\overline{M}_n$  = 4.5 kg/mol as determined using <sup>1</sup>H-NMR spectroscopy. IR: 1527.1 and 1343.6 cm<sup>-1</sup>, assymmetric and symmetric NO<sub>2</sub> bend vibration

#### Reaction of PPE with $\alpha$ -bromo-*p*-toluic acid

1.42 g PPE-OH,  $\overline{M}_n$  = 3.65 kg/mol, was dissolved in a mixture of toluene (20 mL) and THF (20 mL). Subsequently were added: 0.19 g NaOH in 0.5 mL H<sub>2</sub>O and 0.84 g of  $\alpha$ -bromo-*p*-toluic acid. After one hour 0.25 g of an aqueous 40 wt% TBAH solution was added. After 1 day, the solvent was partially evaporated, some chloroform was added and the reaction mixture was extracted with a 10 wt% aqueous HCl solution. The chloroform layer was subsequently precipitated into methanol. <sup>1</sup>H-NMR (CDCl<sub>3</sub>):  $\delta$  8.14 (2H, d, J = 8.1 Hz, arom. C(3)-H of 4-carboxyphenyl endgroup), 7.58 (2H, d, J = 8.2 Hz, arom. C(2)-H of 4-carboxyphenyl endgroup), 4.85 (2H, s, OCH<sub>2</sub>), 7.09 (3H, m, arom. C-H tail-unit), 6.47 (~71H, broad s, arom. C-H repeating unit), 2.09 (~213H, broad s, CH<sub>3</sub> repeating unit).  $\overline{M}_n$  = 4.6 kg/mol as determined using <sup>1</sup>H-NMR spectroscopy. IR  $\nu_{\text{COOH}}$ : 1696.8 cm<sup>-1</sup>.

#### Reaction of telechelic PPE with $\alpha$ -bromo-*p*-tolunitrile

Telechelic PPE-2OH with a tetramethylbisphenol acetone (TMBPA) core (1.03 g,  $\overline{M}_n$  = 3.54 kg/mol) was dissolved in a mixture of toluene (20 mL) and THF (20 mL). Subsequently were added: 1.14 g of  $\alpha$ -bromo-*p*-tolunitrile and 0.23 g NaOH dissolved in 0.5 mL H<sub>2</sub>O. After one hour 0.38 g of an aqueous 40 wt% TBAH solution was added. After 1 day, the solvent was partially evaporated, some chloroform was added and the reaction mixture was extracted with a 10 wt% aqueous HCl solution. The chloroform layer was subsequently precipitated into methanol. <sup>1</sup>H-NMR (CDCl<sub>3</sub>):  $\delta$  7.69 (4H, d, J = 8.2 Hz, arom. C(3)-H of 4-cyanophenyl endgroups), 7.64 (4H, d, J = 8.2 Hz, arom. C(2)-H of 4-cyanophenyl endgroups), 4.83 (4H, s, OCH<sub>2</sub>), 6.96 (4H, s, arom. C-H TMBPA core-unit), 6.47 (~51H, broad s, arom. C-H repeating unit), 6.40 (4H, s, arom. C-H 2,6-dimethylphenoxy headunits) 2.09 (~152H, broad s, CH<sub>3</sub> repeating unit).  $\overline{M}_n$  = 3.6 kg/mol as determined using <sup>1</sup>H-NMR spectroscopy. IR: 2229.9 cm<sup>-1</sup> (CN-stretch).

## 5.5 References

1. Van de Grampel, H.T. *Rapra Rev.*, **5**, 1 (1991).
2. Servens, E., Löwik, D., Bosman, A., Nelissen, L. and Lemstra, P.J. *Macromol. Chem. Phys.*, **198**, 379 (1997).
3. Viersen, F.J., Colantuoni, P. and Mamalis, I. *Ang. Makromol. Chem.*, **206**, 111 (1993).
4. Percec, V. and Nava, H. *Makromol. Chem., Rapid Commun.*, **5**, 319 (1984).
5. Heyde, G., Heitz, W., Karbach, A. and Wehrman, R. *Makromol. Chem.*, **194**, 2741 (1993).
6. Stehlicek, J. and Puffr, R. *Collect. Czech. Chem. Commun.*, **58**, 2574 (1993).
7. Glans, J.H., and Akkapeddi, M.K. *Macromolecules*, **24**, 383 (1991).
8. Bruce, S.B., Trent, J.S., Golba, J.C. and Lowry, R.C. Eur. Pat. Appl. EP 0,374,517 B1 (1989).
9. Campbell, J.R. and Shea, T.J. U.S. US 4,777,221 (1988).



10. Campbell, J.R. and Shea, T.J. U.S. US 4,973,628 (1990).
11. Sybert, P.D., Han, C.Y., Brown, S.B., McFay, D.J., Gately, W.L. and Tyrell J.A. PTC Int. Appl. WO 07279 (1987)
12. Sybert, P.D., Han, C.Y., McFay, D.J., Gately, W.L., Tyrell J.A. and Florence, R.A. U.S. US 5,015,698 (1991).
13. Brown, S.B. Eur. Pat. Appl. EP 0,347,537 A2 (1989).
14. Brown, S.B., Trent, Y.S., Golba, J.C. and Lowry, R.C. Eur. Pat. Appl. EP 0,347,517 B1 (1989).
15. Khouri, F.F., Brown, S.B. and Jackman, J.T. Eur. Pat. Appl. EP 0,475,040 (1992).
16. Khouri, F.F., Brown, S.B. and Jackman, J.T. U.S. US 5,115,042 (1992).
17. Chao, H.S.I., Hovatter., T.W., Johnson, B.C. and Rice, S.T. *J. Polym. Sci., Polym. Chem. Ed.*, **27**, 3371 (1989).
18. Lai, Y.C. *Polym. Mater. Sci. Eng., Proc. Am. Chem. Soc., Div. Polym. Mater. Sci. Eng.*, **64**, 161 (1991).
19. Han, C.H. and Kim, S.C. *Polym. Bull.*, **35**, 407 (1995).
20. Lai, Y.C. *J. Appl. Polym. Sci.*, **54**, 1289 (1994).
21. Grutke, S., Hurley, J.H., Risse, W. *Macromol. Chem. Phys.*, **195**, 2875 (1994)
22. Sato, M., Mangyo, T., Mukaida, K. *Macromol. Chem. Phys.*, **196**, 1791 (1995).
23. Tingerthal, J.M., Nava H. and Percec, V. *J. Polym. Sci., Polym. Chem. Ed.*, **25**, 2043 (1987).
24. Percec, V. and Wang, J.H. *Macromol. Reports*, **A28**, 221 (1991).
25. Müllbach, K. and Percec, V. *J. Polym. Sci, Polym. Chem. Ed.*, **25**, 2605 (1987).
26. Percec, V., Rinaldi, P.L. and Auman, B. C. *Polym. Bull.*, **10**, 397 (1983).
27. Vukovic, R., Bogdanic, G., Kuresevic, V., Srica, V., Karasz, F.E. and Macknight, W.J. *J. Appl. Polym. Sci.*, **52**, 1499 (1994).
28. Vukovic, R., Bogdanic, G., Kuresevic, V., Srica, V., Karasz, F.E. and Macknight, W.J. *Polymer*, **35**, 3055 (1994).
29. Xue, S., Magknight, W.J. and Karasz, F.E. *J. Appl. Polym. Sci.*, **29**, 2679 (1984).
30. Venderbosch, R.W. "Processing of intractable polymers using reactive solvents", PhD thesis, chapter 6, Eindhoven University of Technology, The Netherlands, (1995).
31. De Brabander - Van Den Berg, E.M.M. and Meijer, E.W. *Angew. Chem.*, **105**, 1370 (1993).
32. Van Hest, J.C.M., Delnoye, D.A.P., Baars, M.W.P.L., Van Genderen, M.H.P. and Meijer, E.W. *Science*, **268**, 1592 (1995).
33. Haines, A.H. "Methods for the oxidation of organic compounds", Academic Press, New York, (1985).
34. Kaitayama, T., Nakagawa, O., Kishiro, S., Nishiura T. and Hatada, K. *Polym. J.*, **25**, 707 (1993).
35. Nishimura, H., Aritomi, M., Arashiro, Y., Yamauchi S. Eur. Pat. Appl. EP 0,530,442 A1 (1992)
36. Angle, S.R., Louie, M.S., Mattson H.L. and Yang, W. *Tetrahedron Lett.*, **30**, 1193 (1989)

- 37 . Carson, B.A. and Brown, H.C. *Org. Synth. Coll.*, **6**, 137 (1988).
- 38 . Liska, J. and Borsig, E. *J. Macromol. Sci., Rev. Macromol. Chem. Phys.*, **C35**, 517 (1995).
- 39 . Liska, J., Borsig, E. and Tkac, I. *Ang. Makromol. Chem.*, **211**, 121 (1993).
- 40 . Liska, J. and Borsig, E. *Chem. Listy*, **86**, 900 (1992)
- 41 . Liska, J. and Borsig, E. *J. Macromol. Sci., Pure & Appl. Chem.*, **A31**, 2019 (1994)
- 42 . Bonfanti, C., Lanzini, L., Roggero A. and Sisto, R. *J. Polym. Sci., Polym. Chem. Ed.*, **32**, 1361 (1994).
- 43 . Chao, H.S.I. and Whalen, J.M. *J. Appl. Polym. Sci.*, **49**, 1537 (1993).
- 44 . Bonfanti, C., Lanzini, L., Roggero A. and Sisto, R. *J. Appl. Polym. Sci.*, **32**, 1361 (1994).
- 45 . Mahajan, S.S., Sarwade, B.D. and Wadgaonkar, P.P. *Polym. Bull.*, **20**, 153 (1988).
- 46 . Ishii, Y., Oda, H., Arai, T. and Katayose, T. *Proc. Am. Chem. Soc., Div. Polym. Mat. Sci. Eng.*, **72**, 448 (1995).
- 47 . Percec, S. *J. Appl. Polym. Sci.*, **33**, 191 (1987).
- 48 . Percec, V. and Auman, B.C. *Macromol. Chem.*, **185**, 2319 (1984).
- 49 . Pan, Y., Huang, Y., Liao, B. and Cong, G. *J. Appl. Polym. Sci.*, **61**, 1111 (1996).
- 50 . Risse, W., Heitz, W., Freitag, D. and Bottenbruch, L. *Makromol. Chem.*, **186**, 1835 (1985).
- 51 . Brown, S.B. U.S. US 4,927,894 (1990).
- 52 . Sivavec, T.M. Eur. Pat. Appl. EP 0,338,271 A2 (1989).
- 53 . Ohmura, H. and Aritomi, M. U.S. US 5,128,421 (1992).
- 54 . Sivasec, T.M., Fukuyama, S.M. U.S. US 5,141,999 (1992)
- 55 . Chan, K.P., Argyropoulos, D.S., White, D.M., Yeager, G.W. and Hay, A.S. *Macromolecules*, **27**, 6371 (1994).
- 56 . Ishida H. and Moriaka, M. U.S. US 5,084,496 (1992).
- 57 . Khouri, F.F., Haley, R.J. and Yates, J.B. Eur. Pat. Appl. EP 0,564,244 (1993).
- 58 . Khouri, F.F. Eur. Pat. Appl. EP 0,519,642 A2 (1992)
- 59 . Campbell, J.R. Eur. Pat. Appl. EP 0,395,993 A2 (1990).
- 60 . Sybert, P.D. PTC Int. Appl. WO 07286 (1987).
- 61 . Sybert, P.D. PTC Int. Appl. WO 07280 (1987).
- 62 . Han, C.Y. and Gately, W.L. U.S. US 4,689,372 (1987).
- 63 . Yates, J.B., Brown, S.B., Lowry, R.C., Blubaugh, J.C. and Aycocock, D.F. Eur. Pat. Appl. EP 0,501,155 (1992).
- 64 . Nelissen, L.H.I.H., Meijer, E.W., Lemstra, P.J. *Polymer*, **33**, 3734 (1992).
- 65 . Nelissen, L.N.I.H. and Zijderveld, J.M. U.S. US 5,310,820 (1994).
- 66 . White, D.M. and Socha, L.A. Eur. Pat. Appl. EP 0,334,026 (1989).
- 67 . Starks, C.M. *J. Am. Chem. Soc.*, **93**, 195 (1971).
- 68 . McKillop, A. Fiaud, J.C. and Hug, R.P. *Tetrahedron*, **30**, 1379 (1974).
- 69 . Percec, V. *Am. Chem. Soc. Symp. Ser.*, **326** (Phase Transfer Catal.), 96 (1987).
- 70 . White, D.M. and Louks, G.R. *Polym. Prepr., Am. Chem. Soc., Div. Polym. Chem.*, **25**, 129 (1984).

- 71 . White, D.M. and Louks, G.R. *Am. Chem. Soc. Symp. Ser.*, **282** (React. Oligomers), 187 (1985).
- 72 . Percec, V. and Wang, J.H. *Polym. Bull.*, **24**, 493 (1990).
- 73 . Nava, H. and Percec, V. *J. Polym. Sci., Polym. Chem. Ed.*, **24**, 965 (1986).
- 74 . Wicker, M. and Heitz, W. *Angew. Makromol. Chem.*, **185/186**, 75 (1991).
- 75 . Van Aert, H.A.M., Bürkard, M.E.M., Jansen, J.F.G.A., van Genderen, M.H.P., Meijer, E.W., Oevering H. and Werumeus Buning, G.H. *Macromolecules*, **28**, 7967 (1995).
- 76 . Chapter 3 of this thesis
- 77 . Van Aert, H.A.M., van Genderen, M.H.P., van Steenpaal, G.M.L., Nelissen, L.N.I.H. and Meijer, E.W. *Macromolecules*, submitted.
- 78 . Omura, H., Mitsutoshi, A., Kihira, M., Nakano, H., Eur. Pat. Appl. EP 0,476,619 A2 (1991).
- 79 . Tomita, M., Nakano, H., Uchino, H., Sugano, T., Aritomi, M. Eur. Pat. Appl. EP 0,487,278 A2 (1991).
- 80 . Ohmura, H., Aritomi, M., Kihira, M., Nakano, H. U.S. US 5,191,030 (1993).
- 81 . Ohmura, H., Arotomi, M., Kihira, M., Nakana, H. U.S. US 0,476,619 A2 (1991).
- 82 . Dermer, O.C. and Ham, G.E. "Ethylenimide and other aziridines", Academic Press, New York, (1969).
- 83 . Chapter 2 of this thesis.
- 84 . Van Aert, H.A.M., Venderbosch, R.W., Van Genderen, M.H.P., Lemstra, P.J., Meijer, E.W. *J. Macromol. Sci., Pure & Appl. Chem.*, **A32**, 515 (1995).

## Chapter 6

### Reactive compatibilization of blends of poly(2,6-dimethyl-1,4-phenylene ether) and poly(butylene terephthalate)

#### Summary

*Poly(butylene terephthalate) (PBT) and poly(2,6-dimethyl-1,4-phenylene ether) (PPE) are well-known linear thermoplastic polymers. PBT is a crystalline polymer possessing favorable properties such as resistance to non-polar solvents including gasoline but due to crystallization the dimensional stability, shrinkage during crystallization, is poor. PPE is an amorphous polymer with a high glass transition temperature, appr. 210 °C, possessing an excellent dimensional stability but the resistance to solvents is limited. Blending of PBT with PPE, with PBT as the continuous phase, could yield interesting materials. PBT and PPE, however, are mutually immiscible, and the phase morphologies obtained during blending of these polymers are generally unstable with respect to morphology. When PPE is functionalized selectively, in-situ compatibilization is feasible. Due to the formation of sequential copolymers, which act as compatibilizing agents, stabilization of the morphology formed during blending could be realized. Different types of reactive PPE polymers were investigated, e.g. PPE with hydroxyalkyl, carboxylic acid, methyl ester, amino and t-BOC protected amino endgroups. All these reactive PPE polymers result in better compatibilization after mixing with PBT. PPEs with carboxylic acid endgroups proved to be the most efficient. Promoters, which catalyze or take part in the coupling between PBT and/or functionalized PPEs, such as triphenyl phosphite (TPP), sodium stearate, titanium(IV) isopropoxide and epoxy resins, based on the bisglycidyl ether of bisphenol acetone, were used in order to improve additionally the compatibilization of the PPE/PBT blends. This study on PPE/PBT blends is focused on the chemistry involved in the reactive compatibilization and shows different effectiveness of the type of reaction involved: amidation > esterification > transesterification. The use of a promoters proved to give synergetic compatibilization in combination with functionalized PPEs.*

## 6.1 Introduction

Poly(butylene terephthalate) (PBT) is a thermoplastic polyester possessing a high degree of crystallinity and a high resistance to non-polar solvents like gasoline. The commercial growth of thermoplastic polyesters, such as PBT, has been very rapid among the thermoplastic resins because of their broad and favorable range of properties, including a good chemical resistance, a low moisture uptake, stable electrical-insulation properties, fast processing cycles, an excellent melt flow, good mechanical strength and toughness. However, a major drawback of PBT is its poor dimensional stability due to shrinkage during crystallization. Combining of PBT with a dispersed amorphous polymer, like poly(2,6-dimethyl-1,4-phenylene ether) (PPE), could lead to materials with an improved dimensional stability. Because of the poor processability of PPE, we based our work on blends with a continuous PBT phase with dispersed PPE particles. However, blending of unmodified PPE with PBT will result in unstable morphologies such as large dispersed PPE particles without any significant interaction with the PBT matrix. Molded blends are typically characterized by an extremely low impact strength.<sup>1</sup> Therefore, compatibilization is required to obtain desirable properties. As discussed before, see Chapter 1, *in-situ*, reactive compatibilization is technologically preferred rather than the addition of a specially tailored, usually expensive copolymer.

Compatibilization using added surface-active agents or the *in-situ* generation of surface-active species is generally considered to be the determining factor to make compatible polymer blends. However, next to the chemistry involved in (reactive) compatibilization, rheological parameters are of importance in the process of dispersing polymer A into polymer B.<sup>2</sup> Generally, mixing of immiscible (polymer) liquids involves the deformation of a dispersed phase A in a flow field, resulting in an increased interfacial surface area. In the case of polymer melts the viscosities are relatively large (small Reynolds numbers) and the deformation of the dispersed phase A is mainly governed by the capillary number ( $Ca$ ), the ratio of the (deforming) shear stress  $\tau$  exerted on the dispersed phase by the external flow field and the (shape conserving) interfacial stress  $\sigma/R$  where  $\sigma$  is the interfacial tension and  $R$  the local radius of the dispersed phase:  $Ca = \tau R/\sigma$ . Above a critical value,  $Ca_{crit}$ , the viscous shear stress overrules the interfacial stress and the dispersed phase will break up into smaller fragments. The critical capillary number depends both on the viscosity ratio  $p$  between dispersed and continuous phase ( $p = \eta_d/\eta_c$ ), and the type of flow. In simple shear flow, break up of the dispersed phase is rather easy at viscosities ratios close to unity, at least for Newtonian liquids as shown by Grace.<sup>3</sup> In the case of visco-elastic liquids, i.e. polymer melts, the situation is more complex but, in general, to disperse a polymer A into B (the continuous phase), the viscosity of A should be lower than the viscosity of B. In the case of blending PPE into PBT, the viscosity ratio is difficult to measure and/or to define. PPE is inherently thermally unstable

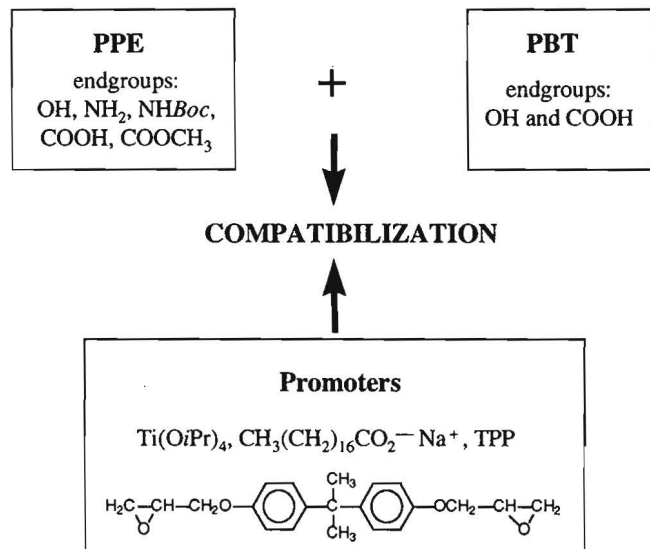
and premature crosslinking and degradation can occur. Consequently, in this Chapter rheological parameters were not taken into account but the emphasis is laid upon *in-situ* reactive compatibilization. The preliminary test for morphology stabilization via *in-situ* compatibilization was annealing at elevated temperatures using electron-microscopy to study the particle size distribution. *The author hastens to add that these annealing test are not conclusive for phase morphology upon the further processing of the compatibilized blends but merely serve the purpose of a first screening on in-situ compatibilization.*

Usually, formation of copolymers during reactive compatibilization is reflected in a shift of the glass transition temperatures of both polymers and can be detected by techniques like differential scanning calorimetry (DSC) and Dynamical Mechanical Thermal Analysis (DMTA). DMTA is more powerful to detect glass transition temperatures especially in blends of PPE and PBT, in which the glass transition temperature ( $T_g$ ) of PPE and melting point ( $T_m$ ) of PBT are close together. The compatibilization can be visualized by a decrease in the  $T_g$  of the PPE phase. The use of PPEs with a higher functionality content (e.g. carboxylic acid), which have in most cases a lower molecular weight, generally yield a shift of the  $\tan \delta$  peak to lower temperatures. However, it is very difficult to differentiate between a shift of the  $T_g$  caused by a higher copolymer content or caused by a lower molecular weight of the functional PPE.<sup>4</sup> Therefore, DMTA is only indicative but not conclusive to determine the extent of compatibilization and in this Chapter conclusions are based on Electron Microscopy.

Extensive studies concerning the development of compatibilizing immiscible blends of PPE and polyesters have been reported, either via addition of an interfacially-active block copolymer<sup>5-7</sup> or using *in-situ* reactive compatibilization.<sup>8-38</sup> However, no detailed information is published on the influence of the type of reactive group attached to the PPE chain on the *in-situ* compatibilization of PPE/PBT blends. Because of the facile synthesis of various types of reactive PPEs as described in previous Chapters, this study is focused on the chemistry in the reactive compatibilization. *In-situ* compatibilization during reactive processing requires modified PPEs that show reactivity towards either the ester functionality or the carboxylic acid and hydroxyalkyl endgroups of PBT. Using the redistribution method, as described in Chapter 3, and the phenolic endgroups modification, as described in Chapter 5, PPEs with various types of endgroups can easily be prepared, like carboxylic acid, hydroxyalkyl, amine and methyl ester functionalities. The effectiveness of these different endgroups in reacting with PBT can then be easily investigated.

Besides the addition or formation of interfacially-active copolymers, the addition of some low molecular weight promoters, such as transesterification catalysts and chain extenders, can influence the morphology of immiscible blends.<sup>39-40</sup> Various transesterification catalysts<sup>41-44</sup>

and chain extenders<sup>45-57</sup> are reported for polyesters. Transesterification catalysts like titanium(IV) isopropoxide (tetra-isopropyl titanate) and sodium stearate (sodium octadecanoate), and chain extenders like triphenyl phosphite (TPP)<sup>58-64</sup> and epoxy resins that mainly consist of the bisglycidyl ether of bisphenol acetone (DGEBA) are known as compatibilization promoters. In combinations with reactive PPE these promoters could possibly yield a synergetic compatibilization of the immiscible PPE/PBT blends (Scheme 6.1).



**Scheme 6.1:** Reactive compatibilization of PPE/PBT blends

In this Chapter, we emphasize the *chemistry* in the *reactive compatibilization* of PPE/PBT blends. Therefore, this investigation may be considered as a *preliminary study* to obtain information on the effectiveness of various reactive PPEs and low molecular weight promoters to form interfacially-active compounds during the reactive processing (Scheme 6.1). Modified PPEs were blended with PBT in a laboratory-scale mini-extruder and the morphology of the obtained blend was mainly investigated by Transmission Electron Microscopy (TEM) and Scanning Electron Microscopy (SEM). The size of dispersed phase, adhesion and stability of the blend morphology are investigated.

## 6.2 Results and Discussion

### 6.2.1 Poly(butylene terephthalate) and blend studies

In the research concerning *in-situ* compatibilization of functionalized PPEs with PBT, a commercial PBT grade was employed, as shown in Table 6.1. In our research, we aimed to obtain an improved crystalline-polymer-based material, combining properties of the continuous PBT phase and dispersed PPE particles. Therefore, we based our work on blends with PPE/PBT weight ratio of 40 : 60 which proved to yield dispersed PPE particles in a continuous PBT matrix for the PBT investigated.

**Table 6.1:** Endgroup concentrations of commercial PBT grade.

polymer	[COOH] ( $\mu\text{eq/g}$ )	[OH] ( $\mu\text{eq/g}$ )	$\bar{M}_w$ (kg/mol) (SEC, PS expressed)
PBT	40	20	108.5

### 6.2.2 Blends of PBT and carboxylic-acid-modified PPE

It should be noted that PPEs that are modified by reacting a functional phenol in a redistribution reaction using tetramethyldiphenoquinone (TMDPQ) as oxidant consist of a mixture of functionalized and unfunctionalized molecules (Chapter 3). This is a direct result of incorporation of both the functional phenol and 3,3',5,5'-tetramethylbiphenyl-4,4'-diol, which is formed from TMDPQ. Therefore, when we describe a redistribution-modified PPE we always will encounter the functionality content, expressed in wt% functional phenol attached to the PPE. The functionality content can be adjusted by varying the amount of reacting phenol and reaction conditions. These modified PPEs can be obtained on a large scale using a fast redistribution catalyzed by TMDPQ.

The several types of carboxylic acid endgroups, capable of reacting with polyesters, are incorporated as a tail-end as illustrated in Chart 6.1. We employed three different carboxylic-acid-modified PPEs in the reactive compatibilization experiments. All types were prepared using the PPE-redistribution method by reacting the following phenols: (4-hydroxyphenyl)propionic acid (HPPA), bis(4-hydroxyphenyl)pentanoic acid (BHPPA) and bis(3,5-dimethyl-4-hydroxyphenyl)pentanoic acid (BDMHPPA).<sup>66</sup> The first two phenols are incorporated as endgroup, while the last *ortho*-methyl substituted bisphenol is incorporated in



the center of the PPE chain. In general, when *ortho*-methyl substituted functional bisphenols are reacted, a redistribution reaction occurs at both sides of the bisphenol-yielding telechelics with the functional group in the center of the polymer chain (Chapter 3). These functional tetramethylbisphenol-modified PPEs yield graft copolymers upon reaction with PBT. The carboxylic acid functionalities are proposed to react with the hydroxyalkyl endgroups of the PBT in a esterification and/or with the main-chain ester units of the PBT in a transesterification reaction.

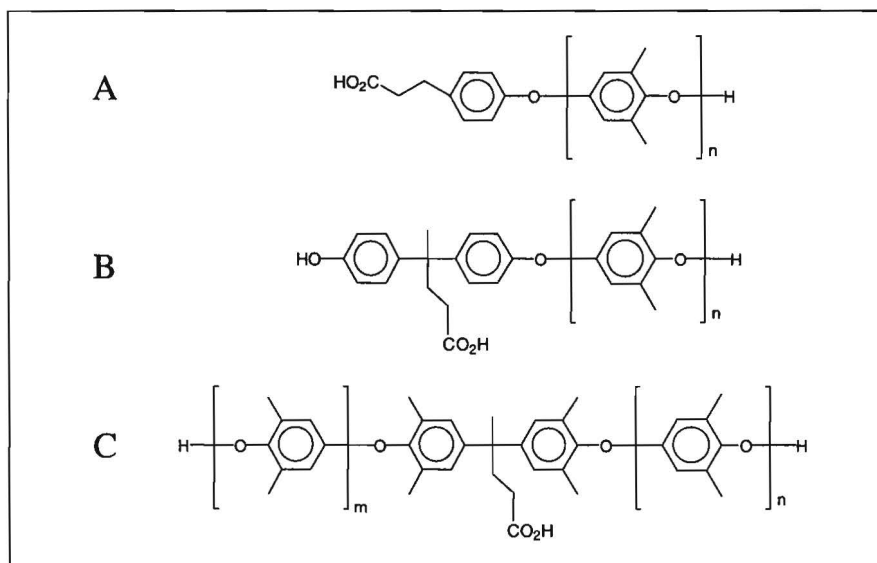


**Chart 6.1:** Carboxylic-acid-modified PPEs prepared by redistribution using A. (4-hydroxyphenyl)propionic acid (HPPA); B. bis(4-hydroxyphenyl)pentanoic acid (BHPPA) and C. bis(3,5-dimethyl-4-hydroxyphenyl)pentanoic acid (BDMHPPA).

Differences between compatibilized (stabilized blend morphologies) with non-compatibilized (unstabilized) morphologies are shown using electron microscopy in Figures 6.1 and 6.2. In these Figures the SEM and TEM pictures of PPE/PBT-1 samples with unmodified PPE and bis(hydroxyphenyl)pentanoic acid (BHPPA)-modified PPEs (Chart 6.1B) are compared. Adhesion of the dispersed PPE particles with the continuous PBT phase can be determined qualitatively using SEM. The PPE/PBT blend with unmodified PPE shows large PPE particles in a continuous PBT matrix and no significant adhesion is observed, while the PPE/PBT blend with BHPPA-modified PPE (Chart 6.1B) shows good adhesion.

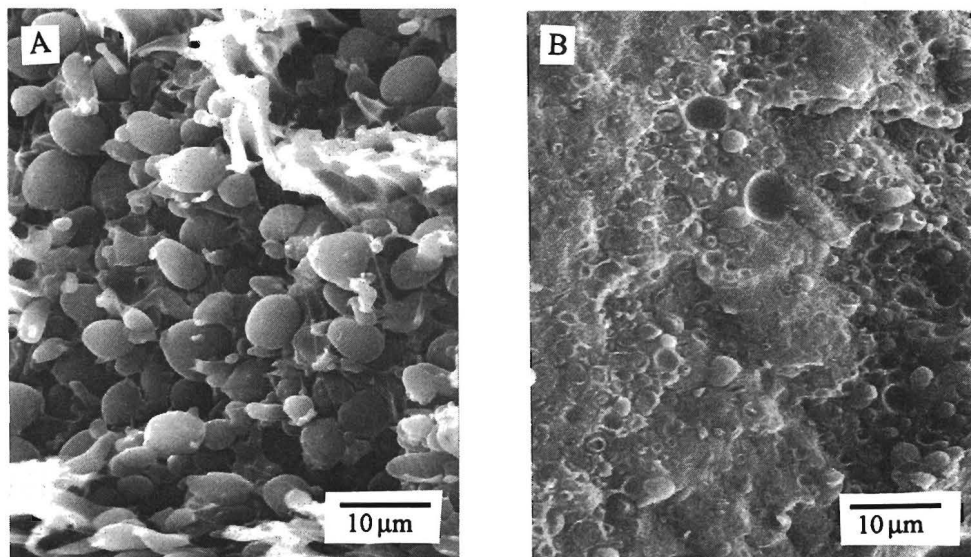


**Figure 6.1:** Scanning Electron Microscopy (SEM) pictures of PPE/PBT-1 blends in a 40/60 weight ratio: A. SEM picture of blend with unmodified PPE ( $IV = 0.4 \text{ dL/g}$ ,  $\overline{M}_w = 46.3 \text{ kg/mol}$ ), B. SEM picture of blend with bis(hydroxyphenyl)pentanoic acid (BHPPA)-modified PPE (functionality content 1.09 wt% BHPPA,  $\overline{M}_w = 12.95 \text{ kg/mol}$ ).

The SEM picture of the blend with modified PPE shows a more compatible phase morphology (Figure 6.1). SEM pictures of cryogenic fracture surfaces give a qualitative indication, whether the compatibilization is successful. We will consider different regimes of compatibilization: a. indicated with “-” having no or bad adhesion, b. indicated with “+/-” having a moderate adhesion and partially disrupted PPE particles, c. indicated with “+” having good adhesion and strongly disrupted PPE particles, d. indicated with “++” having excellent adhesion and fully disrupted and fractured PPE particles.

For successful compatibilization the obtained morphology should be stable upon annealing and after subsequent processing. In this Chapter, as mentioned in the introduction only annealing experiments were performed to test qualitatively the effectiveness of *in-situ* compatibilization as a function of PPE-functionality type and content. This can be determined by SEM, but is more clear from TEM analyses. Figure 6.2 A–D shows the TEM micrographs before and after annealing for unmodified and bis(hydroxyphenyl)pentanoic acid (BHPPA)-modified PPE (Chart 6.1B).

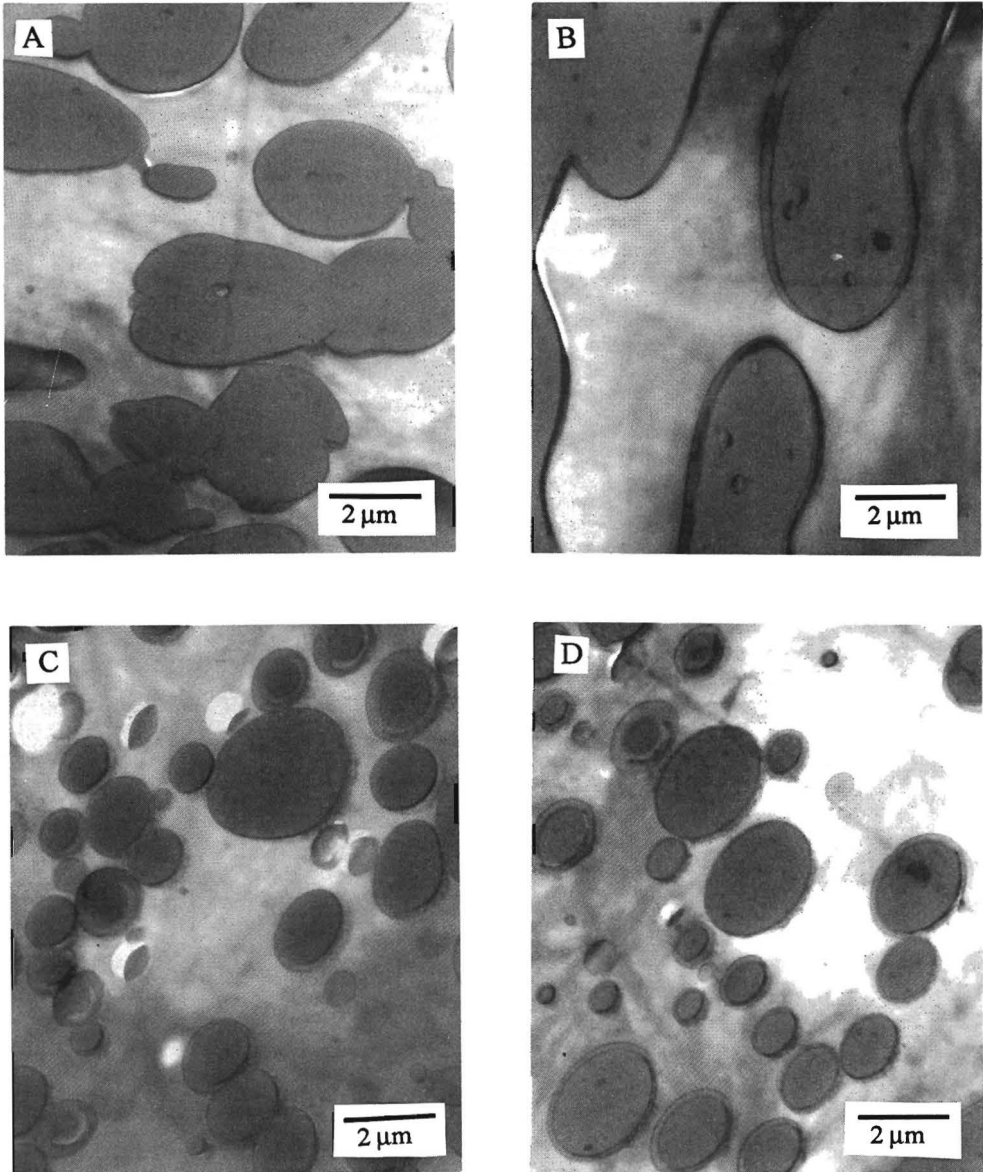


**Figure 6.2:** Transmission Electron microscopy pictures of blends with PPE/PBT-1 weight ratio 40/60 with unmodified PPE ( $IV = 0.4 \text{ dL/g}$ ,  $\overline{M}_w = 46.3 \text{ kg/mol}$ ) or bis(hydroxyphenyl)pentanoic acid (BHPPA)-modified PPE (functionality content 1.09 wt% BHPPA,  $\overline{M}_w = 12.95 \text{ kg/mol}$ ): A. TEM picture of blend with unmodified PPE before annealing; B. TEM picture of blend with unmodified PPE after annealing; C. TEM picture of blend with modified PPE before annealing; D. TEM picture of blend with modified PPE after annealing.

While the PPE particles in blends with unmodified PPE grow macroscopically due to coalescence, the morphology is stable in the PPE/PBT blends with the carboxylic-acid-modified PPE. Morphology stability testing by annealing (at 260 °C) above the melting temperature of PBT (ca. 225 °C) can be considered as a screening test to determine whether compatibilization is successful.

As shown in Figure 6.2, blends of BHPPA-modified PPEs (Chart 6.1B) and PBT show finely dispersed PPE particles which are stable upon annealing. When studying blends containing PPEs with different BHPPA content, the TEM pictures didn't show large differences, although SEM pictures show better adhesion for blends containing PPEs with higher functionality content (Table 6.2). The addition of compatibilization promoter TPP decreases the particle size of the PPE dispersed phase approximately by a factor two.

**Table 6.2:** Influence of BHPPA functionality content on PPE particle size and adhesion in blends of BHPPA-modified PPEs (Chart 6.1B) (40 wt%) with PBT (60 wt %).

Functionality content wt% BHPPA	PPE $\overline{M}_w$ (kg/mol)	PPE particle size ( $\mu\text{m}$ ) before annealing TEM	PPE particle size ( $\mu\text{m}$ ) before annealing SEM	PPE particle size ( $\mu\text{m}$ ) after annealing TEM	Adhesion before annealing SEM
1.09	12.95	2	3	2	+/-
2.71	15.21	2	3	3	++

A larger effect of functionality content on the extent of the compatibilization is found when propionic-acid-modified (HPPA-modified) PPEs (Chart 6.1A) are used instead of BHPPA-modified PPEs. In Table 6.3 the dependence of the obtained morphology and stability on functionalization content is demonstrated for HPPA-modified PPE. In all cases a stable morphology was obtained after annealing, except for the lowest functionalization content. When using an epoxy resin (2 wt%) as co-reactant, morphology, adhesion and stability improve a great deal because of faster reaction of carboxylic acid endgroups with epoxy, epoxy mobility and probable reaction of epoxy with carboxylic acid groups of both components. When the epoxy resin only reacts with the PBT endgroups and not with the carboxylic acid endgroups of the PPE chain, extension of the PBT occurs, resulting in an increase the relative viscosity of the PBT phase. This increase in relative viscosity could also have a positive effect

on the blend dispersion and stability. Similarly to epoxy resins, phenoxy resins have been reported as effective compatibilizing agents for PPE/polyester blends.<sup>65</sup> Phenoxy resins are polyhydroxyethers obtained by condensation of bisphenol acetone and epichlorohydrin leading to polymers with a higher molecular weight than similar epoxy resins. The higher mobility of epoxy resins in comparison with phenoxy resins, benefits their use as compatibilization promoter.

**Table 6.3:** Influence of HPPA functionality content (Chart 6.1A) on PPE particle size and adhesion in blends of HPPA-modified PPEs (40 wt%) with PBT (60 wt %).

Functionality content wt% HPPA	PPE $\overline{M}_w$ (kg/mol)	PPE particle size ( $\mu\text{m}$ ) before annealing TEM	PPE particle size ( $\mu\text{m}$ ) before annealing SEM	PPE particle size ( $\mu\text{m}$ ) after annealing TEM	Adhesion before annealing SEM
1.31	18.82	1	2	> 25	-
1.84	14.18	2	2	4	++
1.87	14.56	0.5	1	2	++
2.66	13.66	1	1	2	++

When PPE modified with the tetramethyl derivative of BHPPA (bis(3,5-dimethyl-4-hydroxyphenyl)-pentanoic acid) (BDMHPPA) (Chart 6.1C) is used in the reactive compatibilization experiments, small particle size and a moderate adhesion are obtained, although the morphology is very unstable after annealing compared to the PPEs modified with the non-methylated carboxylic acid functional phenols. There are two basic differences. First, methylated bisphenols are incorporated in the center of the PPE chain (Chart 6.1C), resulting in graft copolymers, in contrast to non-methylated PPE-derivatives (Chart 6.1A and 6.1B) which yield block copolymers after reaction with PBT. The second difference in regard to reactivity could be steric hindrance of the carboxylic acid group in the tetramethylated derivatives, which might prohibit copolymer formation. This is proposed to be the main reason for the poor compatibilization found in case of the tetramethylated PPE-derivatives (Chart 6.1C). The effect of the shape (block or graft) of the formed interfacially-active copolymer on the compatibilization is not clear from this experiment because a blend of PBT with BDMHPPA-modified PPE (Chart 6.1C) might form less copolymer during reactive extrusion.

Upon comparing carboxylic acid derivatives of PPE (HPPA-, BHPPA- and BDMHPPA-modified PPEs) steric hindrance appears to have a large effect on copolymer formation at its compatibilization. The most freely moving and unhindered carboxylic acids in the HPPA-modified PPEs (Chart 6.1A) and BHPPA-modified PPEs (Chart 6.1B) give the best compatibilization results. Poor compatibilization is achieved using the tetramethylated derivative of the carboxylic-acid-modified PPE (BDMHPPA-modified PPE) (Chart 6.1C), which in addition to the steric hindrance of carboxylic acid group provides graft copolymer instead of block copolymer. In this case the functionality located in the center of the chain is less mobile and its appearance at the surface of a polymer coil is less probable.

### 6.2.3 Blends of PBT and methyl ester-modified PPE

Two types of methyl-ester-modified PPEs are used for *in-situ* compatibilization of PPE/PBT blends, as shown in Chart 6.2, both prepared using PPE redistribution (Chapter 3).

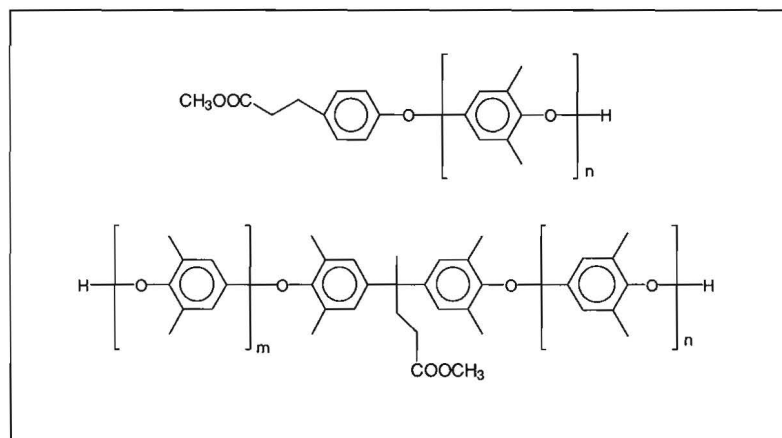


**Chart 6.2:** Methyl-ester-modified PPEs

Methyl-ester-modified PPEs, blended with PBT, show in general a coarse morphology and a poor adhesion and annealing stability, in comparison with the free carboxylic-acid-modified PPEs, especially for the PPEs modified with the methyl ester of bis(3,5-dimethyl-4-hydroxyphenyl)pentanoic acid. These results are related with their lower reactivity towards the hydroxyalkyl endgroups and/or the main-chain ester groups of PBT. Transesterification, which occurs using methyl-ester-modified PPE, is proposed to give slower reaction rates than esterification, which occurs in the case of the reactive blending PBT with carboxylic-acid-modified PPEs.

### 6.2.4 Blends of PBT and hydroxyalkyl-modified PPE

We employed two different hydroxyalkyl-modified PPEs, i.e. hydroxyethylphenol (HEP)-modified PPE prepared by redistribution<sup>66</sup> (Chart 6.3A) and PPE telechelics functionalized with hydroxypropyl (propanol) functionalities prepared via modification of the phenolic endgroups<sup>67</sup> (Chart 6.3B). These hydroxyalkyl-modified are proposed to react with the carboxylic acid endgroups and/or main-chain ester units of PBT.

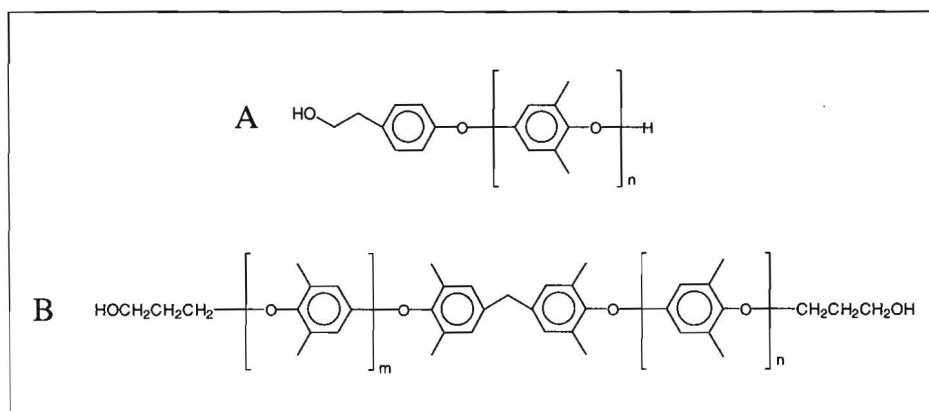


**Chart 6.3:** Hydroxyalkyl-modified PPEs; A. prepared from PPE redistribution with hydroxyethylphenol; B. prepared via modification of phenolic endgroups.

The morphology after extrusion using a 1.85 wt% hydroxyethylphenol (HEP)-modified PPE (Chart 6.3A) or a 1.96 wt% HEP-modified PPE with similar molecular weight ( $\bar{M}_w = 20$  kg/mol) is comparable (TEM, dispersed PPE particles 1–3  $\mu\text{m}$ ). In both cases the morphology, adhesion and morphology stability are substantially better than for an unmodified PPE/PBT blend.

The influence of promoters is illustrated by the example of PPE telechelics functionalized with hydroxypropyl (propanol) functionalities (Chart 6.3B). The most illustrative are SEM pictures after extrusion. Adhesion improvement is clear when using a catalyst to promote esterification reactions between the hydroxypropyl functionality of PPE and the carboxylic acid endgroups of PBT. Sodium stearate is more efficient than titanium isopropoxide. Chain extension agent triphenyl phosphite (TPP) didn't improve adhesion. These examples confirm the dominant effect of reactivity on compatibilization. Figures 6.3A and 6.3B show the difference of a moderate and good adhesion in blends of hydroxypropyl-modified PPEs and PBT obtained

subsequently for a blend without promoter and with addition of 6.5 wt% sodium stearate (modified PPE:  $\overline{M}_w = 39.1$  kg/mol).

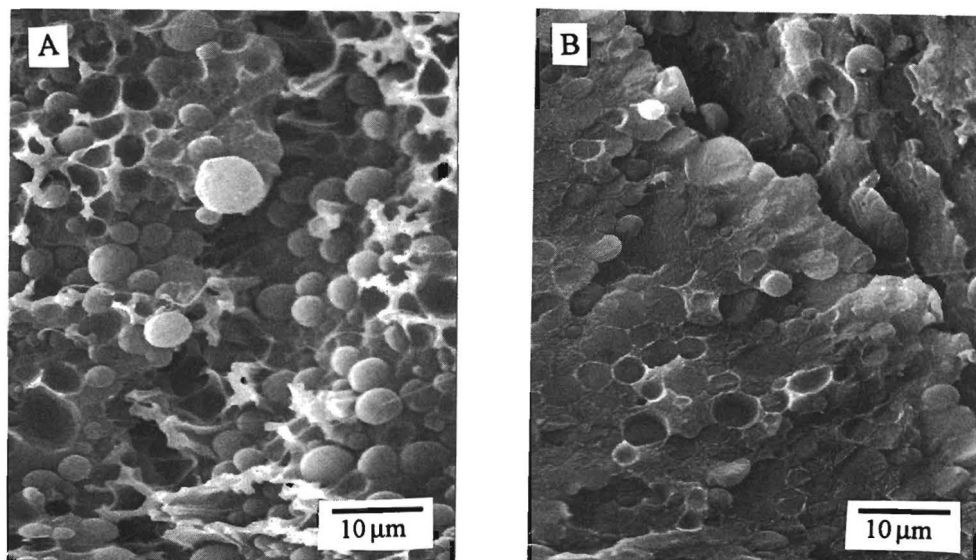


**Figure 6.3:** SEM pictures of blends containing 40 wt% bis(hydroxypropyl)-modified PPE (Chart 6.3B) and 60 wt% PBT: A. without promoter; B. with 6.5 wt% sodium stearate.

### 6.2.5 Blends of PBT and amino-terminated PPE

The amino-terminated PPE, shown in Chart 6.4 was obtained by redistribution of PPE with tyramine (Chapter 3). Amino endgroups could react with the carboxylic acids endgroups in amidation reaction and/or with the main-chain ester units of PBT.

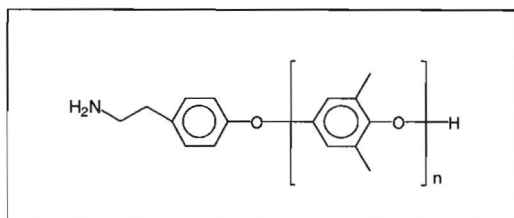


**Chart 6.4:** Amino-terminated PPE



The influence of functionality content is illustrated with the use of amino-terminated PPEs in Table 6.4. A finer morphology of PPE dispersed particles in a PBT matrix is observed for amino-functionalized PPEs with higher functionality content after reactive blending. The blended sample with modified PPE containing 1.74 wt% aminoethylphenol (tyramine) did show the finest morphology, which was stable after annealing.

**Table 6.4:** Influence of functionality content in amino-functional PPEs on particle size and adhesion in PPE/PBT blends.

Functionality content (wt% aminoethyl phenol)	PPE $\overline{M}_w$ (kg/mol)	PPE particle size ( $\mu\text{m}$ ) SEM	Adhesion SEM
1.74	18.22	2	++
1.25	22.25	4	+
0.77	21.87	5	+
< 0.5	19.82	10	-

When 3 wt% triphenyl phosphite (TPP) is added to a blend of amino-modified PPE and PBT, small PPE particle sizes (2  $\mu\text{m}$ ) are obtained, which even decrease further after annealing (1  $\mu\text{m}$ ) (amino-terminated PPE:  $\overline{M}_w = 21.87$  kg/mol, functionality content = 0.77 wt% aminoethylphenol). Without the addition of TPP, no stable morphology is obtained after annealing. This suggests that besides the reaction of hydroxyl endgroups of PBT also the amino endgroups of PPE react as a nucleophile with TPP, yielding a phosphoramidite ( $-\text{NH}-\text{P}(\text{OPh})_2$ ). Subsequent reaction of a carboxylic acid endgroup of PBT with a phosphoramidite (derived from TPP and amino-functional PPE) yields a PPE-PBT copolymer with an amide linkage. While the reaction of a carboxylic acid endgroup of PBT with a modified phosphite ( $-\text{CH}_2-\text{O}-\text{P}(\text{OPh})_2$ ) (derived from reaction of TPP and a hydroxybutyl endgroup of PBT) yields subsequently an extended PBT.<sup>58,59</sup> The coupling of PPE terminated with a phosphoramidite endgroup with carboxylic acid-terminated PBT presumably occurs faster than a traditional amidation reaction of amino-terminated PPE with carboxylic-acid-terminated PBT. Next to the chemistry, which occurs when TPP is used as promoter, not only copolymer formation can be enhanced but also the molecular weight (relative viscosity) of the PBT molecules can increase. A higher relative viscosity of this *in-situ* chain-extended PBT will enhance fine dispersion of the PPE particles in the continuous PBT matrix. The resulting larger interfacial area will promote reaction between the PBT and modified PPE as well.

### 6.2.6 Blends of PBT and *t*-BOC-protected amino-functionalized PPE

Besides the amino-terminated PPEs prepared from redistribution with 4-hydroxyphenylethylamine (tyramine), we studied similar PPEs in which the amino group was protected with a *tert*-butoxycarbonyl (*t*-BOC) group<sup>66</sup> (Chart 6.5).

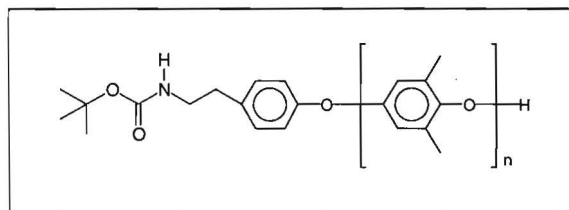
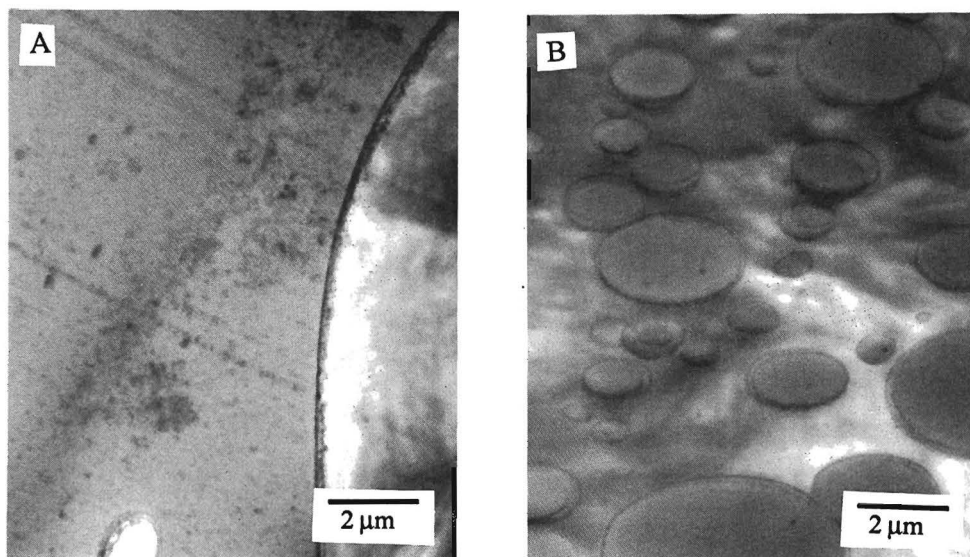


Chart 6.5: *t*-BOC-protected amino-functionalized PPE

The *tert*-butoxycarbonyl (*t*-BOC)-protected amine-modified PPEs can yield the free amine after thermal decomposition. Upon reaction of this modified PPE with PBT, the *t*-BOC groups need to be decomposed first. Decomposition yields carbon dioxide, isobutene and the free amine. When we studied this *t*-BOC-tyramine-functionalized PPE in reactive compatibilization, the influence of the functionality content is reflected, although not as strong when using PPEs with free amino-groups. This is reflected also in the stability of the PPE/PBT blend, which is not stable after annealing. Comparing tyramine versus *t*-BOC-tyramine-functionalized PPEs of the same functionality content (1.7 wt%) results in a stable morphology of the first one, and unstable morphology of the latter. Very unstable morphologies were obtained using the *t*-BOC-tyramine-modified PPEs, even when using PPEs with a functionality content of 3.52 wt% *t*-BOC-protected tyramine. When titanium(IV) isopropoxide is added as compatibilization promoter, a fine morphology is obtained which is stable after annealing (Table 6.5) as shown in Figure 6.4. The titanium catalyst probably promotes both *t*-BOC-decomposition, as well as subsequent amidation.

**Table 6.5:** Compatibilization of blends of 40 wt% *t*-BOC-tyramine-modified PPE and 60 wt% PBT.

Functionality content wt% <i>t</i> -BOC-tyramine	PPE $\overline{M}_w$ (kg/mol)	wt% Ti( <i>i</i> -OPr) <sub>4</sub>	PPE particle size ( $\mu\text{m}$ ) SEM	Adhesion SEM
1.72	18.96	0	4	+/-
3.52	12.99	0	2.5	+
3.52	12.99	0.7	1	++



**Figure 6.4:** TEM pictures of annealed blends of 40 wt% *t*-BOC-tyramine-functionalized PPE ( $\overline{M}_w = 12.99$  kg/mol, functionality content = 3.52 wt% *t*-BOC-tyramine) and 60 wt% PBT: A. Without Ti(*i*-OPr)<sub>4</sub>; B. with 0.7 wt% Ti(*i*-OPr)<sub>4</sub>.

### 6.2.7 Type of reaction, esterification versus amidation

The influence of the type reaction is most clear when different reactive PPEs are used with comparable molecular weight in the PPE/PBT blends (Figure 6.5). For example, we extruded PBT with differently functionalized PPE with comparable molecular weights ( $\overline{M}_w = 18.2$  kg/mol), one case with amino endgroups derived from tyramine, and a second one with 2-hydroxyethyl endgroups derived from 4-hydroxyethylphenol. Both can react with the carboxylic acid endgroups and/or with the ester main-chain units of PBT. Finer and more stable morphology is shown for the blend with the tyramine-modified PPE, despite of the lower functionality content. This means that amidation is more efficient than esterification for these two comparable polymers. When instead of a hydroxyalkyl-modified PPE, a carboxylic-acid-modified PPE is reacted with PBT, esterification might be more efficient than amidation e.g. in the case of HPPA-modified PPEs.

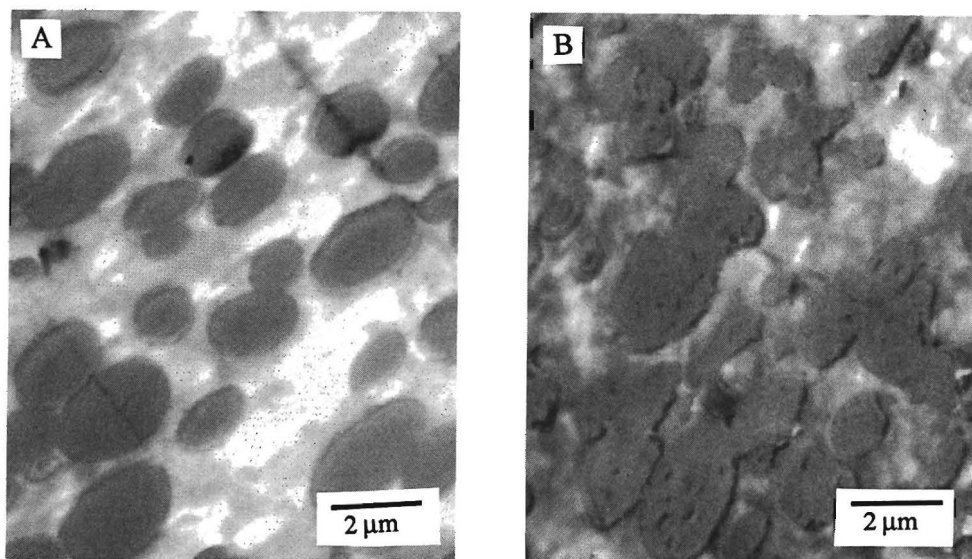


**Figure 6.5:** TEM pictures of PPE/PBT blends, weight ratio PPE/PBT = 40/60, either with amino endgroups (functionality content: 1.74 wt% tyramine) or with hydroxyethyl endgroups (functionality content: 1.96 wt% 4-hydroxyethylphenol), both polymers  $\overline{M}_w = 18.2$  kg/mol: A. Blend with amino-terminated PPE after extrusion; B. Blend with hydroxy-ethyl-functionalized PPE after extrusion.

### 6.3 Conclusions

Reactive compatibilization of blends of functionalized PPE and PBT can result in fine and stable morphologies. The extent of compatibilization largely depends on type and content of reactive endgroups of PBT and PPE. In general, the effectiveness of the type of functionality attached to the PPE chain on the compatibilization decreases in the following order: carboxylic acid > amino > hydroxy alkyl » *t*-BOC protected amino > methyl ester. Generally, the effectiveness of the type of reaction involved in the compatibilization decreases as follows: amidation > esterification » transesterification, however using HPPA-modified PPEs esterification is more efficient than amidation involving tyramine-modified PPE. Generally, the effectiveness of promoters on compatibilization decreases in the following order: epoxy resins > titanium isopropoxide sodium stearate > triphenyl phosphite (TPP). These conclusions, however are based on simple annealing experiments of quiescent systems. Further research is required to explore the effects of flow upon the phase morphology, as encountered during processing.

### 6.4 Experimental

#### *Techniques:*

The PPE/PBT samples were microtomed on a Ultratome Nova at room temperature, yielding coupes of approx. 100 nm. These coupes were etched 11 minutes in OsO<sub>4</sub> vapor and afterwards 11 minutes in RuO<sub>4</sub> vapor. Transmission Electron Microscopy (TEM) was performed on a Philips TEM CM12. Further morphology studies were done on Au/Pd sputtered fracture surfaces using a Cambridge Stereoscan 200 Scanning Electron Microscopy (SEM). Molecular weight determination of all functional PPEs was performed using a chloroform/ethanol mixture (98/2 v/v) as eluent at 40 °C. Dibutyl amine (50 ppm) is added to prevent tailing. Equipment used for this analysis are: a Waters 150-CV ALC/GPC apparatus, PL gel columns 10<sup>3</sup> and 10<sup>5</sup> Å and a Waters 490E programmable multiwavelength detector (PPE detected at 280 nm, polystyrene standards detected at 254 nm).

#### *Materials:*

Commercial grades of PPE and PBT were obtained from General Electric Plastics: unmodified PPE (IV = 0.40 dL/g) and PBT ( $\bar{M}_w = 108.5$  kg/mol, polystyrene expressed).

Epoxy resin, epikote 828, was obtained from Shell. Triphenyl phosphite and titanium isopropoxide were obtained 97% pure from Aldrich. Sodium octadecanoate (sodium stearate) was obtained >98% pure from Fluka.

Hydroxypropyl-modified PPEs were prepared by endgroup modification as described in Chapter 5 of this thesis. A hydroboration/oxidation reaction of bis(allyl)-terminated PPE telechelics yields

bis(hydroxypropyl)-terminated PPE. Allyl-terminated PPE was prepared by reaction of allyl bromide with 2,6-(dimethylphenol)-terminated PPE.

All other PPEs with functional endgroups were prepared by redistribution of PPE with a functional phenol, as described in Chapter 3 of this thesis. Hydroxyethyl-modified PPE was obtained by redistribution of PPE with hydroxyethylphenol (HEP). Amino-terminated PPE was prepared by redistribution of PPE with 4-hydroxyphenylethylamine (tyramine). PPE with *t*-BOC protected amino groups was prepared by redistribution with *t*-BOC-protected tyramine. Carboxylic-acid-modified PPE was prepared by redistribution of PPE with either (4-hydroxyphenyl)propionic acid (HPPA), bis(4-hydroxyphenyl)pentanoic acid (BHPPA) or bis(3,5-dimethyl-4-hydroxyphenyl)pentanoic acid. Methyl-ester-functionalized PPE was prepared from redistribution of PPE with (4-hydroxyphenyl)propionic acid methyl ester or bis(3,5-dimethyl-4-hydroxyphenyl)pentanoic acid methyl ester.

All molecular weights stated in this Chapter are uncorrected molecular weights related to polystyrene standard samples as determined by SEC.

#### *Preparation of PPE/PBT blends:*

PPE/PBT blends are prepared using a laboratory-scale mini-extruder, which operates continuously or batch wise. The device consists of two co-rotating, closely intermeshing, self-wiping, conical screws and is equipped with a recurrent loop and valve system. The device allows processing small quantities of material (volume = 6 cm<sup>3</sup>) at temperatures up to ca. 400 °C in a way equivalent to large scale industrial co-rotating twin screw extruders. Consequently, this is suitable for initial experiments in blending chemically modified PPE with PBT in order to perform a reactive compatibilization. All extrusion experiments were performed at 260 °C, mixing time ca. 3 minutes, after complete filling during 5 minutes.

#### *Annealing of PPE/PBT blends:*

Blended PPE/PBT strands were annealed during 10 minutes at 260 °C in a Linn Elektronik VMK39 oven, equipped with a precise temperature controller.

## 6.5 References

1. Jiang, W., Liang, H., Zhang, J., He, D. and Jiang, B. *J. Appl. Polym. Sci.*, **58**, 537 (1995).
2. Jansen, J.M.H. "Dynamics of Liquid-Liquid mixing", PhD thesis, Eindhoven University of Technology, The Netherlands, (1993).
3. Grace, H.P. *Chem. Eng. Commun.*, **14**, 225 (1982).
4. Araujo, M.A., Stadler, R. and Cantow, H.J. *Polymer*, **29**, 2235 (1988).
5. Quirk, R.P., Ma, J.-J., Chen, C.C., Min, K. and White, J.L. *Contemp. Top. Polym. Sci.*, **6**, 107 (1989).
6. Brown, S.B. and Fewkes, E.J. U.S. US 5,290,863 (1994).

7. Jiang, R., Quirk, R.P., White, J.L. and Min, K. *Polym. Eng. Sci.*, **31**, 1545 (1991).
8. Taubitz, C., Seiler, E. and Lausberg, D. Germ. Offen. DE 3702263 (1988).
9. Liu, W.B., Kuo, W-F., Chiang, C.J. and Chang, F-C. *Eur. Polym. J.*, **32**, 91 (1996).
10. Liu, W.B. and Chang, F.C. *Abstracts of papers of Am. Chem. Soc.*, **206**, 308 (1993).
11. Pan, L. and Liang, B. *J. Chin. Textile University (Engl. Ed.)*, **11**, 51 (1994).
12. Liang, B. and Pan, L. *J. Appl. Polym. Sci.*, **54**, 1945 (1994).
13. Dekkers, M.E.J., Hobs, S.Y. and Watkins, V.H. *Polymer*, **32**, 2150 (1991).
14. Sybert, P.D., Brown S.B. and Tyrell, J.A. PTC Int. Pat. Appl. WO 87/07279 (1987).
15. Sybert, P.D. and King, A.M. PTC Int. Pat. Appl. WO 87/07280 (1987).
16. Sybert, P.D. and King, A.M. PTC Int. Pat. Appl. WO 87/07286 (1987).
17. Sybert, P.D., Han, C.Y., Brown, S.B., McFay, D.J., Gately, W.L., Tyrell, J.A. and Florence, R.A. U.S. US 5,015,698 (1991).
18. Aycock, D.F. and Dert, V. Eur. Pat. Appl. EP 0,550,209 A2 (1992).
19. Aycock, D.F. and Dert, V. Can Pat. Appl. CA 2,082,695 A1 (1993).
20. Khouri, F.F., Halley, R.J. and Yates, J.B. Eur. Pat. Appl. 0. 564,244 A1 (1993).
21. Han, C.Y. and Gately, W.L. U.S. US 4,689,372 (1987).
22. Brown, S.B. and Lowry, R.C. Eur. Pat. Appl. EP 0.349.539 A2 (1989).
23. Brown, S.B. and Lowry, R.C. Eur. Pat. Appl. 0,349,717 A2 (1989).
24. Blubaugh, J.S., Brown, S.B., Dudley, P.R. and Yates, J.B. U.S. US 5,194,517 (1993).
25. Angeli, S.R. and Yates, J.B. Eur. Pat. Appl. 0,550,207 A1 (1993).
26. Angeli, S.R., Smith, G.F. and Whalen, D. Can. Pat. Appl. CA 2,082,735 (1993).
27. Ishida, H. and Morioka, M. U.S. US Pat. 5,084,496 (1992).
28. Yates, J.B., Angeli, S.R., Smith, G.F. and Whalen, D. Can. Pat. Appl. CA 2,082,735 (1991).
29. Yates, B. Eur. Pat. Appl. 0,550,208 A1 (1993).
30. Khouri, F.F. Eur. Pat. Appl. EP 0,519,642 A2 (1991).
31. Colby, R.H., Landry, C.J.T., Long, T.E., Massa, D.J. and Teegarden, D.M. U.S. US 5,276,089 (1994).
32. Arnold-Mauer, B., Bronstert, K. and Baumgartner, E. Eur. Pat. Appl. 0,457,138 A2 (1991).
33. Colby, R.H. and Landry, C.J.T. Eur. Pat. Appl. 0,530, 648 A2 (1993).
34. Kowalczyk, U., Bartman, M. and Pol, G. Eur. Pat. Appl. 0,391,031 A2 (1990).
35. Kowalczyk, U., Mügge, J. and Bartmann, M. Eur. Pat. Appl. 0,461,422 A2 (1991).
36. Kowalczyk, U., Bartman, M. and Poll, H.G. U.S. US 5,128,422 (1992).
37. Yamahita, Y. *Polym. Prepr., Am. Chem. Soc., Div. Polym. Chem.*, **31**, (1990).
38. Tsukahara, T., Nishimura, H., Aritomi, M., Arashiro, Y. and Yamauchi, S. Eur. Pat. Appl. EP 0,530,442 A1 (1992).
39. Heino, M.T. and Seppälä, J.V. "Acta Polytechnica Scandinavica", Chemical Technology and Metallurgy Series No. 214, Finnish Academy of Technology, Helsinki, (1993).
40. Steward, M.E., George, S.E., Miller, R.L. and Paul, D.R. *Polym. Eng. Sci.*, **33**, 675 (1993).
41. Shuster, M., Narkis, M. and Siegman, A. *J. Appl. Polym. Sci.*, **52**, 1383 (1994).

- 42 . Komarova, L.I., Lapina, N.N., Lokshin, B.V., Markova, G.D. and Vasnev, V.A. *Russ. Chem. Bull.*, **42**, 672 (1993).
- 43 . Blandy, C., Pellegatta, J-L. and Gilot, B. *J. Catal.*, **150**, 150 (1994).
- 44 . Siling, M.I. and Laricheva, T.N. *Uspekhi Khii*, **65**, 296 (1996).
- 45 . Inata, H. and Matsumura, S. *J. Appl. Polym. Sci.*, **30**, 3325 (1985).
- 46 . Inata, H. and Matsumura, S. *J. Appl. Polym. Sci.*, **32**, 4581 (1986).
- 47 . Inata, H. and Matsumura, S. *J. Appl. Polym. Sci.*, **34**, 2609 (1987).
- 48 . Inata, H. and Matsumura, S. *J. Appl. Polym. Sci.*, **34**, 2769 (1987).
- 49 . Inata, H. and Matsumura, S. *J. Appl. Polym. Sci.*, **32**, 5193 (1986).
- 50 . Inata, H. and Matsumura, S. *J. Appl. Polym. Sci.*, **33**, 3069 (1987).
- 51 . Böhme, F., Leistner, H. and Baier, A. *Angew. Makromol. Chem.*, **224**, 167 (1995).
- 52 . Akkapeddi, M.K. and Gervasi, J. *Polym. Prepr. (Am. Chem. Soc. Div. Polym. Chem.)*, **29**, 567 (1988).
- 53 . Cardi, N., Po, R., Giannotta, G., Occiello, E., Garbassi, F. and Messina, G. *J. Appl. Polym. Sci.*, **50**, 1501 (1993).
- 54 . Böhme, F., Leistner, H. and Baier, A. *Angew. Makromol. Chem.*, **228**, 117 (1995).
- 55 . Loontjes, T., Belt, W., Stanssens, D. and Weerts, P. *Polym. Bull.*, **30**, 13 (1993).
- 56 . Loontjes, T., Belt, W., Stanssens, D. and Weerts, P. *Makromol. Chem., Macromol. Symp.*, **75**, 211 (1993).
- 57 . Bikiaris, D.N. and Karayannidis, G.P. *J. Polym. Sci., Polym. Chem. Ed.*, **33**, 1705 (1995).
- 58 . Aharoni, S.M., Forbes, C.E., Hammond, W.B., Hindenlang, D.M., Mares, F., O'Brien, K. and Sedgwick, R.D. *J. Polym. Sci., Polym. Chem. Ed.*, **24**, 1281 (1986).
- 59 . Jacques, B., Devaux, J., Legras, R. and Nield, E. *Makromol. Chem., Macromol. Symp.*, **75**, 231 (1993).
- 60 . Jacques, B., Devaux, J., Legras, R. and Nield, E. *Polymer*, **37**, 1189 (1996).
- 61 . Akkapeddi, M.K. and van Buskirk, B. *Abstracts of papers of Am.Chem. Soc.*, **204**, 128 (1992).
- 62 . Akkapeddi, M.K. and van Buskirk, B. *Polym. Prepr., Am Chem. Soc., Div. Polym. Chem.*, **33**, (1992).
- 63 . Glans, J.H. and Akkapeddi, M.K. U.S. US 5,037,897 (1991).
- 64 . Akkapeddi, M.K., van Buskirk, B. and Glans, J.H. "Advances in Polymer Blends and Alloys Technology", ed. Finlayson, K., Technomic Publishing Company, Inc., Lancaster, U.S.A., **4**, 87 (1993).
- 65 . Sugio, A., Okabe, M. and Amagai, A. *Eur. Pat. Appl.* 0,148,774 B1 (1985).
- 66 . Chapter 3 of this thesis.
- 67 . Chapter 5 of this thesis.





## Chapter 7

### Poly(2,6-dimethyl-1,4-phenylene ether) - poly(dimethylsiloxane) triblock copolymers

#### Summary

*PPE-PDMS-PPE triblock copolymers were prepared by redistribution of PPE with  $\alpha,\omega$ -bis(4-hydroxy-3,5-dimethylphenyl)-terminated PDMS. Solution-cast films show microphase-separated morphologies as observed by Transmission Electron Microscopy (TEM). Triblock copolymers with a PDMS volume fraction ( $f_{\text{PDMS}}$ ) between 0.43 and 0.51 have domain dimensions proportional to the 2/3 power of the block copolymer molecular weight, as determined by Small Angle X-ray Scattering (SAXS). This is in fair agreement with the relationship earlier found for block copolymers in the strong segregation limit. Block copolymers with  $0.31 < f_{\text{PDMS}} < 0.35$  show a divergent scaling of the domain spacings proportional to the 0.350 power of the block copolymer molecular weight. The values of the domain spacings determined by SAXS measurements are in our case more reliable than the values obtained by spin diffusion Cross-Polarization Magic Angle Spinning (CP-MAS) solid-state  $^{13}\text{C}$ -NMR experiments, especially for block copolymers with large domain spacings.*

#### 7.1 Introduction

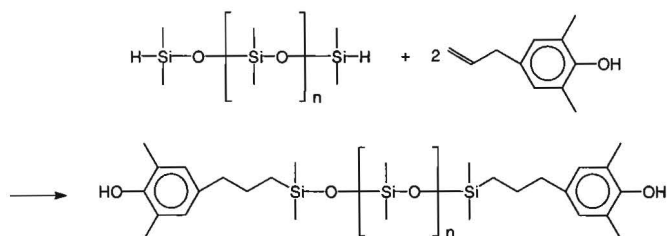
The fundamental principles of microphase separation in block copolymers are most frequently studied in styrene-diene block copolymers.<sup>1,2</sup> An extension to other block copolymers, such as e.g. strongly segregated siloxane block copolymers,<sup>3-6</sup> is now of growing interest. Many theoretical investigations have been carried out to understand the phase diagrams of block copolymers. The conventional representation of the phase behavior is expressed in terms of the volume fraction ( $f$ ) and the product  $\chi N$ , where  $N$  is equal to the degree of polymerization and  $\chi$  the Flory-Huggins segment-segment interaction parameter.<sup>7</sup> Enthalpic effects dominate in the strong segregation limit (SSL),  $\chi N \gg 10$ , leading to a strong spatial variation of concentration for the two constituents composing the block copolymer, along with a very narrow interface separating the domains of the two components. The interfacial composition profile approaches a step function. The entropic contributions become more important in the weak segregation limit (WSL),<sup>8,9</sup>  $\chi N \approx 10$ , leading

to a broad interface with a weakly varying composition profile. In the WSL the chains are not distorted and the molecular weight dependence of domain spacing ( $d$ ) is given by  $d \sim M^{1/2}$ , like in the unperturbed random coil. In the SSL chain-stretching occurs, resulting in a scaling of  $d$  with  $M^{2/3}$ . The scaling law  $d \sim M^{2/3}$  is predicted in several reports<sup>10-19</sup> and confirmed experimentally.<sup>20-23</sup> An even further stretching of chains in other block copolymers with liquid-crystalline (LC) blocks is observed. The exponent of scaling for these LC-block copolymers can become ca. 0.8. All scaling laws are, however, based on the assumption of thermodynamic equilibrium. Cast films of block copolymers are not necessarily in their thermodynamic equilibrium, since any morphology of phase separation could be trapped kinetically. The microdomain structures tend to be frozen-in during the solvent evaporation process.<sup>6,22-25</sup> This non-equilibrium effect is mostly observed in the case of spherical microdomain systems.

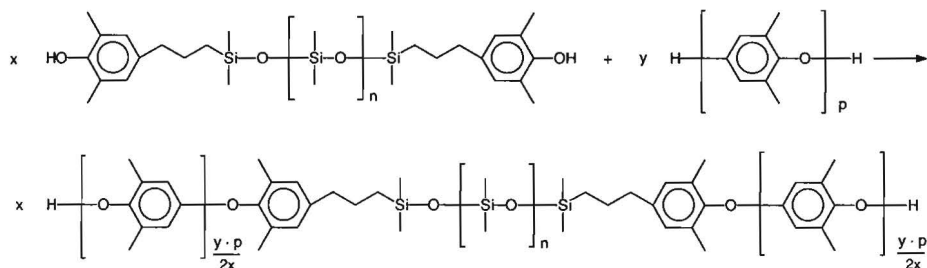
We investigated the microphase separation in triblock copolymers consisting of a central polydimethylsiloxane (PDMS) block and two outer poly(2,6-dimethyl-1,4-phenylene ether) blocks. Such copolymers, albeit less well-defined than our systems, have been prepared previously by the coupling of functional homopolymers in solution<sup>26,27</sup> or in a melt process.<sup>28,29</sup> Copolymerization of 2,6-dimethylphenol with phenol-modified PDMS can yield PPE-PDMS block and graft-copolymers such as reported in patent literature by the General Electric Company.<sup>30-32</sup> These phenol-modified PDMSs were prepared by hydrosilation of hydride-terminated polysiloxanes with allylphenols, such as 2-allyl-6-methylphenol, 2-allyl-4,6-dimethylphenol and 2-allyl-6-methoxyphenol (eugenol). We prepared PPE-PDMS-PPE via the PPE-redistribution method, as introduced in Chapter 3 of this thesis. The required phenol-modified PDMS was also prepared by hydrosilation. In order to obtain less sterically hindered endgroups than those acquired from a hydrosilation with 2-allyl-substituted phenols, we used 4-allyl-2,6-dimethylphenol (Scheme 7.1). Redistribution of  $\alpha,\omega$ -bis(4-hydroxy-3,5-dimethylphenyl)-terminated PDMS with PPE yields more well-defined PPE-PDMS-PPE triblock copolymers (Scheme 7.2) with a facile control of the PPE block length. This is advantageous in comparison with alternative routes for PPE-PDMS-PPE triblock copolymer synthesis and enables a facile study of the block length dependence on the domain size in the microphase-separated block copolymer.

The microphase segregation of the hard PPE and soft PDMS blocks was studied using Transmission Electron Microscopy (TEM) of solution-cast films. It was only possible to visualize the morphology obtained. TEM is not used to quantify the domain sizes since sample deformation during the cryogenic cutting and by beam damage can occur. The domain spacings were determined more accurately using Small Angle X-Ray Scattering (SAXS). A comparison was made between the obtained domain spacings by SAXS with the distances obtained from Cross-Polarization Magic Angle Spinning (CP-MAS) solid-state NMR proton spin diffusion

experiments. The use of spin diffusion experiments has been explored widely by Spiess and co-workers<sup>33-37</sup> and also used by Cho<sup>38,39</sup> for a determination domain spacings in segmented copolymers.



**Scheme 7.1:** Hydrosilylation reaction of 4-allyl-2,6-dimethylphenol and  $\alpha,\omega$ -bis(hydride)-terminated PDMS.



**Scheme 7.2:** Redistribution reaction of PPE and  $\alpha,\omega$ -bis(4-hydroxy-3,5-dimethylphenyl)-terminated PDMS.

## 7.2 Results and discussion

### 7.2.1 Synthesis

We prepared PPE-PDMS-PPE triblock copolymers by reacting  $\alpha,\omega$ -bis(4-hydroxy-3,5-dimethylphenyl)-terminated PDMS with PPE in a redistribution reaction under the action of a CuCl/4-dimethylaminopyridine (DMAP) catalyst in the absence of oxygen in chloroform during ca. 2 weeks at room temperature. The mechanism and scope of this redistribution reaction is described in detail in Chapter 3 of this thesis. The amount of residual homopolymers is less

than 5% as determined by  $^1\text{H-NMR}$  spectroscopy. Block lengths of the obtained copolymer are determined by comparison of the peak integrals of the repeating units with those of the endgroups. PDMS volume fractions were determined also using  $^1\text{H-NMR}$  spectroscopy. When reacting the phenol-terminated siloxane with PPE, the molecular weight of the siloxane remains constant and the PPE-block length in the copolymer depends on the molar ratio of the number of PPE repeating units towards phenolic endgroups attached to PDMS. Triblock copolymers with total number average molecular weights ( $\overline{M}_n$ ) between 10.0 and 71.0 kg/mol and PDMS volume fractions ( $f_{\text{PDMS}}$ ) between 0.31 and 0.76 are prepared.

The strong segregation limit is obtained if  $\chi N \gg 10$ . The Flory-Huggins interaction parameter  $\chi$  can be determined from the solubility parameters ( $\delta$ ) using the following equation:  $\chi = V_0 (\delta_1 - \delta_2)^2 / RT$ , in which  $V_0$  is a reference molar volume of 100 cm<sup>3</sup>/mol. and  $T$  is the temperature. The solubility parameters can be determined from the following equation:  $\delta = (E_{\text{coh}}/V)^{0.5}$ , in which  $E_{\text{coh}}$  is the cohesive energy. Using  $E_{\text{coh}} = 46290 \text{ J/mol}$  and  $V_{\text{PPE}} = 112.3 \text{ cm}^3/\text{mol}$ ,<sup>40</sup> we could calculate  $\delta_{\text{PPE}} = 20.3 \text{ J}^{1/2}/\text{cm}^{3/2}$ . This value corresponds well with  $\delta$  values for PPE:  $\delta = 9.5 \text{ cal}^{1/2}/\text{cm}^{3/2} = 19.4 \text{ J}^{1/2}/\text{cm}^{3/2}$  and  $10.21 \text{ cal}^{1/2}/\text{cm}^{3/2} = 20.9 \text{ J}^{1/2}/\text{cm}^{3/2}$  as reported elsewhere.<sup>41</sup> The molar volumes of homopolymers PDMS and PPE are known to be 69.1 and 112.3 cm<sup>3</sup>/mol.<sup>40</sup> We used a reference molar volume ( $V_0$ ) of 100 cm<sup>3</sup>/mol for the PPE-PDMS-PPE block copolymers. Using  $\delta_{\text{PDMS}} = 15.4 \text{ J}^{1/2}/\text{cm}^{3/2}$  as reported by Chu,<sup>6</sup> we could calculate a Flory-Huggins interaction parameter  $\chi = 0.72$  at 298 K. The SSL is valid when  $\chi N \gg 10$ , so with  $\chi = 0.72$  we require  $N \gg 14$  ( $N = N_{\text{PPE}} + N_{\text{PDMS}}$ ). A PPE-PDMS-PPE triblock copolymer with  $N = 14$  and  $f = 0.5$  would have the following block lengths:  $\overline{M}_n$  (entire triblock) = 1.30 kg/mol,  $\overline{M}_n$  (PPE block) = 0.34 kg/mol,  $\overline{M}_n$  (PDMS block) = 0.62 kg/mol. All copolymers prepared have a higher molecular weight than 1.3 kg/mol and are therefore in the SSL ( $\chi N \gg 10$ ).

## 7.2.2 Electronmicroscopy

Figure 7.1 shows TEM pictures of two lamellar morphologies of block copolymers with different molecular weights, and a PDMS volume fraction  $f$  of approximately 0.5. The dark regions represent the PDMS phase, which has a higher electron density<sup>42</sup> caused by the presence of Si-atoms with high atomic number. The light areas represent the PPE phase. The presented TEM pictures are obtained from films cast from chloroform. The observed morphologies are as expected for this PDMS volume fraction. The increase in molecular weight is reflected in larger domain spacings.

Solution-cast films show often non-equilibrium morphologies. Especially domain systems with a low block content are often in a metastable state, in contrast to domain systems with volume

fractions  $f \approx 0.5$ , which are often very close to the equilibrium state.<sup>22-25</sup> This is illustrated by the TEM picture of block copolymer with PDMS volume fraction  $f = 0.31$  in Figure 7.2. In case of an equilibrium morphology, spherical PDMS microdomains have to be expected. However, a lamellar morphology as a non-equilibrium morphology was seen as earlier reported by Pochan.<sup>24</sup>

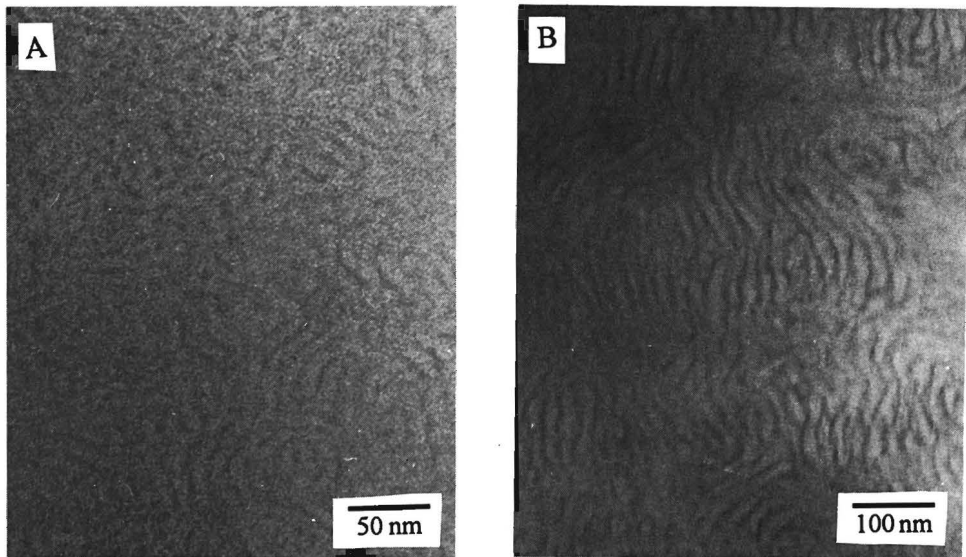


**Figure 7.1:** TEM pictures of films of PPE-PDMS-PPE triblock copolymers, cast from chloroform: A.  $\overline{M}_n$  (PPE block) = 4.55 kg/mol,  $\overline{M}_n$  (PDMS block) = 7.6 kg/mol,  $\overline{M}_n$  (entire triblock) = 16.7 kg/mol,  $f_{PDMS} = 0.47$ ; B.  $\overline{M}_n$  (PPE block) = 5.9 kg/mol,  $\overline{M}_n$  (PDMS block) = 16.2 kg/mol,  $\overline{M}_n$  (entire triblock) = 28.0 kg/mol,  $f_{PDMS} = 0.56$ .

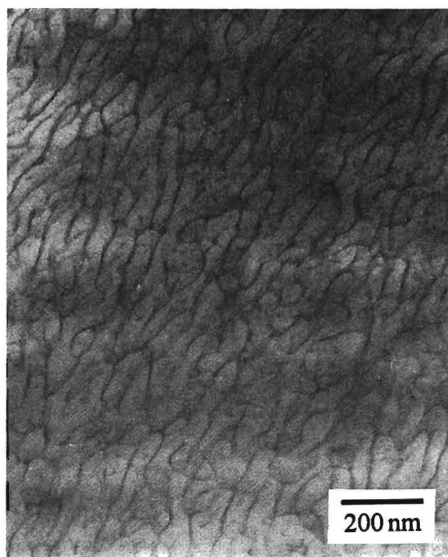


**Figure 7.2:** TEM picture of film of PPE-PDMS-PPE triblock copolymer, cast from chloroform:  $\overline{M}_n$  (PPE block) = 7.7 kg/mol,  $\overline{M}_n$  (PDMS block) = 6.2 kg/mol,  $\overline{M}_n$  (entire triblock) = 21.6 kg/mol,  $f_{PDMS} = 0.31$ .

### 7.2.3 Small Angle X-ray Scattering

Parallel to the TEM analyses, the block copolymers were characterized using SAXS in order to obtain a more accurate domain spacings. The domain spacings were obtained from Lorentz-corrected data plots. As an example, the scattering intensity profile and the Lorentz-corrected plot of a lamellar triblock copolymer is shown in Figures 7.4 and 7.5.

To obtain information about the scaling law relationships concerning the domain size and their dependency on the molecular weight of the domain-forming blocks, block copolymers were synthesized with different molecular weights and their solution-cast films were characterized using SAXS. The results are summarized in Table 7.1. Distances were calculated from the first-order reflections assuming that all structures have lamellar morphologies. An experimental error of 5% was estimated for the determination of domain sizes using SAXS. For all block copolymers with a PDMS volume fraction between 0.31 and 0.35 it is therefore assumed that they have a non-equilibrium lamellar morphology as presented in Figure 7.2.  $\chi N$  values were calculated using  $\chi = 0.72$  (reference molar volume  $V_0 = 100 \text{ cm}^3/\text{mol}$ ) and  $N$  defined as  $N_{PPE} + N_{PDMS}$ .

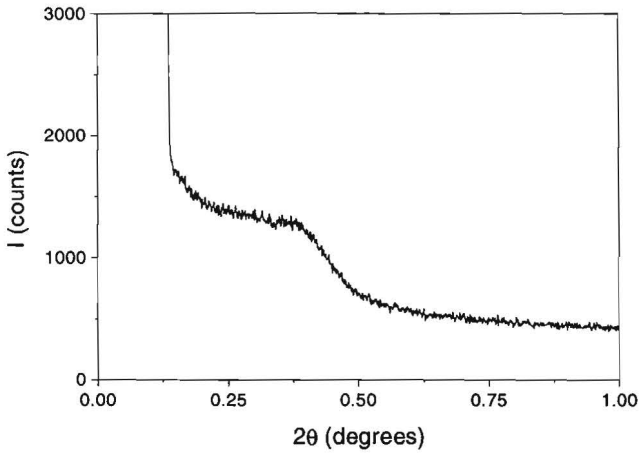


**Figure 7.4:** SAXS intensity profile for a PPE-PDMS-PPE triblock copolymer;  $\overline{M}_n$  (PPE block) = 4.55 kg/mol,  $\overline{M}_n$  (PDMS block) = 7.6 kg/mol,  $\overline{M}_n$  (entire triblock) = 16.7 kg/mol,  $f_{PDMS} = 0.47$ .

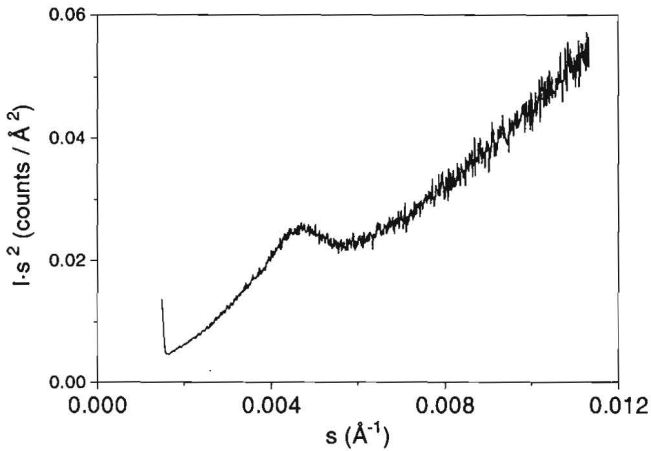


**Figure 7.5:** SAXS experiment; Lorentz-corrected plot for a PPE-PDMS-PPE triblock copolymer;  $\overline{M}_n$  (PPE block) = 4.55 kg/mol,  $\overline{M}_n$  (PDMS block) = 7.6 kg/mol,  $\overline{M}_n$  (entire triblock) = 16.7 kg/mol,  $f_{PDMS} = 0.47$ ,  $I$  = intensity and  $s$  = scattering vector ( $s = 1/d$ , reciprocal distance).



**Table 7.1:** Domain spacings obtained from Lorentz-corrected SAXS data,  $\chi N$  is calculated using a reference volume  $V_0 = 100 \text{ cm}^3/\text{mol}$  and  $N = N_{PPE} + N_{PDMS}$ , at 298 K.

$\overline{M}_n$ (entire triblock) kg/mol	$\overline{M}_n$ (PDMS block) kg/mol	N	$\chi N$	$f_{PDMS}$	d (nm)
21.6	6.2	212	151	0.31	32
14.3	6.1	151	108	0.33	27
64.8	21.2	649	474	0.34	47
71.0	23.0	710	507	0.35	47
30.5	13.3	322	231	0.43	44
11.3	5.4	122	87	0.43	23
13.8	6.8	150	107	0.43	25
29.0	12.4	305	218	0.46	41
14.7	8.1	164	117	0.48	21
16.7	7.6	178	128	0.47	25
28.5	13.1	304	218	0.48	42
30.7	13.3	324	231	0.48	33
11.6	7.2	134	96	0.50	20
45.0	22.0	488	349	0.51	50
10.0	7.6	122	88	0.76	26

The relationships between dependency of molecular weight and domain spacing is illustrated in Figures 7.6, for block copolymers with  $0.43 < f_{PDMS} < 0.51$  and with  $0.31 < f_{PDMS} < 0.35$ , respectively. Although the data points are somewhat scattered, primarily due to variation of the chemical composition, microstructure of the block copolymers, and film preparation conditions, we fitted the data points using linear regression to obtain the scaling law relationships. Linear regression of the data with  $0.43 < f_{PDMS} < 0.51$  gives a slope of 0.662 ( $r = 0.947$ ), while linear regression of the data with  $0.31 < f_{PDMS} < 0.35$  gives a slope of 0.350 ( $r = 0.998$ ). The copolymers with PDMS volume fractions  $0.43 < f_{PDMS} < 0.51$  are expected to be very close to equilibrium and have a lamellar morphology. The scaling factor 0.665 is very close to the 2/3 power relationship, which was expected for block copolymers in the strong segregation limit.<sup>10-23</sup> For block copolymers with lower PDMS volume fractions ( $0.31 < f_{PDMS} < 0.35$ ), a slope of 0.350 is found in contrast to the predicted 2/3 power. This discrepancy in the scaling relationship may be caused by the obtained non-equilibrium morphologies for low volume fractions PDMS.

Solvent casting can dramatically affect bulk domain dimensions and consequently also the scaling relationships. Chain-collapse can occur during the solvent evaporation, causing a smaller scaling factor. Sun<sup>43</sup> reported a scaling factor of 1/3 for polystyrene in the collapsed state, as expected for collapsed homopolymers.<sup>44</sup> Similarly, Bates et al.<sup>25</sup> found a divergent scaling relationship of  $d \sim M^{0.37}$  for styrene-butadiene block copolymers with low butadiene content.

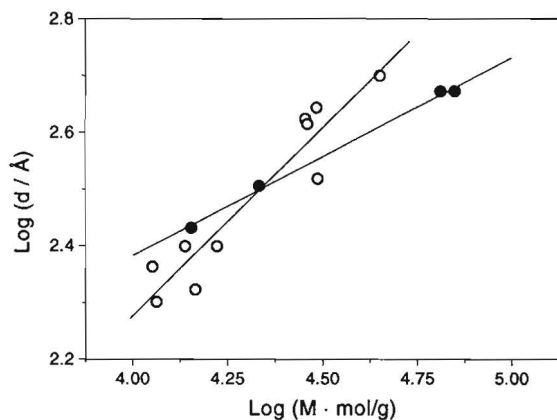


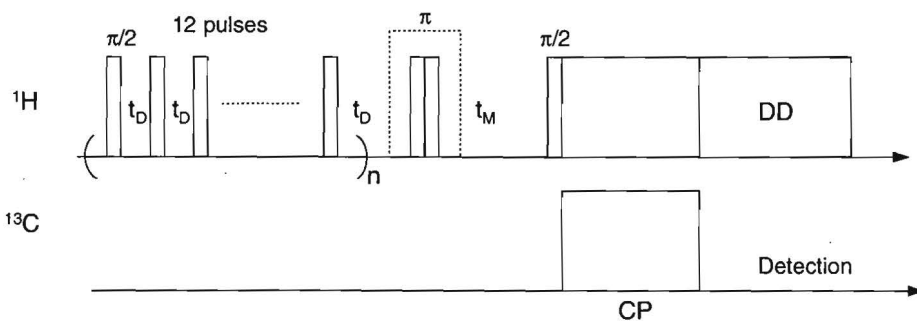
**Figure 7.6:** *Log d versus log M for PPE-PDMS-PPE triblock copolymers with volume fraction PDMS: using open spheres:  $0.43 < f_{PDMS} < 0.51$  and using closed spheres:  $0.31 < f_{PDMS} < 0.35$ .*

#### 7.2.4 Solid state NMR

##### *Spin diffusion technique:*

Besides the SAXS experiments, information about the domain spacings and interfacial distances in microphase-separated PPE-PDMS-PPE triblock copolymers can be obtained from proton spin diffusion in precipitated powder samples of PPE-PDMS-PPE block copolymers as monitored with Cross-Polarization Magic Angle Spinning (CP-MAS) <sup>13</sup>C-NMR. This technique is particularly useful for obtaining information on small domain spacings and the interface. The used block copolymers have a rather broad block length distribution ( $D \approx 2$ ) and are, therefore, supposed to have broad interfaces. For more accurate domain spacings a filter experiment with <sup>1</sup>H-detection can be performed, as described by Spiess and co-workers<sup>45</sup> for characterization of interfaces in core-shell polymers. Using this technique no additional errors are introduced due to variation in CP efficiency for different signals.

Discrimination of rigid and mobile regions in the samples by means of  $^1\text{H-NMR}$  of solid samples is hampered among other things by the lack of resolution (small chemical shift dispersion). In  $^{13}\text{C-NMR}$ , chemical shift differences and hence resolution are much larger. We performed such spin diffusion experiments using the precipitated powder of PPE-PDMS-PPE block copolymers in analogy to a method described by Cho<sup>38</sup> for poly(dimethylsiloxane-urea-urethane) segmented copolymers. The PPE-PDMS-PPE triblock copolymers contain two phases of rather different mobilities. This can be seen clearly from a standard Bloch pulse CP-MAS  $^{13}\text{C-NMR}$  spectrum. Such a spectrum shows only an intense Si-CH<sub>3</sub> signal at 1.6 ppm. Due to the very high mobility of the PDMS phase and because the PPE segment phase is much less mobile with its high  $T_g$ , only a Si-CH<sub>3</sub> signal of the soft segment phase appears in this spectrum, caused by the long  $^{13}\text{C}$  longitudinal relaxation time ( $T_1$ ) of rigid solid samples. In order to determine the domain size, a dipolar filter pulse sequence<sup>46,47</sup> was used as shown in Scheme 7.3. This pulse sequence is designed to partially average dipolar couplings between protons. However, the windows  $\tau$  between the  $\pi/2$  pulses are set to a rather long value of 13  $\mu\text{s}$ . As a result, the averaging is not effective for small dipolar couplings and the z-magnetization of the corresponding protons relaxes. In this way only the magnetization of the protons in the mobile regions of the sample remain after application of the dipolar filter. To improve the selection, the filter pulse sequence is repeated up to 7 times. After the selection sequence the evolution of proton spin diffusion during the mixing time is detected by a normal proton-carbon CP sequence. During the mixing time the proton magnetization not only depends on the spin diffusion but also on the proton  $T_1$  relaxation. A  $\pi$  pulse is introduced in every other scan just after the selection sequence in order to obtain experimental  $^{13}\text{C}$  magnetizations that could be corrected by a factor of  $\exp(t_m/T_1)$ .<sup>33,48</sup> Proton relaxation times  $T_1$  are measured by an inversion-recovery CP sequence.



**Scheme 7.3:** Dipolar filter pulse sequence.

If the spin diffusion coefficients within the soft and rigid segment phase are known, then a dispersed domain size can be calculated from a plot of the intensity versus the square root of the mixing time using the following equation:<sup>34,38</sup>

$$d_{dis} = \left( \frac{\rho_{H, PDMS} \times f_{PDMS} + \rho_{H, PPE} \times f_{PPE}}{f_{PDMS} \times f_{PPE}} \right) \times \frac{4 \times f_{dis} \times \varepsilon \times \sqrt{D_{PDMS} \times D_{PPE}}}{\sqrt{\pi} (\sqrt{D_{PDMS} \times \rho_{H, PDMS}} + \sqrt{D_{PPE} \times \rho_{H, PPE}})} \times \sqrt{t_m^*}$$

in which:  $d_{dis}$  denotes the distance of the dispersed phase,  $\rho_H$  the proton density,  $f$  volume fraction,  $\varepsilon$  the dimensionality,  $D$  the diffusion coefficient, and  $t_m^*$  the mixing time at the intersection of the initial tangent and normalized complete exchange intensity in a plot of the normalized intensity versus the square root of the mixing time. The symbols will be explained in more detail for the employed system in the next section.

The overall domain size can be calculated using the following equation, as described by Cho<sup>38</sup>:

$$d = \frac{d_{dis}}{\varepsilon \sqrt{f_{dis}}}$$

#### *Spin diffusion in PPE-PDMS block copolymers:*

In the equation which defines  $d_{dis}$ , the proton densities of PDMS and PPE are expressed as  $\rho_{H,PDMS}$  and  $\rho_{H,PPE}$ .  $\rho_{H,PDMS} = 0.07848 \text{ g/cm}^3$  is calculated from  $\rho_{PDMS} = 0.97 \text{ g/cm}^3$  and the proton fraction = 6/74 g/g.  $\rho_{H,PPE} = 0.07058 \text{ g/cm}^3$  is calculated from  $\rho_{PPE} = 1.06 \text{ g/cm}^3$  and the proton fraction = 8/120.  $f_{dis}$  is the volume fraction of the dispersed phase. The proton spin diffusion coefficients of phases PDMS and PPE are expressed by the symbols:  $D_{PDMS}$  and  $D_{PPE}$ .  $D_{PDMS}$  is assumed to be  $0.5 \times 10^{-16} \text{ m}^2/\text{s}$ , similar to the reported diffusion coefficient for polybutadiene.<sup>38,48</sup> The proton spin diffusion coefficient of alkane ( $6.2 \times 10^{-16} \text{ m}^2/\text{s}$ )<sup>49</sup> is used as an estimate of  $D_{PPE}$ . This diffusion coefficient is close to the assumption by Feng.<sup>50</sup>  $D_{PPE} = 5.0 \times 10^{-16} \text{ m}^2/\text{s}$ .  $\varepsilon$  indicates the dimensionality of the system:  $\varepsilon = 1$  for lamellar structures,  $\varepsilon = 2$  for cylinders in a matrix and  $\varepsilon = 3$  for spheres in matrix. The square root of  $t_m^*$  is determined from the initial slope of a plot of the normalized intensity versus the square root of the mixing time, as shown in Figure 7.7 for a typical PPE-PDMS-PPE block copolymer. The experimental magnetizations are multiplied by the factor  $\exp(t_m/T_1)$ , where  $T_1$  was obtained from the average of the  $T_1$  values of the signals at 155, 146, 133 and 17 ppm of the PPE phase. For this particular copolymer, we determined  $T_1 = 754 \text{ ms}$ . The maximum intensity ( $I$ ) at high mixing times is normalized as  $I = 1$ . The presented triblock copolymer consists of a central PDMS block ( $\overline{M}_n$  (PDMS block) = 7.0 kg/mol) and two outer PPE blocks ( $\overline{M}_n$  (PPE block) = 6.8 kg/mol). The block copolymer has a total molecular weight of  $\overline{M}_n = 13.8 \text{ kg/mol}$  and a dispersed volume fraction  $f_{dis} = f_{PDMS} = 0.43$ . We used  $\varepsilon = 1$ , since we assumed that the

precipitated powder of the employed block copolymers have a lamellar morphology, like in the solution-cast films, as shown from TEM analysis.

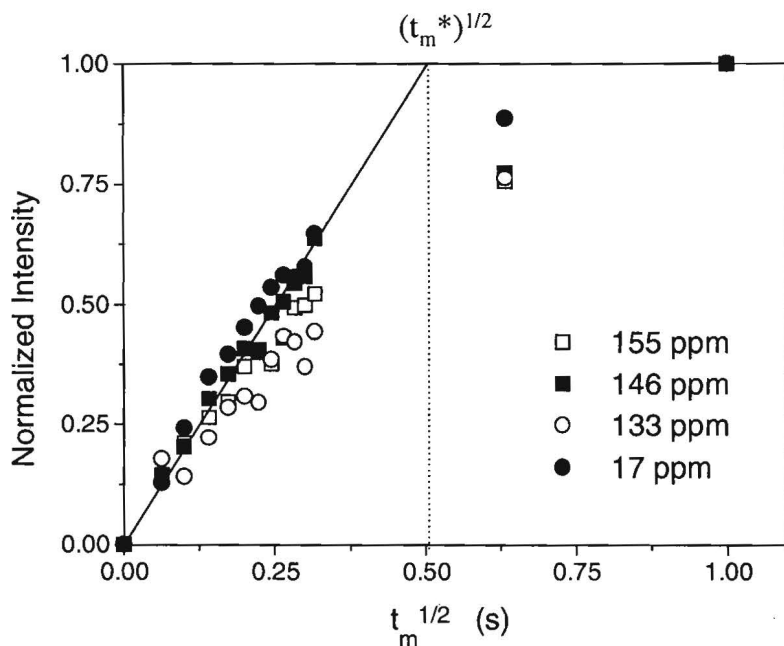


**Figure 7.7:** Magnetization growth of the peaks of the PPE phase as a function of the square root of the mixing time. All intensities were corrected by the factor  $\exp(t_m/T_1)$  and normalized to the highest intensity,  $\bar{M}_n$  (entire triblock) = 13.8 kg/mol,  $f_{PDMS} = 0.43$ , the initial slope is given by the solid line.

For the copolymer presented in Figure 7.8, we could calculate  $(t_m^*)^{1/2} = 0.51 \text{ s}^{1/2}$ , averaged for peaks at different chemical shifts. Subsequently, we calculated  $d_{\text{dis}} = 12.4 \text{ nm}$  and  $d$  (overall) = 26.3 nm. This domain spacing as determined by a spin diffusion experiment is in good agreement with the distance obtained by SAXS:  $d = 25.0 \text{ nm}$ . The accuracy of the determination of by spin diffusion experiment is illustrated in Table 7.2, in which  $d$  (overall) is calculated for each chemical shift separately.

**Table 7.2:** Domain spacings determined for signals at different chemical shift.

peak chemical shift (ppm)	$(t_m^*)^{1/2}$ (s <sup>1/2</sup> )	$d_{\text{dis}}$ (nm)	d (overall) (nm)
155	0.54	13	28
146	0.48	12	25
133	0.60	15	31
17	0.43	10	22

We also performed spin diffusion experiments for PPE-PDMS-PPE samples with higher molecular weights, containing larger domain spacings. Determination of these larger domain sizes requires longer mixing times, resulting in a larger correction factor  $\exp(t_m/T_1)$ . Therefore, the experimental error for the determination of domain spacings in block copolymers with higher molecular weight becomes larger. For experimental spin diffusion data from systems with large domains, determination of complete-exchange intensities values  $I_{\text{PPE}}(t_m \rightarrow \infty)$  becomes more difficult.<sup>33</sup> Moreover, using <sup>13</sup>C-detected proton spin diffusion experiments in these large domain systems, we obtain information about the interfacial distance instead of the total lamellar domain spacing. Therefore, a large deviation in the domain spacing as determined by SAXS compared to the results obtained from solid-state NMR was found for PPE-PDMS-PPE block copolymer with higher molecular weight than in the previous example. For a copolymer with the following parameters:  $\bar{M}_n$  (PPE block) = 8.6 kg/mol,  $\bar{M}_n$  (PDMS block) = 13.3 kg/mol,  $\bar{M}_n$  (entire triblock) = 30.5 kg/mol,  $f_{\text{PDMS}} = f_{\text{dis}} = 0.47$ , we determined d (overall) = 24.0 nm. For this block copolymer we obtained from a SAXS measurement d = 44.0 nm. For a block copolymer with similar block lengths,  $\bar{M}_n$  (PPE block) = 8.3 kg/mol,  $\bar{M}_n$  (PDMS block) = 12.4 kg/mol,  $\bar{M}_n$  (entire triblock) = 29.0 kg/mol,  $f_{\text{PDMS}} = f_{\text{dis}} = 0.46$ , we determined d (overall) = 18.0 nm. For this block copolymer we obtained from a SAXS measurement d = 41.0 nm. From these NMR results obtained for similar polymers, we estimate an experimental error of 20%. However the actual error can be larger due to a structural inaccuracy, in particular for block copolymers with long domain spacings. Generally, using <sup>13</sup>C-detected proton spin diffusion, the interface is characterized. A filter experiment with <sup>1</sup>H-detection can give more accurate distances of lamellar domain spacings also for large systems.<sup>45</sup>

### 7.3 Conclusions

Redistribution of PPE with  $\alpha,\omega$ -bis(4-hydroxy-3,5-dimethylphenyl)-terminated PDMS yields microphase-separated PPE-PDMS-PPE triblock copolymers. Triblock copolymers with a PDMS volume fraction  $0.43 < f_{\text{PDMS}} < 0.51$  show domain spacings (determined by SAXS) proportional to the 0.662 power of the block copolymer molecular weight. This is in agreement with the expected 2/3 power law for lamellar block copolymers in the strong segregation limit. Block copolymers with  $0.31 < f_{\text{PDMS}} < 0.35$  showed a divergent scaling behavior and the domain spacings are proportional to the 0.350 power of the block copolymer molecular weight, probably caused by non-equilibrium morphologies of the solution-cast films with low PDMS content. The domain spacings of PPE-PDMS-PPE block copolymers, obtained from spin diffusion experiments, are more consistent with the domain spacings obtained from SAXS for PPE-PDMS-PPE block copolymers with small domain sizes than for similar block copolymers with large domain sizes. Using  $^{13}\text{C}$ -detected proton spin diffusion experiments in block copolymers with large domain sizes rather yields information on the interface.

### 7.4 Experimental

#### *Materials*

The following  $\alpha,\omega$ -silanol-terminated PDMS grades were obtained from ABCR, Karlsruhe, Germany: DMS-S27 ( $\overline{M}_n = 18$  kg/mol, viscosity 700 cSt), DMS-S21 ( $\overline{M}_n = 4.2$  kg/mol, viscosity 100 cSt) and DMS-S15 ( $\overline{M}_n = 1.5$ -2.0 g/mol, viscosity 50 cSt). The  $\alpha,\omega$ -bishydride-terminated siloxanes with number average molecular weights of 6.0 kg/mol (DMS-H21, viscosity 100 cSt) and 28.0 kg/mol (DMS-H31, viscosity 1000 cSt) were obtained from ABCR as well. The hydrosilation catalyst, a Platinum-divinyltetramethyldisiloxane complex in xylene (ABCR, PC 072) was kept under nitrogen. Chlorodimethylsilane (Acros, 99%), CuCl (Acros, 99%), 4-dimethylaminopyridine (DMAP) (Acros, 99%), ethylenediaminetetraacetic acid (EDTA) (Aldrich), pyridine (Merck, 99%) and methanol (Merck, p.a) were used as received. Dichloromethane (Merck, p.a.) was distilled from  $\text{P}_2\text{O}_5$ . Toluene (Merck, p.a.) was distilled from sodium. Chloroform (Biosolve, p.a.) was degassed by vacuum when frozen.

PPE-1, a commercial PPE grade, was supplied by General Electric Plastics ( $\overline{M}_n = 16.8$  kg/mol,  $D = 2.26$ ,  $IV = 0.46$  dL/g). To obtain PPE-PDMS-PPE block copolymers with a larger PPE total block length than 15 kg/mol, we used PPE-1. For all other block copolymer syntheses we used the low molecular weight PPEs prepared by a precipitation polymerization method, as described in Chapter 2 of this thesis.

#### *Techniques*

$^1\text{H-NMR}$  spectra were recorded in  $\text{CDCl}_3$  on a Bruker AM-400 spectrometer at 400.13 MHz. All  $\delta$  values were given in ppm downfield from TMS but referenced to residual  $\text{CHCl}_3$  ( $\delta = 7.27$  ppm). Infrared measurements were performed on a Perkin Elmer 1600 series FT-IR spectrometer. DSC-

thermograms were recorded on a Perkin Elmer DSC-2, with a heating rate of 20 °C/min. Transmission Electron Microscopy was carried out using a JEOL 2000-FX operated at 80 kV. Thin samples for TEM with an approximate thickness of 80 nm were cut at -122 °C. No additional staining technique was applied. Small Angle X-ray Scattering (SAXS) studies were performed using Cu K $\alpha$  radiation and a Riguka Denki small angle goniometer. Proton-decoupled solid state  $^{13}\text{C}$  NMR spectra were recorded at 100.62 Hz on a Bruker MSL-400 spectrometer using cross-polarization and magic angle spinning at room temperature. The spinning rate was 4 kHz. The proton  $\pi/2$  pulse length was 4.4  $\mu\text{s}$  and the relaxation delay 5 s. The cross-polarization time was 5 ms. The dipolar filter sequence of 12  $\pi/2$  pulses was repeated 7 times. Proton longitudinal relaxation times ( $T_1$ ) were measured with an inversion-recovery pulse sequence.

All reactions were performed under an argon atmosphere. For this, the glassware was first put under vacuum and heated, to remove all the water vapor. After evacuation the flasks were flushed three times with argon. In case of the described polymer reactions, typical examples are given and reactions are performed in a similar way for different molecular weights.

#### $\alpha,\omega$ -Bishydride-terminated PDMS:

$\alpha,\omega$ -Silanol-terminated PDMS (40.13 g, 2.22 mmol,  $\overline{M}_n = 18.0$  kg/mol, number average degree of polymerization  $\overline{P}_n = 243$ , code DMS-S27), was added dropwise into chlorodimethylsilane (4.38 g, 0.046 mol). After 1 day stirring at room temperature the excess of chlorodimethylsilane was removed by applying vacuum. The yield was 38.3 g (95%) of a transparent, highly viscous fluid.  $\overline{M}_n$  determined by  $^1\text{H-NMR}$ ,  $\overline{P}_n = 237$ .  $^1\text{H-NMR}$  ( $\text{CDCl}_3$ ):  $\delta$  0.09 (n times 6H, broad s, repeating unit  $\text{Si}(-\text{CH}_3)_2\text{-O}$ ), 4.71 (2H, s,  $J = 2.8$  Hz,  $\alpha$  and  $\omega$  H-Si). IR (KBr): 2126  $\text{cm}^{-1}$  Si-H stretching mode, 912  $\text{cm}^{-1}$  Si-H bending mode. DSC-scan:  $T_g = -120$  °C ( $\Delta C_p = 0.24$  J/g °C),  $T_c = -80$  °C ( $\Delta H_c = -17.6$  J/g),  $T_{m1} = -41$  °C ( $\Delta H_{m1} = 7.0$  J/g) and  $T_{m2} = -29$  °C ( $\Delta H_{m2} = 12.2$  J/g).

#### 4-Allyl-2,6-dimethylphenol:

4-Allyl-2,6-dimethylphenol is prepared according to a literature procedure.<sup>51</sup>  $^1\text{H-NMR}$  ( $\text{CDCl}_3$ ):  $\delta$  2.24 (6H, s, Ph- $\text{CH}_3$ ), 3.28 (2H, d,  $J = 6.8$  Hz,  $\text{CH}_2=\text{CH}-\text{CH}_2\text{-Ph}$ ), 4.51 (1H, s, HO-Ph), 5.06 (2H, m,  $J = 6.7$  Hz,  $\text{CH}_2=\text{CH}-\text{CH}_2\text{-}$ ), 5.96 (1H, m,  $\text{CH}_2=\text{CH}-\text{CH}_2\text{-Ph}$ ), 6.82 (2H, s, *ortho* aromatic H-Ph). IR (KBr): 1638  $\text{cm}^{-1}$ , 1433  $\text{cm}^{-1}$ , 1309  $\text{cm}^{-1}$ , 994  $\text{cm}^{-1}$  and 913  $\text{cm}^{-1}$  -CH=CH $_2$  vibration modes.

#### $\alpha,\omega$ -Bis(3,5-dimethyl-4-hydroxyphenyl)-terminated PDMS:

$\alpha,\omega$ -Bishydride-terminated PDMS (12.82 g, 2.14 mmol,  $\overline{M}_n = 6.0$  kg/mol, number average degree of polymerization  $\overline{P}_n = 81$ , code DMS-H21) and 4-allyl-2,6-dimethylphenol (0.71 g, 4.36 mmol) were dissolved in 20 mL toluene under nitrogen atmosphere in a glovebox. 7  $\mu\text{L}$  platinum catalyst (code PC 072) was added. Subsequently, the reaction mixture was moved to a fume hood and the temperature was raised to 80 °C. After 12 hours of reaction no 4-allyl-2,6-dimethylphenol and hydride endgroups could be detected by  $^1\text{H-NMR}$  and IR. The solvent was removed by applying vacuum, yielding 12.74 g (94%) of  $\alpha,\omega$ -bis(3,5-dimethyl-4-hydroxyphenyl)-terminated PDMS. The product was highly viscous and yellow.  $\overline{M}_n = 6.5$  kg/mol;  $\overline{P}_n = 83$ , determined by  $^1\text{H-NMR}$  spectroscopy.  $^1\text{H-NMR}$  ( $\text{CDCl}_3$ ):  $\delta$  0.09 (n times 6H, broad s, repeating unit  $\text{Si}(\text{CH}_3)_2\text{-O}$ ), 0.58 (4H, m,  $\alpha$  and  $\omega$  Si- $\text{CH}_2$ ), 1.58 (4H, m,  $\alpha$



and  $\omega$  Si-CH<sub>2</sub>-CH<sub>2</sub>), 2.23 (12H, s,  $\alpha$  and  $\omega$  Ph-CH<sub>3</sub>), 2.49 (4H, m,  $\alpha$  and  $\omega$  Si-CH<sub>2</sub>-CH<sub>2</sub>-CH<sub>2</sub>-Ph), 6.78 (*ortho* aromatic H-Ph).

#### PPE-PDMS-PPE block copolymer:

PPE-1 (2.22 g, 0.132 mmol,  $\overline{M}_n = 16.8$  kg/mol),  $\alpha,\omega$ -bis(3,5-dimethyl-4-hydroxyphenyl)-terminated PDMS (2.00 g, 0.112 mmol,  $\overline{M}_n = 17.9$  kg/mol,  $\overline{P}_n = 237$ ), CuCl (0.058 g, 0.58 mmol), and DMAP (0.12 g, 0.92 mmol) were set under argon by evacuation of the flask and flushing three times with argon. The reaction was started by addition of degassed chloroform (30 ml). After 14 days the reaction mixture was extracted subsequently with an aqueous 10 wt% EDTA solution (60 mL) and an aqueous 10 vol% HCl solution (60 mL). Then the chloroform layer was precipitated in methanol (300 mL) and dried in vacuum (80 °C). The yield was 3.46 g (82%) of a white powder. Molecular weights determined by <sup>1</sup>H-NMR spectroscopy:  $\overline{M}_n = 28.0$  kg/mol (entire triblock),  $\overline{M}_n$  (PDMS block = 16.2 kg/mol),  $\overline{M}_n$  (PPE block) = 5.9 kg/mol,  $\overline{P}_n$  (siloxane block) =  $n = 218$  and  $\overline{P}_n$  (PPE block) =  $\frac{1}{2}p = 48$ . <sup>1</sup>H-NMR (CDCl<sub>3</sub>):  $\delta$  0.09 (( $n+1$ ) times 6H, broad s, repeating unit Si(CH<sub>3</sub>)<sub>2</sub>-O), 0.62 (4H, m,  $\alpha$  and  $\omega$  Si-CH<sub>2</sub>), 1.66 (4H, m,  $\alpha$  and  $\omega$  Si-CH<sub>2</sub>-CH<sub>2</sub>), 2.23 (12H, s,  $\alpha$  and  $\omega$  Ph-CH<sub>3</sub>), 2.58 (4H, m,  $\alpha$  and  $\omega$  Si-CH<sub>2</sub>-CH<sub>2</sub>-CH<sub>2</sub>-Ph), 6.37 (4H, s,  $\alpha$  and  $\omega$  aromatic *meta* C-H PPE heat unit), 6.48 (p times 2H, broad s,  $\alpha$  and  $\omega$  aromatic *meta* C-H PPE repeating unit), 6.90 (4H, s,  $\alpha$  and  $\omega$  *meta* aromatic C-H Si-(CH<sub>2</sub>)<sub>3</sub>-Ph). DSC-scan:  $T_g = -120$  °C ( $\Delta C_p = 0.063$  J/(g·°C)),  $T_c = -92$  °C ( $\Delta H_c = -4.1$  J/g) and  $T_m = -41$  °C ( $\Delta H_m = 7.1$  J/g),  $T_g$  (PPE-phase): not detected.

## 7.5 References

1. Sakurai, S. *Trends Polym. Sci.* **3**, 90 (1995).
2. Hasegawa, H. and Hashimoto, T. *Comprehen. Polym. Sci.*, 2th suppl., Eds. Aggarwal, S.L. and Russo, S., The Bath Press Ltd., Belfast, 497 (1996).
3. Yilgor, I. and McGrath, J.E. *Adv. Polym. Sci.*, **86**, 1 (1988).
4. Almdal, K., Mortensen, K., Ryan, A.J. and Bates, F.S. *Macromolecules*, **29**, 5940 (1996).
5. Feng, D., Wilkes, G.L. and Crivello, J.V. *Polymer*, **30**, 1800 (1989).
6. Chu, J.H., Rangarajan, P., LaMonte Adams, J. and Register, R.A. *Polymer*, **36**, 1569 (1995).
7. Bates, F.S. *Science*, **251**, 898 (1991).
8. Halperin, A., Tirrell, M. and Lodge, T.P. *Adv. Polym. Sci.*, **100**, 33 (1992).
9. Leibler, L. *Macromolecules*, **13**, 1602 (1980).
10. Helfand, E. and Wasserman, Z.R. *Macromolecules*, **9**, 879 (1976).
11. Semenov, A.N. *Sov. Phys. JETP*, **61**, 733 (1985).
12. Whitmore, M.D. and Vavasour, J.D. *Acta Polymer.*, **46**, 341 (1995).
13. Ohta, T. and Kawasaki, K. *Macromolecules*, **19**, 2621 (1986).
14. Matsen M.W. and Schick, M. *Macromolecules*, **27**, 187 (1994).
15. Matsen M.W. and Schick, M. *Macromolecules*, **27**, 7157 (1994).
16. Lescanec, R.L. and Muthukumar, M. *Macromolecules*, **26**, 3908 (1993).
17. Hashimoto, T. *Macromolecules*, **15**, 1548 (1982).
18. Hashimoto, T., Tanaka, H. and Hasegawa, H. *Macromolecules*, **18**, 1864 (1985).

19. Melenkevitz, J. and Muthukumar, M. *Macromolecules*, **24**, 4199 (1991).
20. Shull, K.R., Mayes, A.M. and Russell, T.P. *Macromolecules*, **26**, 3929 (1993).
21. Hashimoto, T. Shibayama, M. and Kawai, H. *Macromolecules*, **13**, 1237 (1980).
22. Hashimoto, T. Fujimura, M. and Kawai, H. *Macromolecules*, **13**, 1660 (1980).
23. Hasegawa, H., Tanaka, H., Yamasaki, K. and Hashimoto, T. *Macromolecules*, **20**, 1651 (1987).
24. Pochan, D.J., Gido, S.P., Pispas, S., Mays, J.W., Ryan, A.J., Fairclough, J.P.A., Hamley, I.W. and Terrill, N.J. *Macromolecules*, **29**, 5091 (1996).
25. Bates, F.S., Berney, C.V. and Cohen, R.E., *Macromolecules*, **16**, 1101 (1983).
26. Allen, R.D. and Hedrick, J.L. *Polym. Prep.*, **28**, 163 (1987).
27. Allen, R.D. and Hedrick, J.L. *Polym. Bull.*, **19**, 111 (1988).
28. Blohm, M.L., Brown, S.B., Seeger, G.T. and Anderson, P.P. U.S. US 5,385,984 (1995).
29. Blohm, M.L., Brown, S.B., Seeger, G.T. and Anderson, P.P. Eur. Pat. Appl. EP 0,649,876 A1 (1995).
30. Banach, T.E., Blohm, M.L. and Snow, K.M. Eur. Pat. Appl. EP 0,540,273 A1 (1993).
31. Blohm, M.L. and Stein, J. Eur. Pat. Appl. EP 0,515,196 A2 (1992).
32. Snow, K.M., Pickett, J.E. and Lewis, L.N. Eur. Pat. Appl. EP 0,433,746 B1 (1995).
33. Schmidt-Rohr, K. and Spiess, H.W. "Multidimensional solid-state NMR and polymers", Academic Press Ltd., London, (1994).
34. Clauss, J., Schmidt-Rohr, K. and Spiess, H.W. *Acta Polymer.*, **44**, 1 (1993).
35. Clauss, J., Schmidt-Rohr, K., Adam, A., Boeffel, C. and Spiess, H.W. *Macromolecules*, **25**, 5208 (1992).
36. Schmidt-Rohr, K., Clauss, J. and Spiess, H.W. *Macromolecules*, **25**, 3273 (1992).
37. Cai, W.Z., Schmidt-Rohr, K., Egger, N., Gerhards, B. and Spiess, H.W. *Polymer*, **34**, 267 (1993).
38. Cho, G., Natansohn, A., Ho, T. and Wynne, K. *Macromolecules*, **29**, 2563 (1996).
39. Cho, G. and Natansohn, A. *Can. J. Chem.*, **72**, 2255 (1994).
40. Van Krevelen, D.W. "Properties of polymers", third edition, Elsevier Science Publishers, Amsterdam, (1990).
41. Krause, S. "Polymer Blends", Eds. Paul D.R. and Newman, S., Volume 1, Academic Press, Inc., London, (1991).
42. Feng, D., Wilkes, G.L. and Crivello, J.V. *Polymer*, **30**, 1800 (1994).
43. Sun, S.F. and Fan, J. *Polymer*, **34**, 655 (1993).
44. De Gennes, P.G. *J. Phys. Lett.*, **36**, L-55 (1975).
45. Landfester, K., Boeffel, C., Lambla, M. and Spiess, H.W. *Macromolecules*, **29**, 5972 (1996).
46. Egger, N., Schmidt-Rohr, K., Blümich, B., Domke, W.D. and Stapp, B. *J. Appl. Polym. Sci.*, **44**, 289 (1992).
47. Bovey, F.A. and Mirau, P.A. "NMR of polymers", Academic Press, San Diego, 281 (1996).

- 48 . Spiegel, S., Schmidt-Rohr, K., Boeffel, C. and Spiess, H.W. *Polym. Commun.*, **34**, 4566 (1993).
- 49 . Douglass, D.C. and Jones, G.P. *J. Chem. Phys.*, **45**, 956 (1966).
- 50 . Feng, H., Feng, Z., Ruan, H. and Shen, L. *Macromolecules*, **25**, 5981 (1992).
- 51 . Tarbell, D.S., Kincaid, J.F. *J. Am. Chem. Soc.*, **62**, 128 (1940).

## Chapter 8

# Poly(bisphenol A carbonate)-poly(dimethylsiloxane) multiblock copolymers

### Summary

*A versatile technique for the synthesis of multiblock copolymers of polydimethylsiloxane (PDMS) and poly(bisphenol A carbonate) (PC) is described. Specific reaction of the phenol endgroups of  $\alpha,\omega$ -bis(bisphenol A)-terminated PDMS with the activated endgroups of  $\alpha,\omega$ -bis(ortho-nitrophenylcarbonate)-endcapped PC yields PC-PDMS multiblock copolymers and ortho-nitrophenol. The morphology and influence of crystallization of the polycarbonate blocks is studied using solution-cast films. When THF is used as casting solvent instead of chloroform, the crystallinity of the PC blocks increases resulting in smaller domain spacings as measured by Small Angle X-Ray Scattering (SAXS) and the solution-cast film has a lower strain at fracture as measured by tensile testing.*

### 8.1 Introduction

Block copolymers based on poly(bisphenol A carbonate) (PC) and polydimethylsiloxane (PDMS) provide elastomeric products with excellent toughness at low temperatures. Due to the microphase separation of the soft siloxane blocks and the hard polycarbonate blocks, these materials can be regarded as thermoplastic elastomers (TPEs). The most common synthetic procedure for obtaining these block copolymers involves the reaction between phosgene and bisphenol acetone (BPA) in the presence of BPA-terminated polysiloxanes, as introduced by Vaugh.<sup>1-5</sup> The latter polymers are synthesized via a Lewis-acid-catalyzed equilibration of dimethyldichlorosilane with octamethylcyclotetrasiloxane, yielding a chloro-terminated siloxane, which is phenol terminated upon reaction with excess BPA in the presence of an acid scavenger, like pyridine.<sup>6</sup> Based on the initial work of Vaugh, new synthetic procedures were developed for such PC-PDMS block copolymers and their properties are studied to a large extent.<sup>7-26</sup> Most previously reported routes for the synthesis of PC-PDMS copolymers involve a reaction of a modified PDMS reacting as nucleophile, with phosgene and BPA,<sup>7</sup> cyclic carbonates<sup>22</sup> or poly(bisphenol A carbonate). However, due to side-reactions occurring in most

of these synthetic procedures, which result in chain extension of the siloxane blocks or chain cleavage of the polycarbonate blocks, the block lengths are rather polydisperse. The extent of microphase separation between the hard and the flexible segments is significantly influenced by the sequential distribution of the various species.<sup>6</sup>

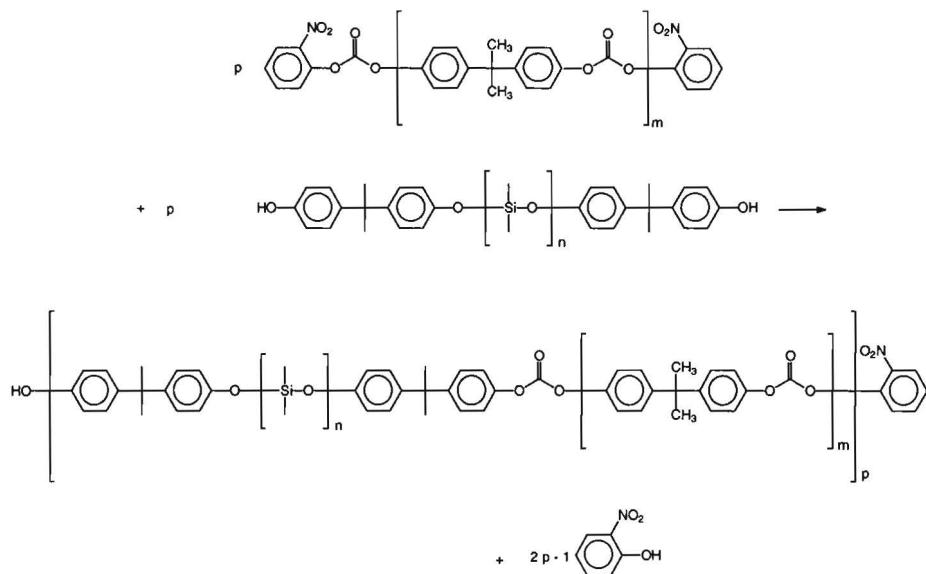
The transesterification reaction of a phenol with a carbonate unit is well-known in the synthesis of PC using the melt reaction of diphenylcarbonate and BPA at high temperature in the presence of a base as catalyst.<sup>28-30</sup> Phenol is produced as a condensation by-product and must be removed to facilitate the chain growth reaction. Generally, the preparation of high molecular weight polycarbonate with activated chain ends,<sup>31</sup> or with phenolic chain ends is rather difficult, and requires a specific synthetic procedure. As confirmed by experiments in our laboratories, depolymerization (chain cleavage) readily occurs, e.g. the transesterification reaction of BPA with PC under the action of a base, like 4-dimethylaminopyridine (DMAP), yields low molecular weight oligomers.

To prevent the reacting phenol-terminated polymer from reaction with the internal carbonate units, we activated the carbonate group at the endgroups of the polycarbonate by using *ortho*-nitrophenylcarbonate-endcapped PC, as prepared by D. Brunelle. Previously, Brunelle<sup>31</sup> showed that *ortho*-nitrophenylcarbonates can give a fast transesterification upon reaction with BPA under the action of a basic catalyst. This transesterification reaction affords a clean formation of polycarbonates at or below ambient temperatures. Polycarbonates with the same *ortho*-nitrophenylcarbonate incorporated as endgroup can be used as well to favour the reaction of a nucleophile preferentially at those activated endgroups. In particular, we studied the reaction of BPA-terminated polysiloxanes with *ortho*-nitrophenylcarbonate endgroup activated PC, yielding pure PDMS-PC multiblock copolymers. The occurrence of less side-reactions, which affect the block lengths in the obtained copolymer, results in a more distinct microphase separation of the soft PDMS and hard PC blocks. This is the basis for a more facile characterization of the morphology obtained. In contrast to most other reports about PC-PDMS copolymers,<sup>11,23</sup> crystallization of the polycarbonate blocks could be detected in the prepared multiblock copolymers. The influence of crystallization of the PC blocks on the morphology and stress-strain behavior is investigated.

## **8.2 Results and discussion**

The transesterification reaction of a phenol with this nitrophenyl carbonate endgroup can be used for the preparation of PC-block copolymers. We now require a phenol-terminated polymer, instead of a low molecular weight phenol, which preferentially has free *ortho*-

positions. We studied the formation of block copolymers using BPA-terminated polysiloxanes in a reaction with *ortho*-nitrophenylcarbonate-endcapped PC, as presented in Scheme 8.1. *Ortho*-nitrophenyl carbonate endcapped PC can be prepared by copolymerization of BPA and phosgene with *ortho*-nitrophenol. We reacted the modified PDMS and activated PC, both dissolved in chloroform, under the action of DMAP. The occurring reaction is visualized by the formation of *ortho*-nitrophenol, which is orange.



**Scheme 8.1:** Synthesis PC-PDMS multiblock copolymers.

We studied the microphase segregation of the hard PC and soft PDMS block using Transmission Electron Microscopy (TEM) of solution-cast films. The PC-PDMS copolymer dissolves easily in chloroform at room temperature, while dissolving in THF requires elevated temperatures (ca. 50 °C). TEM pictures of copolymer films, cast either from THF or  $\text{CHCl}_3$ , showed similar morphologies as presented in Figure 8.1. The dark regions represent the PDMS phase, which has a higher electron density<sup>37</sup> caused by the presence of Si-atoms with high atomic number. The light areas represent the PC phase. The observed morphology is mainly lamellar with some cylindrical structures, as expected from the polymer volume ratios: 59.4 % (v/v) PC and 40.6 % (v/v) PDMS. No accurate domain spacings could be determined from the TEM pictures, because of the presence of a distribution in domain spacings and possible deformation during sample preparation. Therefore, we studied the solution-cast films with Small Angle X-Ray Scattering (SAXS).

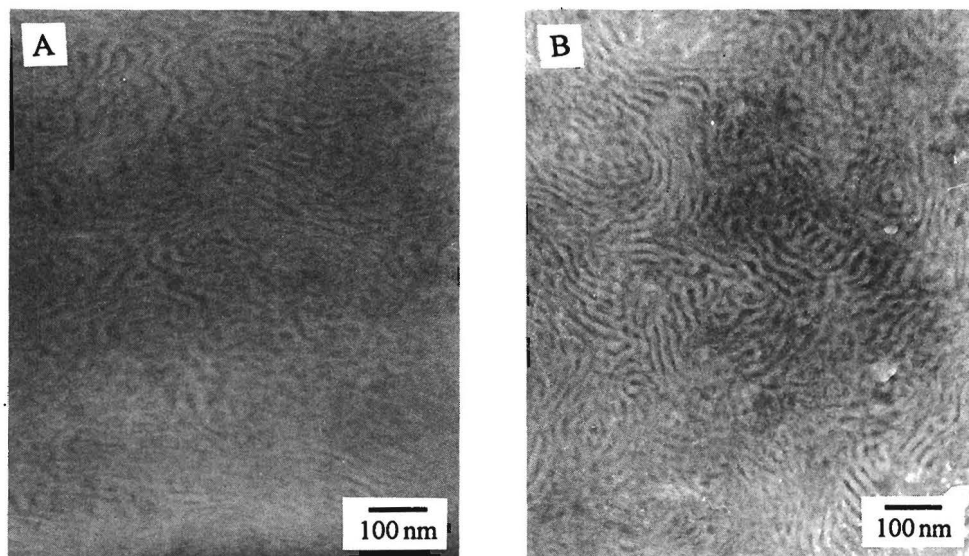


**Figure 8.1:** TEM pictures of solution-cast film of PC-PDMS copolymers: A. cast from THF; B. cast from  $\text{CHCl}_3$ .

Due to the microphase separation in the block copolymer, the SAXS analysis shows a reflection corresponding to the double lamellar distance, i.e. belonging to one PC block and one PDMS block. A clearer reflection is shown in a Lorentz-corrected plot, in which the  $I \cdot s^2$  is plotted as a function of  $s$ , where  $s$  represents the scattering vector ( $s$ ) and  $I$  the scattering intensity ( $I$ ). The scattering vector is defined as the reciprocal value of the distance ( $d$ ). Figure 8.2 shows the intensity profile of the solution-cast films of the prepared block copolymer, whereas Figure 8.3 shows the corresponding Lorentz-corrected plots. The PC-PDMS film cast from THF shows a reflection at larger scattering angle ( $2\theta$ ) in the intensity profile and at larger scattering vector ( $s$ ) in the Lorentz-corrected plot, corresponding to a smaller domain spacing ( $d$ ). From the Lorentz-corrected plots a domain spacing of  $424 \pm 10 \text{ \AA}$  could be determined for a copolymer cast film from chloroform, while a copolymer film cast from THF shows a domain spacing of  $371 \pm 20 \text{ \AA}$ . This difference in domain spacings can be explained by a difference in density<sup>32</sup> due to a difference in crystallinity, which will be shown by Wide Angle X-Ray Scattering (WAXS) studies in this chapter. Furthermore, the reflection peak from the cast film from THF is broader due to a decrease in electron density difference between the PC phase and PDMS phase. This decrease in electron density is caused by a higher density of crystalline PC ( $\rho_c = 1.31 \text{ g/cm}^3$ )<sup>32,35</sup> in comparison with amorphous PC ( $\rho_a = 1.20 \text{ g/cm}^3$ ).

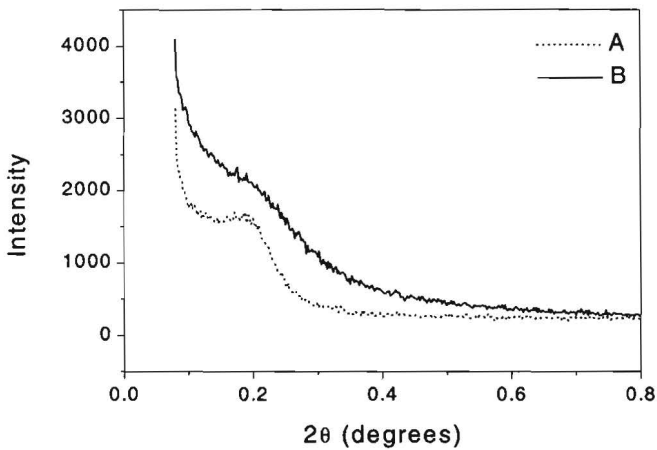


**Figure 8.2:** SAXS results of PC-PDMS copolymer film, intensity as a function of scattering angle ( $2\theta$ ): A. cast from  $\text{CHCl}_3$ , B. cast from THF

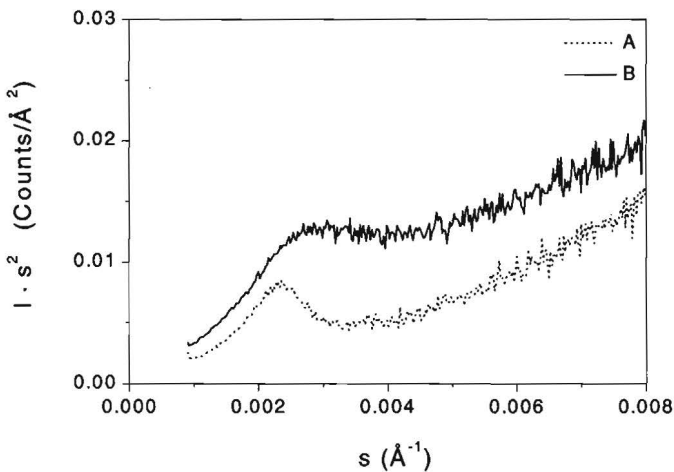


**Figure 8.3:** SAXS results of a PC-PDMS copolymer film, Lorentz corrected plot: A. cast from  $\text{CHCl}_3$ , B. cast from THF.

The determined domain distances can be compared with distances theoretically predicted from the polymer molecular weights. If we assume that Gaussian chain statistics can be utilized and that the average block length only depends on block molecular weight, then we can estimate the domain spacings by calculation of the unperturbed chain dimensions of the PC and PDMS blocks.<sup>33</sup> The root mean square unperturbed end-to-end distance for PDMS chains can be expressed as:  $(\langle R_0^2 \rangle)^{1/2} = (6.3 n l^2)^{1/2}$ , where  $l = 1.64 \text{ \AA}$  and  $n$  is the number of Si-O bonds.<sup>34</sup>



For PC chains, the unperturbed chain dimensions can be calculated using the equation:  $\langle R_0^2 \rangle^{1/2} = (3.55 n \cdot l^2)^{1/2}$ . In our calculations, we used  $l = 7.01 \text{ \AA}$ , corresponding with the distance from the carbonyl to the isopropylidene unit.<sup>35,36</sup> We calculated the unperturbed end-to-end distance for the PDMS block ( $\overline{M}_n = 7.8 \text{ kg/mol}$ ,  $n = 210.6$ ) as  $59.7 \text{ \AA}$  and for the PC block ( $\overline{M}_n = 14.2 \text{ kg/mol}$ ,  $n = 104.9$ ) as  $135.3 \text{ \AA}$ . For the less crystalline block copolymer cast from chloroform, we determined a domain spacing of  $424 \text{ \AA}$  using SAXS. Calculation of the domain spacings via the unperturbed chain dimensions results in smaller distances. Similar discrepancies were found for PDMS-PS multiblock copolymers.<sup>37</sup> The higher value obtained by SAXS can be caused by deviation of the characteristic ratio (i.e. 6.3 for PDMS and 3.55 for PC) for lower molecular weights. The larger chain dimensions as measured by SAXS can be caused as well by a chain extension near the junction points in the block copolymer and mobility restriction due to linkage of the different blocks. Consequently these chains can not be considered as unperturbed chains following the Gaussian approximation. Therefore the assumption that the distance in strongly segregating block copolymers scales with  $M^{2/3}$ , will be more accurate than scaling with  $M^{1/2}$  in the case of unperturbed chain dimensions.

This difference in domain spacings between the two samples cast from different solvents obtained by SAXS can be due to a difference in crystallinity. Therefore, we extended our investigation with Differential Scanning Calorimetry (DSC) and Wide Angle X-Ray Scattering (WAXS). Poly(bisphenol A carbonate) is known to crystallize slowly from the melt.<sup>38</sup> Much faster rates of crystallization may be obtained by solvent-induced crystallization,<sup>39-41</sup> vapor-induced crystallization<sup>42,43</sup> or nucleation using organic salts.<sup>44,45</sup> PC crystallization using a non-solvent like acetone is well-known.<sup>46</sup> However, PC crystallization using solution casting from a good solvent, like chloroform, or from poor solvents, like THF,<sup>39</sup> has only been studied to a limited extent. Therefore, we studied also crystallization of the PC homopolymer, as a comparison to the crystallization in the PC-PDMS block copolymers.

We used DSC and WAXS to obtain information about the degree of crystallinity<sup>46</sup> and the crystal lattice size of the semi-crystalline PC blocks in the PC-PDMS block copolymer. If the starting PC homopolymer is slowly cast from THF or chloroform, crystallization occurs, which yields a sharp peak in the WAXS pattern as shown in Figure 8.4. When the PC-PDMS film is prepared by solution casting, a more pronounced crystallization occurs in film cast from THF. During evaporation of the solvent, chain collapse and aggregation can occur when the polymer solution becomes more concentrated.<sup>27</sup> This chain collapse and aggregation can induce crystallization. In films prepared from THF the crystallization is more pronounced, probably caused by the low solubility of the PC blocks in THF, in comparison with  $\text{CHCl}_3$ . The crystallization can start already during aggregation in concentrated solutions or is enhanced by the microphase separation of the PC and PDMS blocks in the solid polymer film. Figure 8.5

shows the WAXS patterns of the PC-PDMS copolymer, cast either from THF or  $\text{CHCl}_3$ . A sharp reflection is detected in the wide-angle area for the crystalline PC ( $2\theta = 11.7^\circ$ ), besides the reflection corresponding to the interchain distance of the PDMS ( $2\theta = 16.7^\circ$ ). These WAXS results are consistent with the DSC results as shown in Table 8.1. The melting peak of crystalline PC is only detected in the first heating run using DSC, which is in agreement with the slow melt crystallization rates. Crystallinities are calculated using  $\Delta H_0 = 109.6 \text{ J/g}$  (26.2 cal/g) as reported by Mercier.<sup>46</sup> The presence of more crystallinity in the copolymer films in combination with smaller domain spacings as determined by SAXS in films prepared from THF solutions in comparison with films prepared from  $\text{CHCl}_3$  can be explained by a higher density in crystalline PC.<sup>32</sup> However, more research is required to predict whether folded-chain or extended-chain crystallization dominates in these block copolymers.

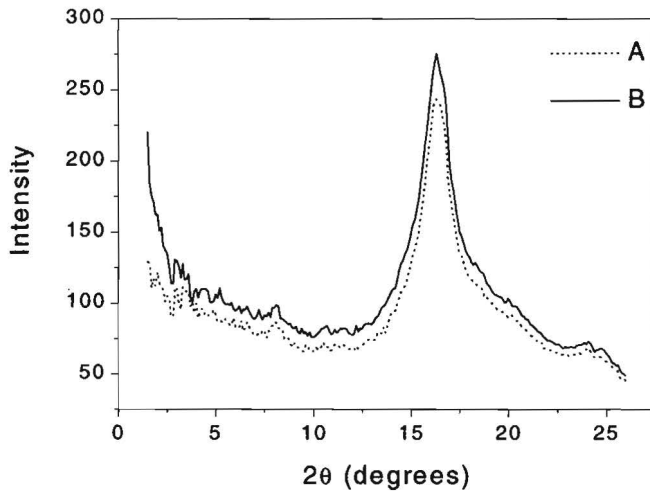


**Figure 8.4:** WAXS patterns of solution-cast PC films: A. cast from  $\text{CHCl}_3$ ; B. cast from THF.

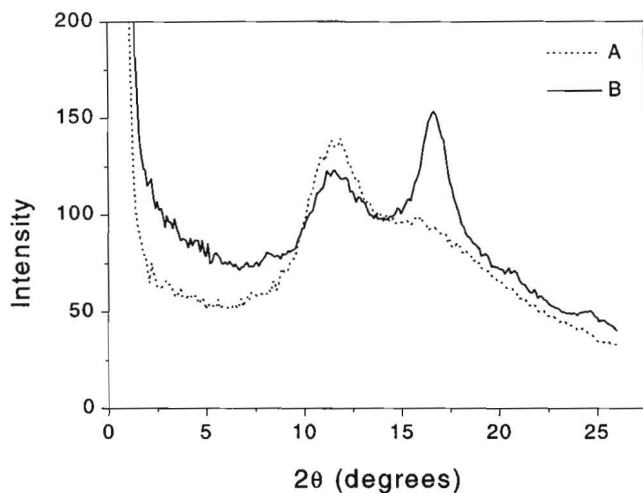


**Figure 8.5:** WAXS patterns of solution-cast PC-PDMS copolymer films: A. cast from  $\text{CHCl}_3$ ; B. cast from THF.

**Table 8.1:** DSC results of solution cast films.

	Parameters phase transitions	PC cast from THF	PC cast from $\text{CHCl}_3$	PC-PDMS cast from THF	PC-PDMS cast form $\text{CHCl}_3$
1st heating run 20 °C/min	Tg (°C)	148.9	154.3	155.2	154.7
	$\Delta\text{Cp}$ (J/g·K)	0.076	0.025	0.027	0.036
	Tm (°C)	224.0	227.4	216.7	211.7
	$\Delta\text{H}$ (J/g)	21.68	22.54	10.9	4.43
	% Cryst.	19.8	20.6	15.4	6.3
2nd heating run 20 °C/min	Tg (°C)	144.3	146.2	150.0	151.8
	$\Delta\text{Cp}$ (J/g·K)	0.169	0.124	0.099	0.041

The crystallization of the PC is also reflected in the stress-strain behaviour. If crystallization takes place, disentanglement can occur in these relatively low molar mass polymers. This brittle fracture at low strain is especially observed in tensile test of the homopolymer PC films. Introducing elastomeric PDMS blocks yields a higher strain at break, especially for copolymers cast from chloroform with very low crystallinity. The obtained tensile testing results are summarized in Table 8.2. The stress-strain behavior of a PC-PDMS copolymer cast film is shown in Figure 8.6. The film cast from THF shows a lower strain, essentially because of its higher crystallinity. Besides the difference in crystallinity, the variation in mechanical properties could be caused by a difference in development of the morphology during the solvent-casting.

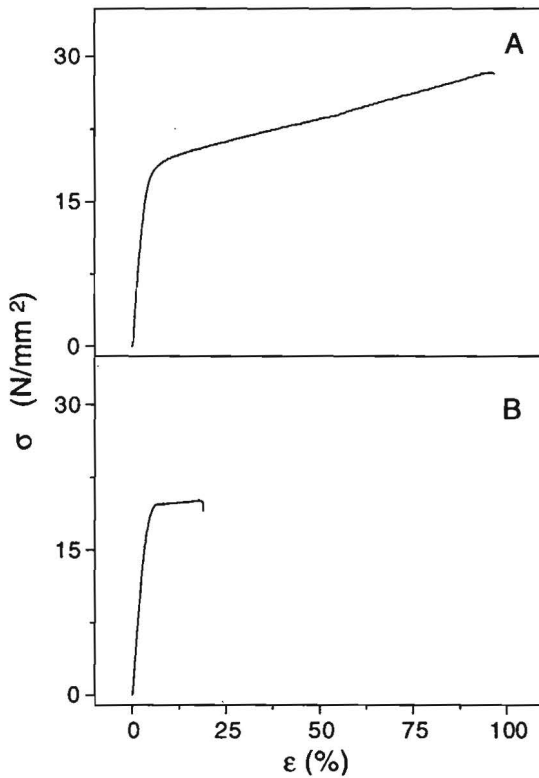


**Figure 8.6:** Stress-strain behaviour of solution cast PC-PDMS copolymer films: A. cast from  $\text{CHCl}_3$ ; B. cast from THF.

**Table 8.2:** Stress-strain behaviour PC homopolymer and PC-PDMS copolymer cast films.

Material films	casting solvent	E (N/mm <sup>2</sup> )	$\sigma_{\text{fracture}}$ (N/mm <sup>2</sup> )	$\epsilon$ (%)
PC	CHCl <sub>3</sub>	1930	11.6	0.66
PC	THF	1150	3.1	0.32
PC-PDMS	CHCl <sub>3</sub>	570	28.3	96.6
PC-PDMS	THF	580	19.1	18.9

### 8.3 Conclusions

A new method is described for the preparation of PC-PDMS multiblock copolymers with well-defined block length. For this purpose PC with *ortho*-nitrophenylcarbonate activated endgroups was reacted with bis(bisphenol A)-terminated PDMS. The resulting copolymer shows a microphase-separated morphology, as is evident from TEM analysis. The observed morphology is mainly lamellar with some cylindrical structures, as expected from the polymer volume ratios: 59.4% (v/v) PC and 40.6% (v/v) PDMS. As a comparison to previous reports, this research gave more insight on the influence of solvent casting on the crystallinity obtained in these materials. The copolymer films cast from THF show a higher crystallinity than those from CHCl<sub>3</sub>, resulting in shorter domain spacings as measured by SAXS. Films cast from THF have a lower strain at fracture, possibly due to disentanglement when the PC crystallizes. The relatively low molar mass PC homopolymer is toughened by the addition of PDMS blocks, like in the PC-PDMS block copolymer. In comparison to the reported studies on crystallized PDMS-PC block copolymers,<sup>23</sup> this research extends the understanding in the structure-property relationships of these polymers. This can be of importance when crystallized PC-PDMS copolymers are used as selective membranes for gas separation.<sup>23</sup>

## 8.4 Experimental

### Materials:

$\alpha,\omega$ -Bis(*ortho*-nitrophenylcarbonate)-terminated poly(bisphenol A carbonate) was prepared by P. Phelps and D. Brunelle, General Electric Corporate Research and Development in Schenectady, NY, USA.  $\alpha,\omega$ -Bis(bisphenol acetone)-terminated polydimethylsiloxane was prepared by the reaction of  $\alpha,\omega$ -bis(chloro)-terminated polysiloxane with an excess of BPA according to a literature procedure.<sup>5,6</sup> All other chemicals were obtained commercially and used without further purification.

### Techniques:

The  $^1\text{H-NMR}$  spectra were recorded using a Bruker AM 400 spectrometer ( $^1\text{H}$ : 400.13 MHz).  $\delta$  values are given in ppm relative to TMS, but were referenced to residual  $\text{CHCl}_3$  at 7.27 ppm when siloxanes were present in the sample. X-ray diffraction patterns of copolymers were taken using  $\text{Cu K}\alpha$  radiation and a multi-wire area detector X-1000 coupled with a graphite monochromator. Small Angle X-Ray Scattering (SAXS) studies were performed using a Rigaku Denki small angle goniometer. Transmission Electron Microscopy (JEOL 2000-FX) was operated at 80 kV. Cryosections of approximately 80 nm were cut with a diamond knife at  $-122\text{ }^\circ\text{C}$ . No additional staining was applied. Tensile testing of solution-cast films was performed at room temperature using a Zwick 1445 tensile tester. Testing specimen with a length of 20 mm, width of 5 mm and thickness of ca. 1 mm were tested using a DIN 53455 tensile test and a testing speed of 5 mm/min.

### Synthesis of $\alpha,\omega$ -bis(*ortho*-nitrophenylcarbonate)-terminated poly(bisphenol A carbonate):

A 5 neck 1 L morton flask equipped with mechanical stirrer, pH electrode, phosgene dip tube, caustic addition port and a chilled brine condensor vented to a phosgene scrubber was charged with BPA (68.4 g, 0.30 mol), dichloromethane (400 mL), water (100 mL) and 1 mL of a aqueous 75% methyltributylammonium chloride solution (0.003 mol). Phosgene was added at 2.00 g/min while pH maintained at  $\sim 8$  by addition of a 50 wt% aqueous NaOH solution. After phosgenation was complete, the pH was trimmed to 11.0 and 0.012 mol of *ortho*-nitrophenol was added, producing a dark orange color that quickly disappeared as the carbonates are formed. Next 1.0 mL of trimethylamine was added and the pH was kept  $> 11$ , until all chloroformates were gone. At this time the reaction mixture was slightly yellow again so another 2.0 g of phosgene was added to consume any phenolics in solution. In total 63 g of a 50 wt% NaOH solution was required. The polycarbonate was isolated by washing the organic phase, twice with 1 M HCl solution and three times with water. The washed organic layer ( $\sim 0.5$  L) was added to 1 L methanol in a blender, then another 1 L of methanol was added. The solid was collected on a filter and returned to the blender, where it was mixed with 2 L water. The polymer was collected and dried in vacuum at  $110\text{ }^\circ\text{C}$ .  $^1\text{H-NMR}$  (400 MHz,  $\text{CDCl}_3$ ):  $\delta$  8.17 (d, 2H,  $J=8.2$  Hz, arom. C-H endgroup *meta* towards carbonyl, *ortho* towards nitro) 7.70 (t, 2H,  $J = 7.8$  Hz, arom. C-H endgroup *meta* towards carbonyl, *para* towards nitro)  $\overline{M}_n = 14.2$  kg/mol (according to  $^1\text{H-NMR}$ ). SEC (eluens = THF,  $40\text{ }^\circ\text{C}$ , RI detection): uncorrected molecular weights using polystyrene standards  $\overline{M}_n = 19.1$  kg/mol,  $D = 2.75$ .

*Synthesis of the  $\alpha,\omega$ -bis(BPA)-endcapped PDMS:*

The  $\alpha,\omega$ -bis(BPA)-terminated polydimethylsiloxane was prepared according to a literature procedure.<sup>56</sup> <sup>1</sup>H-NMR (400 MHz, CDCl<sub>3</sub>):  $\delta$  1.63 (s, 12H, CH<sub>3</sub> of BPA endgroups), 6.72 (d, 4H, J = 8.7 Hz, arom. C-H of BPA endgroups, *ortho* towards hydroxyl), 6.79 (d, 4H, J = 8.6 Hz, arom. C-H of BPA endgroups, *ortho* towards carbonate), 7.08 (m, 8H, arom. C-H of BPA endgroups, *ortho* towards isopropopylidene unit).  $\overline{M}_n$  = 7.81 kg/mol (according to <sup>1</sup>H-NMR).

*Synthesis of PC-PDMS multiblock copolymer:*

$\alpha,\omega$ -Bis(*ortho*-nitrophenylcarbonate)-terminated PC (28.89 g, 2.04 mmol) was dissolved in 800 mL chloroform at room temperature. Subsequently were added,  $\alpha,\omega$ -bis(BPA)-endcapped PDMS (15.93 g, 2.04 mmol) and DMAP (0.32 g, 2.62 mmol). Upon reaction the colorless solution turns yellow upon reaction. After stirring for 1 day at room temperature, the reaction mixture was precipitated in methanol (10 L). The obtained polymer was dried in vacuum oven at 70 °C. Yield: > 95%. SEC (eluent = THF, 40 °C, RI detection): uncorrected molecular weights using polystyrene standards  $\overline{M}_n$  = 39.5 kg/mol, D = 2.16. Solution-cast films were prepared from 10 wt% solutions in THF or chloroform. Films were dried in a vacuum oven during 1 day at 160 °C to eliminate all residual solvent.

## 8.5 References

1. Vaugh, H.A. Brit. Pat. 989,379 (1965).
2. Vaugh, H.A. U.S. US 3,189,662 (1965).
3. Vaugh, H.A. U.S. US 3,419,634 (1968).
4. Vaugh, H.A. U.S. US 3,419,635 (1968).
5. Vaugh, H.A. *J. Polym. Sci., Poly, Lett.*, **7**, 569 (1969).
6. Niznek, G.E. and LeGrand, D.G. *J. Polym. Sci., Polym. Symp.*, **60**, 97 (1977).
7. Noshay, A. and McGrath, J.E. "Block copolymers, overview and critical survey", Academic Press, New York, (1977).
8. Merrit, W.D. and Vestergaard, J.H. U.S. US 3,821,325 (1974).
9. Kambour, R.P., Faulkner, D.L., Holik, A.S., Miller, S. and Smith S.A. *Org. Coat. Plast.Chem., Am Chem. Soc.*, **38**, 18 (1978).
10. Kambour, R.P. *J. Polym. Sci., Poly, Lett.*, **7**, 573 (1969).
11. Legrand, D.G. *J. Polym. Sci., Poly, Lett.*, **7**, 579 (1969).
12. Knauss, D.M., Yamamoto, T., Yoon, T.H. and McGrath, J.E. *Polym. Mater. Sci. Eng.*, **72**, 232 (1995).
13. Knauss, D.M., Yamamoto, T. and McGrath, J.E. *Polym. Prep., Am Chem. Soc.*, **34**, 622 (1993).
14. McDermott, P.J., Krafft, T.E. and Rich, J.D. *J. Polym. Sci., Polym. Chem. Ed.*, **29**, 1681 (1991).
15. Dwight, D.W., McGrath, J.E., Beck, A.R. and Rifle, J.S. *Polym. Prep., Am Chem. Soc.*, **20**, 702 (1979).
16. Riffle, J.S., Freelin, R.G., Banthia, A.K. and McGrath, J.E. *J. Macromol. Sci., Macromol. Chem.*, **A15**, 967 (1981).

17. Rosenquist, N.R. U.S. US 5,344,908 (1994).
18. Peters, E.N. U.S. US 5,194,524 (1993).
19. Hoover, J.F. *Eur. Pat. Appl.* EP 0,522,751 A2 (1992).
20. Okamoto, M. and Kanesaki, T. *Eur. Pat. Appl.* EP 0,434,848 B1 (1995).
21. Silva, J.M. and Pyles, R.A. *Eur. Pat. Appl.* EP 0,374,508 A2 (1989).
22. Evans, T.L. and Carpenter, J.C. *Macromol. Chem., Macromol. Symp.*, **42/43**, 177 (1991).
23. Legrand, D.G. U.S. US 3,679,774 (1972).
24. Gur'yanonva, V.V., Alkayeva, O.F., Narinyan, T.A., Zhdanova, V.V. and Arshava, B.M. *Polym. Sci. U.S.S.R.*, **31**, 1266 (1989).
25. Maung, W. and Leverne Williams H. *Polym. Eng. Sci.*, **25**, 113 (1985).
26. Gorelova, M.M., Levin, V.Y. Dubchak, I.L. Zhdanov, A.A., Makarova, L.J. Storozhuk, I.P. and Koroleva, S.S. *Polym. Sci. U.S.S.R.*, **31**, 643 (1989).
27. Listvoin, G.I., Raigorodskii, I.M., Gol'dberg, E.S., Kireyev, V.V. and Tsvinskaya, L.K. *Polym. Sci.*, **33**, 695 (1991).
28. Fox, D.W. U.S. US 3,153,008 (1964).
29. Kim, Y., Choi, K.Y., Chamberlin, T.A. *Ind. Eng. Chem. Res.*, **31**, 2118 (1992).
30. Ko, A.W. and Starr, J.B. U.S. US 4,383,092 (1983).
31. Brunelle, D.J. *J. Macromol. Sci., Macromol. Reports*, **A28**, 95 (1991).
32. Van Krevelen, D.W. "Properties of polymers", Elsevier, Amsterdam, 3 th edition, 799 (1990).
33. Kurata, M. and Tsunashima, Y. "Polymer Handbook", Eds. Brandrup, J. and Immergut, E.H., Wiley-Interscience, VII/1 (1989).
34. Crescenzi, V. and Flory, P.J. *J. Am. Chem. Soc.*, **86**, 141 (1964).
35. Bonart, R. *Macromol. Chem.*, **92**, 149 (1966).
36. Pietralla, M., Schubach, H.R., Dettenmaier and Heise, B. *Progress Coll. Polym. Sci.*, **71**, 125 (1985).
37. Feng, D., Wilkes, G.L. and Crivello, J.V. *Polymer*, **30**, 1800 (1994).
38. Radhakrishnan, R., Iyer, V.S. and Sivaram S. *Polymer*, **35**, 3789 (1994).
39. Schorn, H., Hes, M. and Kosfeld, R. "Integration of fundamental polymer science and technology - 2", Eds. Lemstra, P.J. and Kleintjes, L.A., 385 (1988).
40. Di Filippo, G., Gonzalez, M.E., Gasiba, M.T. and Müller, A.V. *J. Appl. Polym. Sci.*, **34**, 1959 (1987).
41. Ji, G., Xue, G., Ma, J., Dong, C. and Gu, X. *Polymer*, **37**, 3255 (1996).
42. Mercier, J.P., Groeninckx, G. and Lesne, M. *J. Polym. Sci., Part C*, 2059 (1967).
43. Jonza, J.M. and Porter, R.S. *J. Polym. Sci., Polym. Phys. Ed.*, **24**, 2459 (1986).
44. Legras, R., Bailley, C., Daumerie, M., DeKoninck, J.M., Mercier, J.P., Zichy, V. and Nield, E. *Polymer*, **25**, 835 (1984).
45. Bailley, C., Daumerie, M., Legras, R. and Mercier, J.P. *J. Polym. Sci.*, **23**, 751 (1985).
46. Mercier, J.P. and Legras, R. *Polym. Lett.*, **8**, 645 (1970).





## Chapter 9

# Microphase-separated multiblock copolymers of poly(dimethylsiloxane) and photo-crosslinkable unsaturated polyesters

### Summary

*New multiblock copolymers based on dimethylsiloxanes and cinnamic acid derivatives have been prepared by hydrosilation polymerization. Copolymerization was performed using either low molecular weight monomers or high molecular weight macromers. The organic macromer was prepared by acyclic diene metathesis (ADMET) polymerization of para-phenylenediacrylic acid dipent-4-enyl ester. Hexamethyl-trisiloxane and  $\alpha,\omega$ -bishydride-terminated polydimethylsiloxane (PDMS) were used as inorganic macromers. The copolymers show microphase separation of the soft siloxane block and the hard semi-crystalline organic block, as observed by differential scanning calorimetry (DSC), X-ray scattering experiments (SAXS and WAXS) and transmission electron microscopy (TEM). Upon irradiation of the polyester-PDMS copolymer with linearly polarized light ( $\lambda = 254$  nm), crosslinking occurs due to a selective photochemical [2+2] cycloaddition yielding anisotropy in the polymer film. The polarizing efficiency of the resulting polarizer is 67 %, which is much higher than observed by irradiating the polyester homopolymer. The cause of this difference is discussed. The crosslinking rate upon UV-irradiation is slightly higher for the microphase-separated copolymer than for the corresponding homopolymer.*

### 9.1 Introduction

Recently, there is an increasing interest in photo-crosslinkable polymers. In particular, crosslinking of photosensitive moieties, like cinnamate derivatives, that can crosslink via a selective [2+2] cycloaddition, has been studied extensively.<sup>1-6</sup> Selective photochemical crosslinking using linearly polarized light can produce optically anisotropic polymer films. Anisotropic aligning and simultaneous crosslinking of photopolymers by linearly polarized light has been reported by Schadt.<sup>7</sup> These novel photopolymers were found not only to induce planar uniaxial alignment in adjacent monomeric liquid crystals (LCs) but also in polymeric liquid crystals (LCPs).

We are interested to use photo-crosslinkable microphase-separated block copolymers in order to obtain a topological fixation of the photosensitive cinnamate moieties. Selective crosslinking with polarized light via the photochemical [2+2] cycloaddition should yield a crosslinked polymer film, which behaves as a polarizer. Topological fixation of the cinnamate units can improve the polarizing efficiency. In order to obtain a microphase-separated photo-crosslinkable copolymer, we combined siloxanes with photoactive cinnamate derivatives. Other synthetic procedures for photo-<sup>8,9</sup> or thermally<sup>10</sup> crosslinkable siloxanes copolymers have been recently reported, however, these synthetic procedures cannot be used for a selective crosslinking.

Polysiloxanes are known as a unique class of inorganic polymers. Poly(dimethylsiloxane) (PDMS) is the most common polysiloxane. PDMS exhibits some interesting features such as: low glass transition temperature, low surface tension, good thermal and UV stability and a small variation of physical constants over a wide temperature range.<sup>11</sup> The increasing interest in multiphase copolymers<sup>12-15</sup> is mainly due to their unique combination of properties, which is directly related to their chemical structure and macromolecular architecture. Microphase separation in these block copolymers systems creates well-defined periodic structures on the sub-micron length scale.

In principle there are two techniques to produce siloxane-organic polymer conjugate materials. The first is based on polymerization of siloxane monomers initiated from telechelic organic polymers, e.g. living polystyrene initiating the polymerization of cyclic siloxanes.<sup>16-18</sup> A second technique to produce siloxane multiblock copolymers is a reaction in which telechelic polysiloxanes are reacted with either organic monomers<sup>19,20</sup> or telechelic organic polymers. Very often, hydrosilation is used in this method, either to produce more reactive endgroups or to couple PDMS with other polymers. The hydrosilation reaction with a variety of allylic compounds has been studied to introduce several endgroups like hydroxyalkyl,<sup>20,21</sup> dimethylamino,<sup>22</sup> glycidyl,<sup>23</sup> and thiophene.<sup>24</sup> These functional siloxanes are useful as precursors in the synthesis of block copolymers<sup>25-27</sup> and well-defined networks.<sup>28,29</sup>  $\alpha,\omega$ -Bis(hydrosilyl)-terminated siloxanes have also been employed to react directly with  $\alpha,\omega$ -divinyl-terminated organic compounds.<sup>30-33</sup> Hydrosilation polymerization under the action of platinum catalysts and using low molecular weight monomers is known as a very fast and efficient polymerization technique.<sup>34,35</sup>

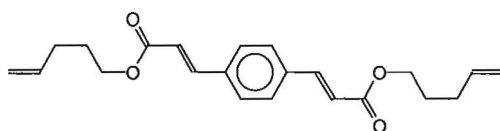
Block lengths and crystallization of independent blocks can determine morphology in PDMS block copolymers.<sup>36,37</sup> As shown in this Chapter, microphase separation in the block copolymers of PDMS with semi-crystalline unsaturated polyesters also can have a large effect

on the crosslinking reaction. This is illustrated by characterization of spin coated crosslinked films of a PDMS-polyester copolymer and the corresponding homopolymer by UV spectroscopy, varying the irradiation time, as presented in this Chapter. Thermal properties, crystallization behaviour and microphase separation of these copolymers are investigated using Differential Scanning Calorimetry (DSC), X-ray diffraction and Transmission Electron Microscopy (TEM). Selective crosslinking of the block copolymer films is investigated by irradiation with linearly polarized UV light ( $\lambda = 254 \text{ nm}$ ).

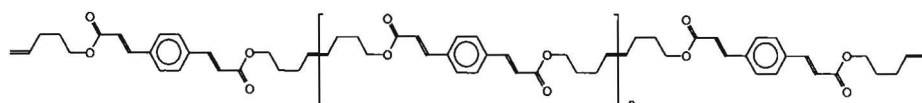
## 9.2 Results and Discussion

### 9.2.1 Synthesis of cinnamic acid derivatives and siloxane copolymers

*Para*-phenylenediacrylic acid dipent-4-enyl ester (**9.1**) was obtained in two steps. The first step is a Perkin synthesis,<sup>38</sup> where the reaction of terephthalaldehyde with sodium acetate and acetic anhydride yields *para*-phenylenediacrylic acid. In the second step, the acid chloride of *para*-phenylenediacrylic acid was prepared using thionylchloride and then reacted with 4-pentene-1-ol, yielding *para*-phenylenediacrylic acid dipent-4-enyl ester (**9.1**) in 78% yield. The monomer (**9.1**) was employed in an acyclic diene methathesis (ADMET) polymerization,<sup>39,40</sup> catalyzed by a ruthenium catalyst ( $\text{RuCl}_2(\text{=CHPh})(\text{PCy}_3)_2$ ).<sup>41,42</sup> The molecular weight of the oligomer or polymer (**9.2**) obtained strongly depends on the reaction conditions. Solution polymerization of **9.1** yields polymers with a higher molecular weight than melt polymerizations. For photo-crosslinking experiments, we used polyesters, prepared from solution polymerization, with  $\bar{P}_n = 60$  and oligoesters, prepared from melt polymerization, with  $\bar{P}_n = 11$ . The polymers were fully characterized and the end groups were analyzed as being of olefinic nature.

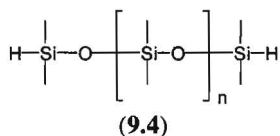
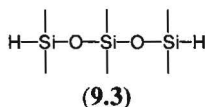


(9.1)



(9.2)

$\alpha,\omega$ -Bishydride-terminated hexamethyltrisiloxane (**9.3**) and PDMS (**9.4**) were obtained commercially. These siloxane macromonomers were copolymerized with *para*-phenylenediacrylic acid dipent-4-enyl ester or its oligomers via a hydrosilation polymerization. This platinum-catalyzed polymerization yields multiblock copolymers of an unsaturated (poly)ester and a (poly)siloxane.



The hydrosilations were performed by heating a solution containing equimolar amounts of each component and 0.0092–0.0265 mol% Pt as a hydrosilation catalyst in toluene for at least 8 hours at 80 °C under a nitrogen atmosphere. The monomer *p*-phenylenediacrylic acid dipent-4-enyl ester (**9.1**), its oligomers (**9.2**), the hydrosilation reaction mixture and the products were kept in the dark to prevent crosslinking of the cinnamate groups present. The reactions were quenched by evaporation of the solvent toluene without removal of the platinum catalyst. The reaction products were characterized by <sup>1</sup>H-NMR spectroscopy. The <sup>1</sup>H-NMR spectrum shows disappearance of the Si–H signal at 4.7 ppm of the siloxane (macro)monomer and disappearance of the terminal vinyl protons of the cinnamate (macro)monomer, as a result of the hydrosilation polymerization. Furthermore, a characteristic signal corresponding to the methylene unit adjacent to the siloxane (CH<sub>2</sub>–Si) is detected in the <sup>1</sup>H-NMR spectrum of the products. This is most clearly observed in a hydrosilation reaction between two low molecular weight compounds, like the cinnamate derivative *p*-phenylenediacrylic acid dipent-4-enyl ester (**9.1**) and  $\alpha,\omega$ -bishydride-terminated hexamethyltrisiloxane (**9.3**). The <sup>1</sup>H-NMR spectrum of this transparent copolymer, referred to as the 3/1 copolymer (**9.5**), is shown in Figure 9.1. The molecular weights were determined by means of Size Exclusion Chromatography (SEC). The uncorrected molecular weights are:  $\overline{M}_n = 5.8$  kg/mol and  $\overline{M}_w = 18.9$  kg/mol. These values show that the hydrosilation yielded a rather efficient polymerization.

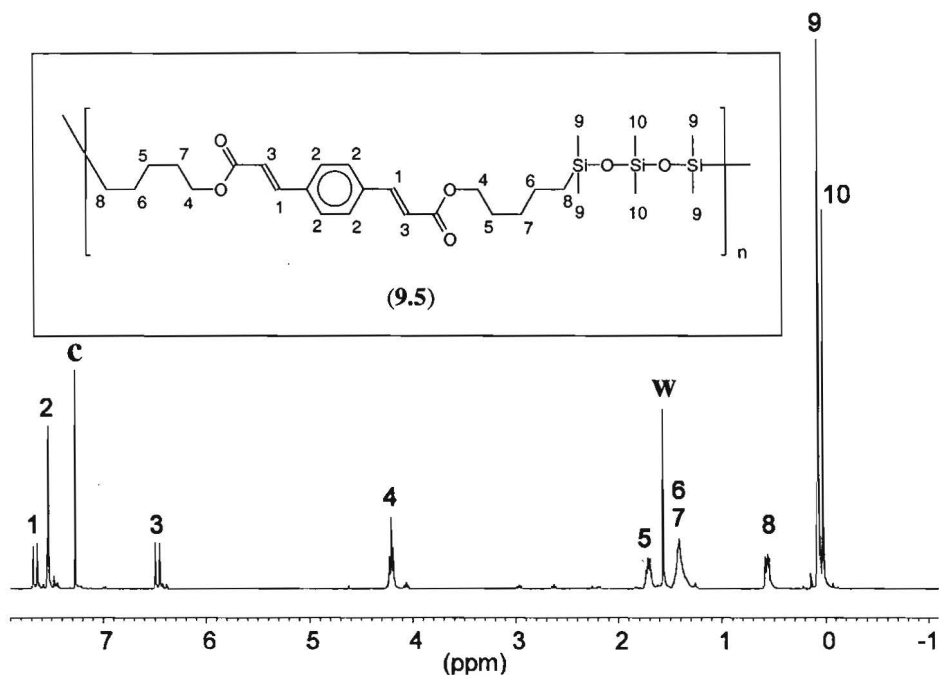


**Figure 9.1:**  $^1\text{H-NMR}$  spectrum of the 3/1 copolymer (9.5) in  $\text{CDCl}_3$ ; the signals marked with *c* and *w* are assigned to residual  $\text{CHCl}_3$  and  $\text{H}_2\text{O}$ , respectively, unmarked signals are assigned to the polymer endgroups.

A  $^1\text{H-NMR}$  spectrum similar to that of the 3/1 copolymer (9.5), is obtained from the polymer of *p*-phenylenediacrylic acid dipent-4-enyl ester and a PDMS with longer chain length ( $\bar{P}_n = 81$ ). However, the  $^1\text{H-NMR}$  spectrum of the reaction product (9.6) shows a smaller peak integral of the Si-CH<sub>3</sub> protons in comparison to the peak integrals corresponding to the other protons (Figure 9.2). No signals of the starting compounds are visible in the  $^1\text{H-NMR}$  spectrum. The reaction product (9.6) will be referred to as the 81/1 copolymer. Comparison of the SEC analyses of the starting PDMS with that of the reaction product shows that polymerization has occurred. Molecular weights determined by SEC analysis according to polystyrene standards are: for the bishydride-terminated PDMS ( $\bar{M}_n = 6.0$  kg/mol according to the supplier)  $\bar{M}_n = 7.8$  kg/mol and  $\bar{M}_w = 13.3$  kg/mol, and for the reaction product  $\bar{M}_n = 44.7$  kg/mol and  $\bar{M}_w = 140.3$  kg/mol. These uncorrected molecular weights are not absolute numbers and can only be used as a qualitative indication of the molecular size.

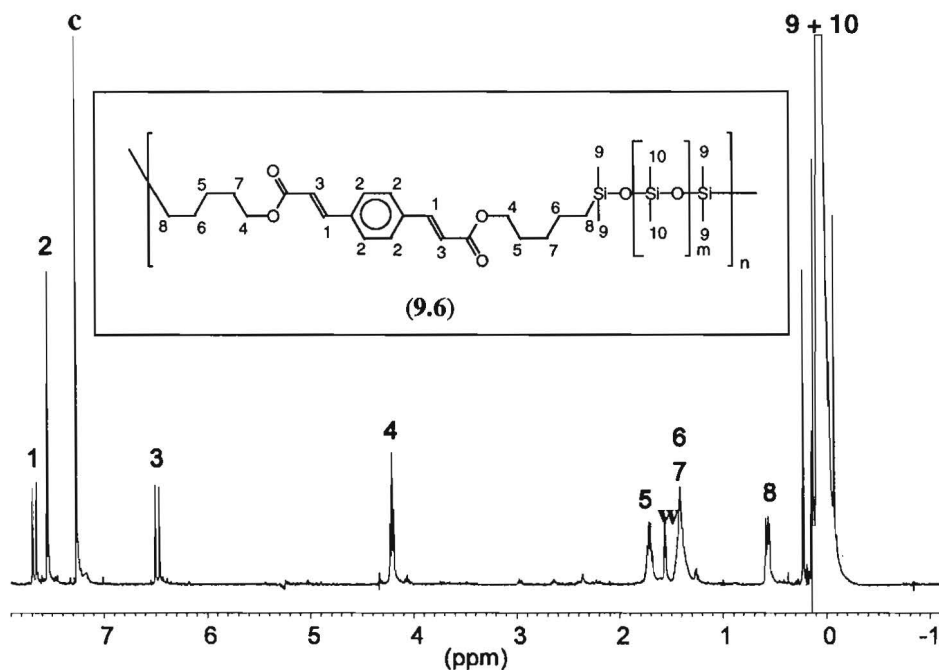


**Figure 9.2:**  $^1\text{H-NMR}$  spectrum of the 81/1 copolymer (9.6) recorded in  $\text{CDCl}_3$ . The signals marked with *c* and *w* are assigned to residual  $\text{CHCl}_3$  and  $\text{H}_2\text{O}$ , respectively, unmarked signals are assigned to the polymer endgroups.

In addition, the  $\alpha,\omega$ -bishydride-terminated PDMS was copolymerized with a  $\alpha,\omega$ -bisvinyl-terminated unsaturated polyester oligomer (9.2). The  $^1\text{H-NMR}$  spectrum of the polymerization product (9.7) shows a new signal of the methylene unit attached to the silicon atom ( $\delta = 0.56$  ppm,  $\text{CH}_2\text{-Si}$ ) and the disappearance of the proton signal of vinyl endgroup ( $\delta = 5.04$  ppm,  $\text{CH}=\text{CH}_2$ ). The product of the hydrosilylation polymerization of the  $\alpha,\omega$ -bishydride-terminated PDMS macromonomer (number average degree of polymerization  $\bar{P}_n = 81$ ) with the polyester oligomer ( $\bar{P}_n = 11$ ) will be indexed as the 81/11 copolymer (9.7). Its  $^1\text{H-NMR}$  spectrum is shown in Figure 9.3. From the  $^1\text{H-NMR}$  spectrum and the SEC analysis it can be concluded that only a few blocks of PDMS and polyester are linked by the hydrosilylation reaction. From the SEC analyses of the polyester oligomer ( $\bar{M}_n = 3.6$  kg/mol,  $\bar{P}_n = 11$  as determined from  $^1\text{H-NMR}$ ) the following molecular weights were determined:  $\bar{M}_n = 4.01$  kg/mol,  $\bar{M}_w = 9.7$  kg/mol (uncorrected molecular weights according to polystyrene standards). Molecular weights were determined by SEC analysis of the 81/11-copolymer are:  $\bar{M}_n = 8.9$  kg/mol,  $\bar{M}_w = 35.4$  kg/mol (uncorrected molecular weights according to polystyrene standards).

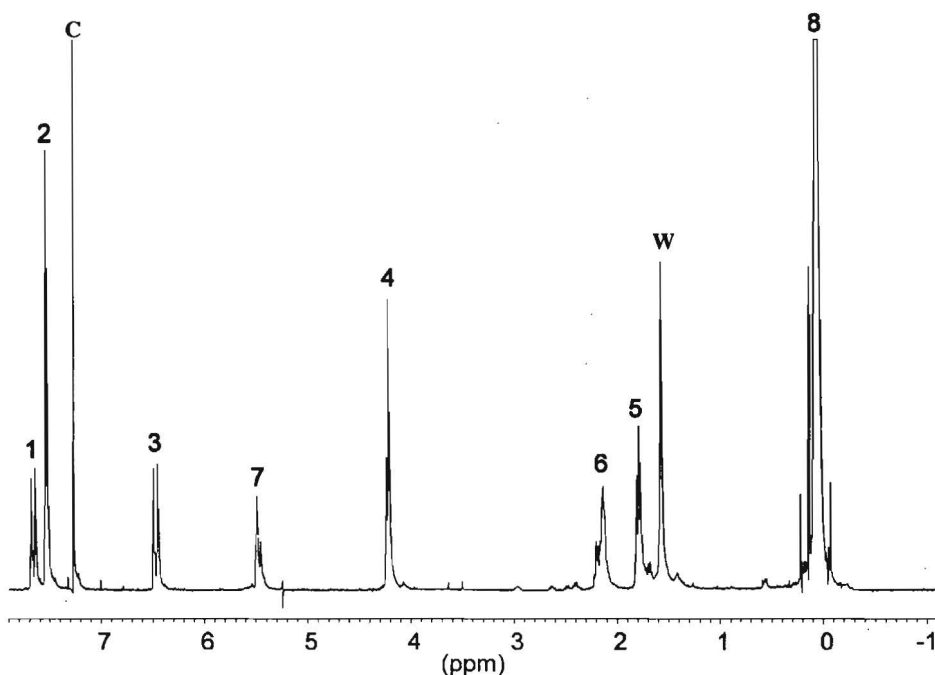
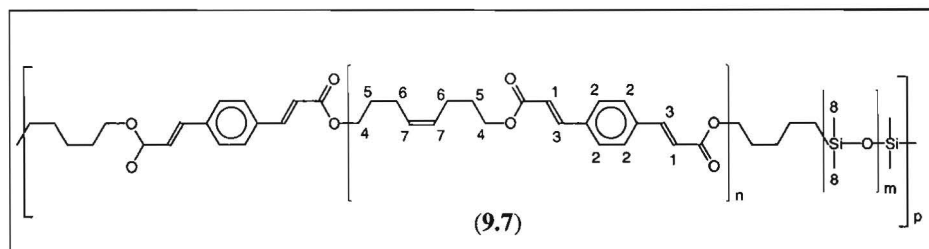


**Figure 9.3:**  $^1\text{H-NMR}$  spectrum of the 81/11 copolymer (9.7) in  $\text{CDCl}_3$ , the signals marked with *c* and *w* are assigned to residual  $\text{CHCl}_3$  and  $\text{H}_2\text{O}$ , respectively, unmarked signals are assigned to the polymer endgroups.

### 9.2.2 Thermal properties of copolymers

The phase transition temperatures and enthalpies of the copolymers and starting compounds were determined using DSC and are collected in Table 9.1. The siloxane homopolymer with  $\bar{P}_n = 81$  (9.4) has two melting endotherms, while copolymers prepared from this poly(dimethylsiloxane) show only one broad melting peak. Melting peaks of the polyester block in the 81/11 copolymer (9.7) have a similar melting enthalpy and are detected at lower temperatures than in the corresponding polyester homopolymer. No liquid crystalline



behaviour is observed in the melting regime between 107 and 138 °C of the homo- and copolyesters with  $\bar{P}_n = 11$  using polarization microscopy and during melting no change in X-ray pattern but only a decrease in intensity is observed in the X-ray diffraction pattern. Therefore, we interpret these transitions as melting of different crystal modifications.

Earlier work has shown that high molar mass PDMS crystallizes quite easily.<sup>43,44</sup> Furthermore, the rate of crystallization is high because of the unhindered rotation about the backbone.<sup>45</sup> Generally, higher molar mass PDMS shows a higher glass transition temperature ( $T_g$ ).<sup>44</sup> It has been reported that when high molar mass PDMS is cooled below  $T_g$ , four thermal transitions are detected when the samples are reheated. These transitions are: a) the glass transition, b) an exothermal crystallization and melting of c) one crystalline form, and d) a second crystalline form of the polymer.<sup>43,44</sup> We observed similar thermal behaviour for the employed PDMS homopolymer. Only small differences are found in melting temperatures and glass transition temperatures for the copolymers in comparison with the corresponding siloxane starting material.

When we compare the melting enthalpy of the oligo(ester) block in the 81/11 copolymer (**9.7**) ( $\Delta H_{\text{total}} = 12.0$  J/g, weight fraction oligo(ester) = 37.5 %) with the melting enthalpy ( $\Delta H_{\text{total}} = 29.1$  J/g) of the pure oligo(ester) ( $\bar{P}_n = 11$ ), we can conclude that the oligo(ester) block in the copolymer has a similar crystallinity as the corresponding oligo(ester) (**9.2**).

**Table 9.1:** DSC results, using a heating rate of 10 K/min.

Polymer / monomer type	$\bar{P}_n$ (siloxane block/ polyesterblock)	Phase transitions
<i>p</i> -phenylenediacrylic acid-dipent-4-enyl ester ( <b>9.1</b> )	1	$T_m = 60.7 \text{ }^\circ\text{C}$ , $\Delta H = 132.2 \text{ J/g}$
polyester oligomer ( <b>9.2</b> )	11	$T_g = 54.7 \text{ }^\circ\text{C}$ , $T_{m1} = 119.8 \text{ }^\circ\text{C}$ , $T_{m2} = 137.8 \text{ }^\circ\text{C}$ , $\Delta H_{\text{total}} = 29.1 \text{ J/g}$
siloxane oligomer ( <b>9.3</b> )	3	$T_g = -43.4 \text{ }^\circ\text{C}$
PDMS homopolymer ( <b>9.4</b> )	81	$T_g = -120.9 \text{ }^\circ\text{C}$ , $T_{m1} = -41.1 \text{ }^\circ\text{C}$ , $T_{m2} = -29.4 \text{ }^\circ\text{C}$ $\Delta H_{\text{total}} = 44.0 \text{ J/g}$
copolymer ( <b>9.5</b> )	3/1	$T_g = -47.2 \text{ }^\circ\text{C}$
copolymer ( <b>9.6</b> )	81/1	$T_g = -118.8 \text{ }^\circ\text{C}$ , $T_m = -44.2 \text{ }^\circ\text{C}$ , $\Delta H = 37.9 \text{ J/g}$
copolymer ( <b>9.7</b> )	81/11	$T_{g1} = -115.4 \text{ }^\circ\text{C}$ , $T_{m1} = -39.7 \text{ }^\circ\text{C}$ , $\Delta H = 18.9 \text{ J/g}$ , $T_{g2} = 50.2 \text{ }^\circ\text{C}$ , $T_{m2} = 107.3 \text{ }^\circ\text{C}$ , $T_{m3} = 125.9 \text{ }^\circ\text{C}$ , $\Delta H_{2+3} = 12.0 \text{ J/g}$

### 9.2.3 X-ray scattering experiments

X-Ray scattering<sup>46</sup> is used to investigate the domain spacing (small angle area) and crystal lattice size (wide angle area) of the homo and block copolymers. The determined reflections and corresponding distances of the homo and block copolymers are summarized in Table 9.2.

**Table 9.2:** X-ray scattering results

Structure	$\bar{P}_n$ (siloxane block/ polyesterblock)	Scattering angle $2\theta$ ( $^\circ$ )	d ( $\text{\AA}$ )
<b>9.5</b>	3/1	2.53	35.0
<b>9.6</b>	81/1	10.18	8.69
<b>9.7</b>	81/11	0.465 10.58	190 8.36
<b>9.2 and 9.7</b>	11 and 81/11	17.58 18.98 21.48	5.04 4.67 4.14

The intensity profile of the X-ray diffraction of the 3/1 copolymer shows a pronounced reflection in the small-angle area at  $2\theta = 2.53^\circ$  corresponding to a domain spacing  $d = 35.0 \text{ \AA}$  in the microphase separated system. The intensity profile of the X-ray diffraction of the 81/1 shows a characteristic broad reflection at  $2\theta = 10.18^\circ$  corresponding to a distance of  $8.69 \text{ \AA}$ . A related reflection is also detected in the 81/11 copolymer at  $2\theta = 10.58^\circ$  corresponding to a distance of  $8.36 \text{ \AA}$ . These reflections at approximately  $2\theta = 10.4^\circ$  correspond to the interchain distance of PDMS of approximately  $8.5 \text{ \AA}$ . Analogously, poly(*n*-alkylsiloxane)s with *n*-alkyl side groups larger than methyl show reflections belonging to the interchain distance at smaller angles.<sup>47</sup>

The intensity profile of the X-ray diffraction pattern of the 81/11 copolymer shows some weak reflections from the crystalline polyester block in the wide angle area. Similar reflections can clearly be seen in the intensity profile of the polyester oligomer ( $\bar{P}_n = 11$ ). Three distinct reflections are detected at  $2\theta = 17.58, 18.98$  and  $21.48^\circ$ , corresponding to distances of  $5.04, 4.67$  and  $4.14 \text{ \AA}$ , respectively. The presence of a crystalline polyester block besides the amorphous polysiloxane block in the 81/11 copolymer indicates that microphase separation of the soft and hard polymer blocks occurs in this copolymer. The reflections of the crystalline polyester blocks in the 81/11 copolymer are clearly shown in the presented X-ray diffraction

pattern (Figure 9.4), however, the reflections are less pronounced than in the X-ray diffraction pattern of the pure polyester oligomer (Figure 9.5).

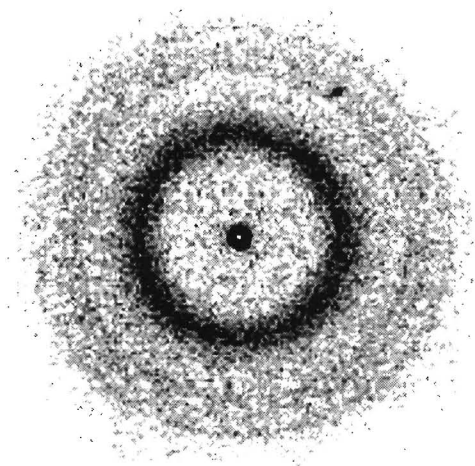


**Figure 9.4:** X-ray diffraction pattern of the 81/11 copolymer.

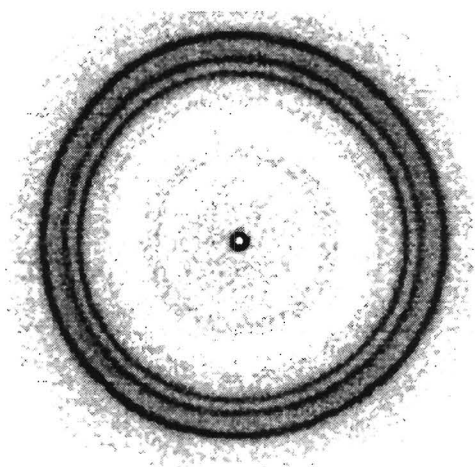


**Figure 9.5:** X-ray diffraction pattern of the polyester homopolymer ( $\bar{P}_n = 11$ ).

The microphase separation as observed by the presence of a crystalline phase, is more clearly seen with TEM. The 81/11 copolymer has a lamellar structure as determined by TEM (Figure

9.6). The polymer film used for the TEM analysis was obtained by slow evaporation of a toluene solution. Small angle X-ray scattering experiments were performed to obtain the lamellar thickness of the microphase-separated 81/11 copolymer. Only one reflection at a scattering angle  $2\theta$  of  $0.465^\circ$  was observed, indicating a thickness of the double layer lamellae of 190 Å.

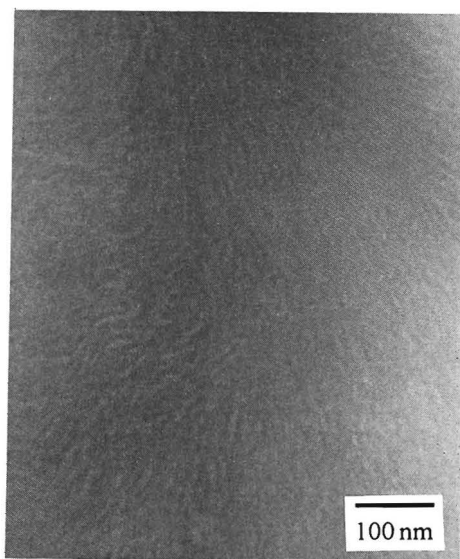


*Figure 9.6: TEM picture solution cast film of 81/11 copolymer*

#### 9.2.4 Photo-crosslinking experiments

To investigate the influence of the siloxane blocks and microphase segregation upon crosslinking, spin-coated films were characterized by UV spectroscopy after irradiation with UV light (254 nm) at room temperature. The crosslinking is reflected in a decrease of the absorption maximum at approximately 300 nm, caused by the reduction of  $\pi$ -electron conjugation of the cinnamic acid units in the chain upon transformation into cyclobutane derivatives upon crosslinking. UV spectra at different irradiation times of the 81/11 copolymer are shown in Figure 9.7. A corresponding polyester oligomer gives similar UV spectra, however, crosslinking is somewhat slower. We predominantly investigated a polyester oligomer with a number average degree of polymerization of 60 ( $\bar{P}_n = 60$ ), which provides films with a better optical transparency than films obtained from the corresponding polyester oligomer with  $\bar{P}_n = 11$ .

Anisotropy can be introduced in the polymeric film by crosslinking with linearly polarized light. The linearly polarized light selectively crosslinks the chromophores having their transition dipole moment aligned with the polarization of the UV light. Spin-coated films of the polyester copolymers and homopolymers were irradiated with linearly polarized light and characterized using polarized UV spectroscopy. The optical anisotropy of the crosslinked film can be analyzed by measuring its efficiency as a polarizing filter, with a maximum absorption for light that is polarized in the plane of the UV source. Upon irradiation of polyester homopolymers, only a minor selectivity of crosslinking in the direction of the polarized light could be obtained. However, upon irradiation of the 81/11 copolymer selective crosslinking in the direction of the polarized light was obtained. In Figure 9.8, the normalized intensity of the absorbance band at ca. 300 nm is given as a function of the irradiation time for a polyester homopolymer ( $\bar{P}_n = 60$ ) and the 81/11 PDMS-polyester copolymer using polarized light perpendicular to ( $90^\circ$ ) and parallel with ( $0^\circ$ ) the direction of the linearly polarized light used for irradiation. In general the photoinduced crosslinking of the block copolymer proceeds somewhat faster than that of the homopolymer.

In order to determine the polarizing efficiency of the irradiated film, UV spectra were recorded between  $0^\circ$  and  $90^\circ$  at intervals of  $10^\circ$ . We irradiated for 150 s, which was estimated as the irradiation time with maximum difference in absorbance between the parallel and perpendicular direction. Figure 9.9 shows the  $\cos^2(\theta)$  dependence of the transmission (T) on the measurement angle  $\theta$ . The transmissions corresponding to angles  $90$ - $360^\circ$  were derived from the measured transmissions at  $0$ - $90^\circ$ . The transmission of a common polarizing filter evolves via the cosine of the polar angle. The irradiated sample also behaves as a polarizer giving a cosinus dependence. Both polarizers give therefore a  $\cos^2(\theta)$  dependance (a least-squares fit gives:  $T = 0.022 \cdot \cos^2(\theta) + 0.011$ ). The polarization efficiency (PE) of the obtained polarizer was 67 %, as calculated by difference of the transmission parallel ( $T_{\parallel}$ ) and perpendicular ( $T_{\perp}$ ) divided the by the parallel transmission ( $T_{\parallel}$ ):  $PE = ((T_{\parallel} - T_{\perp}) / T_{\parallel}) * 100\%$ . This value is lower than the efficiency of the polarization filter used for UV irradiation (95.3%).

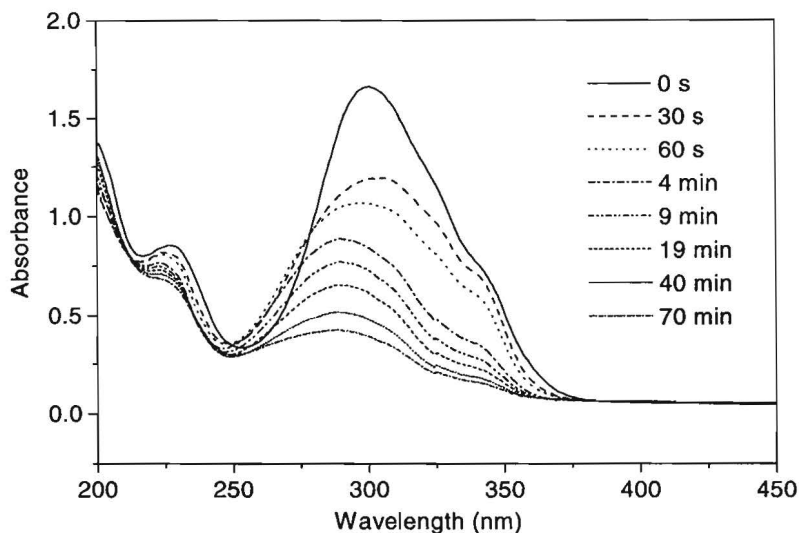


**Figure 9.7:** UV spectra of a spin-coated film of the 81/11 copolymer varying the irradiation time

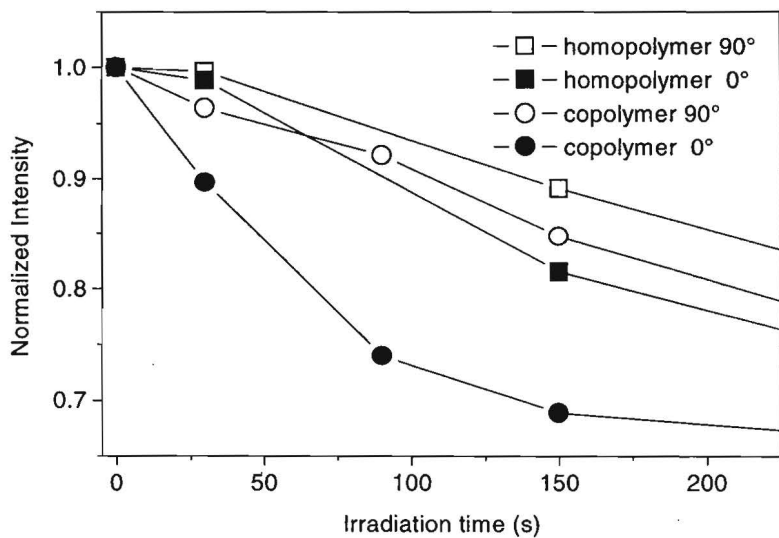


**Figure 9.8:** UV absorbance at  $\lambda_{max}$  ( $\approx 300$  nm) as a function of the irradiation time for the 81/11 copolymer and polyester homopolymer, parallel ( $0^\circ$ ) and perpendicular ( $90^\circ$ ) towards the direction of the polarized light used for irradiation.

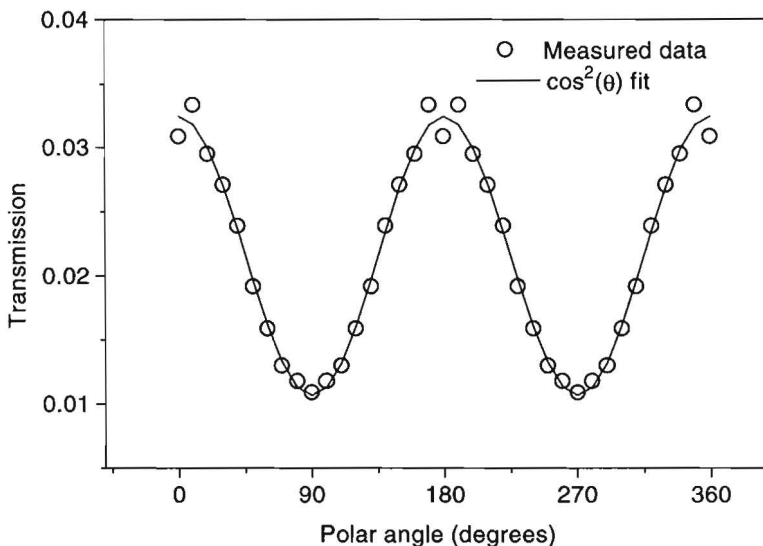


**Figure 9.9:** Transmission of the band at 300 nm as a function of the polar angle towards the direction of the polarized light used for irradiation.

### 9.3 Conclusions

Microphase-separated polyester-PDMS copolymers give higher crosslinking rates than corresponding polyester homopolymers. Selective crosslinking in the direction of the polarized light yielding anisotropy in the polymer film can be obtained using the polyester-PDMS copolymer. However, further investigations are required to understand the higher polarizing efficiency and crosslinking rate for the block copolymer compared to the polyester homopolymer.

### 9.4 Experimental

#### Materials:

Bishydride-terminated polydimethylsiloxanes, hexamethyltrisiloxane and the hydrosilylation catalyst, a 2.1–2.4 wt% platinum-divinyltetramethylsiloxane complex solution in xylene (PC072), were obtained from ABCR GmbH & Co, Karlsruhe, Germany. Toluene was used distilled from sodium before use and kept under nitrogen. All other chemicals were obtained commercially and used without any further treatment unless stated otherwise.



*Techniques:*

All hydrosilylation experiments were started in a glovebox under a nitrogen atmosphere and subsequently moved to a fume hood to react further at 80 °C. The NMR spectra were recorded using a Bruker 400 AM spectrometer ( $^1\text{H}$ : 400.13 MHz) or using a Varian Gemini 300 ( $^1\text{H}$ : 300.08 MHz and  $^{13}\text{C}$ : 75.46 MHz). Chemical shift values are given in ppm, relative to TMS but were referenced to residual  $\text{CHCl}_3$  at 7.27 ppm when siloxanes were present in the sample. UV spectra were obtained using a Perkin Elmer Lambda 3B UV-VIS spectrophotometer. IR spectra were recorded on a Perkin Elmer 1600 series FTIR. SEC analyses were performed on a Waters model 510 SEC apparatus with THF as eluent at 40 °C using 2 Shodex KF 80-M linear columns, a Waters 410 differential refractometer and a Waters 486 tunable absorbance detector (UV detection at 254 nm). Molecular weights were not corrected but referenced to polystyrene standards. Homopolymer bishydride-terminated PDMS is only analysed using the differential refractive index (DRI) detector. Molecular weights were determined using the universal calibration method, employing polystyrene standards. DSC spectra were taken using a Perkin-Elmer DSC-2 under nitrogen atmosphere with a heating rate of 20 K/min. X-ray diffraction patterns of copolymers were taken using  $\text{Cu K}\alpha$  radiation and a multi-wire area detector X-1000 coupled with a graphite monochromator and a Linkam THM 600 hot stage for X-ray studies at elevated temperatures. Small Angle X-Ray Scattering (SAXS) studies were performed using  $\text{Cu K}\alpha$  radiation and a Rigaku Denki small angle goniometer. Transmission Electron Microscopy (JEOL 2000-FX) was operated at 80 kV. Cryosections of approximately 80 nm were cut with a diamond knife at  $-122$  °C. No additional staining was applied. Optical properties were studied using a Jenaval polarisation microscope equipped with a Linkam THMS 600 heating device, with crossed polarizers. Spin-coated films were prepared from preferably THF solutions on quartz glass plates ( $0.85 \times 1.28 \times 0.10$  cm) at a spinning rate of 1500 rpm using a Convac ST145 spincoater. Due to the moderate solubility of polyester homopolymers in THF, high molecular weight polyesters were spin-coated from  $\text{CHCl}_3$  and low molecular weight polyesters from a 1/1 v/v  $\text{CHCl}_3$ /THF mixtures. Spin-coated films were irradiated at 254 nm using a Philips TUV PL-S 9W "long life" germicidal lamp without fluorescent powder. UV spectra of spincoated samples were obtained using a Unicam 8700 Series UV-VIS spectrophotometer. In between the light source of the UV spectrophotometer and the sample, first a depolarization filter and secondly a polarization filter was placed, to obtain linearly polarized light. The used polarization filter used for irradiation has a polarization efficiency of 95.3%, which was defined as the difference of parallel and perpendicular transmission divided by the parallel transmission.

*Synthesis of p-phenylenediacrylic acid dipent-4-enyl-ester (9.3):**Step 1: Synthesis of p-phenylenediacrylic acid:*

A mixture of terephthalaldehyde (28.8 g, 21.5 mmol), anhydrous sodium acetate (57 g, 69.5 mmol) and acetic anhydride (100 gram, 97.9 mmol) was heated under reflux for 14 days. Water (200 mL) was added dropwise after which the water/acetic acid mixture was distilled off. The residue was cooled to room temperature, an aqueous KOH solution (1.0 L, 5 M) was added and the mixture was heated under reflux for 8 hours. The mixture was filtered and concentrated HCl was added to the filtrate until pH = 3. After filtration and drying under vacuum *p*-phenylene-diacrylic acid was obtained as a light yellow solid (45.9 g, 98%).  $^1\text{H-NMR}$  ( $\text{D}_2\text{O}$  + anhydr.  $\text{Na}_2\text{CO}_3$ , 300 MHz):  $\delta$  7.61 (s, 4H,  $\text{C}_6\text{H}_4$ ), 7.34 (d, J = 16 Hz,

2H, C<sub>6</sub>H<sub>4</sub>CHCH), 6.51 (d, J = 16 Hz, 2H, Ph-CH). <sup>13</sup>C-NMR (D<sub>2</sub>O + anhydr. Na<sub>2</sub>CO<sub>3</sub>, 300 MHz): δ 182.7 (COOH), 147.1 (CH-C<sub>6</sub>H<sub>4</sub>-CH), 143.3 (2C, arom., C<sub>ipso</sub>), 135.2 (4C, arom., C<sub>ortho</sub>), 131.9 (CH=CH-C<sub>6</sub>H<sub>4</sub>-CH=CH). IR: ν(C=O) = 1708 cm<sup>-1</sup>.

*Step 2: Synthesis of p-phenylenediacrylic acid dipent-4-enyl ester:*

*Para*-phenylenediacrylic-acid (10 g, 45.9 mol) was added to thionyl chloride (30 g, 352 mmol) and the mixture was heated under reflux for 6 hours under an argon atmosphere. The excess thionyl chloride was removed by distillation under reduced pressure. The crude acid chloride was used without further purification for the esterification. Pyridine (20 mL) and 4-pentene-1-ol (8.68 g, 100 mmol) were added under argon atmosphere and the mixture was heated under reflux for 5 hours. The pyridine was removed under reduced pressure and the product was dissolved in dichloromethane (200 mL). The solution was extracted with water (100 mL) and washed with a 0.1 M HCl solution (100 mL), a saturated aqueous Na<sub>2</sub>CO<sub>3</sub> solution (2 × 100 mL) and a saturated aqueous NaCl solution (100 mL). After column chromatography with an ethylacetate-hexane mixture (1:9, v/v) and distillation (250 °C, 0.04 mbar), *p*-phenylene-diacrylic acid dipent-4-yl ester resulted as a white solid (13.2 g, 80%). GC showed 99.5% purity. <sup>1</sup>H-NMR (CDCl<sub>3</sub>, 300 MHz): δ 7.65 (d, J = 16 Hz, PhCHCH), 7.55 (s, 4H, C<sub>6</sub>H<sub>4</sub>), 6.46 (d, J = 16 Hz, 2H, PhCH), 5.85 (m, 2H, CH=CH<sub>2</sub>), 5.04 (dd, 4H, CH=CH<sub>2</sub>), 4.24 (t, J = 6.1 Hz, 4 H, OCH<sub>2</sub>), 2.18 (m, 4H, OCH<sub>2</sub>CH<sub>2</sub>CH<sub>2</sub>), 1.82 (m, 4H, OCH<sub>2</sub>CH<sub>2</sub>). <sup>13</sup>C-NMR (D<sub>2</sub>O + anhydr. Na<sub>2</sub>CO<sub>3</sub>, 300 MHz): δ 167.3 (COOH), 144.0 (CH-C<sub>6</sub>H<sub>4</sub>-CH), 138.0 (CH=CH<sub>2</sub>), 136.7 (C<sub>6</sub>H<sub>4</sub>-CH=CH), 129.0 (2C, arom., C<sub>ipso</sub>), 119.8 (4C, arom., C<sub>ortho</sub>), 115.8 (CH=CH<sub>2</sub>), 64.6 (CH<sub>2</sub>-CH<sub>2</sub>-CH<sub>2</sub>-CH=CH<sub>2</sub>), 30.6 (CH<sub>2</sub>-CH<sub>2</sub>-CH=CH<sub>2</sub>), 28.5 (CH<sub>2</sub>-CH=CH<sub>2</sub>). IR: ν(C=O) = 1705 cm<sup>-1</sup>, ν(CH=CH-Ar) = 1632 cm<sup>-1</sup>, ν(CH=CH) = 917 cm<sup>-1</sup>. Anal. calculated for C<sub>22</sub>H<sub>26</sub>O<sub>4</sub>: C: 74.55%, H 7.39%, found: C 74.75%, H 7.13%. UV (CHCl<sub>3</sub>): λ<sub>max</sub> = 320 nm. DSC: T<sub>m</sub> = 60.7 °C, ΔH = 132.2 J/g.

*Acyclic Diene Methathesis (ADMET) bulk polymerization of para-phenylenediacrylic acid-dipent-4-enyl ester:*

A mixture of *para*-phenylenediacrylic acid dipent-4-enyl ester (1 g, 2.82 mmol) and a ruthenium catalyst<sup>41,42</sup> (RuCl<sub>2</sub>(=CHPh)(PCy<sub>3</sub>)<sub>2</sub>) (20 mg, 0.041 mmol) was heated at 80 °C under vacuum (0.003 mbar). Rapid evolution of ethene was observed upon melting of the monomer. The mixture was heated under vacuum for 24 hours. The reaction product was dissolved in hot chloroform and filtered. The chloroform solution containing a oligomeric fraction was precipitated in a 10-fold excess of methanol, yielding a white product (0.354 mg, 35.4%). <sup>1</sup>H-NMR (CDCl<sub>3</sub>, 300 MHz) δ 7.65 (d, J = 16 Hz, 2H, PhCHCH), 7.55 (s, 4H, C<sub>6</sub>H<sub>4</sub>), 6.46 (d, J = 16 Hz, 2H, PhCH), 5.85 (m, CH=CH<sub>2</sub>, external), 5.45 (m, CH=CH, internal), 5.04 (dd, CH=CH<sub>2</sub>, external), 4.24 (t, J = 6.1 Hz, 4H, OCH<sub>2</sub>), 2.22 (m, 4H, OCH<sub>2</sub>CH<sub>2</sub>CH<sub>2</sub>), 1.83 (m, 4H, OCH<sub>2</sub>CH<sub>2</sub>) Degree of polymerization  $\bar{P}_n = 11$ , as determined by <sup>1</sup>H-NMR spectroscopy. SEC (THF):  $\bar{M}_n = 3.6$  kg/mol. IR ν(C=O) 1705 cm<sup>-1</sup>, ν(CH=CH-Ar) = 1636 cm<sup>-1</sup>. UV (spincoated film): λ<sub>max</sub> = 306 nm. DSC: T<sub>g</sub> = 54.7 °C, T<sub>m1</sub> = 119.8 °C, T<sub>m2</sub> = 137.8 °C, ΔH<sub>total</sub> = 29.1 J/g.

*Acyclic Diene Methathesis (ADMET) solution polymerization of para-phenylenediacrylic acid dipent-4-enyl ester:*

*Para*-phenylenediacrylic acid dipent-4-enyl ester (0.500 g, 1.41 mmol) was dissolved in dry dichloromethane (2.5 mL). A solution of the ruthenium catalyst ( $\text{RuCl}_2(\text{=CHPh})(\text{PCy}_3)_2$ ) (5.5 mg, 0.007 mmol) was added using a syringe. The mixture was stirred at 30 °C for 24 hours under an argon atmosphere; solvent evaporates during this time. The obtained polymer was dissolved in 5 mL of chloroform and precipitated in a 10 fold-excess of methanol. The polymer was collected by centrifugation, yielding a white product (0.390 mg, 78.0 %). Degree of polymerization  $\overline{P}_n = 60$ , as determined by  $^1\text{H-NMR}$  spectroscopy. Proton assignments in the  $^1\text{H-NMR}$  spectrum are as in the bulk polymerization. UV (spincoated film):  $\lambda_{\text{max}} = 303 \text{ nm}$ .

*Synthesis of the 3/1 copolymer (9.5):*

Hexamethyltrisiloxane (0.135 g, 0.649 mmol) and *para*-phenylenediacrylic acid dipent-4-enyl ester (0.229 g, 0.647 mmol) were dissolved in 4 mL of toluene under nitrogen atmosphere in the absence of light in a 10 mL Schlenk tube. Subsequently, 3  $\mu\text{L}$  of the hydrosilation catalyst (PC072) dissolved in 1 mL of toluene was added. Subsequently, the reaction mixture was moved from the glove box to a fume hood to react at 80 °C under nitrogen. After 24 hours reaction time the toluene was removed by applying vacuum. The reaction product was stored at room temperature in the absence of light.  $^1\text{H-NMR}$  (400 MHz,  $\text{CDCl}_3$ ) only chemical shifts of protons of the repeating units are indicated:  $\delta$  7.66 (2H, d,  $J = 16.1 \text{ Hz}$ ,  $\text{CH}=\text{CH-Ar}$ ), 7.54 (4H, s, arom. C-H), 6.47 (2H, d,  $J = 15.9 \text{ Hz}$ ,  $\text{CH}=\text{CH-Ar}$ ), 4.21 (4H, t,  $J=6.7 \text{ Hz}$ ,  $\text{OCH}_2$ ), 1.71 (2H, m,  $\text{OCH}_2\text{CH}_2$ ), 1.44 (8H, m,  $\text{OCH}_2\text{CH}_2\text{CH}_2$  and  $\text{CH}_2\text{CH}_2\text{Si}$ ), 0.56 (4H, m,  $\text{CH}_2\text{Si}$ ), 0.07 (24H, s, outer Si- $\text{CH}_3$ ), 0.03(12H, s, inner Si- $\text{CH}_3$ ). SEC (THF):  $\overline{M}_n = 5.8 \text{ kg/mol}$ ,  $\overline{M}_w = 18.9 \text{ kg/mol}$ . DSC:  $T_g = -43.4 \text{ }^\circ\text{C}$ .

*Synthesis of the 8/1/1 copolymer(9.6):*

Bishydride-terminated PDMS (2.42 g, 0.403 mmol,  $\overline{M}_n = 6.0 \text{ kg/mol}$ ) and *para*-phenylenediacrylic acid dipent-4-enyl ester (0.143 g, 0.403 mmol) were dissolved in 8 mL of toluene under nitrogen atmosphere in the absence of light in a 25 mL Schlenk tube. Subsequently, 3.5  $\mu\text{L}$  of the hydrosilylation catalyst (PC072) dissolved in 1 mL of toluene was added. Subsequently, the reaction mixture was moved from the glovebox to a fumehood to react at 80 °C under nitrogen. After 13 hours reaction time the toluene was removed by applying vacuum. The reaction product was stored at room temperature in the absence of light.  $^1\text{H-NMR}$  (400 MHz,  $\text{CDCl}_3$ )  $\delta$  7.67 (2H, d,  $J = 16.0 \text{ Hz}$ ,  $\text{CH}=\text{CH-Ar}$ ) 7.55 (4H, s, arom. C-H) 6.48 (2H, d,  $J = 16.0 \text{ Hz}$ ,  $\text{CH}=\text{CH-Ar}$ ) 4.21 (4H, t,  $J=6.7 \text{ Hz}$ ,  $\text{OCH}_2$ ) 1.71 (2H, m,  $\text{OCH}_2\text{CH}_2$ ) 1.42 (8H, m,  $\text{OCH}_2\text{CH}_2\text{CH}_2$  and  $\text{CH}_2\text{CH}_2\text{Si}$ ) 0.57 (4H, m,  $\text{CH}_2\text{Si}$ ) 0.07 ( $\checkmark$ 500H, broad s, Si- $\text{CH}_3$  siloxane repeating unit). SEC (THF):  $\overline{M}_n = 44.7 \text{ kg/mol}$ ,  $\overline{M}_w = 140.3 \text{ kg/mol}$ . DSC:  $T_g = -118.8 \text{ }^\circ\text{C}$ ,  $T_m = -44.2 \text{ }^\circ\text{C}$ .

*Synthesis of the 8/1/1 copolymer (9.7):*

Bishydride terminated PDMS (0.244 g, 0.04 mmol,  $\overline{M}_n = 6.0 \text{ kg/mol}$ ) and the polyester oligomer of *para*-phenylenediacrylic acid dipent-4-enyl ester (0.144 g, 0.04 mmol,  $\overline{M}_n = 3.6 \text{ kg/mol}$ ) were dissolved in 5 mL of toluene under nitrogen atmosphere in the absence of light in a 10 mL Schlenk tube. Subsequently, 1  $\mu\text{L}$  of the hydrosilation catalyst (PC072) dissolved in 1 mL of toluene was added. Subsequently, the reaction mixture was moved from the glove box to a fumehood to react at 80 °C.

After 13 hours reaction time the toluene was removed by applying vacuum. The reaction product was stored at room temperature in the absence of light.  $^1\text{H-NMR}$  (400 MHz,  $\text{CDCl}_3$ ) only chemical shifts of repeating units are indicated:  $\delta$  7.66 (2H, d,  $J = 16.0$  Hz,  $\text{CH}=\text{CH-Ar}$ ), 7.54 (4H, s, arom. C-H), 6.47 (2H, d,  $J = 16.0$  Hz,  $\text{CH}=\text{CH-Ar}$ ), 5.49 (4H, m,  $\text{OCH}_2\text{CH}_2$ ), 1.71 (2H, m,  $\text{OCH}_2\text{CH}_2$ ), 4.22 (4H, t,  $J=6.5$  Hz,  $\text{OCH}_2$ ), 2.16 (4H, m,  $\text{CH}_2-\text{CH}=\text{CH}$ ), 1.79 (4H, m,  $\text{CH}_2\text{CH}_2\text{CH}=\text{CH}$ ), 0.07 (12H, broad s, Si- $\text{CH}_3$ ). UV (spincoated film):  $\lambda_{\text{max}} = 300$  nm. SEC (THF):  $\overline{M}_n = 8.9$  kg/mol,  $\overline{M}_w = 35.4$  kg/mol. DSC:  $T_{g1} = -115.4$  °C,  $T_{m1} = -39.7$  °C,  $\Delta H = 18.9$  J/g,  $T_{g2} = 50.2$  °C,  $T_{m2} = 107.3$  °C,  $T_{m3} = 125.9$  °C,  $\Delta H_{2+3} = 12.0$  J/g

## 9.5 References

1. Maekawa, Y., Kato, S., Saigo, K., Hasegawa, M. and Ohashi, Y. *Macromolecules*, **24**, 2314 (1991).
2. Stumpe, J., Ziegler, A., Berfhahn, M. and Kricheldorf, H.R. *Macromolecules*, **28**, 5306 (1995).
3. Allen, N.S., Mallon, D., Timms, A., Green, A.W. and Catalina, F. *Eur. Polym. J.*, **29**, 533 (1993).
4. Akabor, S., Kumagai, T., Habata, Y. and Sato, S. *Bull. Chem. Soc. Jpn.*, **61**, 2459 (1988).
5. Scigalski, F., Toczek, M. and Paczkowski, J. *Polymer*, **35**, 692 (1994).
6. Egerton, P.J., Pitts, E. and Reiser, A. *Macromolecules*, **14**, 95 (1981).
7. Schadt, M., Seiberle, H., Schuster, A. and Kelly, S.M. *Jpn. J. Appl. Phys., Part 1*, **34**, 3240 (1995).
8. Boutevin, B., Abdellah, L. and Dinia, M.N. *Eur. Polym. J.*, **31**, 1127 (1995).
9. Lai, Y.C. and Quinn, E.T. *J. Polym. Sci., Polym. Chem. Ed.*, **33**, 1783 (1995).
10. Son, D.Y. and Keller, T.M. *Macromolecules*, **28**, 399 (1995).
11. Tezuka, Y. *Prog. Polym. Sci.*, **17**, 47 (1992).
12. Bates, F.S., Schulz, M.F., Khandpur, A.K., Förster, S., Rosedale, J.H., Almdal, K. and Mortensen, K. *Faraday. Discuss.*, **7**, 98 (1994).
13. Yilgör, I. and McGrath, J.E. *Adv. Polym. Sci.*, **86**, 1 (1988).
14. Thomas, E.L. and Lescanec, R.L. *Phil. Trans. R. Soc. Lond. A*, **348**, 149 (1994).
15. Sakurai, S.S. *Trends Polym. Sci.*, **3**, 90 (1994).
16. Saam, J.C., Gordon, D.J. and Lindsey, S. *Macromolecules*, **3**, 1 (1970).
17. Selby, C.E., Stuart, J.O., Clarson, S.J., Smith, S.D., Sabata, A., van Ooij, W.J. and Cave, N.G. *J. Inorg. Organomet. Polym.*, **4**, 85 (1994).
18. Dems, A. and Strobin, G. *Macromol. Chem.*, **192**, 2521 (1991).
19. Cameron, G.G. and Chisholm, M.S. *Polymer*, **27**, 1420 (1986).
20. Simionescu, C.I., Harabagiu, V., Comanita, E., Hamciuc, V., Giurgiu, D.G. and Simionescu, B.C. *Eur. Polym. J.*, **5**, 565 (1992).
21. Kazama, H., Tezuka, Y. and Imai, K. *Polym. J.*, **19**, 1091 (1987).
22. Kazama, H., Tezuka, Y., Imai, K. and Goethals, E.J. *Macromol. Chem.*, **189**, 985 (1988).
23. Rao, B.S., Madec, P.J. and Marechal, E. *Macromol. Chem. Rapid Commun.*, **7**, 703

- (1986).
- 24 . Pratt, L.M., Waugaman, M. and Khan, I. M. *Polym. Prep., Am Chem. Soc., Div. Polym. Chem.*, **36**, 263 (1995).
  - 25 . Nagase, Y., Masubuchi, T., Ikeda, K. and Sekine, Y. *Polymer*, **22**, 1607 (1981).
  - 26 . Allen, R.D. and Hedrick, J.L. *Polym. Prep., Am Chem. Soc., Div. Polym. Chem.*, **28**, 163 (1987).
  - 27 . Lai, Y.C., Ozark, R. and Quinn., E. T. *J. Appl. Polym. Sci.*, **33**, 1773 (1995).
  - 28 . Kazama, H., Tezuka, Y. and Imai, K. *Macromolecules*, **24**, 122 (1991).
  - 29 . Friedmann, G., Herz, J. and Brossas, J. *Polym. Bull.*, **6**, 251 (1982).
  - 30 . He, X., Herz, J. and Guenet, J.M. *Macromolecules*, **20**, 2003 (1987).
  - 31 . Schmitt, D., Beinert, G., Zilliox, J.G. and Herz, J. *Angew. Makromol. Chem.*, **165**, 181 (1989).
  - 32 . Auman, B.C., Percec, V., Schneider, H.A. and Cantow, H. *Polymer*, **28**, 1407 (1987).
  - 33 . Auman, B.C., Percec, V., Schneider, H.A., Jishant, J. and Cantow, H. *Polymer*, **28**, 119 (1987).
  - 34 . Mathias, L.J. and Lewis, C.M. *Macromolecules*, **26**, 4070 (1993).
  - 35 . Itsuno, S., Chao, D. and Ito, K. *J. Polym. Sci., Polym. Chem. Ed.*, **31**, 287 (1993).
  - 36 . Shih, H-Y., Kuo, W.F., Pearce, E.M. and Kwei, T.K. *Polym. Adv. Techn.*, **6**, 413 (1995).
  - 37 . Li, W. and Huang, B.T. *J. Polym. Sci., Polym. Phys. Ed.*, **30**, 727 (1992).
  - 38 . Koepp, E. and Vögtle, F., *Synthesis*, 177 (1987).
  - 39 . Smith D.W. and Wagener, K.B. *Macromolecules*, **26**, 1633 (1993).
  - 40 . Patton, J.T., Boncella, J.M. and Wagener, K.B. *Macromolecules*, **25**, 3862 (1992).
  - 41 . Schwab, P., France, M.B., Ziller, J.W. and Grubbs, R.H. *Angew. Chem., Int. Ed. Engl.*, **28**, 7248 (1995).
  - 42 . Schwab, P., Grubbs, R.H. and Ziller, J.W. *J. Am. Chem. Soc.*, **118**, 110 (1996).
  - 43 . Orrah, D.J., Semlyen, J.A., Dodgson, K. and Ross-Murphy, S.B. *Polymer*, **28**, 985 (1987).
  - 44 . Clarson, S.J., Dodgson, K. and Semlyen, J.A. *Polymer*, **26**, 930 (1985).
  - 45 . Polmanteer, K.E., Servais, P.C. and Konkle, G.M. *Ind. Eng. Chem.*, **44**, 1576 (1952).
  - 46 . Lodge, T. *Mikrochim Acta*, **116**, 1 (1994).
  - 47 . Out, G.J.J. "Poly(di-n-alkylsiloxane)s - Synthesis and Molecular Organization", PhD thesis, University of Twente, Enschede, The Netherlands, (1994).

## Summary

This thesis describes the design and synthesis of polymeric building blocks with well-defined chain length, chain architecture, and nature of endgroups. These building blocks are applied in multicomponent polymer systems, such as block copolymers and blends and their morphology is investigated. We emphasized on systems based on poly(2,6-dimethyl-1,4-phenylene ether) (PPE) in particular, but also systems with poly(bisphenol A carbonate) (PC) and poly(dimethylsiloxane) (PDMS) with well-defined chain lengths are investigated.

The traditional synthesis of PPE is based on the oxidative coupling of 2,6-dimethylphenol. When this polymerization is performed in a non-solvent, like methanol or 2-propanol, the polymer produced precipitates and can easily be isolated in pure form. The molecular weight can be adjusted by performing the reaction in a mixture of 2-propanol and toluene, where a higher amount of toluene in the reaction mixture yields higher polymers with higher molecular weight.

The molecular weight of PPEs can also be adjusted conveniently by applying by the reaction of a phenol with PPE in a redistribution reaction. Such redistribution reactions are examined in detail in this thesis. Redistribution reactions are known to occur next to the oxidative coupling polymerization in the PPE synthesis. The absence or presence of several copper/amine catalysts and oxygen allows control over these two reaction processes. We used redistribution reactions to prepare various types of modified PPE. When a substituted phenol is reacted with PPE in the redistribution the tail-end in the product consists of the phenolic compound. This redistribution method is advantageous because besides an easy control over molecular weight, the functionality of endgroups can easily be varied using this method. Reactive PPEs are prepared using a phenol with a reactive functionality in the PPE redistribution. Besides the synthesis of reactive PPEs, star-shaped PPEs and di- or triblock copolymers can be prepared using redistribution. The synthesis of star-shaped PPEs is illustrated by the reaction of multifunctional phenols based on poly(propylene imine) dendrimers. Polystyrene-PPE diblock copolymers are prepared via reaction of a phenol-terminated polystyrene with PPE. Redistribution reactions of  $\alpha,\omega$ -bis(4-hydroxyphenyl)-terminated PDMS with PPE yield PPE-PDMS-PPE triblock copolymers.

Next to the preparation of modified PPEs via redistribution, the synthesis of endgroup-modified PPEs is described in this thesis via etherification of the phenolic endgroups using phase-transfer-catalysis. The reactive PPEs, prepared either by redistribution or modification of the phenolic endgroups, are used in the reactive compatibilization of immiscible blends of PPE and poly(butylene terephthalate) (PBT). *In-situ* formation of interfacially active copolymers

during reactive extrusion of these reactive PPEs with PBT can yield a fine dispersion of PPE particles in a PBT matrix, which is stable after annealing. Besides the addition of reactive PPEs, the addition of low molecular weight promoters like chain-extenders or transesterification catalysts can be beneficial for the compatibilization of the PPE/PBT blends. Other blends that are investigated in this thesis are blends of star-shaped PPEs and linear atactic polystyrene. The miscibility of these blends decreases with increasing number of arms of the star-shaped PPE.

Facile control over the PPE molecular weight in redistribution reactions allows an easy variation of PPE block lengths in PPE-PDMS-PPE triblock copolymers. The microphase separation in this triblock copolymer is investigated. Triblock copolymers with a PDMS volume fraction of ca. 0.50 show a scaling behaviour of the domain size ( $D$ ) with the total molecular weight ( $M$ ) to the power 0.662, that is in agreement with theory that predicts  $2/3$  as scaling value. In contrast, block copolymers with a low PDMS content show divergent scaling behaviour,  $D \sim M^{0.350}$ . The lower scaling factor is proposed to be a result of collapsed chains a non-equilibrium morphology. Microphase separation is also studied in well-defined multiblock copolymers of PDMS and poly(bisphenol A carbonate) (PC). These PDMS-PC are prepared in a reaction of  $\alpha,\omega$ -bis(bisphenol A)-terminated poly(dimethylsiloxane) (PDMS) with endgroup-activated PC. The influence of crystallization in solution-cast films on the obtained morphology and stress-strain behaviour is investigated. Microphase separation also plays an important role in the selective photocrosslinking of multiblock copolymers of PDMS and unsaturated polyesters. A selective crosslinking, which was more efficient for microphase-separated copolymers than for polyester homopolymers, yields optically anisotropic polymer films that behave as polarizers.

Generally, there is an increasing interest in polymers with a well-defined chain-architecture, chain length, and nature of endgroups. The use of synthetic organic and polymer chemistry in the development of these well-defined polymeric building blocks can open pathways for new materials and applications, as has been illustrated in this thesis for a few examples.

## Samenvatting

Dit proefschrift beschrijft het ontwerp en de synthese van polymere bouwstenen met goed gedefinieerde ketenlengte, ketenarchitectuur en eindgroepfunctionaliteit. Deze bouwstenen zijn toegepast in multicomponent systemen, zoals blok copolymeren en blends, waarbij metname de morfologie werd bestudeerd. De nadruk ligt hierbij in het bijzonder op systemen gebaseerd op poly(2,6-dimethyl-1,4-fenyleen ether) (PPE), echter ook systemen met goed gedefinieerde ketenlengte gebaseerd op polycarbonaat (PC) en polydimethylsiloxaan (PDMS) zijn onderzocht.

De traditionele synthese van PPE maakt gebruik van de oxidatieve koppeling van 2,6-dimethylfenol. Als deze polymerisatie wordt uitgevoerd in een non-solvent, zoals 2-propanol, precipiteert het zuivere polymeer en kan het eenvoudig geïsoleerd worden. Het molecuulgewicht is eenvoudig instelbaar door de reactie uit te voeren in een mengsel van 2-propanol en toluen, waarbij een hoger gehalte aan toluen polymeren geeft met een hoger molecuulgewicht.

Het molecuulgewicht van PPE kan ook eenvoudig geregeld worden door de reactie van een fenol met PPE in een redistributie reactie. Deze redistributie reacties zijn in detail onderzocht in dit proefschrift. Redistributie reacties treden altijd op naast de oxidatieve koppelingspolymerisatie in de synthese van PPE. De af- of aanwezigheid van diverse koper/amine katalysatoren en zuurstof geeft de mogelijkheid de twee reactieprocessen te controleren. De redistributiereactie werd gebruikt om verschillende gemodificeerde PPE's te maken. Als een gesubstitueerd fenol reageert met PPE in een redistributie reactie dan wordt het gereageerde fenol ingebouwd als staart-uiteinde van het polymeer. De redistributiemethode is aantrekkelijk doordat eenvoudig het molecuulgewicht en de eindgroepfunctionaliteit kunnen worden ingesteld. Reactieve PPE's kunnen worden verkregen door gebruik te maken van fenol met een reactieve groep. Naast de synthese van reactieve PPE's, biedt de redistributiemethode de mogelijkheid tot synthese van sterpolymeren en di- of triblok copolymeren. De bereiding van sterpolymeren werd geïllustreerd aan de hand van de reactie van multifunctionele fenolen gebaseerd op poly(propyleen imine) dendrimeren. Polystyreen-PPE diblok copolymeren zijn bereid door reactie van een fenol-getermineerd polystyreen met PPE. Redistributie van  $\alpha,\omega$ -bis(4-hydroxyfenyl)-getermineerde polydimethylsiloxaan geeft PPE-PDMS-PPE triblok copolymeren.

De bereiding van gemodificeerde PPE's kan naast door redistributie ook gebeuren door veretheringsreacties aan de fenolische eindgroep met gebruik van fase-transfer-katalyse. De reactieve PPE's, bereid met behulp van redistributie of modificatie van de fenolische



eindgroepen, zijn toegepast in de reactieve compatibilisering van niet-mengbare blends van PPE en poly(butyleen tereftalaat) (PBT). De *in-situ* vorming van grensvlak-actieve copolymeren tijdens de reactieve extrusie van deze reactieve PPE's met PBT geeft aanleiding tot een fijne dispergering van PPE deeltjes in een PBT matrix, die stabiel is na temperen (annealen). De toevoeging van laag moleculaire verbindingen, welke ketenverlenging of transesterificatie geven, kunnen de compatibilisering verder verbeteren. Andere onderzochte blends zijn blends van stervormig PPE met lineair ataktisch polystyreen. De mengbaarheid van deze blend neemt af bij toenemend aantal armen van het stervormige PPE.

Het eenvoudig te sturen molecuulgewicht van PPE bij redistributie reacties maakt een gemakkelijke variatie van PPE blok lengtes in bijvoorbeeld PPE-PDMS-PPE triblok copolymeren mogelijk. De microfasenscheiding in deze triblok copolymeren is onderzocht. Triblok copolymeren met een PDMS volumefractie van circa 0.50 geven overeenkomend met theoretische beschouwingen ( $D \sim M^{2/3}$ ), een schaling van de domeingrootte als functie van het totale molecuulgewicht met de exponent 0.662. Blok copolymeren met laag PDMS gehalte geven daarentegen een afwijkend schalingsgedrag,  $D \sim M^{0.350}$ . De lagere schalings factor kan verklaard worden door gekrompen polymeer kluwens die zich bevinden in een niet-evenwichtsmorfologie. De microfasenscheiding is tevens onderzocht in goed-gedefinieerde multiblok copolymeren van PDMS en PC. Deze PC-PDMS multiblok copolymeren zijn bereid door de reactie van  $\alpha,\omega$ -bis(bisphenol A)-getermineerde PDMS met eindgroep-geactiveerde PC. De invloed van kristallisatie op de morfologie en het trek-rek gedrag van de vanuit oplosmiddel gegoten films is bestudeerd. Microfasenscheiding speelt ook een belangrijke rol in de selectieve fotocrosslinking van multiblok copolymeren van PDMS en onverzadigde polyesters. Een selectieve crosslinking, welke het meest efficiënt was voor microfase gescheiden copolymeren in vergelijking met de polyester homopolymeren, resulteert in optisch anisotrope polymere films die zich gedragen als polarisatoren.

In het algemeen is er in toenemende mate interesse voor polymeren met een goed-gedefinieerde ketenarchitectuur, ketenlengte en eindgroepfunctionaliteit. Het gebruik van synthetisch organische chemie en polymeerchemie bij de ontwikkeling van deze polymere bouwstenen zoals beschreven in dit proefschrift kan leiden tot routes voor nieuwe materialen en toepassingen.

## **Curriculum Vitae**

De auteur van dit proefschrift werd geboren op 6 januari 1966 te Huybergen. Na het behalen van zijn HAVO (1983) en VWO (1985) diploma aan het Moller Lyceum te Bergen op Zoom werd gestart met de studie aan de Hogeschool West-Brabant, sectie Chemie. In 1989 sloot hij deze studie in Etten-Leur cum laude af met als afstudeerrichting Organische Chemie en extra specialisatie-richting Analytische Chemie. Aansluitend werd aan de Rijksuniversiteit te Groningen aangevraagd met de verkorte opleiding bij de faculteit Scheikunde. Het afstudeeronderzoek betreffende polymeer-gebonden hydroformyleringskatalysatoren werd uitgevoerd bij de vakgroep Polymeerchemie onder begeleiding van prof.dr. G. Challa in een samenwerkings project met prof.dr. P.W.N.M van Leeuwen van het Koninklijk Shell Laboratorium te Amsterdam. Het doctoraal examen werd in mei 1992 behaald waarna hij in september van dat zelfde jaar startte met een tweejarige onderzoekers opleiding aan de Technische Universiteit Eindhoven in de vakgroep Polymeerchemie en Kunststoffotechnologie (TPK) onder leiding van prof.dr. P.J. Lemstra. In nauwe samenwerking met prof.dr. E.W. Meijer van de vakgroep Organische Chemie (TOC) aan dezelfde universiteit en DSM Research te Geleen werd gewerkt aan modificatie van poly(2,6-dimethyl-1,4-fenyleen ether). Dit onderzoek werd als promotie onderzoek voortgezet en resulteerde in dit proefschrift onder begeleiding van prof.dr. E.W. Meijer en in nauwe samenwerking met de vakgroep TPK en General Electric Plastics te Bergen op Zoom.

## **Dankwoord**

Mijn boekje is nu klaar en een drukke maar vooral leuke promotietijd zit er op. Tijdens mijn onderzoek hebben vele personen een essentiële bijdrage geleverd aan dit proefschrift. Zonder jullie hulp had dit proefschrift er zeker anders uitgezien. Een aantal personen wil ik met name bedanken.

Allereerst natuurlijk mijn promotoren Prof. Bert Meijer en Prof. Piet Lemstra. De grote mate van vrijheid die ik van jullie kreeg tijdens mijn AIO-2 en later tijdens mijn promotie heb ik altijd enorm gewaardeerd. Bert, jou wil ik bedanken voor je motiverende begeleiding en omdat ik altijd bij je terecht kon met vragen, probleempjes of voor het corrigeren van manuscripten. Dankzij jou heb ik mijn promotietijd ervaren als een leerzame en prettige tijd. Piet, ook jou dank ik voor al je hulp en kritische blik op mijn proefschrift.

Mijn co-promotor Marcel van Genderen wil ik vooral danken voor al zijn hulp en de snelle correctie van vele manuscripten. De leesbaarheid werd hier vaak flink door verbeterd en zelfs na al vele correcties door anderen wist je er altijd nog wel een spelfout uit te halen. Dankzij Hartmut Fisher heb ik veel geleerd over blokcopolymeren, en zijn hulp bij verschillende fysische metingen heb ik enorm gewaardeerd. Laurent Nelissen bedank ik vooral voor de vele nuttige werkbesprekingen. Verder wil ik Prof. Jan Bussink en Prof. Ton German bedanken voor de snelle en kritische beoordeling van dit proefschrift. Alhoewel tijdens mijn promotie Prof. Bussink niet meer werkzaam was aan de TUE, kreeg ik als ik met hem sprak diverse tips en ideeën, vooral door zijn enorme kennis op het gebied van PPE en polycarbonaat. Ook door zijn opgewekte humeur vond ik het altijd fijn om met hem te spreken.

Milko Burkard, Grègory van Steenpaal en Leon Beekmans dank ik voor hun inzet tijdens hun afstudeerperiode. Alhoewel slechts maar een klein gedeelte van al de experimenten die we hebben uitgevoerd in dit boekje staan, heb ik enorm veel geleerd door met jullie samen te werken. Milko, jij bent de pionier op het gebied van de PPE sterpolymeren, bedankt hiervoor, ook voor je inzet bij de DLS experimenten die je hebt uitgevoerd bij DSM Research in Geleen. Grègory, bedankt voor je werk aan de reactieve compatibilisering van de PPE/PBT blends en de redistributie opschalings-experimenten die je hebt uitgevoerd bij General Electric Plastics in Bergen op Zoom. Leon, jou wil ik bedanken voor het enorme enthousiasme waarmee je aan blokcopolymeren hebt gewerkt, ook al tijdens je researchstage. Andere researchstagiaires die ik wil danken zijn: Leon Nelissen, Mark Roos, Christian Widdershoven en Willy Zelen.

Tijdens mijn onderzoek heb ik veel samengewerkt via industriële contacten, in het bijzonder met DSM Research, General Electric Plastics en Philips. Ik dank al hun werknemers die

hebben bijgedragen aan dit proefschrift door hun inbreng bij wetenschappelijke discussies en/of door experimentele hulp. DSM medewerkers, die ik met name wil noemen zijn: Henk Oevering, Gerard Werumeus Buning, Ron Out, Giovanna di Pietro, Abdellatif Moussaïd, Prof. Jacques Joosten en Ellen de Brabander. Hun hulp bij het werk aan de PPE redistributie en sterpolymeren tijdens het begin van mijn promotie heeft tot mooie resultaten geleid. Medewerkers bij General Electric Plastics te Bergen op Zoom die in het bijzonder hebben bijgedragen aan dit proefschrift zijn: Juraj Liska, Gert de Wit, Jan Lohmeijer, Christian Bailley, Bernard Klazema, Arno Hagenaars, Martin Hetem en Adri Landa. De samenwerking met deze GEP medewerkers vooral tijdens het eind van mijn promotie heeft mij in het bijzonder geholpen door hun grote know-how op het gebied van synthese en karakterisering van diverse PPEs en PPE/PBT blends. Daniel Brunelle en Pete Phelps, werkzaam bij General Electric Corporate Research te Schenectady (NY) in Amerika, wil ik bedanken de synthese van het geactiveerde polycarbonaat en het kritisch lezen van het hoofdstuk over PC-PDMS blok copolymeren. Prof. Dick Broer van Philips Research ben ik erkentelijk voor zijn hulp bij het werk aan de foto-crosslinkbare polyester co- en homo-polymeren.

Anderen die ik wil bedanken zijn o.a. Patrick Baesjou en Prof. Reedijk van de Rijksuniversiteit Leiden en Prof. Challa van de Rijksuniversiteit te Groningen, voor nuttige discussies en synthese van het PPE-dimeer. Mark Hempenius van de Universiteit Twente dank ik voor nuttige tips betreffende hydrosileringsreacties en voor synthese van het fenol-getermineerde polystyreen. Een discussie betreffende mengsels van sterpolymeren en lineaire polymeren met Prof. Jacques Roovers van de National Research Council te Ottawa, Ontario te Canada was voor mij erg leerzaam. Bert Postma van Viscotek te Oss en Joop Vorenkamp van de Rijksuniversiteit Groningen wil ik bedanken voor de GPC metingen. Hans-Joachim Räder van het Max-Planck Institut für Polymerforschung ben ik erkentelijk voor FD-MS metingen.

Verder wil ik ook al mijn (ex-)collega's bij TOC, TPK en WFW bedanken voor de prima werksfeer, gezelligheid en de steun tijdens mijn promotietijd. Jullie vriendschap zal me altijd bijblijven. Jullie gezelschap bij uitstapjes naar de Ardennen of Maastricht, tijdens een hapje eten in de Mensa, Trafagar Pub of de Connaisseur, en het geouwehoer tijdens wat drinken in de benedenbar, gaf voor mij een aangename afwisseling. Ook vond ik het fijn als ik 's avonds laat of 's weekends weer eens aan het werk was dat jullie er vaak ook waren. Ik hoop dat we elkaar in de toekomst nog vaak zien en dat onze vriendschap niet verloren gaat, ook al verblijven sommigen van jullie een korte tijd in het buitenland na het promoveren.

Een aantal mensen van 't lab wil ik nog met name bedanken. Bij de vakgroep Polymeertechnologie en Kunststoftechnologie (TPK) ben ik erkentelijk: Johan Boekholt voor hulp bij mechanische testen, Alfons Franken voor DSC assistentie, Wieb Kingma voor vele

GPC analyses, Erik Nies voor uitleg aangaande thermodynamica en fysica van polymeren en hulp bij enige hoofdstukken, Anne Spoelstra-Govaert voor vele TEM foto's en Theo Tervoort voor het lezen van een manuscript. Bij de vakgroep Organische Chemie (TOC) wil ik met name bedanken: Joost van Dongen voor de verschillende analyses, Rint Sijbesma voor zijn bijdrage aan het laatste hoofdstuk van dit proefschrift, Jef Vekemans voor alle synthese tips en Henk Eding voor diverse dingen. Jan de Haan en Leo van de Ven van de vakgroep Instrumentele Analyse (TIA) ben ik erkentelijk voor de vaste stof NMR spindiffusie metingen. Ik vond het leuk om samen te werken met o.a. de volgende (ex-)collega's in gezamenlijke projecten: Annemieke Aerds-Vermeijlen, Felix Beijer, Joris Gilberts, Ky Hirschberg, Johan Jansen, Joost Maas, Rob Venderbosch en Bas de Waal. Mijn collega's van vloer 8, Jan van de Bos, Hans Damen, Tamme Doornbos, Pieter van Lier, Bas de Waal en Du Yinjun dank ik vooral voor de goede sfeer.

Tenslotte wil ik mijn familie en vrienden bedanken voor hun steun en getoonde belangstelling.

# Stellingen

behorende bij het proefschrift

## Design and Synthesis of Reactive Building Blocks for Multicomponent Polymer Systems

New options for poly(2,6-dimethyl-1,4-phenylene ether)

van

Huub A.M. van Aert

1. Het opnieuw publiceren van essentiële artikelen uit het verleden, maar nu met commentaar gebaseerd op huidige inzichten, is aan te bevelen.  
*Hay, A.S. J. Polym. Sci., Polym. Chem. Ed., 34, 1373 (1996).*
2. De term ‘telechelic’ wordt door veel auteurs op verschillende manieren geïnterpreteerd. De definitie gegeven door de IUPAC commissie voor macromoleculaire nomenclatuur maakt de bestaande verwarring groter.  
*IUPAC Commission on Macromolecular Nomenclature, Pure & Appl. Chem., 68, 2287 (1996).*  
*Percec, V., Pugh, C., Nuyken, O., Pask, S.D. Compr. Polym. Sci., 6, 281 (1989).*  
*Tezuka, Y. Prog. Polym. Sci., 17, 471 (1992).*  
*Jerome, R., Henriouille-Granville, M., Boutevin B. and Robin, J.J. Prog. Polym. Sci., 16, 837 (1991).*
3. De door Kallos et al. bepaalde dispersiegraad van 1,0007 voor een 4e generatie polyamidoamine dendrimeer is niet betrouwbaar.  
*Kallos, G.J., Tomalia, D.A., Hedstrand, D.M., Lewis, S. and Zhou, J. Rapid Commun. Mass. Spectrom., 5, 383 (1991).*

4. Het voordeel van uitsluiting van oplosmiddel bij gebruik van CO<sub>2</sub> als reactiemedium voor de synthese van poly(fenyleen ether), zoals beschreven door Kapellen et al., wordt teniet gedaan als voor de zuivering van het polymeer dit opgelost dient te worden in toluen.  
Kapellen, K.K., Mistele, C.D. and DeSimone J.M. *Macromolecules*, **29**, 495 (1996).
5. De bereiding van polycarbonaat (PC) – polystyreen (PS) diblok copolymeren uit de copolymerisatie van fenol-getermineerd PS met fosgeen en bisfenol A, zoals beschreven door Jiang et al., zal naast het gewenste diblok copolymeer en eventueel kleine hoeveelheden vrij PS en triblok copolymeer, ook PC homopolymeer bevatten.  
Jiang, R., Quirk, R.P., White, J.L. and Min, K. *Polym. Eng. Sci.*, **31**, 1545 (1991).  
Hoofdstuk 8 van dit proefschrift.
6. De door Camus et al. gemeten molecuulgewichten van poly(2,6-dimethyl-1,4-fenyleen ether) zoals bereid met gebruik van oxidatieve koppeling, zijn niet in overeenstemming met de gemeten intrinsieke viscositeiten.  
Camus, A., Garozzo, M.S., Marsich, N. and Mari, M. *J. Mol. Catal. A: Chem.*, **112**, 353 (1996).
7. Bij een reorganisatie zijn niet alleen de ontslagen werknemers de dupe.
8. Flatbewoners die een hond als huisdier hebben zijn geen echte dierenvrienden.
9. De gemiddelde prijzen van 3-jarige rijpaarden zijn veel te laag in verhouding met het betaalde dekgeld en de fokkosten.
10. De uitdrukking “gebelgd zijn” doet onrecht aan het opgewekte karakter van onze zuiderburen.
11. Het is vreemd dat het aantal soorten abdij-bieren toeneemt, terwijl het aantal kloosterlingen gestaag afneemt.
12. Het gebruik van een varken als spaarpot impliceert niet dat er momenteel veel geld te verdienen valt in de varkenshouderij.